SAFETY ANALYSIS REPORT

for

THE MODEL BMI-1 SHIPPING CASK

Revision A

March 28, 1980

from

BATTELLE'S COLUMBUS LABORATORIES
505 KING AVENUE
COLUMBUS, OHIO 43201

TABLE OF CONTENTS

TABLE OF CONTENTS
(Continued)

TABLE OF CONTENTS
(Continued)

TABLE OF CONTENTS
(Continued)

TABLE OF CONTENTS
(Continued)

TABLE OF CONTENTS
(Continued)

TABLE OF CONTENTS
(Continued)

<u>TABLE OF CONTENTS</u>
(Continued)

LIST OF TABLES

LIST OF TABLES
(Continued)

LIST OF FIGURES

LIST OF FIGURES
(Continued)

LIST OF DRAWINGS

0. PREFACE FOR REVISION A, 3-28-80

0.1 Document Index

This revised Safety Analysis Report for Packaging (SARP) for the BMI-1 cask contains a compilation of 17 documents including the original license application of 1963, 15 subsequent revisions amendments, or communications, and the certificate of compliance. In this revised SARP, the 17 documents have been reorganized into the standard format suggested in Regulatory Guide 7.9.1.* The information in those 17 documents is presented unchanged except in a few instances. In addition, some new sections prepared specifically for this revision have been included. In order to enable ready identification of the source of the data and information presented, the following identification system is used:

> The 17 documents previously submitted are listed in Table 0.1 in chronological order. Each document has been assigned a "Document" Number as shown in Table 0.1. The appropriate Document Number appears at the upper right side of each page that contains data from any of these 17 documents. Where new data or information is included or changes to the previously submitted data have been made, the bottom of the page bears the identification "REV. A, 3-28-80" and the changed lines are identified by a solid vertical bar in the right hand margin. If the entire page is new or has been changed, the vertical bar is omitted. When the only change to

*U.S. Nuclear Regulatory Guide 7.9, Standard Format and Content of Part 71 Applications for Approval of Packaging of Type B, Large Quantity, and Fissile Radioactive Material, Revision 1, January, 1980.

a page is to the section titles, in order to conform to those suggested in Regulatory Guide 7.9, the vertical bar and the identification "REV. A, 3-28-80" are omitted.

TABLE 0.1 INDEX OF DOCUMENTS PREVIOUSLY SUBMITTED

Document Number	Title of Document
1.	Safety Analysis for Battelle Research Reactor Spent Fuel Shipping Cask, dated November 14, 1963.
2.	Addendum to Structural Integrity Analysis, BMI-1 Shipping Cask, dated January 27, 1964.
3.	Safety Analysis for the Shipment of Power Reactor Development Company, Irradiated Fermi Fuel Subassemblies, dated July 19, 1965.
4.	Addendum to Safety Analysis for BRR Spent Fuel Shipping Cask BMI-1, to Show Compliance with 10CFR-71 Regulations and to List Maximum Quantities of Nuclear Materials to Be Shipped, dated September 8, 1969.
5.	Addendum II to Safety Analysis for Nuclear Material Shipping Cask BMI-1, to Show Compliance with 10CFR-71 Regulations and to List Maximum Quantities of Nuclear Material to Be Shipped, dated May 7, 1970.
6.	Addendum III to Safety Analysis for Nuclear Material Shipping Cask BMI-1, to Show Compliance with 10CFR-71 Regulations and to List Maximum Quantities of Nuclear Material to Be Shipped, dated July 15, 1970.
7.	Telegram to Transportation Branch/D.M.L. from B.C.L. correcting Addendum Number II, dated July 24, 1970.

TABLE 0.1 (Continued)

Document Number	Title of Document
8.	Addendum IV to Safety Analysis for Nuclear Shipping Cask BMI-1 to Show Compliance with 10CFR-71 Regulations for Shipment of Battelle Research Reactor Fuel Having an Increased Loading of U-235, dated September 21, 1970.
9.	Addendum V to Safety Analysis for Nuclear Shipping Cask BMI-1 to Show Compliance with 10CFR-71 Regulations for Shipment of Battelle Research Reactor Fuel Having an Increased Loading of U-235, dated January 18, 1971.
10.	Safety Analysis Report for Shipment of TRIGA Fuel by the University of Arizona, dated December 8, 1971.
11.	Safety Analysis Report for Shipment of TRIGA Fuel by the University of Arizona, Upgraded Analysis, dated December 8, 1971.
12.	Supplement Number 1 to Request for License to Transport Irradiated TRIGA Fuel in BMI-1 Shipping Cask, dated June 15, 1972.
13.	Results of Loading-to-Critical Experiment in the University of Arizona TRIGA, dated September 14, 1972.
14.	Safety Analysis Report for Shipment of MTR Fuel by Texas A&M University, dated September 29, 1972.
15.	Safety Analysis Report for Shipment of PULSTAR Fuel by The State University of New York at Buffalo, dated October 13, 1977.

TABLE 0.1 (Continued)

Document Number	Title of Document
16.	U.S. Nuclear Regulatory Commission Certificate of Compliance 5957, Revision 5, Docket Number 71-5957; Package Identification Number USA/ 5957B ( ) F.
17.	Safety Analysis Report for Shipment of EPRI Crack Arrest Capsules in BMI-1 Shipping Cask, dated February 8, 1980.

1. GENERAL INFORMATION

1.1 Introduction

The Safety Analysis Report for Packaging (SARP) demonstrates that the Model No. BMI-1 shipping cask meets the current regulatory requirements[1] for shipment of the contents listed below in Section 1.2.3. as Fissile Classes I. II, and III. This SARP shows that an infinite number of packages can be transported per shipment with Fissile Class I contents, and up to 25 packages may be transported per shipment with Fissile Class II contents.

1.2 Package Description

1.2.1 Packaging

1.2.1.1 Description of Cask

Cask Design Drawing Number 43-6704-0001 Rev. A accompanying this safety analysis report presents the configuration of the modified BMI-1 nuclear-material-shipping cask. The modified cask has a measured shipping weight of 23,660 pounds. The total envelope dimensions, including the lifting trunnions, are 59.12 inches in diameter x 78 inches high.

The basic cask body is 33.37 inches in diameter x 73.37 inches high. It consists of two concentric stainless steel shells which form an annular region which is filled with lead. The outer shell is of a laminated steel construction. The innermost layer of the two laminates is made of 0.50-inch Type 304 stainless plate. This layer is the body of the cask as first constructed. The 0.12-inch outer layer of the laminated outer shell is welded to the inner layer at the corners of the cask and at all penetrations of the shell. This added outer shell is spaced 0.06 inch from the original shell by weld spots spaced on approximate 8-inch centers.

(1) References to Section 1. found in Section 1.3.1.

The inner shell is made of 0.25-inch-thick stainless steel plate and is unchanged from the original design. With the cover in place, the internal cavity dimensions are 15.5 inches in diameter x 54 inches long. The cover fits into a recess in the cask body formed by stepping the internal cavity diameter to about 18.5 inches. This recess is about 8-inches deep and has tapering sides. The top of the cask body is made of 0.75-inch-thick steel plate welded to the inner and outer shells. Lead shielding consists of an 8.0-inch annulus on the sides with a 7.75-inch slab section in the cover and a 7.5-inch slab section in the bottom under the cavity. Lead-expansion space was provided in the former design by peripheral cones welded in both ends of the cask. In the modified design, the void space at the top end of the cask will be filled with lead.

A liquid drain line penetrates the inner cavity at about the center of the cavity bottom. The drain line terminates in the side of the shell about 5.5 inches from the bottom. A stainless steel needle valve with the discharge end closed with a pipe plug affords a closure of this drain. The closure is protected from mechanical damage by a housing made of 0.50-inch thick stainless steel welded to the 0.50-inch thick cask shell. Safety plugs (Patent Number 3,466,444*) are welded into the cask wall and cover plate as an added safety feature in case water should enter the lead cavity or in case the cask should be exposed to a fire which exceeds the prescribed test fire.

The safety plug, shown on Drawing 420040, consists of a nominal 1/4-inch stainless steel pipe plug, which screws into a stainless steel body. The body, which is 1.0-inch diameter x 0.62-inch thick, has stainless steel filter welded to the back side. The body is welded in the shell of the cask with the filter toward the lead. The 1/4-inch pipe plug has a 1/8-inch hole drilled clear through and is filled with a low melting alloy. The pipe plug screws into the body so it is flush at the outside surface.

---

* Patent included in Section 1.3.3

In the event of extreme temperature, the low melting alloy melts and permits venting of gases through the filter and pipe plug. The porous stainless steel disc readily passes gases, including steam, but it is substantially impermeable to liquid lead, thus retaining the shielding material, should it become molten.

Four lugs are welded to the top plate of the cask as a means of tying the cask to the vehicle. The thickness of these lugs has been increased to 1.5-inch, to comply with the 10G, 5G, and 2G combined load prescribed in the regulations.

Twelve 1.0-inch-diameter stainless steel studs are welded into the top plate of the cask on a 23.37-inch-diameter bolt circle to secure the cover. Two alignment pins are provided in the same bolt circle to protect the threads on the studs. A tapered surface is machined on the circular edge at the joint between the inner cavity shell and the top plate of the cask. This surface is the seat for the O-ring used to provide a seal for the cask cavity.

The cover of the cask is nominally 26.5 inches in diameter x 9.75 inches thick. The sides are tapered to fit the recess in the cask body. The sides of the cover are 0.25 inch thick and the bottom is 0.75 inch thick. The top plate of the cover is laminated. The inner layer is 1.0-inch-thick stainless steel and the outer layer is 0.12-inch-thick stainless steel. The outer layer is cut out and seal welded at all penetrations and around the outer periphery. The cover-lift device is made of two 0.25-inch-thick Type 304 stainless steel plates. An alternate cover lifting device consists of a U-bolt welded to the top of the cover. The chemical lead-filled section between the top and bottom plates of the cover is 7.75 inches thick providing 0.25 inch of space between the top cover plate and the lead. The cover is fitted with a thermocouple/thermometer well for monitoring internal cavity temperatures.

Lifting trunnions 3.5 inches in diameter are mounted on the sides of this cask and are positioned above the shell of the cask. In this position, it is not possible for the trunnions to act as rods to penetrate the shell in an accident. The trunnions have outboard supports to fit unloading equipment at ICPP.

The cask is mounted on a mild steel beam-type skid measuring 6 ft x 8 ft. This skid serves to spread the weight of the cask on the floor and to add stability in shipment. Four tie rods 1.5 inches in diameter with adjustable turnbuckles are attached to the cask at a height of 38 inches from the skid and extend to the corners of the skid. In addition, eight 1-inch-diameter A325 steel bolts are used to anchor the cask to the skid. Bumper blocks are also used to prevent shearing of the bolts between the cask and skid. A 0.75-inch-thick stainless steel plate is positioned between the cask proper and the skid. This plate is attached to the skid by the same bolt-block system as the cask base plate. The plate is used to comply with the unloading facility at the ICPP. This plate also provides greater resistance to heat flow through the cask bottom from the fire test than does the laminated construction used on the side wall of the cask.

The BMI-1 cask is designed to be used either for dry or water-filled shipments. A pressure gauge, pressure-relief valve, and filter are provided at the top of the cask. These items are protected by a housing of 0.50-inch-thick stainless steel similar to that which protects the drain valve.

Some of the basic information pertaining to the cask is summarized in the following information.

(a) Total maximum weight, 23,660 pounds
(b) Outside diameter, 33.37 inches
(c) Inside cavity diameter, 15.5 inches
(d) Outside shell thickness, 0.50 inch
(e) Inside shell thickness, 0.250 inch
(f) Over-all length, 73.37 inches
(g) Operating pressure, 50 psig
(h) Design pressure, 100 psig

(i) Maximum operating temperature (inside cavity), 320 F
(j) Lid weight, 1,100 pounds
(k) Contents weight, 1,110 pounds
(l) Skid weight, 1,700 pounds

1.2.1.2 Description of Product Containers And Baskets

a) BMI-1 Canister

The containment canister to be used inside the BMI-1 cask cavity, as shown on Drawing 00-000-421 Rev. C., is constructed of 304 type stainless steel. The wall of the can is 0.125 inch thick, and the ends are 0.50 inch thick. Ten 0.213-inch socket head cap screws secure the cover to the can. A silastic rubber O-ring located in a groove in this cover provides the seal. The canister is designed to fit into the cask cavity with 0.25-inch clearance on the diameter and 0.50-inch clearance on the length.

(b) BMI-1 Basket

Fuel assemblies are positioned within the central cavity by two identical stainless steel baskets, with one basket supported on top of the other, BMI Drawing Number 41-4409-0004, Rev. B. A permanent neutron poison is provided by boral clad with stainless steel used as dividing plates in the baskets.

(c) Enrico Fermi Copper Basket

The copper basket shown on Drawing K5928-5-0049D, Rev. to May 12, 1966, may be used as needed as additional radial gamma shielding and as a device to better conduct heat from a load of small dimensions to the cask wall. It was designed, licensed, and used for shipping a single fuel element from the Enrico Fermi reactor. It was also used for shipping a load of 40,000 curies of stainless steel encapsulated Co-60, with a decay heat output of 1.25 kw.

(d) University of Arizona Basket for TRIGA Fuel

A special basket has been designed (BMI Drawing 1020, Rev. B) to individually support 38 TRIGA fuel elements in the BMI-1 cask. The TRIGA fuel will be shipped dry in this basket. The basket is a sealed container made of stainless steel to serve as a secondary containment of this shipment.

(e) Texas A&M Basket

Basket assembly defined by BMI Drawing Number 41-4409-0004, Rev. B, as modified by BMI Drawing Number 00-000-236, Rev. A.

(f) S8DR Fuel Basket

Basket assembly and storage can defined by BMI Drawing Number 00-000-391, Rev. C, and Atomic International Drawing Number AIHL, S8DR 0019-01, respectively.

(g) Pulstar Fuel Basket and Canisters

Basket assembly as shown in BMI Drawing Number 41-4409-0004, Rev. B, as modified by BMI Drawing Number 00-001-376, Rev. A, and fuel canister as shown in BMI Drawing Number 00-001-375, Rev. 0.

The BMI-1 fuel basket, modified to Battelle Memorial Institute Drawing Number 00-001-376, Rev. A, will be used to ship 12 canisters containing 21 Pulstar fuel pins each. The basket modification drawing and the Pulstar fuel pin canisters, Drawing Number 00-001-375, Rev. C, are attached.

(h) BMI-1 Basket Spacer

BMI-1 Cask Basket Spacer for ALRR Converter Fuel; Ames Laboratory Research Reactor, (File Drawing) Number RRM 245, dated 4/3/77.

1.2.2 Operational Features

Operation of the BMI-1 is discussed in Section 1.2.1. That Section and the referenced drawings clearly explain operation of the cask and show all valves, openings, seals, etc.

1.2.3 Contents of Packaging

1.2.3.1 Description of Cask Contents

In accordance with the requirements of § 71.22(b) of 10-CFR-71-Subpart B, the materials planned for shipment in the BMI-1 cask are described as follows.

(1) Radioactive Constituents - Identification and Maximum Radioactivity

(a) Shipments by Any Transport Vehicle (Except Aircraft) Assigned for Sole Use. The radioactive contents of the cask may include any radionuclides(s) classified according to the transport grouping in Appendix C of 10-CFR-71. Quantities (in curies) of the respective radionuclides may be equal to or less than any of the following group limits:

Transport Group*	Quantity (in curies)
I	1,000
II	8,120
General Mixed fission products	Unlimited**
III	4,960
IV	11,070
V	8,120
VI and VII	800,000

* As defined in § 173.390 of 49 CFR and Appendix C of 10-CFR-71.

** Limit will be imposed by dose-rate limits specified in § 173.393 (i) of 49 CFR.

Also, 40,000 curies of Co-60, as licensed in Amendment 71-3, License Number SNM-7, Docket Number 70-8, July 17, 1969, or equivalent sources of nonfissile isotopes having gamma or Bremsstrahlung emission energies less than 1.33 Mev may be shipped in the modified BMI-1 cask with the copper basket or other additional internal shielding.

(b) Shipments by Commercial, Contract, Governmental, and Private Carriers. The radioactive contents of the cask may include any radionuclide(s) classified according to the transport grouping in Appendix C of 10-CFR-71. Quantities (in curies) of the respective radionuclides may be equal to or less than any one of the following group limits:

Transport Group*	Quantity (in curies)
I	1,000
II	2,520
General mixed fission products	Unlimited**
III	1,540
IV	3,440
V	5,000
IV and VII	800,000

(2) Identification and Maximum Quantities of Fissile Constituents

(a) Without Leakproof Inner Container. Fissile constituents planned for shipment in the cask without the leakproof inner container along with respective quantities are as follows:

U-233 . . . . 280 grams
Pu-239. . . . . 280 grams
U-235 . . . . 500 grams

---

* As defined in § 173.390 of 49 CFR and Appendix C of 10-CFR-71.

** Limit will be imposed by dose-rate limits specified in § 173.393 (i) of 49 CFR.

(b) With Leakproof Inner Container. Fissile constituents planned for shipment in the cask with the leakproof inner container along with respective quantities are as follows:

U-233 . . . . 480 grams
Pu-239. . . . . 480 grams
U-235 . . . . 800 grams

(3) Chemical and Physical Form

Radioactive and fissile radioactive materials of the following chemical and physical forms may be shipped in the BMI-1 cask:

(a) Special form, as defined in § 71.4(0) of 10-CFR-Part 71.

(b) Normal form, providing that the materials are solid and are securely confined in the leakproof inner container, Drawing 00-000-421, Rev. C., during all normal and accident conditions.

(c) Normal form providing that all materials are packaged and securely confined in the cask cavity. Normal form shall be defined as solid material nonpowder that must remain solid up to 500 F. Only special form materials may be shipped in the cask with water coolant.

(4) Extent of Reflection, Neutron Absorbers, and H/X Atomic Ratios

(a) Without Inner Container. Reflection, absorption, and atomic characteristics of the package contents without the inner container are summarized as follows:

Extent of reflection . . . . . Maximum reflection
Nonfissile neutron
absorbers present. . . . . . None assumed (although various types would be present)

Atomic ratio of moderator to fissile constituents*:

Isotope	H/X
U-233	450
U-235	500
Pu-239	800

(b) With Inner Container. Reflection, absorption, and atomic characteristics of the package contents with the inner container are summarized as follows:

Extent of reflection . . . . . Maximum reflection
Nonfissile neutron
absorbers present. . . . . . Not assumed (although various types would be present)

Atomic ratio of moderator to fissile constituents*:

Isotope	H/X
U-233	20
U-235	20
Pu-239	20

(5) Maximum Weight

The maximum weight of the package contents is 1,800 pounds.

(6) Maximum Amount of Decay Heat

A decay heat load of 1.5 kw is the maximum analyzed for the package contents.

1.2.3.2 Type and Form of Contents Material

(a) BRR/MTR Type Fuel Elements

Intact irradiated MTR or BRR fuel assemblies containing not more than 200 grams U-235 per assembly prior to irradiation. Uranium may be enriched to a maximum 93 w/o in the U-235 isotope. Active fuel length shall be 25 inches.

This report presents a safeguards evaluation of the design and proposed uses of a shielded cask for transporting irradiated fuel assemblies from the Battelle Research Reactor to the Idaho Falls Chemical Processing Plant. The shipment of irradiated fuel is to be made by truck-trailer according to regular commercial conditions and regulations.

---

* Most reactive H/A (Reference 2).

The Texas A&M University requests a special permit to make shipments of MTR reactor fuel in the BMI-1 Shipping Cask (Number SP5957). This request involves the shipment of 23 partially irradiated and 13 unirradiated elements from the Texas A&M Nuclear Science Center to the University of Virginia.

The BMI-1 fuel basket has been modified according to Battelle Memorial Institute Drawing Number 00-000-236, Rev. A, (attached) to individually support 12 MTR fuel elements in the BMI-1 cask.

(b) Enrico Fermi Fuel Elements

Intact irradiated Enrico Fermi Core. A fuel assembly containing not more than 4.77 kgs U-235 prior to irradiation. Uranium may be enriched to 25.6 w/o in the U-235 isotope.

This report presents an evaluation of the proposed use of the BMI-1 spent fuel shipping cask to transport one Enrico Fermi Atomic Power Plant core-A fuel subassembly per trip from the Enrico Fermi plant located near Monroe, Michigan, to the Battelle Nuclear Center near Columbus, Ohio, and then to the Nuclear Fuels Services reprocessing plant near West Valley, New York. The BMI-1 cask was approved in July, 1964, and given License Number SNM 807 (Docket Number 70-813) for use in shipping 24 spent BRR fuel elements per trip to SRL. Shipment in this cask of one Fermi fuel subassembly, removed from the reactor 10 days prior to shipment, requires a different fuel element basket and basket support inside the cask. Enclosed Drawing Number 0049D, Rev. 5/12/66, provides a description and details of the proposed modifications. The main part of this modification is a copper casting which provides mechanical support, additional shielding, and a good thermal path for the removal of decay heat from the subassembly. There are no other cask modifications necessary.

The analysis given in this report is based on shipment of fuel elements with the maximum fuel burnup expected during the program, about 1.6 a/o of the uranium. Initial shipments will involve fuel elements with burnups of about 0.2 a/o. Because of the nature of the reactor power cycle, the maximum decay heat from the fuel will be 1.5 kw.

The major problem encountered in development of a method for shipment of the Fermi fuel subassemblies was the loss-of-coolant condition. Without some type of coolant, the fuel subassemblies with 1.6 a/o burnup would reach excessive temperatures. The use of fine copper shot as a heat transfer medium in the cask, in conjunction with water, has been demonstrated as a reliable means of preventing excessive fuel temperatures if the water is accidentally lost from the cask.

The fuel element will be loaded and unloaded under water employing the normal operating instructions for this cask. In loading, the copper shot will be added in a slurry through a tube into the fuel element cavity. Unloading will be accomplished by removing the stainless steel basket from the shot-filled cavity and then removing the shot from the element.

Operating instructions for the cask handling and loading procedure will be followed to ensure that:

(1) The characteristics of the fuel assemblies as shipped are in compliance with the conditions of the license
(2) External radiation and surface contamination of the cask do not exceed prescribed limits
(3) The cask closures are leak-tight at the maximum operating pressures; the cask and skid are fastened securely to the transporting vehicle
(4) All administrative procedures relating to the recording and transfer of pertinent data are executed.

Details of the assumptions and calculations used in formulating this method of shipping Fermi fuel subassemblies are included in the following sections.

ENRICO FERMI CORE-A FUEL SUBASSEMBLY SPECIFICATIONS

(1) Dimensions: 34 x 2.646 x 2.646 inches
(2) Type: Pin type with 140 active pins
(3) Pin Diameter: 0.156 inch
(4) Cladding: 0.005 inch zirconium
(5) Loading: Total uranium 18.616 kg
(6) Enrichment: 25.6 percent
(7) Reactor Operating Power: 110 megawatt
(8) Peaking Factor: Axial maximum to average 1.23
(9) Estimated Maximum Burnup: 1.6 a/o
(10) Irradiation Time: Alternating 28-day on-off cycles
(11) Cooling Time: 10 days
(12) Void Volume per Element: 1902 cc
(13) Maximum Decay Heat: 1.5 kw (based on alternate 28-day on, 28-day off power cycles).

(c) TRIGA Fuel Elements

Irradiated Triga Type III fuel assemblies containing not more than 40 grams U-235 per assembly prior to irradiation. Uranium may be enriched to a maximum 20 w/o in the U-235 isotope. Active fuel length shall be 15 inches for stainless steel clad assemblies and 14 inches for aluminum clad assemblies.

The University of Arizona requests a special permit to make a Fissile Class III shipments of TRIGA III reactor fuel in the BMI-1 Shipping Cask (Number SP5957). This request involves the shipment of 63 Al-clad elements from the University of Arizona

TABLE 1.1 COMPARISON OF REQUESTED SHIPMENT OF TRIGA FUEL TO PRESENT LICENSE

Item	Conditions of Present Request	Conditions of Present License SNM-7[a]
Contents	38 Irradiated Triga Type III fuel assemblies 8.5 w/o U^{235} Al or SS clad	Various fuels and radiation sources
Maximum decay heat generation per package	112.5 Watts	1,500 Watts maximum
Maximum external dose rate	0.6 mr/hr maximum at 3 ft from the cask external surface	10 mr/hr at 3 ft from external surface of the cask
Criticality	Subcritical (60 assemblies required for criticality - 38 assemblies maximum to be shipped)	All packages subcritical
Contents in maximum impact accident situation	Basket maintains integrity after experiencing 87 G impact force	Maximum impact force of 87 G experienced

(a) BMI License SMN 7, Amendment Number 71-4.

to the University of Utah and the shipment of 87 partially spent stainless steel clad elements from Gulf General Atomics, San Diego, California, to the University of Arizona.

The BMI-1 License SMN 7, Amendment Number 71-4, does not specifically provide for the shipment of TRIGA fuel. Table 1.1 summarizes the pertinent aspects of the shipment of this fuel in the BMI-1 cask and compares this shipment to the present cask license. As shown in Table 1.1, the TRIGA fuel to be shipped has a very low heat and radiation content and the number of elements to be shipped is well below the number required to achieve criticality. The following discussion expands on the areas of criticality, thermal, and structural analysis of this shipment and also provides a shipping procedure for the TRIGA fuel.

The cask has a maximum capacity of 38 TRIGA fuel elements Number 103. The fuel assemblies are stainless steel and aluminum clad, 8.5 percent U^{235} in a zirconium hydride matrix.

(d) Pulstar Fuel Elements

Irradiated Pulstar Zircaloy clad fuel pins containing not more than 31 grams U-235 per pin prior to irradiation. Uranium may be enriched to a maximum 6 w/o in the U-235 isotope. Active fuel length shall be 24 inches.

The State University of New York at Buffalo, requests a special permit to make shipments of Pulstar reactor fuel in the BMI-1 Shipping Cask (Number SP5957). This request involves the shipment of 600 irradiated element pins from the S.U.N.Y. Nuclear Science and Technology Facility to the Idaho Chemical Processing Plant.

(e) S8DR Fuel Elements

Irradiated S8DR fuel elements 0.56 inch OD by 18.7 inches long by 0.010-inch wall thickness of Hastelloy-N. The fuel material is UZrH fully enriched in U-235.

(f) CP-5 Fuel Elements

Intact irradiated CP-5 fuel assemblies containing not more than 176 grams U-235 per assembly prior to irradiation. Uranium may be enriched to a maximum 93 w/o in the U-235 isotope. Active fuel length shall be 28 5 inches.

(g) Fissile Material

Greater than Type A quantities of radioactive material which may include the uranium enriched in the U-235 isotope, U-233, plutonium, as metal, oxides, or compounds which are thermally stable up to 600 F.

(h) Byproduct Material

Greater than Type A quantities of byproduct material in special form.

Greater than Type A quantities of byproduct material in normal form as metal, oxides, or compounds which are thermally stable to 600 F.

(i) EPRI Crack Arrest Capsules

This Safety Analysis Report shows that the EPRI Crack Arrest Capsules shown in Figure 1.1 can be shipped in the BMI-1 cask. The capsules are essentially rectangular parallelepipeds made of aluminum and containing carbon steel specimens. Lesser amounts of other materials are present as shown in Table 1.2.

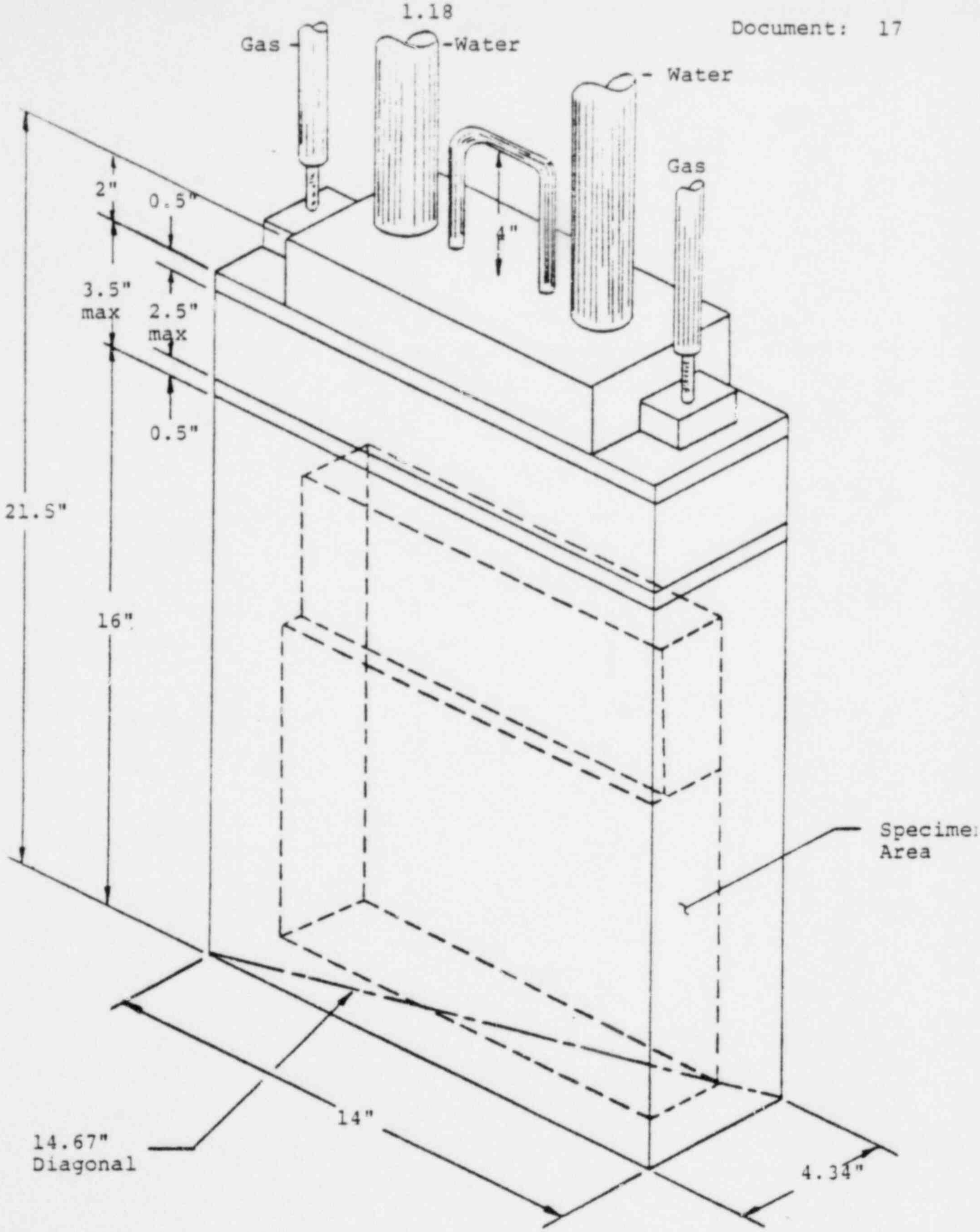

FIGURE 1.1. CRACK ARREST IRRADIATION CAPSULE

TABLE 1.2. MATERIALS IN THE EPRI CRACK ARREST CAPSULES

Material	Component	Weight, lb
Aluminum	Capsule walls Piping	68 5
Carbon Steel	Specimens	123
Stainless Steel (Type 304 and 347)	Seal Plugs, T/C & Heater Sheath	10
Constantan Wire	Thermocouples	~1
Magnesium Oxide	T/C Insulation	6
Nickel	Heaters	~2
Inconel	Heaters	~2
U^{238}	Fission Monitor	36 mg
Np^{237}	Fission Monitor	60 mg

1.3 Appendix

1.3.1 References

(1) Packaging of Radioactive Material for Transport and Transportation of Radioactive Material Under Certain Conditions; U.S. Nuclear Regulatory Commission, Title 10, Chapter 1, Part 71, June 30, 1978.

(2) Paxton, H. C., et al, "Critical Dimensions of Systems Containing U-235, Pu-239, and U-233", USAEC, TID 7028 (1964).

1.3.2 Drawings

The drawings of the cask, skid, and the various canisters and baskets follow.

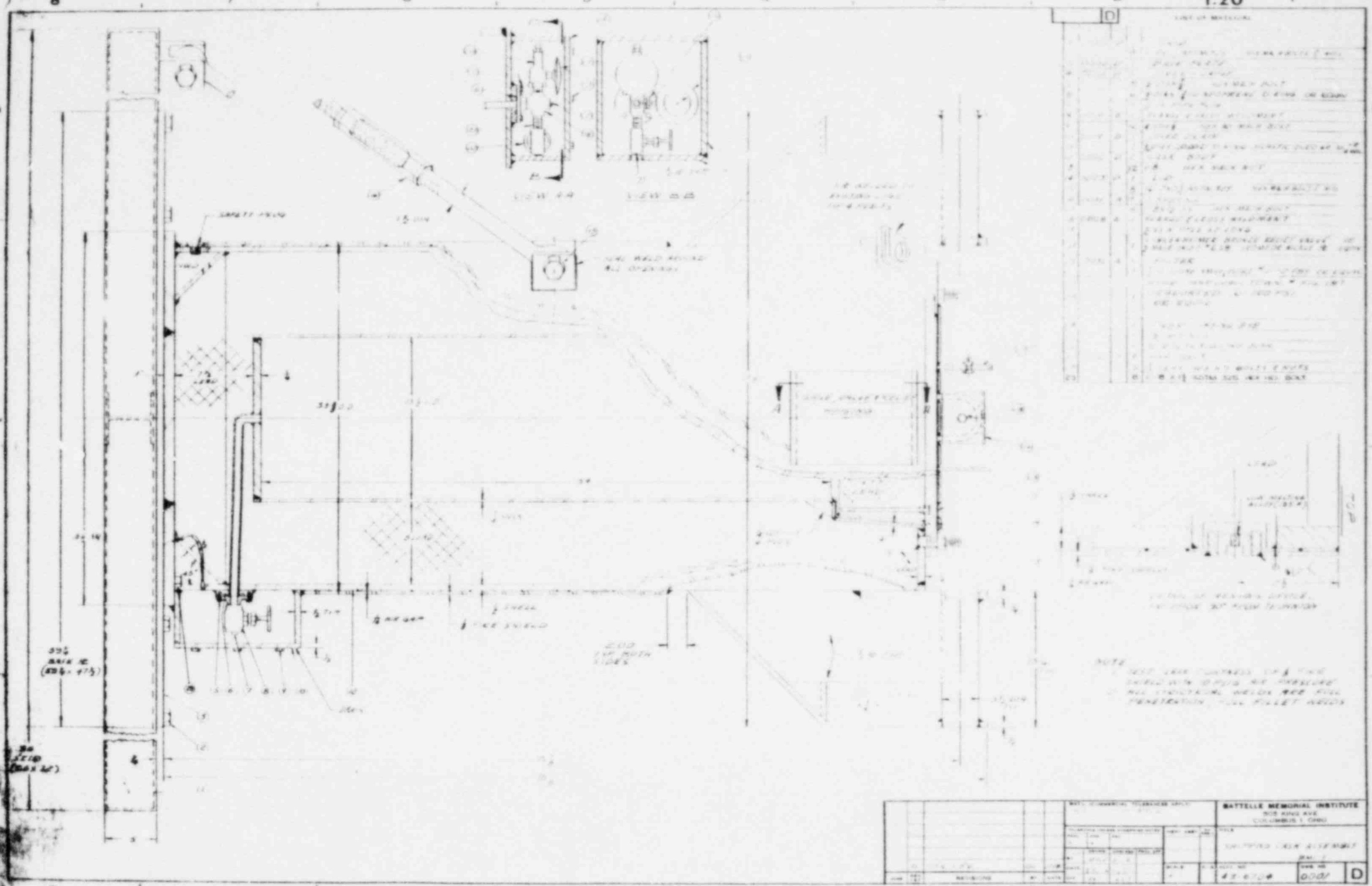
VIEW A-A
VIEW B-B
SAFETY PLUG
TOP
NOTE
BATTELLE MEMORIAL INSTITUTE
505 KING AVE
COLUMBUS 1, OHIO
0001
D

1.20 A

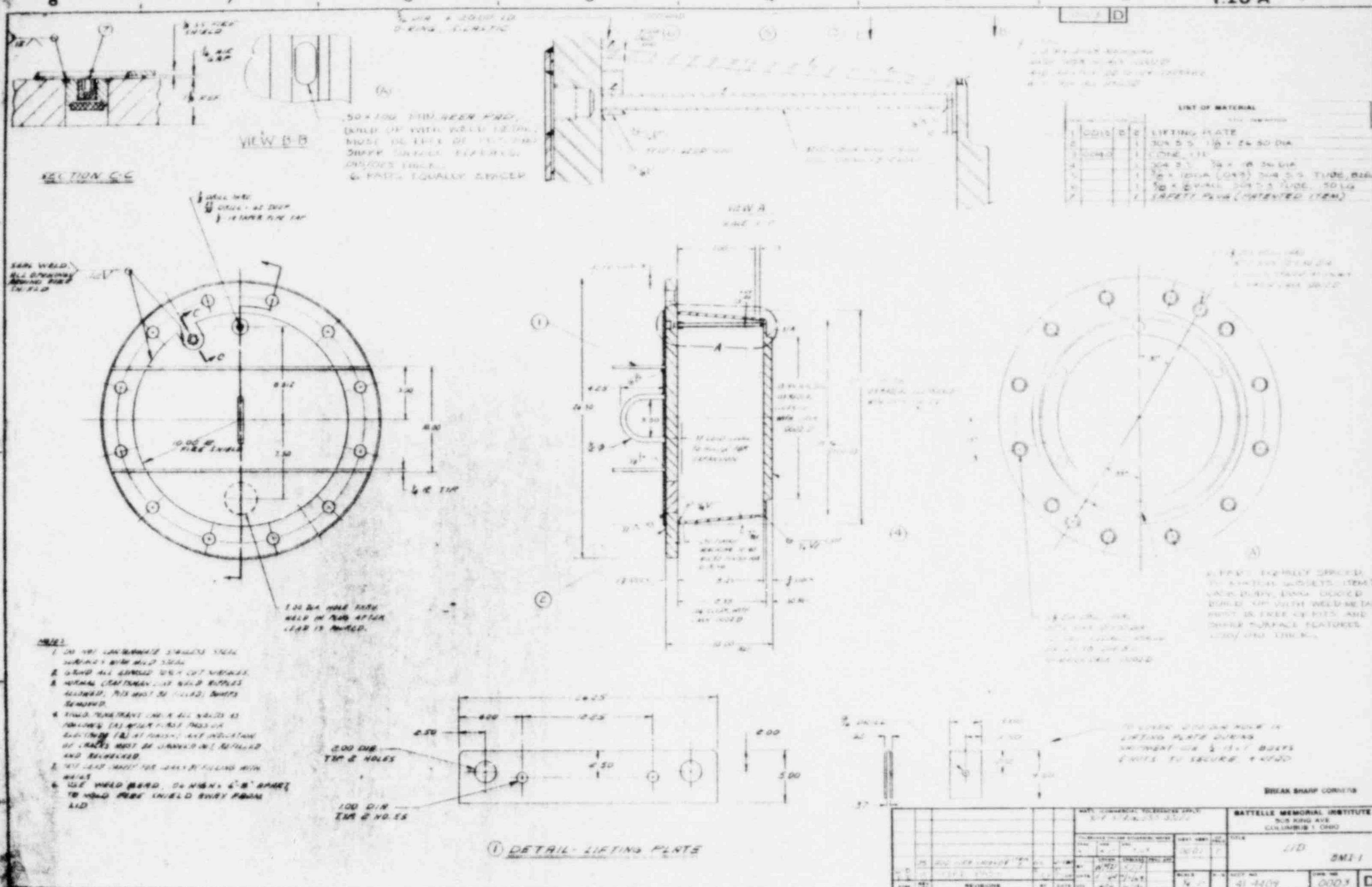
SECTION C-C
VIEW B-B
VIEW A
LIST OF MATERIAL
1 | 0013 | D | 2 | LIFTING PLATE
2 | | | 1 | 304 S.S. 1 5/8 × 26.50 DIA
3 | 0040 | | 1 | CONE (1)
4 | | | 1 | 304 S.S.
5 | | | 1 | 304 S.S. TUBE
6 | | | 1 | 304 S.S. TUBE, 50 LG
7 | | | 2 | SAFETY PLUG (PATENTED ITEM)
SEAL WELD ALL AROUND
6 PADS EQUALLY SPACED
1.00 DIA HOLE. SEAL WELD IN PLUG AFTER LEAD IS POURED.
NOTES:
1. DO NOT CONTAMINATE STAINLESS STEEL SURFACES WITH MILD STEEL.
2. GRIND ALL EXPOSED TORCH CUT SURFACES.
3. NORMAL CRAFTSMANLIKE WELD RIPPLES ALLOWED; THIS MUST BE FILLED; BURRS REMOVED.
4. LIQUID PENETRANT CHECK ALL WELDS AS FOLLOWS: (A) AFTER FIRST PASS OR ELECTRODE (B) AT FINISH; ANY INDICATION OF CRACKS MUST BE GROUND OUT, REFILLED AND RECHECKED.
5. TEST LEAD CAVITY FOR LEAKS BY FILLING WITH WATER.
6. USE WELD BEAD, 04 HIGH × 6"-8" APART TO HOLD PROBE SHIELD AWAY FROM LID.
2.00 DIA TYP 2 HOLES
1.00 DIA TYP 2 HOLES
(1) DETAIL - LIFTING PLATE
BREAK SHARP CORNERS
BATTELLE MEMORIAL INSTITUTE
505 KING AVE
COLUMBUS 1, OHIO
TITLE
LID
BMI-1
41-4409
0003
D

LIST OF MATERIAL					
ITEM	DWG. NO.	SIZE	NO. REQ'D	TITLE - DESCRIPTION
1	420041	A	1	BODY PLUG
2	420042	A	1	PLATE
3	[illegible]	A	1	PLUG

420040 **B**

1.21

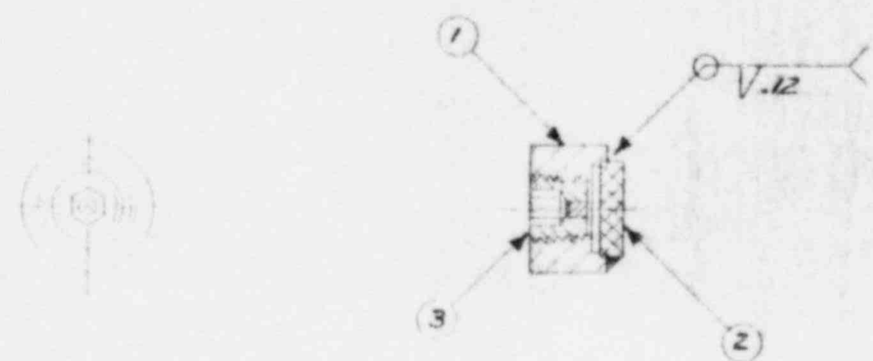

NOTES:
1. PATENTED ITEM FURNISHED BY THE EDWARD [illegible] COLUMBUS, OHIO
2. REMOVE ITEM 3 BEFORE WELDING

BATTELLE MEMORIAL INSTITUTE

SAFETY PLUG ASSEMBLY

B

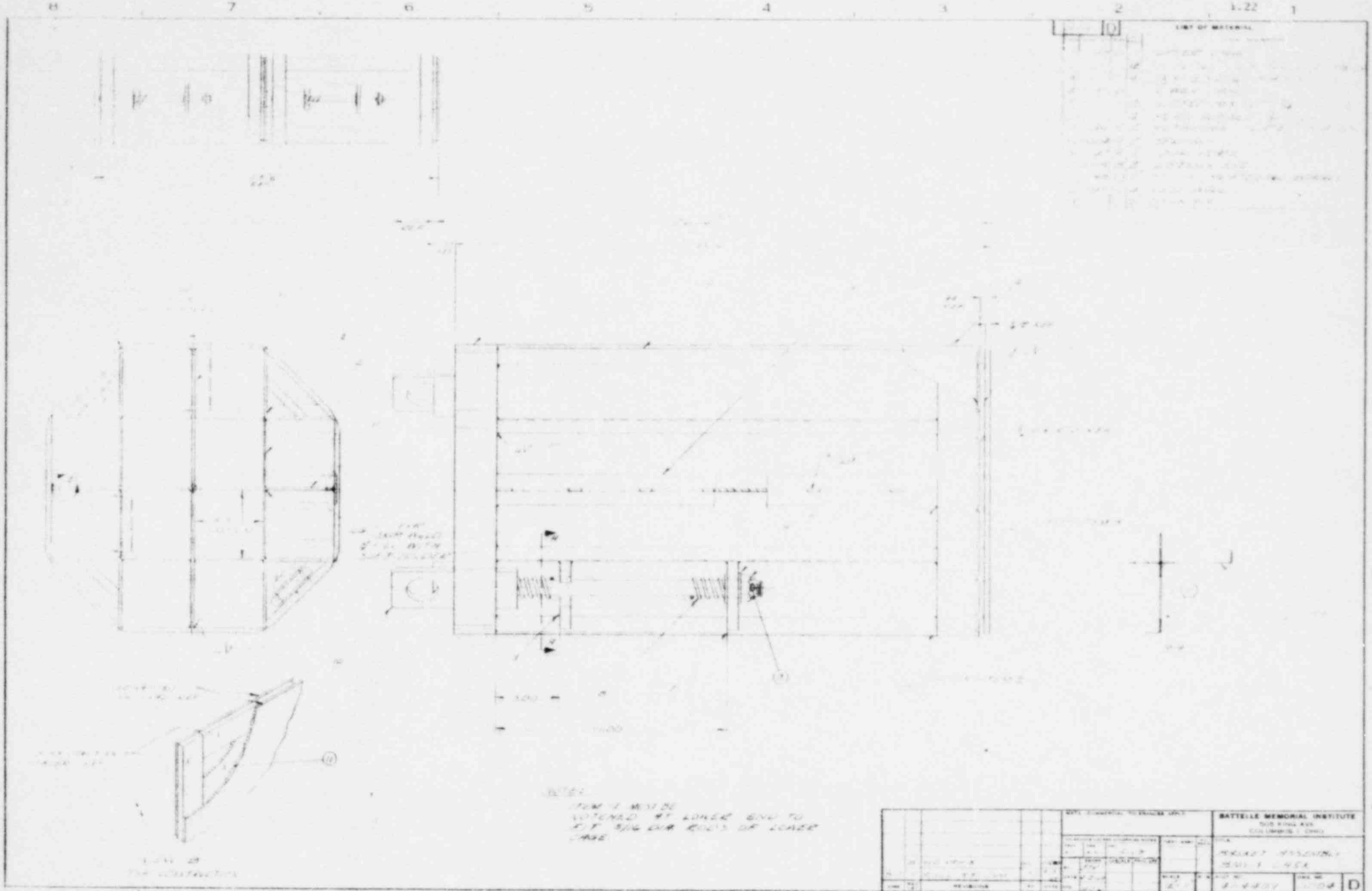
1.22
LIST OF MATERIAL
BATTELLE MEMORIAL INSTITUTE
505 KING AVE
COLUMBUS 1, OHIO
D

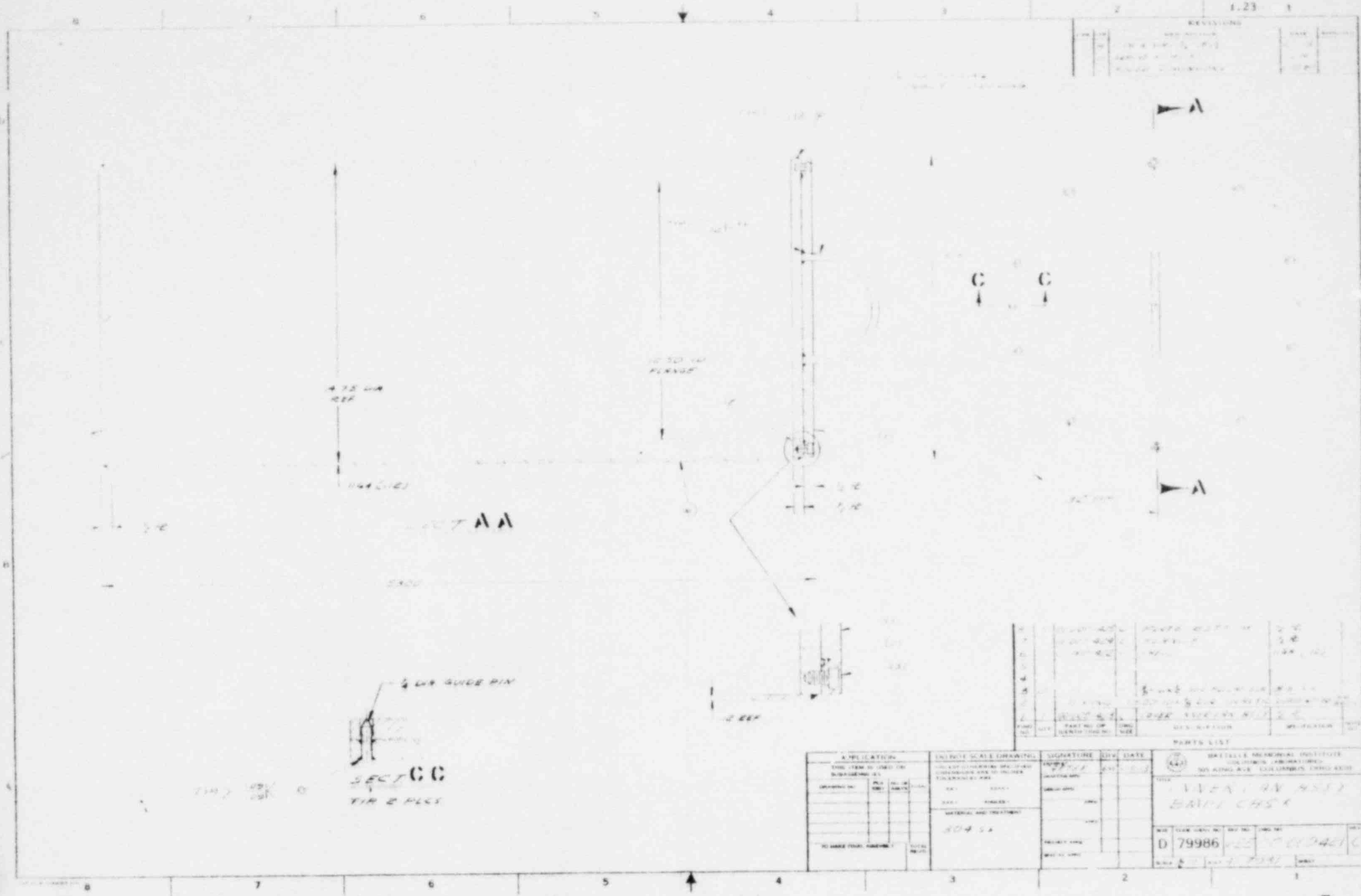
1.23
REVISIONS
10.50 DIA
FLANGE
4.75 DIA
REF
SECT AA
¼ DIA GUIDE PIN
SECT CC
TYP 2 PLCS
PARTS LIST
DESCRIPTION
APPLICATION
DO NOT SCALE DRAWING
SIGNATURE
DATE
304 SS
BATTELLE MEMORIAL INSTITUTE
COLUMBUS LABORATORIES
505 KING AVE COLUMBUS OHIO 43201
D
79986

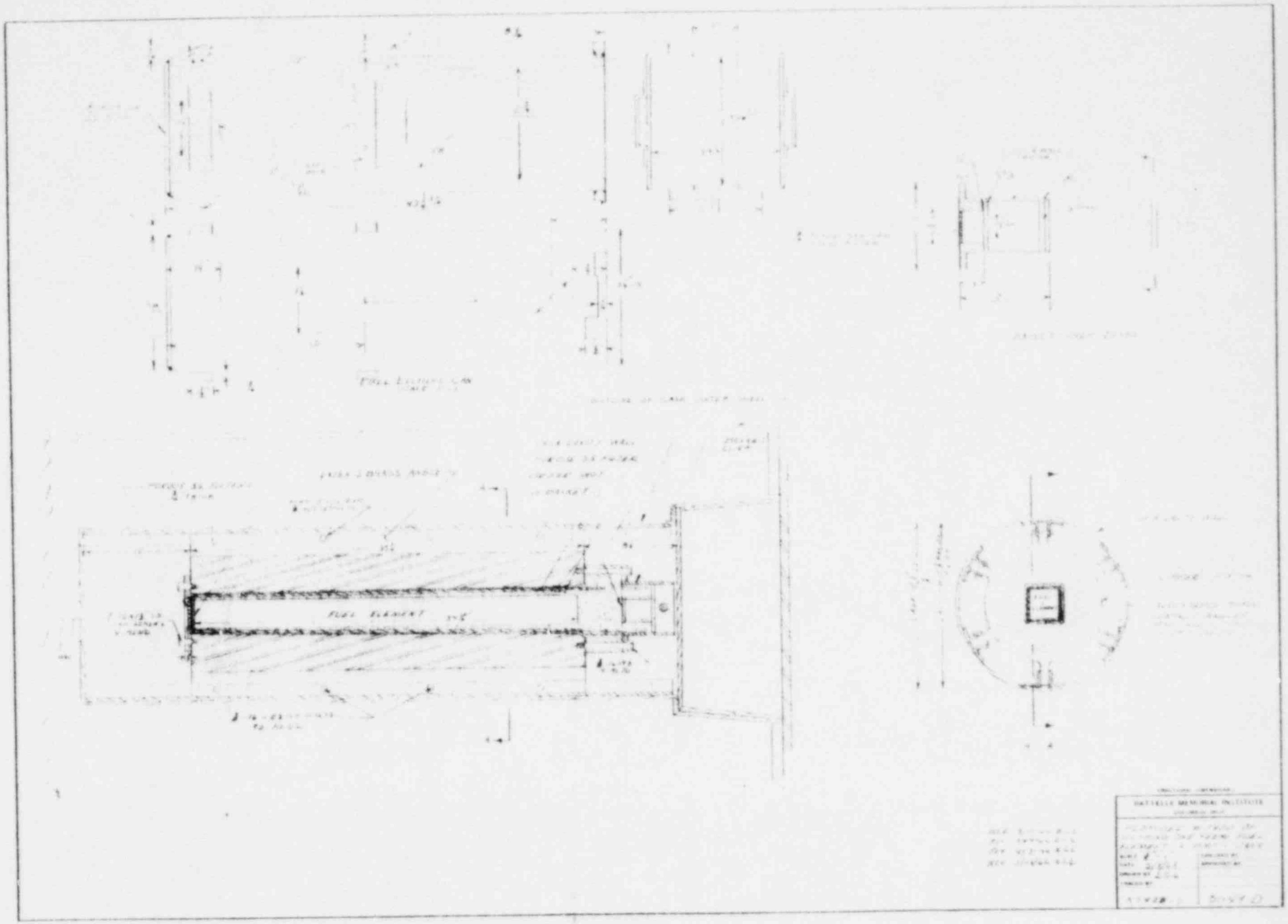
FUEL ELEMENT
BATTELLE MEMORIAL INSTITUTE

1.26

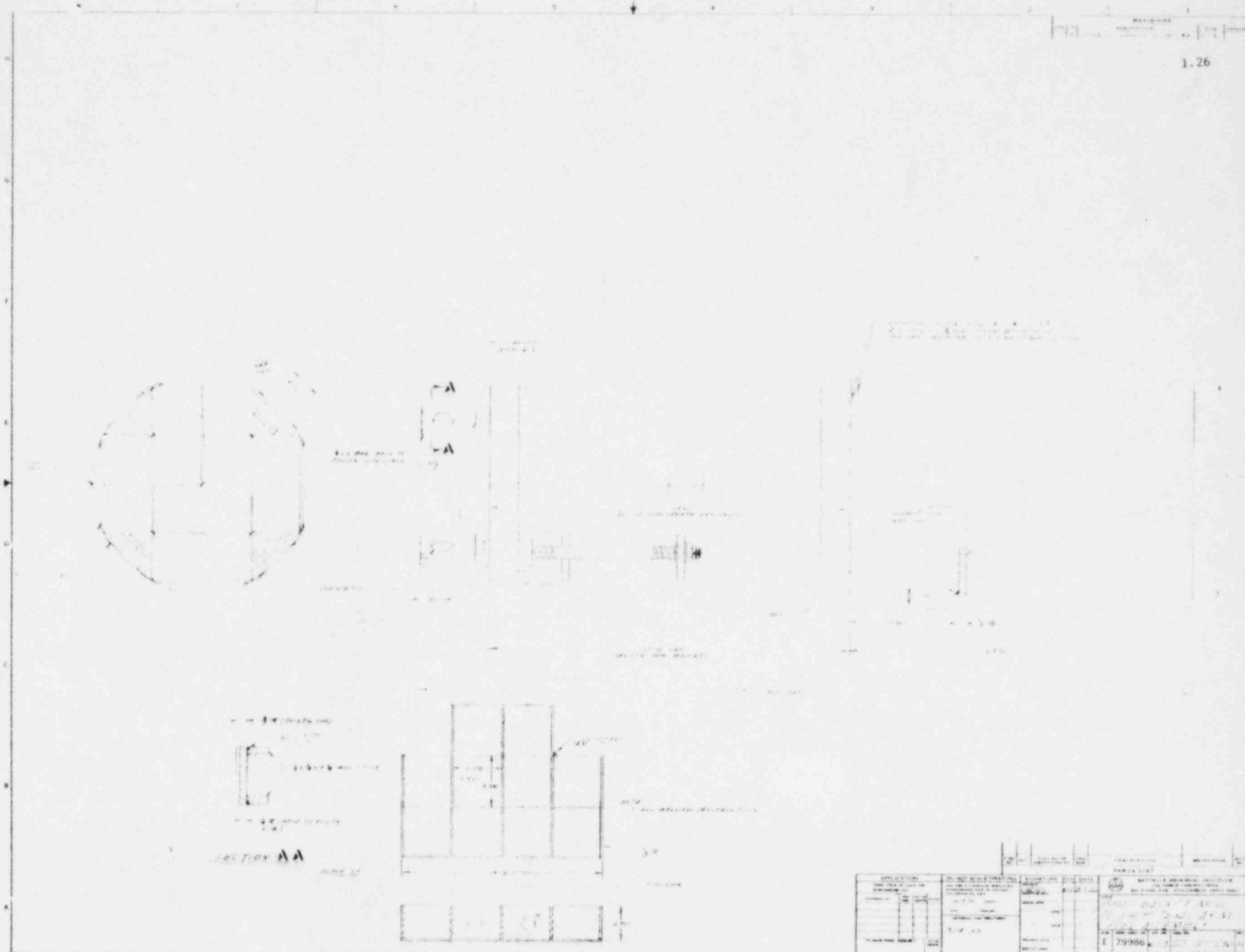


1.27
SECTION AA
Battelle
GASKET
E
79986

REVISIONS			
LTR	DESCRIPTION	DATE	APPROVED
A	ADD REF STORAGE AT TOP	5-4-73	

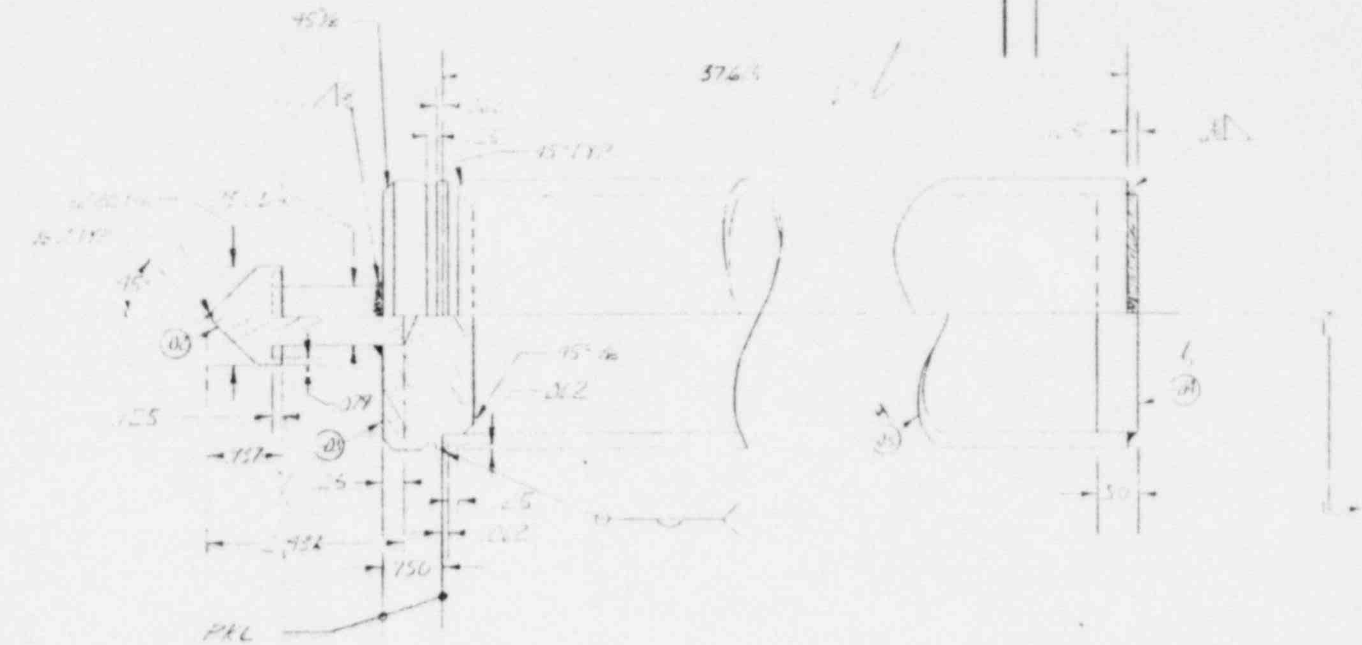

- NOTE -
-03 TO SLIP FIT -04

QTY REQD	PART OR IDENTIFYING NO	NOMENCLATURE OR DESCRIPTION	CODE IDENT	MATERIAL	DATA SPECIFICATIONS SIZES NOTES VENDORS	ITEM NO.
1	05	[illegible]		MS	[illegible]	005
1	04	TUBE		MS	[illegible]	004
1	03	LID		MS	[illegible]	003
1	02	[illegible]		MS	[illegible]	002
	01	ASSY				001

LIST OF MATERIALS OR PARTS LIST

UNLESS OTHERWISE SPECIFIED
DIMENSIONS ARE IN INCHES
TOLERANCES ON
DECIMALS ANGLES FRACTIONS
XX = ± .03 ± 30' ± 1/32
.XXX = ± .010
HOLES NOTED "DRILL"
.013 THRU .040 + .001 - .001
.041 THRU .130 + .002 - .001
.131 THRU .229 + .003 - .001
.230 THRU .500 + .004 - .001
.501 THRU .750 + .005 - .001
.751 THRU 1.000 + .007 - .001
1.001 THRU 2.000 + .010 - .001
DO NOT SCALE PRINT

DR BY
CHK BY
APPROVED BY

ATOMICS INTERNATIONAL
A Division of North American Rockwell
CANOGA PARK, CALIFORNIA

SBDC
STORAGE CAN

CODE IDENT NO 09974 | SIZE C | AIHL-SBDC 0017 01

SCALE | SHEET

ITEM	QTY	MODEL	NEXT USING DRAWING
REQD PER END ITEM			

APPLICATION (USAGE) DATA

NOTES UNLESS OTHERWISE SPECIFIED

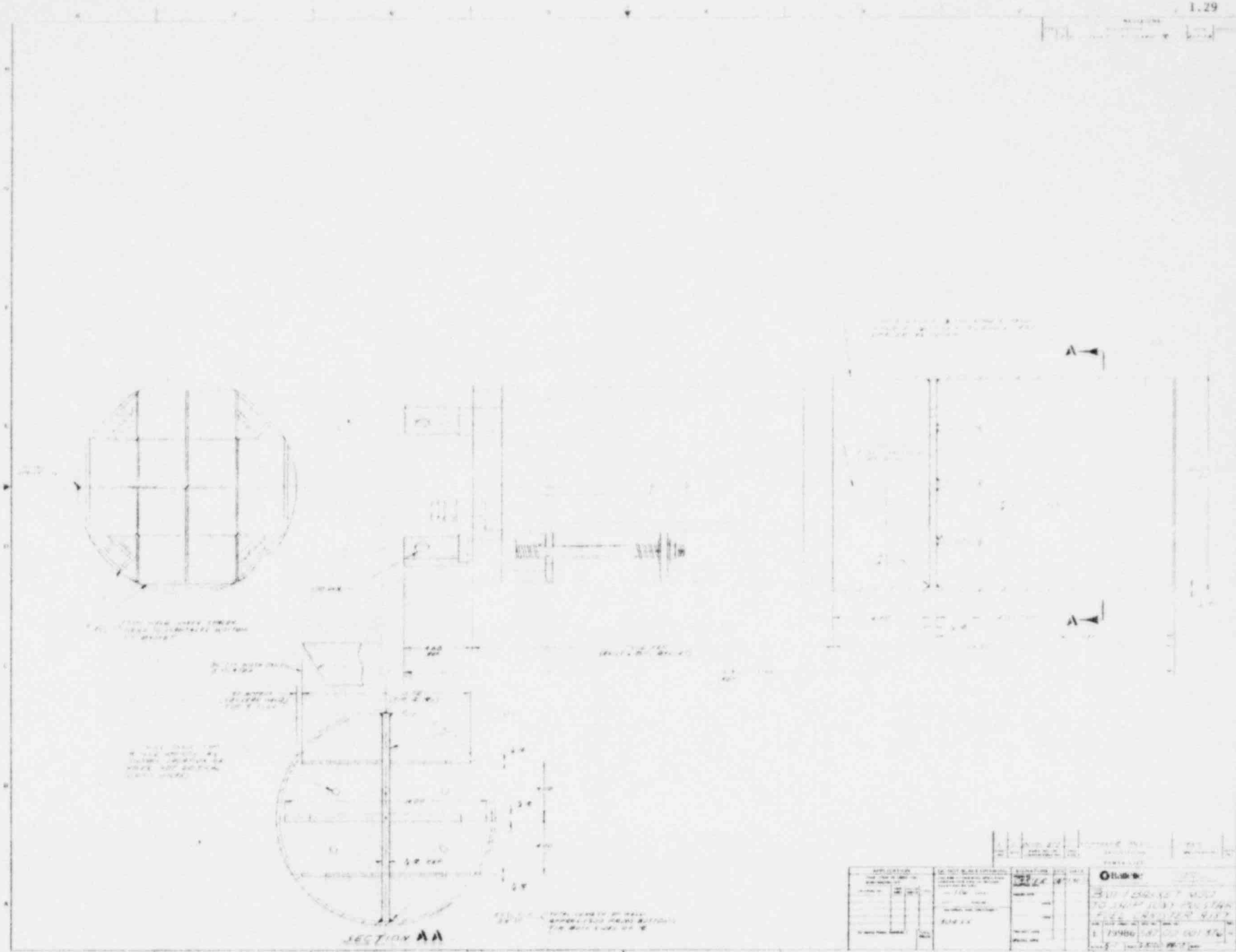
SECTION AA
A
A


1.30
REVISIONS
35.00
(REF ONLY)
PARTS LIST
DESCRIPTION
SPECIFICATION
APPLICATION
DO NOT SCALE DRAWING
SIGNATURE
DIV
DATE
Battelle
TITLE
STORAGE CANISTER
D
79986


1.31
818C199
DESCRIPTION
END CAP
DETAIL G
SEE NOTE 2
REFERENCE ONLY
THIS PRINT IS NOT TO BE USED FOR MANUFACTURING AND WILL BE REPLACED BY REVISED PRINT ONLY ON REQUEST.
FEB 15 1977
WESTINGHOUSE CANADA LIMITED
TITLE
SCALE
818C199

ITEM	DESCRIPTION	MAT'L	REQ'D
	PROJECT TITLE	SCALE	
	AMES LABORATORY RESEARCH REACTOR	DESIGNER	
		DRAFTSMAN	
		DATE	
		FILE NO	

1.3.3 Patent for Safety Plugs

Sept. 9, 1969 E. C. LUSK **3,466,444**

DIFFERENTIALLY VENTED CARRYING CASK FOR RADIOACTIVE MATERIALS

Filed Aug. 24, 1965

FIG. 1

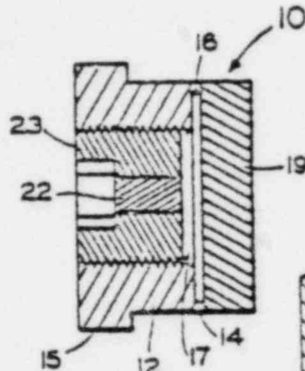

FIG. 2

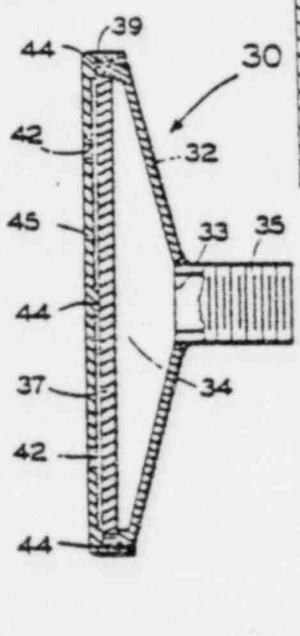

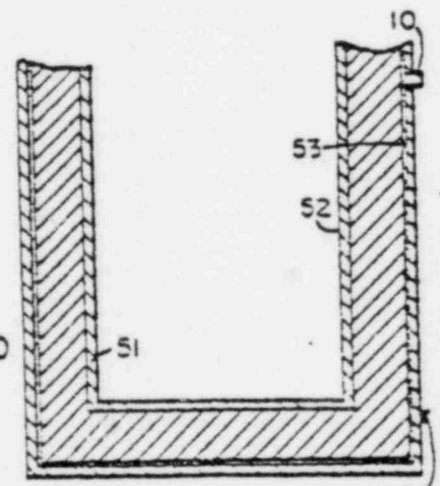

FIG.3

INVENTOR.
ELMER C. LUSK
BY John B. [signature]

REV. A, 3-28-80

United States Patent Office

1.35

3,466,444

Patented Sept. 9, 1969

3,466,444

DIFFERENTIALLY VENTED CARRYING CASK FOR RADIOACTIVE MATERIALS

Elmer C. Lusk, Columbus, Ohio, assignor, by mesne assignments, to Edward Lead Company, Columbus, Ohio, a corporation of Ohio

Filed Aug. 24, 1965, Ser. No. 483,905

Int. Cl. G21f 5/00

U.S. Cl. 250—108 9 Claims

ABSTRACT OF THE DISCLOSURE

There is disclosed a carrying cask structure for radioactive materials, and the cask is characterized by having a fusible solid shielding material disposed interiorly thereof in a substantially filled space, there further being in the cask structure a differential material vent, the vent comprising a porous outlet-defining arrangement having pores of a mean pore size in a vent path from the aforementioned space for the pores to vent gas from that space at a pressure at which the pores are substantially impermeable to molten shielding material in the space and to vent molten shielding material at an increased pressure from the space.

This invention relates to differential material venting devices and more particularly, it relates to a differential vent for the removal of gases from a container while retaining molten liquid within the container. The invention further relates to a differential material venting device used in combination with a lead-lined shipping cask for radioactive materials.

In the transportation of radioactive materials, shipping casks are used which generally comprise an inner container and an outer shell with lead shielding material contained in the annular cavity defined therebetween. The area within the container carries radioactive materials being shipped. In the fabrication of these shipping casks, molten lead is poured within the annular space defined by the inner container and outer shell. Because of the high coefficient of thermal expansion of lead as compared to the container and shell materials, the lead shrinks upon solidification and pulls away from the outer shell. This leaves a void between the outer surface of the lead and the inner surface of the outer shell. Safety requirements dictate that the void volume thus formed must remain to provide room for expansion of the lead in the event of fire in the vicinity of the shipping cask. In fact, sufficient void volume must be allowed to take up the expansion of the lead resulting from temperature rise and transformation to the liquid state at temperatures equivalent to those that would be encountered in a fire. Lack of sufficient space for expansion of lead would result in rupture of the outer shell and loss of shielding material with attendant radiation hazards. The presence of the required void volume in the wall of the shipping cask has caused another significant danger. In some cases, cracks in the outer shell have allowed moisture to enter into the void volume. This is a particular hazard where radioactive materials are loaded into the shipping cask under water. The cracks through which water has been admitted may subsequently become sealed by the action of corrosion, dirt, paint, lead packing or shifting, and by yielding of the metal shell. It has been found that when the shipping cask is exposed to high temperature, the moisture entrapped as described above transforms to steam and produces dangerously high pressures within the lead-filled cavity. Even where the crack remains open, considerable pressure is still generated to a dangerously high level because the area of the opening through which steam may escape is insignificant. Catastrophic explosions of shipping

casks have resulted from transformation of entrapped moisture to vapor as described above. The venting of entrapped steam is made difficult by the likelihood of the presence of molten lead at temperatures of steam formation. Loss of lead must be avoided to minimize the risk of a radiation hazard.

It is therefore an object of this invention to provide a vent for a container which allows gases to escape therefrom but which retains molten liquids therein.

It is a still further object of the present invention to provide a shipping cask for radioactive material having little likelihood of explosion from the presence of entrapped moisture within the container wall and thus increased utility over conventional containers.

It is another object of this invention to provide a vent for the lead-filled walls of shipping casks for radio-active materials.

It is still another object of this invention to provide a vent for the lead-filled wall of shipping casks characterized by the ability to allow vaporized moisture to escape from the void volumes defined therein without allowing molten lead to flow therefrom.

Various other objects and advantages will appear from the description of the embodiments of the invention in the ensuing specification, which is to be read in conjunction with the attached drawings wherein:

FIG. 1 is a vertical sectional view through a vent constructed in accordance with one embodiment of the invention;

FIG. 2 is a vertical sectional view through a vent constructed in accordance with another embodiment of the invention; and,

FIG. 3 is a fragmentary view of a shipping cask having a wall thereof combined with a venting device.

Briefly described, the invention includes within its scope the preferential venting of materials and a differential material venting device therefor comprising a body fitted with a porous metal plate member adapted to vent steam and other gases under pressure but to restrain the flow of molten liquids therethrough.

Referring to FIG. 1, an assembly of a differential material venting device 10 according to this invention is shown comprising a cylindrical body 12 with a centrally located threaded opening 17 extending therethrough. Circumferential shoulder 14 is outwardly disposed from one extremity of cylindrical body 12 to define a shallow opening 16 therein while flanged portion 15 is provided at the opposing extremity of cylindrical body 12. A porous metal member 19 is suitably affixed to the face of circumferential shoulder 14. The dependent threads in opening 17 of cylindrical member 12 are threaded with plug member 23 having a centrally located opening therethrough filled with a material 22 automatically removable at a predetermined temperature above room temperature.

In operation, the assembly is connected into the wall of a container with flanged portion 15 extending outwardly. Gas pressure that develops within the container is vented through porous plate member 19 and the large area defined by space 16. Material 22 is selected so as to be automatically removable at temperatures just below the temperature at which significant vaporization of the liquid is likely to occur within the container.

Material 22 can be a solder having a melting range within the required temperature limits. Bi-metallic snap out disks are equally suitable. In this way, porous metal plate member 19 is protected from possible contaminating influences from without the container during the time that assembly 10 is not in active operation. It should be understood that material 22 is not absolutely essential for the operation of the differential material venting assembly but merely is convenient. In some applications, it will be obvious that water entering the container from without the vent is merely vented back out as steam when elevated temperatures arise.

Assembly of the pressure venting device is relatively simple. Porous metal member is merely welded by convenient means to circumferential shoulder 14. Plug member 23 is tapped by convenient means and the opening extending therethrough fitted with material 22. The threaded exterior of plug 23 engages threads on the interior of opening 17 extending through cylindrical member 12.

Referring to FIG. 2, a pressure venting device 30, also according to this invention, comprises a funnel-shaped body 32 terminating respective in openings 33 and 34. A centrally located vent port 35 communicates with smaller diameter opening 33 in funnel-shaped body 32. Vent port 35 is provided with threads for fixed attachment to dependent threads provided within the wall of a container, thus allowing assembly 30 to communicate with the interior. At the larger diameter opening 34 of funnel-shaped body 32, a porous metal plate member 37 is disposed within recess 39 provided on the inside diameter defined by larger opening 34 of funnel-shaped member 32. A cap 45 is provided for engagement with larger diameter opening 34. Projections 44—44 on the inside face of cap 45 force the porous metal plate 37 to fit snugly into recess 39 while maintaining a suitable spacing of cap 45 from the same. Numerous small diameter openings 42—42 filled with a material automatically removable at a preferred temperature range extend through the face of cap 45 at various locations thereon.

In assembly of the pressure venting device described above, porous metal plate 37 is merely disposed within recess 39 provided within the inside diameter of larger diameter opening 34 defined at one extremity of funnel-shaped body 32. Cap 45 is secured tightly so that projections 44—44 on the inside face thereof engage porous member 37 to secure the same in place on recess 39 and to seal the assembly 30.

The porous metal plate member comprises the key member of the material venting device of this invention. The porous metal member is available commercially with a variety of different pore sizes. Where high pressures or high-liquid heads may be developed, a small pore size is selected. Similarly, for a given pore size, a thicker porous metal member is selected where high metal heads may be encountered. Generally it is advisable to select a pore opening size and thickness of porous metal member to restrain the flow of the contained liquid and allow the passage of gases therethrough. The actual size of the differential material vent depends on the active surface area needed for the porous metal plate. This, in turn, depends on the gas flow capacity of the porous metal plate, the strength of the porous metal plate, the volume of gas estimated to be generated in the container, and the length of time during which gas would be formed. When these factors are known, the surface area required to vent gas can be determined by simple calculation. Where the calculated surface area is large it may be convenient to assemble a plurality of differential material vents for use in the container. The sum of the areas presented by each vent being equal to or greater than the required area. The use of a plurality of vents would also provide an additional safety factor in the event of injury to one of the vents during transit.

In FIG. 3 one of the hereinbefore described devices 10 is represented connected for venting the space 53 between an inner container 51 and an outer shell 52 of a shipping cask 50 for radioactive elements and very satisfactorily includes a porous metal plate member fabricated from stainless steel. For example, for a porous plate member of stainless steel having a thickness of 0.187-inch and a mean pore diameter of 0.0002 inch, molten lead will be restrained at pressures over 42 p.s.i.g. This is equivalent to a metal head of 8 feet. In a cask having a void volume of 1521 in.^{3}, a surface area of 56 in.^{2} in porous stainless steel plate as described above vented the quantity of steam that would be expected to form within the lead-filled wall without achieving pressures in excess of 50 p.s.i.g.

In operation in the lead-filled wall of a shipping cask for radioactive elements, the porous metal plate member can be protected at its outer surface by a material that is automatically removable to open and exit for gases at temperatures slightly below the boiling point of water. Upon encountering conditions such as fire wherein the temperature of the atmosphere surrounding the cask rises rapidly, the material in the exit gas opening is automatically removed thus leaving free openings to communicate with the porous metal plate. As temperature continues to increase, steam begins to form and is vented through the porous metal plate. Further increase of temperature causes the lead to become molten but the molten lead is retained within the wall of the cask by the porous metal plate. Should temperatures in the vicinity of the cask exceed values currently foreseen by safety requirements, it has been found that the differential material vent of this invention will still not cause catastrophic rupture of the outer shell of the container. The higher pressures occassioned by these higher temperatures will merely result in a slow leakage of molten lead through the porous plate member thus relieving the excess pressure caused by expansion of molten lead.

The body of the differential material vent may be made from a variety of materials, though it has been found that components of stainless steel are very satisfactory. In the embodiments of the invention shown, the porous metal member is a disk configuration. It is obvious that any configuration disposed between the contents of the outer shell and an opening entering the atmosphere would be satisfactory.

One advantage of this invention is that a material venting device is provided to exhaust steam or other gases at a safe pressure from a cavity filled with molten liquid.

Still another advantage of this invention is that a material venting device is characterized by a porous metal plate having substantial strength and resistance to breakage in service.

In its application to shipping casks for radioactive elements, the material venting device of this invention provides several significant advantages which make the shipping of radioactive elements less hazardous.

It will be apparent that new and useful means for differential venting of materials have been described. Although several preferred embodiments of the invention have been described, it is apparent that modifications may be made therein by those skilled in the art. Such modifications may be made without departing from the spirit or scope of the invention, as is set forth in the appended claims.

What is claimed is:

1. In a carrying cask for radioactive materials which includes an inner container; an outer shell spaced outwardly from said inner container; and a fusible solid shielding material substantially filling the space between said outer shell and said inner container; the improvement comprising a differential material vent including a porous structure having pores of a mean pore size in a vent passage from said space for said pores to vent gas from said space at a pressure at which said pores are substantially impermeable to molten said shielding material and said pores to vent molten said shielding material at an increased pressure from said space.

2. The carrying cask of claim 1, wherein said fusible solid shielding material is a monolithic casting within said space.

3. The carrying cask of claim 2, wherein said monolithic casting includes lead.

4. The carrying cask of claim 3, wherein said porous structure comprises porous stainless steel.

5. The carrying cask of claim 1, and including thermally sensitive sealing means arranged in said vent passage to seal said space closed and to be automatically displaced to vent said space through said pores after temperature of said thermally sensitive sealing means exceeds a minimum value.

6. The carrying cask of claim 1, wherein a vent member is connected having an opening therein for communicating with said pores and with said space, and said cask is further characterized by including thermally sensitive sealing means arranged to close said vent member opening and to be automatically displaced to vent said space through said vent member opening and through said pores after temperature of said thermally sensitive sealing means exceeds a minimum value.

7. The carrying cask of claim 6, wherein said thermally sensitive sealing means comprises a low-melting range solder which fuses when said minimum temperature is exceeded.

8. The carrying cask of claim 6, wherein said porous structure is arranged having said pores interposed between said space and said vent member opening.

9. The carrying cask of claim 6, wherein said vent member has said opening therein interposed between said space and said pores.

No references cited.

RALPH G. NILSON, Primary Examiner

SAUL ELBAUM, Assistant Examiner

U.S. Cl. X.R.

220—44, 89; 250—106

REV. A, 3-28-80

2. STRUCTURAL EVALUATION

2.1 Structural Design

2.1.1 Discussion

The principal members and systems of the BMI-1 cask are identified and discussed in Section 1.2.1.1.

2.1.2 Design Criteria

The cask was designed to have a positive margin of safety based on the yield strength for all normal conditions and for a positive margin of safety based on the yield strength or ultimate strength for all accident conditions.

2.2 Weights and Center of Gravity

Calculated weights of the BMI-1 cask and skid and the allowable contents weight are presented in Table 2.1. All structural calculations were performed on the basis of the calculated weights. The total measured weight is about 0.3 percent greater than that calculated. This difference is considered neglible and thus the results of the structural analyses based on the calculated weight are considered acceptable.

TABLE 2.1. BMI-1 CASK WEIGHT

Component	Weights, pounds	
	Calculated	Measured
Body	19,200	19,750
Cover	1,200	1,100
Skid	1,400	1,700
Contents (maximum)	1,800	1,110 [(a)]
TOTAL	23,600	23,660

(1) Weight of heaviest basket and contents, the copper basket for the Fermi Fuel Elements.

The center of gravity is assumed at the geometric center of the cask.

2.3 Mechanical Properties of Materials

The cask is constructed entirely of stainless steel plate. The material properties used in the analyses were obtained from MIL-HDBK-5A.[1] In cases where property data were not specified, the values were estimated by referencing to similar properties of the same or similar materials. The ASTM A3´5 bolts specified in the design correspond to the Type 4 fasteners included in MIL-HDBK-5A. The maximum surface temperature of the cask during normal operation is 190 F. At this temperature, the properties of the cask construction materials are essentially unchanged from room-temperature conditions. Therefore, room-temperature properties were used in the analyses. Table 2.2 summarizes the properties of the cask construction materials.

TABLE 2.2 MATERIAL PROPERTIES UTILIZED IN BMI-1 CASK DESIGN

Material	Property	Design Stress, psi
Type 304 stainless steel	Tensile yield stress	30,000
	Tensile ultimate stress	75,000
	Compressive yield stress	35,000
	Shear yield stress	20,000
	Shear ultimate stress	40,000
	Bearing yield stress	50,000
ASTM A325 bolts	Tensile ultimate stress	120,000
	Shear ultimate stress	89,000

(1) References to Section 2, found in Section 2.12.1.

2.4 General Standards for All Packages

2.4.1 Chemical and Galvanic Reactions

The materials used--stainless steel and lead--do not react with each other in such a way as to cause deleterious amounts of corrosion products.

2.4.2 Positive Closure

Closure of the cask is accomplished by 12 Type 304 stainless steel studs. These studs provide positive closure of the cask during normal shipping conditions. The closure, with respect to accident conditions, is analyzed in a subsequent section.

2.4.3 Lifting Device

This section demonstrates the safety of the lifting devices associated with the package. The adequacy of lifting devices associated with the baskets are presented in Section 2.11.

2.4.3.1 Cask

According to § 72.34(e), the cask-lifting must be capable of lifting 6 times the weight of the cask without exceeding the yield strength of the materials in the device.

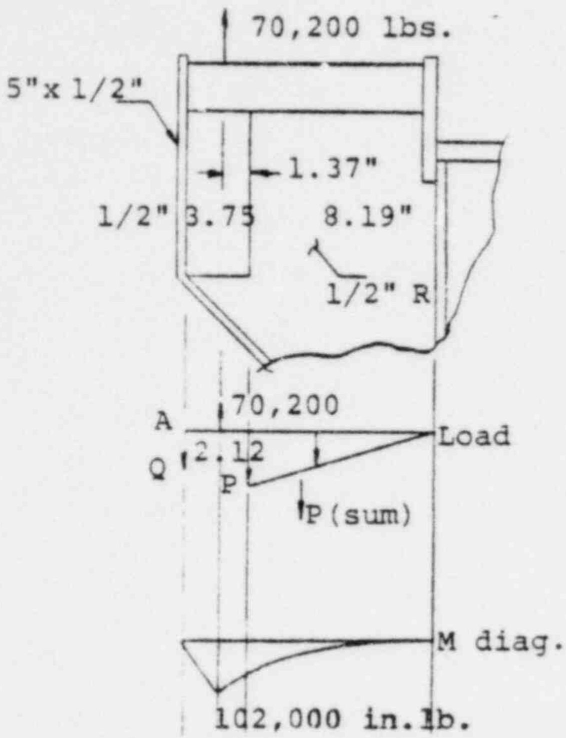

$$\Sigma M_A = 0 = 70,200(2.12) - P(2.12 + 1.87 + 8.19/3)$$

$$P = \frac{70,200(2.12)}{6.72} = 22,200\#$$

$$\Sigma V = 9 = 70,200 - 22,200 - Q$$
$$Q = 48,000\#$$

$$P(1/2)(8.14) = 22,200\#$$

$$P = 5420\#/m.$$

The tensile stress in the 5 x 1/2 inch plate is:

$$\sigma = \frac{P}{A} = \frac{48,000}{5 \times 0.5} = 19,200 \text{ psi} \quad .$$

The maximum tensile stress in the web is:

$$\sigma = \frac{P}{A} = \frac{5420}{1 \times 0.5} = 10,850 \text{ psi} \quad .$$

The bending stress in the 3.5-inch bar is:

$$\sigma = \frac{M}{S} = \frac{102,000}{4.22} = 26,600 \text{ psi} < 30,000 \text{ psi yield} \quad .$$

The average shear stress in the 3.5 inch bar is:

$$\tau = \frac{P}{A} = \frac{48,000(4)}{\pi(3.5)^2} = 5,000 \text{ psi} < 15,000 \text{ psi shear yield} \quad .$$

Checking attachment to the cask, the maximum bending stress is 1,000 psi and the average shear stress is 1,950 psi, as shown below.

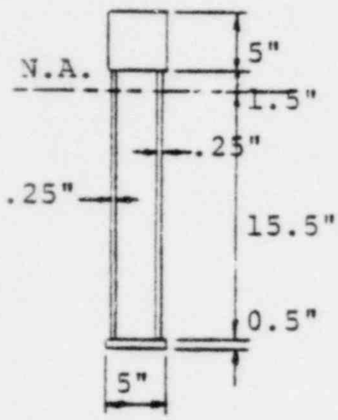

$I_{N.A.} = 11,278$ in.

$A = 36^{11}$

$$\sigma = \frac{Mc}{I} = \frac{(70,200)(8.19 + 1.87)(16)}{11,278} = 1000 \text{ psi}$$

$$\tau_{avg} = \frac{P}{A} = \frac{70,200}{36} = 1950 \text{ psi}$$

Cross-section
of Trunnion
of Cask Surface

2.4.3.2 Cover

To meet the requirements of ∮ 72.34 (f), the lid-lifting device must be capable of lifting six times the weight of the lid and contents without exceeding the yield strength of the materials in the device.

The lifting device must be capable of lifting 6(1,690) = 10,130 pounds. The following calculations show that the device is adequate to lift the lid. It should be stated that the attachment plates have purposely been made as thin as possible for lifting purposes so that in the event of a top impact, they will collapse and not penetrate the lid.

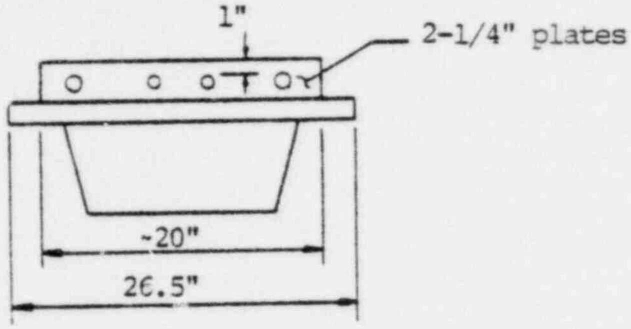

Force to shear out holes

$$F = 4(15{,}000)(2)(1x1/4) = 30{,}000 \text{ lbs} - \text{O.K. if only 2 holes are used}$$

Tensile stress in weld

$$\sigma = \frac{P}{A} = \frac{10{,}130}{2(20x1/4)} = 1013 \text{ psi}$$

The alternate lifting device (U-bar) was tested at 3 times the cover weight to show adequacy. The test report is presented in Section 2.12.2. The lifting device on the cover and the cover closure is not designed to permit its use as a cask-lifting device. Therefore, a U-plate, which bolts onto the device, is provided to prevent inadvertent use of the component as a cask-lifting device.

2.4.3.3 Failure of the Lifting Device Would not Impair Containment or Shielding

Impairment of containment or shielding due to failure of the lifting device would be less severe than in the case of the 30 foot drop which is considered in a subsequent section.

2.4.4 Tiedown Devices

2.4.4.1 No Yielding with 10G Longitudinal, 5G Transverse, and 2G Vertical Forces

The design analysis assumes that the cask and skid act as a single unit. Therefore, the four tiedown ears must withstand the applicable 10G, 5G, and 2G forces applied to combined weight of the cask and skid. As is customary, it was assumed that the cask is adequately blocked so that tipping, rather than sliding or tipping and skidding, is impeded. The critical tipping orientation is when the 10G force is acting in the direction of the 72 inch dimension of the cask skid, i.e., the tipping axis is 36 inches from the vertical axis of the cask, Figure 2.1.

For purposes of analysis, it was assumed that the cask will tip on the assumed tipping axis, Figure 2.1, rather than the side of the cask. The assumed axis was taken, however, at the same distance from the center of the cask as the true tipping axis, i.e., 36 inches. This is a conservative assumption since the skid provides greater stability for tipping from a diagonal force (11.18 G) than for a force directed perpendicular to the long side of the cask skid.

Direct solution of the tiedown forces is not possible because the system is statically indeterminate. It was, therefore, assumed that the force in each tiedown ear is proportional to the distance of the ear from the vertical plane through the tipping axis. Thus:

$$\frac{F_1}{L_1} = \frac{F_2}{L_2} = \frac{F_3}{L_3} = \frac{F_4}{L_4} \quad ,$$

where:

$$L_1 = t + r \left[\cos(\theta - \psi)\right]$$

$$L_2 = t - r \left[\cos(\theta + \psi)\right]$$

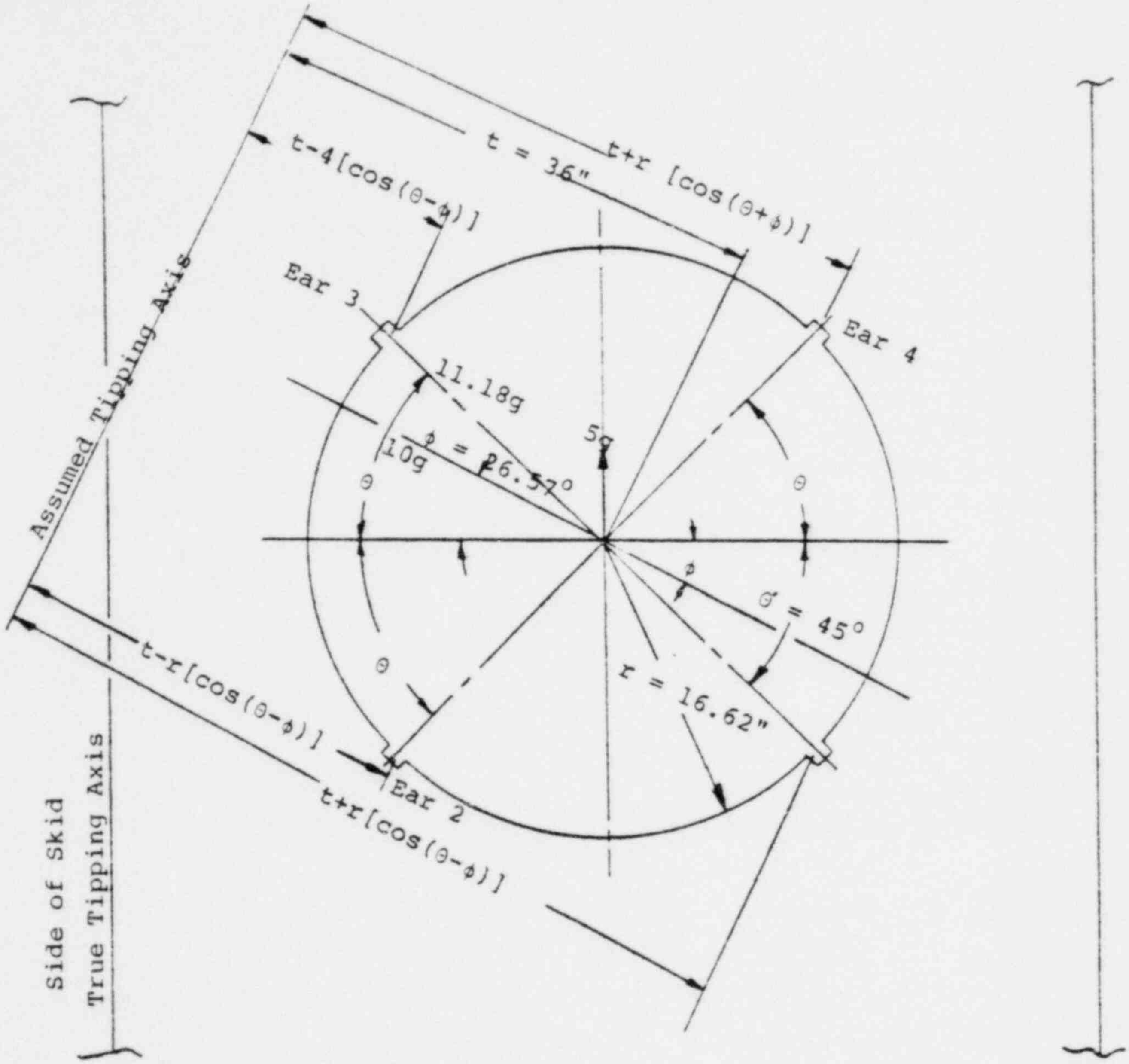

FIGURE 2.1. CRITICAL TIPPING ORIENTATION

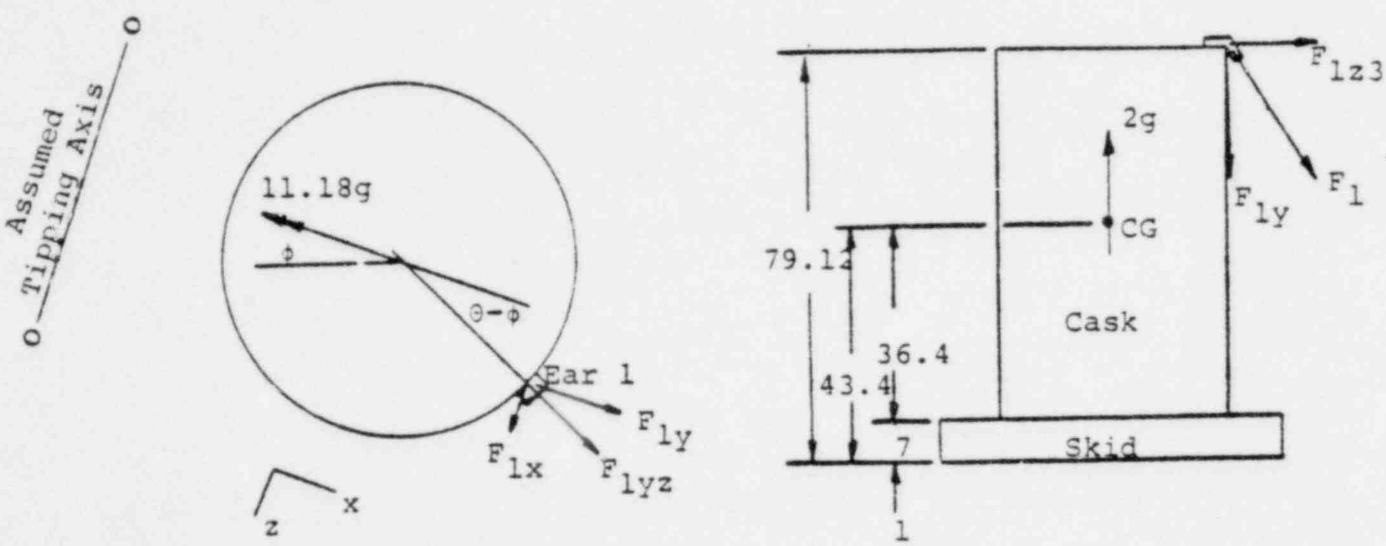

FIGURE 2.2. TYPICAL FORCE SYSTEM ON TIEDOWNS

$$L_3 = t - r \left[\cos(\theta - \psi) \right]$$

$$L_4 = t + r \left[\cos(\theta + \psi) \right]$$

t = 36 inches

r = 16.62 inches

θ = 45 degrees

= 26.57 degrees.

Substituting and solving for the forces in terms of F_1 yields:

$$F_2 = 0.5945\ F_1$$

$$F_3 = 0.3910\ F_1$$

$$F_4 = 0.7975\ F_1 \quad .$$

The components of each force were then determined. The force vector coordinate axes and the vectors for the force on a typical ear are shown in Figure 2.2. The force vectors which will produce a moment about the tipping axis are the x and y components. They are:

$$F_{1x} = F_1 \sin\alpha \cos(\theta - \psi)$$

$$F_{1y} = F_1 \cos\alpha$$

$$F_{2x} = F_2 \sin\alpha \cos(\theta - \psi)$$

$$F_{2y} = F_2 \cos\alpha$$

$$F_{3x} = F_3 \sin\alpha \cos(\theta - \psi)$$

$$F_{3y} = F_3 \cos\alpha$$

$$F_{4x} = F_4 \sin\alpha \cos(\theta - \psi)$$

$$F_{4y} = F_4 \cos\alpha$$

Then, for α = 35 degrees, the components, in terms of F_1, are:

$$F_{1x} = 0.5440\ F_1$$

$$F_{1y} = 0.8192\ F_1$$

$$F_{2x} = 0.1078\ F_1$$

$$F_{2y} = 0.4865\ F_1$$

$$F_{3x} = 0.2126\ F_1$$

$$F_{3y} = 0.3200\ F_1$$

$$F_{4x} = 0.1448\ F_1$$

$$F_{4y} = 0.6530\ F_1 \quad .$$

Moments can then be summed about the assumed tipping axis to determine the maximum force, F_1, at impending tipping.

$\curvearrowleft$	=	$\curvearrowright$
$(W)\ (11.18\ G)\ (C)$		$(F_{1x})\ (H)$
$(W)\ (2\ G)\ (t)$		$(F_{1y})\ (L_1)$
$(F_{2x})\ (H)$		$(F_{2y})\ (L_2)$
$(F_{3x})\ (H)$		$(F_{3y})\ (L_3)$
		$(F_{4x})\ (H)$
		$(F_{4y})\ (L_4)$

where:

W = 23,600 pounds

C = 43.4 inches (Figure 2.2)

t = 36.0 inches (Figure 2.1)
H = 79.12 inches (Figure 2.2)

and the values for the force components and the lever arms, L_1, L_2, L_3, and L_4 are given above. Solving the above equation yields:

$$F_1 = 110{,}000 \text{ lb} \quad .$$

The ear and cask can fail by:

(1) Tensile failure in the eye
(2) Shear through the eye
(3) Bearing in the eye
(4) Shear bending in the weld between the doubler plate and the original 1-inch-thick ear
(5) Shear bending of the ear in the weld to the cask
(6) Compression of the cask shell
(7) Shear in bolts at the base of the cask.

These are evaluated below.

(a) Tensile Failure in the Eye

The minimum stress area (see sketch below) is:

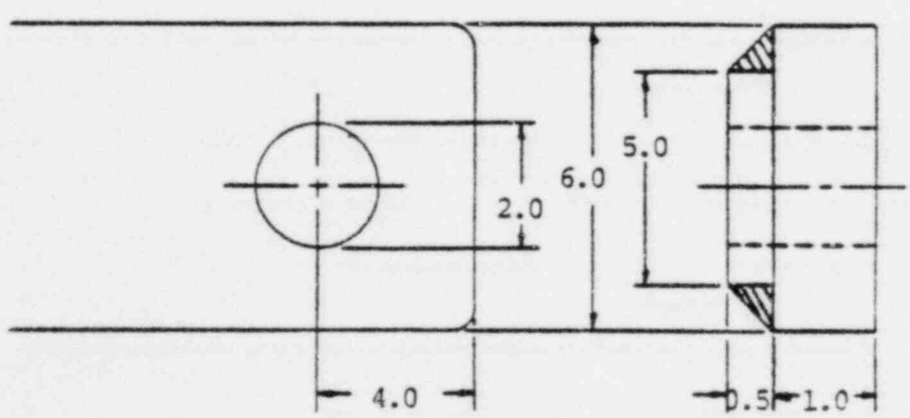

$$A = (6 - 2)(1) + (5 - 2)(0.5) + (0.5)(0.5)(\tfrac{1}{2})(2)$$
$$= 5.75 \text{ inches}^2 \quad .$$

The stress is:

$$\sigma = \frac{F_1}{A} = \frac{110,000}{5.75} = 19,130 \text{ psi} \quad ,$$

and the margin of safety is:

$$MS = \frac{F_{tu}}{\sigma} -1 = \frac{30,000}{19,130} -1 = 0.57 \quad .$$

(b) Shear Through the Eye

It was conservatively assumed that a 1-1/2 inch nominal shackle bolt might be used through the eye. Therefore, for purposes of analysis, the length of the shear area was reduced to 3.5 inches (from 4.0 inches for the centerline distance of the hole). The area for shear is:

$$A = 2\left[(3.5)(1.5)\right] = 10.5 \text{ inches}^2 \quad .$$

The stress is:

$$\sigma_s = \frac{F_1}{A} = \frac{110,000}{10.5} = 10,500 \text{ psi} \quad .$$

The margin of safety is:

$$MS = \frac{F_{su}}{\sigma_s} -1 = \frac{20,000}{10,500} -1 = 0.90 \quad .$$

(c) Bearing in the Eye

Assuming that a 1-1/2 inch shackle bolt would be used, the e/D for bearing in the eye is:

$$e/D \cong \frac{3.5}{1.5} > 2.0 \quad .$$

Therefore, the design bearing strength is:

$$F_{bry} = 50{,}000 \text{ psi} \quad .$$

The bearing area is:

$$A = (1.5)(1.5) = 2.25 \text{ inches}^2 \quad .$$

The stress is:

$$\sigma_{br} = \frac{F_1}{A} = \frac{110{,}000}{2.25} = 48{,}900 \text{ psi} \quad .$$

The margin of safety is:

$$MS = \frac{F_{bry}}{\sigma_{br}} -1 = \frac{50{,}000}{48{,}900} -1 = 0.02 \quad .$$

(d) Shear-Bending in Doubler Weld

That portion of the force, F_1, restrained by the doubler plate must be transferred to the original ear member by the weld between the doubler and the original ear. If it is assumed that the entire force, F_1, is carried by the weld at the top of the cask (see the sketch on the following page) the weld would be in combined bending and shear.

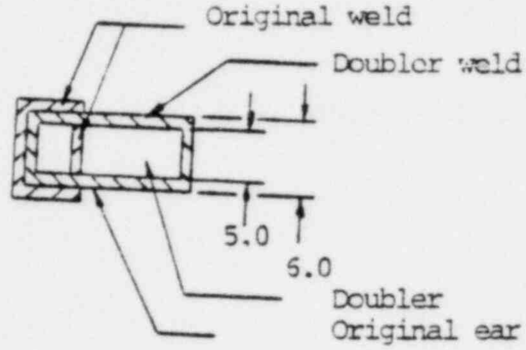

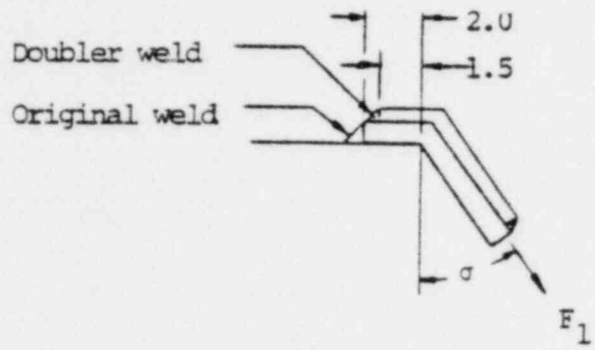

The area in shear is:

$$A = \Big[(2)(1.5) + (5) \Big] \ (\tfrac{1}{2})(0.707) = 2.828 \text{ inches}^2 \quad .$$

It is assumed that $\frac{1}{3}$ of force, F_1, is carried in the doubler. Then, the stress is:

$$\sigma_{sh} = \frac{\frac{1}{3} F_1 \sin\alpha}{A} = \frac{(110{,}000)(0.5736)}{(3)(2.828)} = 7300 \text{ psi} \quad .$$

If it is assumed that the bending moment is equal to the product of the vertical force component and a lever arm equal to half the length of the doubler over the cask (i.e., $\ell = \frac{1}{2}(1.5)$ in the sketch), the moment is:

The area moment of inertia about this axis is:

$$M = \left[\frac{1}{3} F_1 \cos\alpha\right] \left[(\tfrac{1}{2})(1.5)\right] = \frac{110,000}{3} (0.8192)(\tfrac{1}{2})(1.5)$$

$$= 22,500 \text{ inches-pounds} \quad .$$

The area moment of inertia about this axis is:

$$I = 2(\frac{bh^3}{12})_{side} + \left[\frac{bh^3}{12} + Ad^2\right]_{end}$$

$$= 2\left[\frac{(0.707)(0.5)(2)^3}{12}\right] + \left[\frac{(6)(0.707 \times 0.5)^3}{12} + (0.707)(6)(0.5)(0.75)^2\right]$$

$$= 0.471 + 0.022 + 1.192$$

$$I = 1.685 \text{ inches}^4 \quad .$$

The maximum fiber distance is:

$$C = 1/2\ \ell = \tfrac{1}{2}(1.5) = 0.75 \quad .$$

The stress is:

$$\sigma_b = \frac{Mc}{I} = \frac{(22,500)(0.75)}{1.685} = 10,000 \text{ psi} \quad .$$

The total stress on the area is the vector sum of the shear and bending forces or:

$$\sigma_{tot} = \sqrt{\sigma_{sh}^2 + \sigma_b^2} = \sqrt{7,300^2 + 10,000^2}$$

$$= 12,400 \quad .$$

The margin of safety is:

$$MS = \frac{F_{tu}}{\sigma_{tot}} - 1 = \frac{30,000}{12,400} - 1 = 1.42 \quad .$$

(e) Shear-Bending in Original Weld

The area for shear in the weld between the original ear and the cask is:

$$A = \Big[(2)(2) + (2)(6) \Big] \quad (1)(0.707) = 11.30 \text{ inches} \quad .$$

The stress is:

$$\sigma_{sh} = \frac{F_1 \sin\alpha}{A} = \frac{(110,000)(0.5736)}{11.3} = 5,580 \text{ psi} \quad .$$

For the case of bending of the weld, it is assumed that the moment is:

$$M = (F_1 \cos\alpha)(\tfrac{1}{2} \ell)$$

$$= (110,000)(0.8192)(\tfrac{1}{2})(2) = 90,000 \text{ inch-pounds} \quad .$$

The area moment of inertia is:

$$I = 2 \left[\left(\frac{bh^3}{12}\right)_{side} + \left(\frac{bh^3}{12} + Ad^2\right)_{end} \right]$$

$$= 2 \left[\frac{(0.707)(1)(2)^3}{12} + \frac{(6)(0.707 \times 1.0)^3}{12} + (6)(1)(0.707)(1)^3 \right]$$

$$= 2 \left[0.472 + 0.177 + 4.240 \right]$$

$$= 9.778 \text{ inch}^4 .$$

The maximum fiber distance is:

$$C = \frac{1}{2}(\ell) = \frac{1}{2}(2) = 1.0 \text{ inch} \quad .$$

The stress is:

$$\sigma_b = \frac{Mc}{I} = \frac{(90,000)(1)}{9.778} = 9210 \text{ psi} \quad .$$

The total combined stress is:

$$\sigma_{tot} = \sqrt{\sigma_{sh}^2 + \sigma_b^2}$$

$$= \sqrt{5580^2 + 9210^2}$$

$$= 10,900 \text{ psi} \quad .$$

The margin of safety is:

$$MS = \frac{F_{tu}}{\sigma_{tot}} - 1 = \frac{30,000}{10,900} - 1 = 1.75 \quad .$$

(f) Compression of Cask Shell

Considering only the original 1/2-inch-thick cask shell, the area in compressive loading directly under the ear is:

$$A = (t)(\ell) = \frac{1}{2}(6) = 3 \text{ inches}^2.$$

The stress is:

$$\sigma_C = \frac{F_1 \cos\alpha}{A} = \frac{(110,000)(0.8192)}{3} = 30,000 \quad .$$

The margin of safety is:

$$MS = \frac{F_{cy}}{\sigma_C} - 1 = \frac{35,000}{30,000} - 1 = 0.17 \quad .$$

(g) Shear in Bolts at Base

The shearing force on the eight 1-inch A325 bolts holding the cask to the skid is:

$$F_{sh} = (11.18\ G)(W) + F_{2x} + F_{3x} - (F_{1x} + F_{4x}) \quad .$$

If W is taken to include the skid weight:

$$F_{sh} = (11.18)(23,600) + (0.1078 + 0.2126 - 0.544$$

$$- 0.1448)(110,000) = 222,400 \text{ pounds} \quad .$$

The area of eight bolts is:

$$A_{sh} = (8)(0.6331) = 5.06 \text{ inches}^2.$$

The stress is:

$$\sigma_{sh} = \frac{F_{sh}}{A_{sh}} = \frac{222,400}{5.06} = 44,000 \text{ psi} \quad .$$

The margin of safety is:

$$MS = \frac{F_{su}}{\sigma_{sh}} - 1 = \frac{89,000}{44,000} - 1 = 1.02 \quad .$$

(h) Stress in Turnbuckles

The question was raised about the response of the turnbuckles and their points of attachment to the cask in the event of an incident such as the 30 foot fall conditions included in the regulations. Our analyses indicate that the turnbuckle will fail before damage could occur to the cask. These analyses are shown below.

The turnbuckles are attached to the cask through two, 1/2 inch plates welded to the outer shell of the casks as shown in the sketch following.

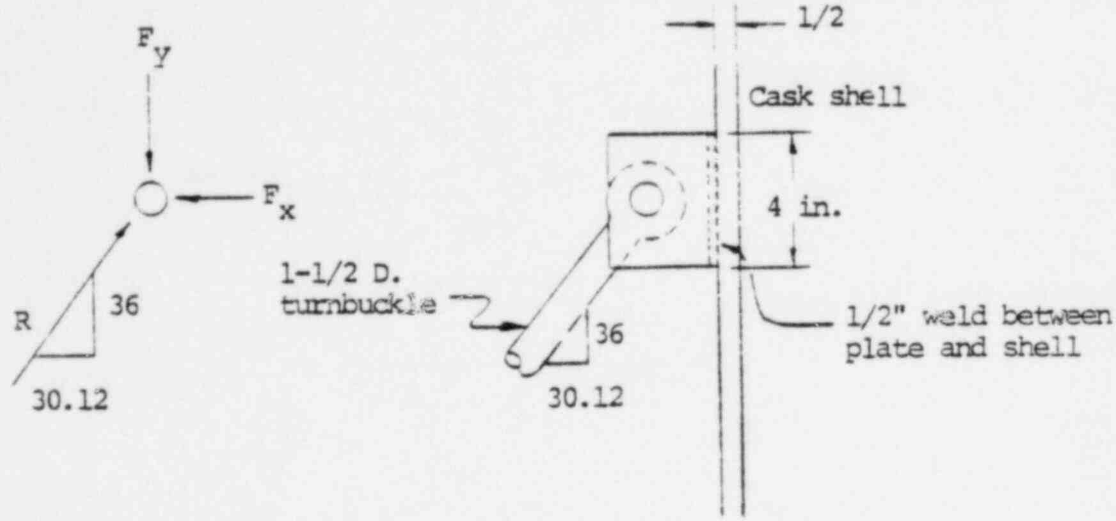

The force required to cause shear in the welds between the two plates and the cask shell is:

$$F_y = \sigma_{su} A = \sigma_{su} t L (.707)$$

where σ_{su} = the shear strength = 40,000 psi

t = the weld thickness = .5 inch

L = total length of weld = (4) (4) = 16 inches .

Then

$$F_y = (40,000)(.5)(16)(.707) = 226,000 \text{ pounds} .$$

The force required to cause puncture of the two plates through the cask shell (using the punch press shear stress technique) is:

$$F_x = \sigma_{su} A = \sigma_{su} t L$$

where σ_{su} = the shear strength = 40,000 psi

t = the shell thickness = .5 inch

L = length of the shear plane = 2 (4 + 4 + .5 + .5)

= 18 inches. .

Then

$$F_x = (40,000)(.5)(18) = 360,000 \text{ pounds} \quad .$$

If the case of incipient shear in the weld is assumed, F_y = 226,000 pounds as above, and

$$F_x = \left(\frac{30.12}{36}\right) F_y = 189,000 \text{ pounds} \quad .$$

Since the value of F_x is less than that required to produce penetration through the shell (360,000 pounds), the weld will shear first. The force in the turnbuckle is:

$$R = \sqrt{F_x^{\,2} + F_y^{\,2}}$$

$$= \sqrt{189{,}000^2 + 226{,}000^2} = 294{,}000 \text{ pounds} \quad .$$

The turnbuckle is 1-1/2 inches in diameter and 47 inches long. From the Euler buckling formula, the force required to cause instability buckling of the turnbuckle under a compressive load is:

$$P = \frac{A\pi^2 E}{\left(\frac{L}{r}\right)^2}$$

where

$$A = \text{area} = \frac{\pi d^2}{4} = \frac{(\pi)(1.5)^2}{4} = 1.765 \text{ inches}$$

$$E = \text{the elastic modulus} = (29)(10^6) \text{ psi}$$

$$\frac{L}{r} = \text{the slenderness ratio} = \frac{47.0}{0.375} = 125 \quad .$$

Then

$$P = \frac{(1.765)(\pi^2)(29)(10^6)}{(125)^2} = 32{,}300 \text{ pounds} \quad .$$

Thus, the case of a compressive load on the turnbuckle, the turnbuckle will collapse by column instability before the attachment plates will shear away from the cask shell.

In the event the load on the turnbuckle is a tensile load, failure will occur when the load is:

$$F = \sigma_{tu} A$$

where

F_{tu} = the tensile ultimate strength = 120,000 psi

A = area = 1.765 inches^2 .

Then

$$F = (120{,}000)(1.765) = 212{,}000 \text{ pounds} \quad .$$

Since the force in the turnbuckle required to cause shear of the attachment welds (R) is 294,000 pounds, the turnbuckle will break before shear failure would occur. In addition, since the tensile ultimate strength of the cask shell is 75,000 psi, or about twice the shear ultimate strength used in the calculations above, the turnbuckle would fail in tension before the cask shell would fail due to the tensile force applied at the plate attachments.

2.4.4.2 Nontiedown Devices Covered or Locked

The nontiedown devices will be covered as described above in Section 2.4.3.2.

2.4.4.3 Failure of the Tiedown Device Would Not Impair Meeting Other Requirements

Failure of the tiedown device would not impair meeting other requirements of the cask as described above in Section 2.4.3.3 and in the subsequent section on accident conditions.

2.5 Standards for Type B and Large Quantity Packaging

2.5.1 Load Resistance

A question has been raised as to the accuracy of the beam strength calculation provided in the Hazards Report on this cask. The purpose of this section is to provide an answer to this question.

The original beam strength calculation was based on a 10-g loading uniformly applied as required in 10CFR Section 72.32(a). The maximum stress was calculated using the common beam stress equation $\frac{Mc}{I}$. The maximum stress calculated was 5,160 psi. This stress is only approximately correct for the given loading and support condition because the cask tends to flatten at mid-span introducing additional bending stresses.

A more accurate solution to the problem is outlined by Wojtaszak[2]. The solution applies to the case of a circular cylindrical shell freely supported at the edges as shown below and submitted to the pressure of liquid within the shell.

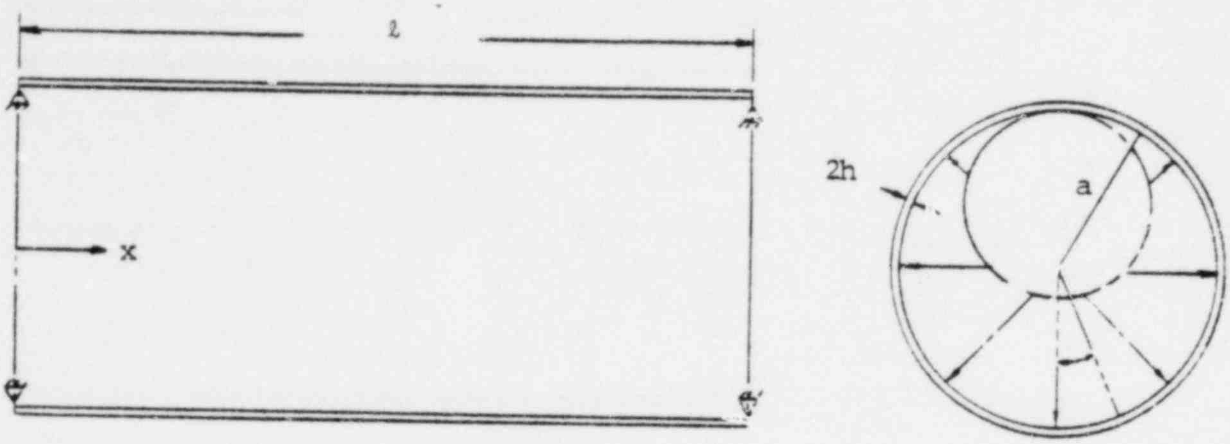

The loads and displacements in the Wojtaszak solution are in the form of a double-summation trigonometric series.

$$q = \Sigma\Sigma\, D_{mn} \cos n\phi \sin \frac{m\pi x}{\ell} \quad .$$

To simplify the solution and reduce the number of terms needed in the series solution m was taken as 1, which makes the x-axis load distribution a sine wave. This approximation of a uniform load with a sine wave loading was necessary to obtain a solution to the problem in a reasonable length of time. The sine wave loading, however, is a conservative approximation of the uniform loading. The total load applied as a sine wave, was taken to equal 10 times the weight of the cask, 23,200 pounds.

Following through the solution as outlined by Wojtaszak, the displacements for the n = 0, mode were found to be:

$$u = 327 \frac{\gamma h}{D} \cos \frac{\pi x}{\ell} \quad \text{(longitudinal)}$$

$$v = 0 \qquad \text{(circumferential)}$$

$$w = 750 \frac{\gamma h}{D} \sin \frac{\pi x}{\ell} \quad \text{(radial)}$$

For the n = 1 mode, the displacements are:

$$u = -1,885 \frac{\gamma h}{D} \cos\phi \cos \frac{\pi x}{\ell}$$

$$v = -6,850 \frac{\gamma h}{D} \sin\phi \sin \frac{\pi x}{\ell}$$

$$w = +7,150 \frac{\gamma h}{D} \cos\phi \sin \frac{\pi x}{\ell}$$

where

γ = 3.98 pound/inches^3 obtained by equating the total cask weight to the inside volume.

$$D = \frac{2Eh^3}{3(1 - \nu)^2} = \frac{2(30 \times 10^6)(0.25)^3}{3(1 - 0.3^2)} = 342,000 \text{ inch-pound}$$

flexural rigidity.

With the displacements known, it is possible to calculate the strains, and, in turn, the stresses. The final circumferential and longitudinal stresses (including membrane and bending), are calculable from the following equations for the cask under consideration:

$$\sigma_L = \left\{ 2700 \left[1 + 3.08 \cos\phi \right] + 33.4 \left[1 + 9.77 \cos\phi \right] \right\} \sin \frac{\pi x}{\ell}$$

$$\sigma_C = \left\{ 4640 \left[1 + 0.868 \cos\phi \right] + 10 \left[1 + 12.1 \cos\phi \right] \right\} \sin \frac{\pi x}{\ell}$$

By inspection, it can be observed that the maximum longitudinal and circumferential stresses occur at $x = \frac{l}{2}$ and the maximum stresses are tensile and occur at $\phi = 0$, the bottom of the shell.

The maximum tensile stresses were found to be:

$$\sigma_L = 11,360 \text{ psi}$$

$$\sigma_C = 8,800 \text{ psi} \quad .$$

Since these stresses are less than ultimate, the cask meets the requirement of 10CFR, Section 72.32(a).

2.5.2 External Pressure

The requirements are that the cask must be able to withstand an external pressure of 25 psig without loss of contents. The cask will operate normally at 100 psig internal pressure and was designed for this condition.* The pressure condition under the application of this requirement is a net 75 psig internal pressure. Therefore, the cask complies with the requirement.

2.6 Normal Transport Conditions

The structural requirements of the cask for normal transport conditions, as specified in § 71.35 of 10-CFR-71, are less severe than those analyzed in previous sections, as well as those analyzed in subsequent sections for accident conditions.

The following analysis shows that the inner cask wall, inner cask bottom head, and lid are sufficient to withstand the design pressure of 100 psig at 320 F as required in § 72.32(d) of the 10-CFR-72.

---

* Section 2.6

Inner Cask Wall Thickness

The wall thickness of the inner cask wall is 0.250 inch, which is adequate according to § UG-27(c) of Section VIII of the 1962 ASME Boiler and Pressure Vessel Code.

$$t_{reqd} = \frac{PR}{SE-0.6P} = \frac{100(7.75)}{15,890(0.8) - 0.6(100)} = 0.0613 \text{ inch} \quad .$$

where

t_{reqd} = minimum wall thickness

P = 100 psig, design pressure

R = 7.75 inches, inside radius

S = 15,800 psi, allowable stress from Table UHA-23, ASME Code

E = 0.8 joint efficiency for single-welded butt joint with a backing strip--spot radiographed.

Inner Cask Bottom Head

The thickness of the bottom head is 0.75 inch, which is adequate according to Section UG-34(2) of the ASME Code as shown below:

$$t_{reqd} = D\sqrt{\frac{CP}{S}} = 15.5\sqrt{\frac{0.3(100)}{15,890}} = 0.675 \text{ inch} \quad .$$

where

t_{reqd} = minimum head thickness

D = 15.5 inches, inside cask diameter

C = a geometry co‹ᶠficient which, according to the ASME Code for the configuration used, is 0.3.

Cask Lid

Lid Thickness. The thickness of the lid is 1.125 inches, which is adequate according to Section UG-34(2) of the ASME Code as shown below:

$$t_{reqd} = d\sqrt{\frac{CP}{S} + \frac{1.78\ Wh_G}{Sd^3}}$$

$$t_{reqd} = 20.75\sqrt{\frac{0.3(100)}{15,890} + \frac{1.78(34,130)(1.375)}{15,890(20.75)^3}} = 1.04 \text{ inches} \quad .$$

where

d = 20.75 inches, diameter of gasket circle

C = 0.3, constant which is a function of geometry

$W = \frac{\pi d^2}{4} P + \pi d(F_G)$ = 33,800 + 330 = 34,130 pounds, pressure head

h_G = 1.375 inches, distance from gasket to bolt ring circle .

Lid Bolts

The total force W, acting on the lid as a result of the pressure and rubber sealing gasket, was calculated above to be 34,130 pounds.

Twelve 1-inch-diameter stainless steel studs have been provided to hold the lid in place. The stress in these bolts is 5,160 psi as shown in the calculation following:

$$\sigma = \frac{P}{A} = \frac{34,130}{12(0.551)} = 5160 \text{ psi}$$

2.7 Hypothetical Accident Conditions

This section demonstrates the safety of the packaging under the hypothetical accident conditions. Response of the product containment and the baskets are presented in Sections 2.10 and 2.11, respectively.

2.7.1 Free Drop

The first condition which the cask must withstand in the hypothetical accident sequence is a 30-foot fall onto a flat, unyielding surface. There are three critical orientations which the cask can assume at the moment of impact. These include direct impact on an end, direct impact on the cylindrical side, and impact on an edge at such an angle that the reaction force is directed through the center of mass of the cask.

2.7.1.1 End Drop

(a) Bottom

For impact on the bottom, the collapse of the skid would absorb some energy and the remainder would be absorbed by deformation of the cask. If it is assumed that the skid absorbs no energy, a conservative value of cask deformation can be determined. The impact area, from the sketch following, is:

$$A = \frac{\pi}{4} d^2 = \frac{\pi}{4}(23.75)^2 = 441 \text{ inches}^2 \quad .$$

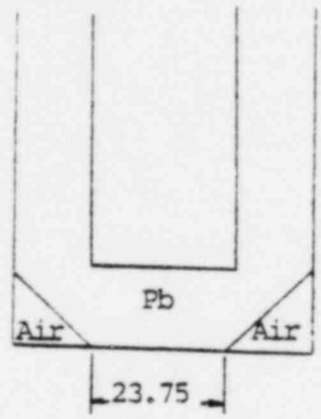

The kinetic energy to be absorbed is:

$$KE = 360(W) = (360)(23,600) = 8.5(10^6) \text{ inch-pounds} \quad .$$

Then, if the lead flow pressure, P, is 10,000 psi, the depth of deformed lead is:

$$\delta = \frac{KE}{PA} = \frac{(8.5)(10^6)}{(10,000)(441)}$$

$$\delta = 1.92 \text{ inches}$$

The lead thickness on the end is 7.5 inches. Therefore, the thickness of lead shielding remaining is:

$$t = t - \delta = 7.5 - 1.92 = 5.58 \text{ inches} \quad .$$

The question that has come up is whether the bottom plate of the lid is adequate since the thickness is reduced at the edge.

In a bottom impact, the force on the bottom plate of the lid would tend to shear the plate around the edge. Using the requirements of Section 72.32(c), the bottom plate must be able to withstand a force of 60 times the lid weight. The force is, therefore, 60(1,050) = 63,000 pounds.

The average shear stress at the edge for the above loading is 3450 psi as shown in the following calculation. This is well below the 15,000 psi yield stress of this material in shear and, therefore, should be adequate.

$$\tau = \frac{P}{A} = \frac{63.000}{\pi(15.5)(0.375)} = 3450 \text{ psi} \quad .$$

(b) Top

Trunnion Weld Shear. For the case of an impact on the top end, the lifting trunnions would strike the flat surface first. If it is assumed that the trunnion welds shear off, the weld area in shear on each trunnion is, from the sketch below:

$$A_{sh} = 2(6 + 12)(0.75)(0.707) + (16 + 16 + 5)(0.25)(0.707)$$

$$= 25.65 \text{ inches}^2 \text{ per trunnion}$$

$$= 51.3 \text{ inches}^2 \text{ for both trunnions} \quad .$$

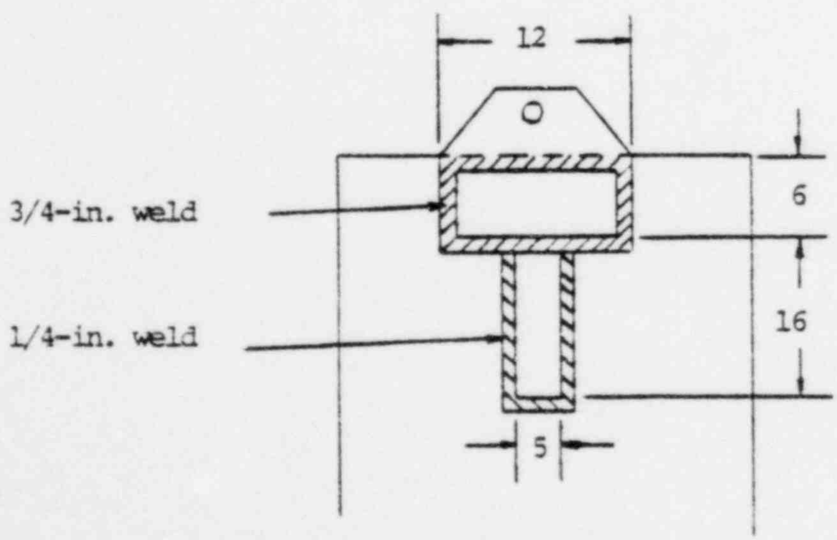

The maximum force developed in shearing the weld is:

$$F = (F_{su})(A_{sh}) = (40,000)(51.3) = 2,050,000 \text{ pounds} \quad .$$

The deceleration is:

$$a = \frac{F}{m} = \frac{FG}{W} \quad ,$$

$$a = \frac{2,050,000}{23,600} G = 86.8 G \quad .$$

This deceleration, applied to the weight of the lid and contents, would produce a tensile load in the lid bolts:

$$F_{deceleration} = a(W_{lid} + W_{contents})$$

$$= (86.8)(1,200 + 1,800) = 260,000 \text{ pounds} \quad .$$

The maximum stress in the 12 bolts is:

$$\sigma = \frac{F_{deceleration}}{12(A)} = \frac{260,000}{(12)(0.6331)} = 34,200 \text{ psi} \quad .$$

The margin of safety is:

$$MS = \frac{F_{tu}}{\sigma} -1 = \frac{75,000}{34,200} -1 = 1.19$$

Cask Deformation. If it is assumed that energy absorbed by the shearing of the trunnions is negligible compared to the kinetic energy of the cask at the moment of impact, the kinetic energy which must be absorbed by deformation of the cask body is:

$$KE = HW = (360)(23{,}600) = 8.5\ (10^6)\ \text{inch-pounds} \quad .$$

The area presented by the deformed volume (see sketch below), is approximately:

$$A = \frac{\pi}{4}\,(32.0)^2 = 804\ \text{inches}^2 \quad .$$

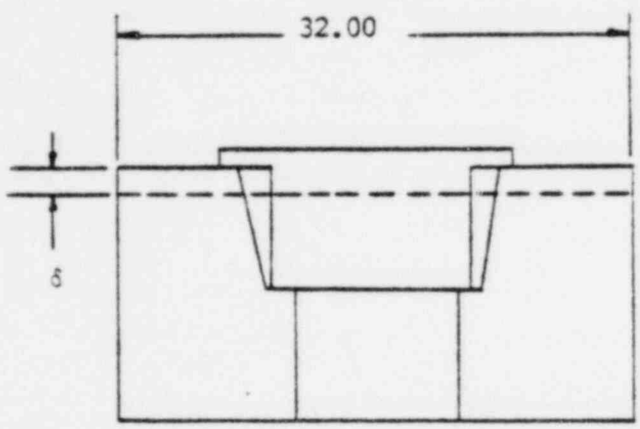

If it is assumed that the flow pressure of lead is taken as 10,000 psi, and all of the energy is dissipated in the lead, the deformation, δ, is:

$$\delta = \frac{KE}{(A)\quad(P)} = \frac{(8.5)(10^6)}{(804)(10{,}000)} = 1.06\ \text{inches} \quad .$$

The lead in the cover is 7.75 inches thick. Therefore, the thickness of lead remaining after impact is:

$$t_{left} = 7.75 - 1.06 = 6.69\ \text{inches} \quad .$$

Fire Shell. Drawing 43-6704-001, Rev. A has been revise the region immediately below the trunnions. The 1/8-inch-thick steel shell added to the cask is terminated two inches below the bottom of the trunnion. Thus, thr trunnion would not tend to remove the shell should it be sheared off the cask body during a top end impact.

Penetration of Cover Lifting Device. The cover lifting device consists of two 1/4-inch plates, 5 inches high, and 20 inches long. Roark[3] shows that for a long thin flange which has one end free and one end fixed, and which is loaded on the edge, (see sketch below) the buckling stress is:

$$\sigma^1 = \frac{1.09\ E}{1 - \gamma^2} \left(\frac{t}{b}\right)^2$$

where

E = elastic modulus = 29.0×10^6 psi

γ = possoins ratio = 0.3

t = thickness = 0.25 inch

b = width = 20 inches

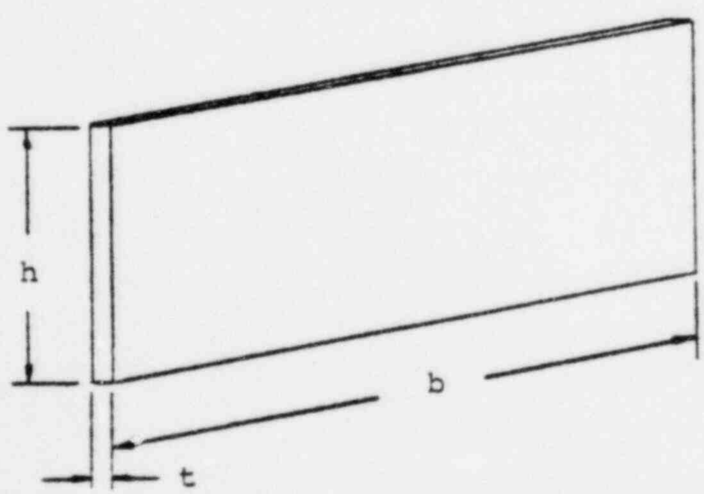

Then the buckling stress is:

$$\sigma^1 = \frac{(1.09)(29)(10^6)}{1 - (.3)^2} \left(\frac{.25}{20}\right)^2$$

$$\sigma^1 = 5430 \text{ psi} \quad .$$

The force to product this stress is:

$$F^1 = \sigma^1 \, tb = (5430)(.25)(20) = 27{,}000 \text{ pounds} \quad .$$

The force required to cause the lifting device to shear through the top plate of the cover is:

$$F_s^1 = \sigma_s A_s = F_s \, w(2 \, bt)$$

where

F_s = ultimate shear stress = 40,000 psi

w = the thickness of the top plate
= 1.25 inches

and b and t as above .

Then

$$F_s^1 = (40{,}000)(1.25)(2)(20)(.25) = 2.02 \, (10^6) \text{ pounds} \quad .$$

The margin of safety is

$$MS = \frac{F_s^1}{F^1} - 1 = \frac{(2.02)(10^6)}{27{,}000} - 1 = \text{large} \quad .$$

2.7.1.2 Side Drop

In the event of an accident in which the cask falls on its side, the highest impact load is experienced if the cask is separated from the skid. The deformed shape of the cask then is as shown below.

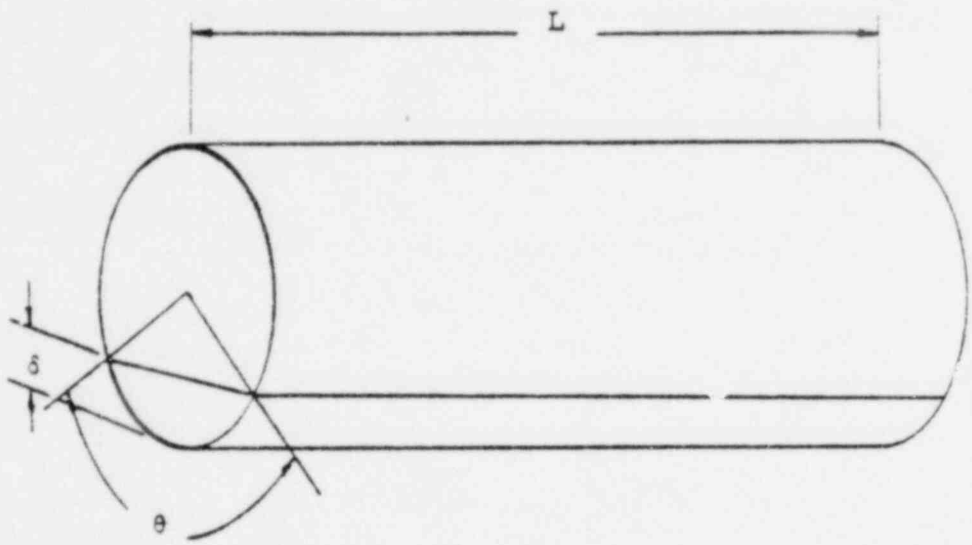

$$\theta - \sin\theta = \frac{8V}{d^2 L} = \frac{(8)(850)}{(32)^2\ (66)}$$

$$= .1007$$

then θ = 49.0 degrees.

The corresponding depth of the deformed lead is:

$$\delta = (1 - \cos\frac{\theta}{2})\ \frac{d}{2} = (1 - \cos\ \left[24.5 \text{ degrees}\right]\ )(\frac{32}{2})$$

δ = 1.44 inches .

The equivalent "g" load is:

$$G = 2\ \frac{h}{\delta} = (2)\ \frac{360}{1.44} = 500\ g$$

In Drawing 43-6704-0003, Area 2-c, it is noted that the holes in the cover for the studs are 1-1/8 inch diameter. Thus, the holes provide a 0.062 inch radial clearance. In Area 3 c of this drawing, it is noted that the radial clearance between the cover and the cask cavity is 0.03 inch. Thus, should the cover be moved in the radial direction by a side impact, the sides of the cover will contact the cask cavity before the holes in the cover can contact the closure studs and product a shear load upon them. Therefore, the closure is maintained for the case of a side impact.

2.7.1.3 Corner Drops

In the case of impact on an edge, the deformed lead volume may be represented as shown in the sketch below.

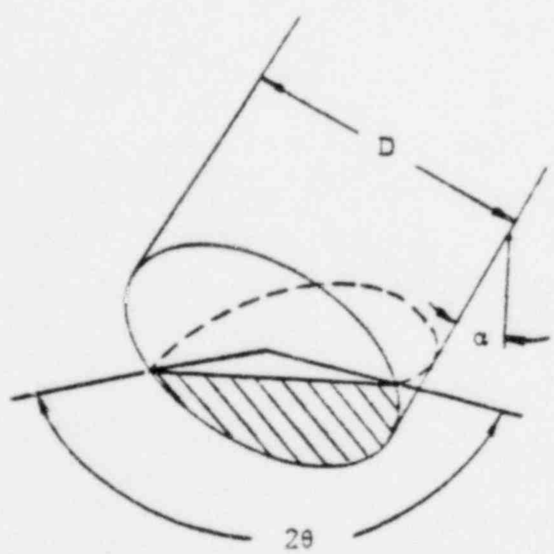

The volume is given by:

$$V = \left(\frac{D}{2}\right)^3 \tan\alpha \left(\sin\theta - \frac{\sin^3\theta}{3} - \theta\cos\theta\right) \quad .$$

For the edge impact:

$$\alpha = 24.75 \text{ degrees } \left(\tan\alpha = \frac{\text{cask diameter}}{\text{cask height}} = \frac{33.25}{72.12}\right) \quad .$$

If the flow pressure of lead, P, is taken as 10,000 psi, the volume of lead deformed in order to absorb the kinetic energy at impact is:

$$V = \frac{KE}{P} = \frac{360W}{P} = \frac{(360)(23,600)}{10,000}$$

$$V = 850 \text{ inches}^3$$

The equation above for the volume of the deformed lead shown in the sketch can be solved by trial and error for θ. Then for:

$$D = 33.25 \text{ inches}, \; \theta = 79.0 \text{ degrees} \quad .$$

The lead thickness on the side is 8 inches and on the end it is 7.5 inches. Using solid geometry, it can be shown that depth of deformed lead, δ (measure perpendicular to the deformed surface) is 5.63 inches and that the minimum thickness of lead shielding left at the edge is 4.53 inches. The deceleration is:

$$G = \frac{Ht}{\delta} 2$$

$$= \frac{360}{5.63} (2) = 128 \text{ G} \quad .$$

<u>Cover bolts.</u> For impact on the top edge, the deceleration of the cask lid and contents would produce both shear and tensile stresses in the bolts. If the combined weight of the cover and contents are assumed to act at the center of the bottom face of the cover as shown in the sketch following, the maximum loan the bolts can be evaluated.

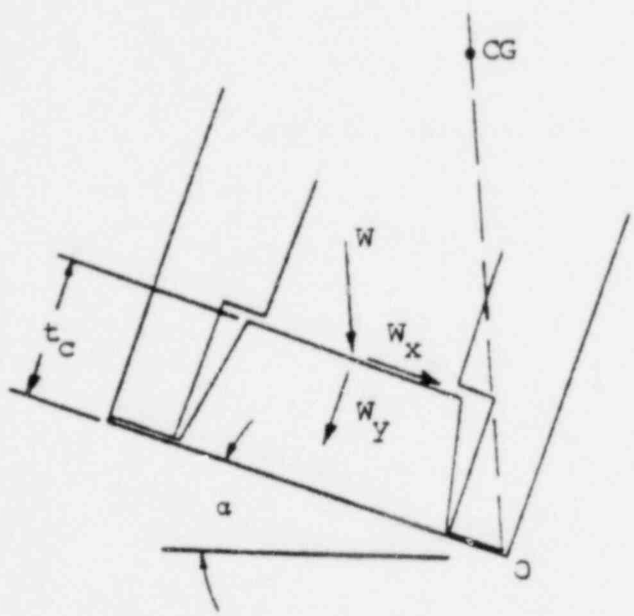

The maximum tensile stress in the bolts will occur in the bolt farthest away from the point of impact, 0, and is evaluated by the following equation:

$$\sigma = \left(\frac{Mc}{I}\right) O \quad ,$$

where:

$$M = \left[(W_y) \frac{D}{2} - (W_x)\ t_c \right] G = WG \left(\frac{D}{2} \cos\alpha - t_c \sin\alpha\right)$$

$$c = \frac{1}{2}(D + D_{BC})$$

$$I_o = \Sigma (I_c + Ad^2)$$

where:

W = the weight of the cover and contents = 3,000 pounds

G = the "G" impact load = 128 G

D = the cask diameter = 33.25 inches

t_c = the cover thickness = 8.88 inches

D_{BC} = the bolt circle diameter = 23.38 inches

I_c = area moment of inertia for one bolt about its own neutral axis = 0.0319 inches^4

A = the effective area of one bolt - 0.633 inch^2

d = the distance of each bolt from a horizontal axis through "0"

α = 24.75 degrees .

Therefore,

$M = (4.36)(10^6)$ inches-pounds

c = 28.3 inches

I = 2,619 inches^4

and

$$\sigma_t = \frac{Mc}{I} = \frac{(4.36)(10^6)(28.3)}{2,619} = 47,200 \text{ psi} \quad .$$

The corresponding margin of safety is:

$$MS = \frac{F_{tu}}{\sigma_t} - 1 = \frac{75,000}{47,200} - 1 = 0.59 \quad .$$

In addition, the shear stress:

$$\sigma_{sh} = \frac{WG}{nA} = \frac{W_{cover} G \sin \alpha}{nA}$$

where:

$$W_{cover} = \text{weight of the cover only} = 1,200 \text{ pounds} \quad .$$

The shear stress then is:

$$\sigma_{sh} = \frac{(1,200)(128)(\sin 24.75)}{(12)(0.633)} = 8,500 \quad .$$

The margin of safety is:

$$MS = \frac{F_{su}}{\sigma_{sh}} - 1 = \frac{40,000}{8,500} - 1 = 3.7 \quad .$$

2.7.2 Puncture

An empirical equation for the minimum steel shell thickness required for lead-filled casks has been developed by the Oak Ridge National Laboratory.[4] The equation has the form:

$$t = \left(\frac{W}{F_{tu}}\right)^{0.71} \quad ,$$

where:

t = minimum shell thickness, inch
W = weight of lead-lined cask, pourd
F_{tu} = ultimate tensile strength, psi .

Therefore, the required shell thickness is:

$$t = (\frac{W}{F_{tu}})^{0.71} = (\frac{23,600}{75,000})^{0.71} = 0.44 \text{ inch}$$

On the basis of an outer shell thickness of 0.68, the cask design is shown to comply with the regulatory puncture criteria.

2.8 Special Form

The BMI-1 shipping cask is capable of transporting a variety of radioactive materials, including various special form materials, as stated in the Certificate of Compliance, Revision 5, as follows:

> Paragraph 5(b) (1) (iv) - Greater than type A quantities of by-product material in special form.
>
> Paragraph 5(b)(2)(iv) - For the contents described in 5(b)(1)(iv): Gamma sources securely confined in the cask cavity to preclude secondary impacts during accident conditions of transport. Thermal heat generation rate shall be limited to 200 watts.

Materials shipped under these conditions will be shown to meet the special form requirements of Paragraph 71.4(0) of Appendix D, to 10CFR, Part 71.

2.9 Fuel Rods

To meet licensing requirements for shipment of the Fermi fuel subassemblies, it is necessary that the element not fail under credible shipping conditions. The failure temeperature, as defined in 10CFR, Part 72, is the minimum temperature at which the element will release 100 curies of beta-gamma activity or one curie of alpha activity over a 48-hour period.

There are two different means by which failure could occur during shipment of the Fermi fuel subassemblies. These are: (1) corrosion in water, air and steam, or a dry air atmosphere, and (2) swelling and subsequent rupturing of the fuel pins caused by the expansion of gaseous fission products in the fuel alloy at an elevated temperature. Swelling of the fuel is not expected, since the in-reactor fuel operating temperature of 800 F is well above that which will be encountered during shipment.

The fuel pins are not expected to fail by corrosion since the corrosion rate of zirconium in 680 F water is 0.004 mils/day, in 750 F steam, at 15 psi, the corrosion rate is 0.007 mils/100 hrs, and in 750 F steam, at 1,500 psi, the corrosion rate is 0.21 mils/100 hrs.[5] Also, the corrosion rate of zirconium in air is such that at 930 F, oxidation would penetrate the clad to a depth of only 1.2 mils in a 100-hour period.[6] It can be concluded that temperatures in excess of 900 F would have to be maintained for a period of over 400 hours before failure in a dry oxidizing atmosphere would occur, and that temperatures in excess of 750 F would have to be maintained for a period of over 2,000 hours before failure of the 5-mil clad would occur in a steam and air atmosphere. From these data, it is expected that corrosion of the cladding in steam or air at 521 F would proceed very slowly. The normal trip from Monroe, Michigan, to Columbus, Ohio, should require less than 5 hours.

Discussions with corrosion specialists at BMI indicate that with the presence of copper shot in water, there would probably be some plating out of the copper but there would be no effect on the corrosion rate of the zirconium.[7]

2.10 Product Containers

2.10.1 BMI-1 Canister

In the event of a 30-foot free fall accident condition, the inner container will be subjected to an impact load due to its inertia. There is a minimal radial clearance between the inner container and the inner cavity. Thus, in the event of a side impact, the cavity walls would support the inner container over its entire length. However, in the event of an end or corner impact, the inner container would experience an end loading that would produce axially-oriented compressive stresses in the walls of the can due to the inertia of the can. The weights of the various components of the can, Drawing 00-000-421 Rev. C, are shown on the sketch below:

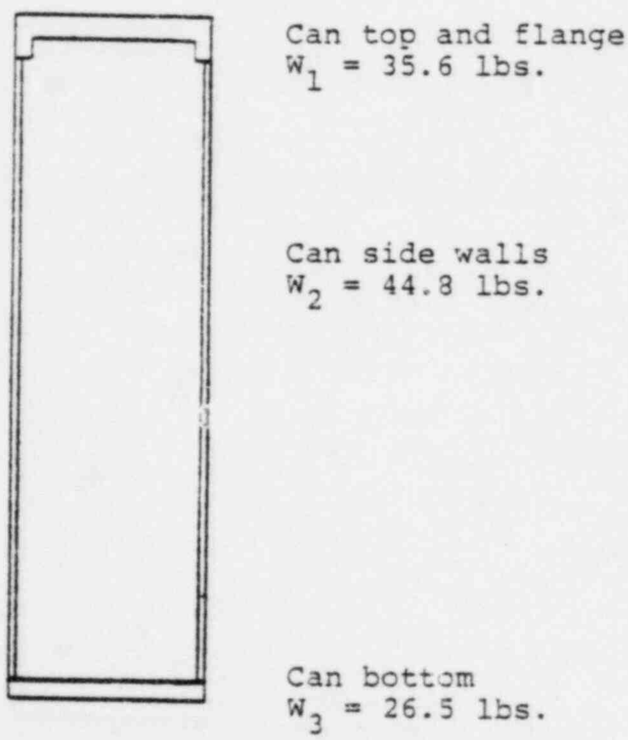

For impact on the bottom, the cask deforms 1.92 inches. The associated g load is:

$$g = \frac{2(\text{drop height})}{\delta} = \frac{(2)(360)}{1.92} = 375 \text{ G} \quad .$$

The load experienced by the can will be less than this since significant damping occurs in the cask body. If however, it is conservatively assumed that the can experiences the full g load, the impact force is:

$$F_{I_{bottom}} = g(w_1 + w_2) = 375(35.6 + 44.8) = 30{,}200 \text{ pounds} \quad .$$

The cross section of the can wall is:

$$A = \pi dt = \pi(14.88)(.062) = 2.90 \text{ square inches} \quad .$$

The compressive stress in the can wall is:

$$\sigma_{I_{bottom}} = \frac{F_{I_{bottom}}}{A} = \frac{30{,}200}{2.90} = 10{,}400 \text{ psi} \quad .$$

The margin of safety is:

$$MS = \frac{F_{cy}}{\sigma_{I_{bottom}}} - 1 = \frac{35{,}000}{10{,}400} - 1 = 2.37 \quad .$$

For impact on the top, the cask deforms 1.06 inches. The associated g load is:

$$g = \frac{2(\text{drop height})}{\delta} - 1 = \frac{2(360)}{1.06} = 680 \text{ G} \quad .$$

If, as before, it is assumed that the can experiences the full g load, the impact force is:

$$F_{I_{top}} = g(w_2 + w_3) = 680(44.8 + 26.5)$$

$$= 48,500 \text{ pounds} \quad .$$

The compressive stress in the can wall is:

$$\sigma_{I_{top}} = \frac{F_{I_{top}}}{A} = \frac{48,500}{2.90} = 16,700 \text{ psi} \quad .$$

The margin of safety is:

$$MS = \frac{F_{cy}}{\sigma_{I_{top}}} - 1 = \frac{35,000}{16,700} - 1 = 1.10 \quad .$$

In addition, the end impact will produce a shock wave pattern which will travel the length of the can. The inner container can be represented by a bar with free ends. For the condition of an end impact, Roark[8] shows that the stress produced is:

$$\sigma_{dy} = v\sqrt{\frac{\rho E}{386.4}}$$

where:

σ is the stress produced by the traveling wave induced by the end impact

v is the relative velocity between the impacting body and the inner container

ρ is the density of the inner container material $= 0.29$ pound per inch^3 .

E is the elastic modulus of the inner container
$= 29 \times 10^6$ psi .

The velocity can be represented by:

$$v^2 = v_o^2 + 2as$$

where:

v_o is the initial velocity before free fall = 0

a is the acceleration of gravity = 32.2 fps^2 = 386.4 ips^2

s is the fall distance = 30 feet = 360 inches .

Then

$$v = \sqrt{0 + (2)(386.4)(360)}$$

$$= 528 \text{ ips}$$

It should be noted this is conservative in that no credit is taken for energy absorption in the deformation of the cask.

Substituting above:

$$\sigma_{dy} = 528 \sqrt{\frac{(.286)(29)(10^6)}{386.4}}$$

$$\sigma_{dy} = 77{,}300 \text{ psi}$$

This stress will initially be a compressive stress traveling with the wave front. If it is conservatively assumed that no internal damping occurs, the wave will rebound from the opposite (free) end and produce a tensile stress of equal magnitude traveling behind the rebounding shock wave. Thus, if no credit is taken for internal damping, the maximum tensile stress which the inner container could experience is 77,300 psi.

It has been shown that materials under dynamic load exhibit greater apparent strength than under static loads. For austenitic stainless steels, Brown and Edmonds[9] indicate that the dynamic yield strength is about 11 percent greater than the static yield strength. If it is assumed that the ultimate strength exhibits a similar relationship, the dynamic ultimate strength will be:

$$F_{TU_{dy}} = (1.11)(F_{TU}) = (1.11)(75{,}000)$$

$$= 83{,}200 \text{ psi} \quad .$$

The margin of safety is:

$$MS = \frac{F_{TU_{dy}}}{\sigma_{dy}} - 1 = \frac{83{,}200}{77{,}300} - 1 = 0.08$$

The condition for an impact on a corner is less severe than a direct end impact since part of the load will be transmitted to the side wall of the cask cavity.

2.10.2 TRIGA Fuel Shipping Assembly

In a letter dated March 10, 1972, additional information was requested by the Division of Material Licensing to support the request by the University of Arizona to transport TRIGA fuel assemblies in the BMI-1 shipping cask. The BMI-1 cask has previously been licensed and the license application concerned the use of a Fuel Shipping Assembly (fuel can) to hold the TRIGA fuel assemblies in the cask during transport, University of Arizona, Drawing 1020, Rev. B. The request for additional information concerned substantiation of the fuel can integrity in the event of the 30 foot free fall hypothetical accident, confirmation in the use of specific sealant materials and a request for a copy of the report upon which the criticality analyses were based.

2.10.2.1 Free Drop

In a telephone conversation with the DML reviewer, clarification was obtained of the specific questions underlying some of the items noted in the request for additional information. It was noted that for the 30 foot free fall incident, the cask impact forces calculated by DML during their review differ slightly from those presented in the Safety Analysis Report for the cask. For the purpose of consistency, the impact forces determined by DML are used in this response. They are presented in Table 2.3. It should be noted that the impact forces presented in Table 2.3 are those calculated to exist at the outer surface of the cask in the region of impact. No credit is taken for energy attenuation through the walls of the cask and at the interface of the cask cavity and the fuel can. This conservative approach is taken since the exact degree of attenuation cannot be accurately predicted.

TABLE 2.3 IMPACT FORCES USED IN ANALYSES FOR FUEL CAN INTEGRITY

Orientation	Impact Force, G
End Fall, on top	87.5
End Fall, on bottom	368
Side Fall	400
Corner (oblique)	153

(a) Top End

The cover plate of the fuel can has been modified as shown on the attached University of Arizona drawing, Sheet 1020, Revision B. A solid ring of rectangular cross section has been added at the outer edge of the cover to support the edge of the cover in the event of a top impact. Since the ring thickness is the same as the head of the draw bolt, the bolt and the ring will strike the end of the cavity simultaneously in the event of a top end impact. In order to evaluate the stresses on the fuel can, in the event of a top end fall incident, the can was modeled and analyzed with the aid of a computer program MONSA (Multilayer Orthotropic Nonsymmetric Shell Analysis), used by the Applied Solid Mechanics Division at Battelle. This program, based on the work of Dr. A. Kalnins, is discussed briefly in Section 2.12.3. A paper by Dr. Kalnins which is the basis for the computer program is also included in Section 2.12.3.

The can is sketched in Figure 2.3 and the model used in the analyses for the top end impact incident is presented in Figure 2.4. Because of the massiveness of the anchor nut relative to the thickness of the bottom, a fully fixed condition was assumed for the can bottom at the location of the anchor nut. The stresses in the can bottom and walls were analyzed by superimposing the effect of the static load of the draw bolt and the inertia load of the can and comparing the result with the effect of the static load and inertia load of the draw bolt. A seal load of 10 pounds per inch is usually considered adequate for the type of seal used on the fuel can. However, as an extra assurance factor, a seal load of 20 pounds per inch has been selected. This would require a draw bolt tensile load of 945 pounds. The operations manual was revised to indicate that the bolt should be tightened to a torque of 22 feet/pounds, which will result in about 1,000 pounds of tensile load in the bolt (~21 pounds per inch, seal load).

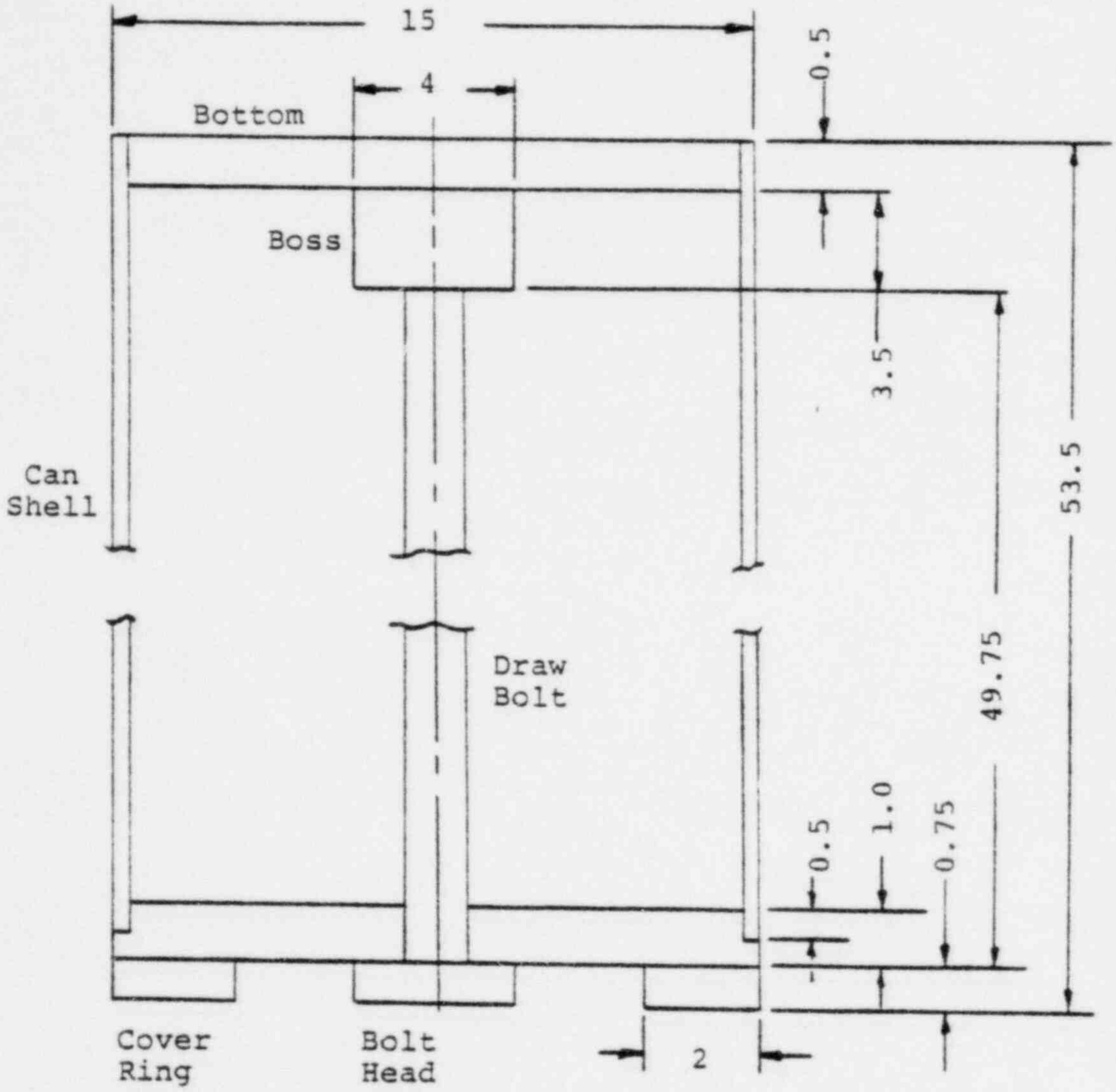

FIGURE 2.3 SKETCH OF FUEL CAN FOR THE TRANSPORT OF TRIGA FUEL ASSEMBLIES

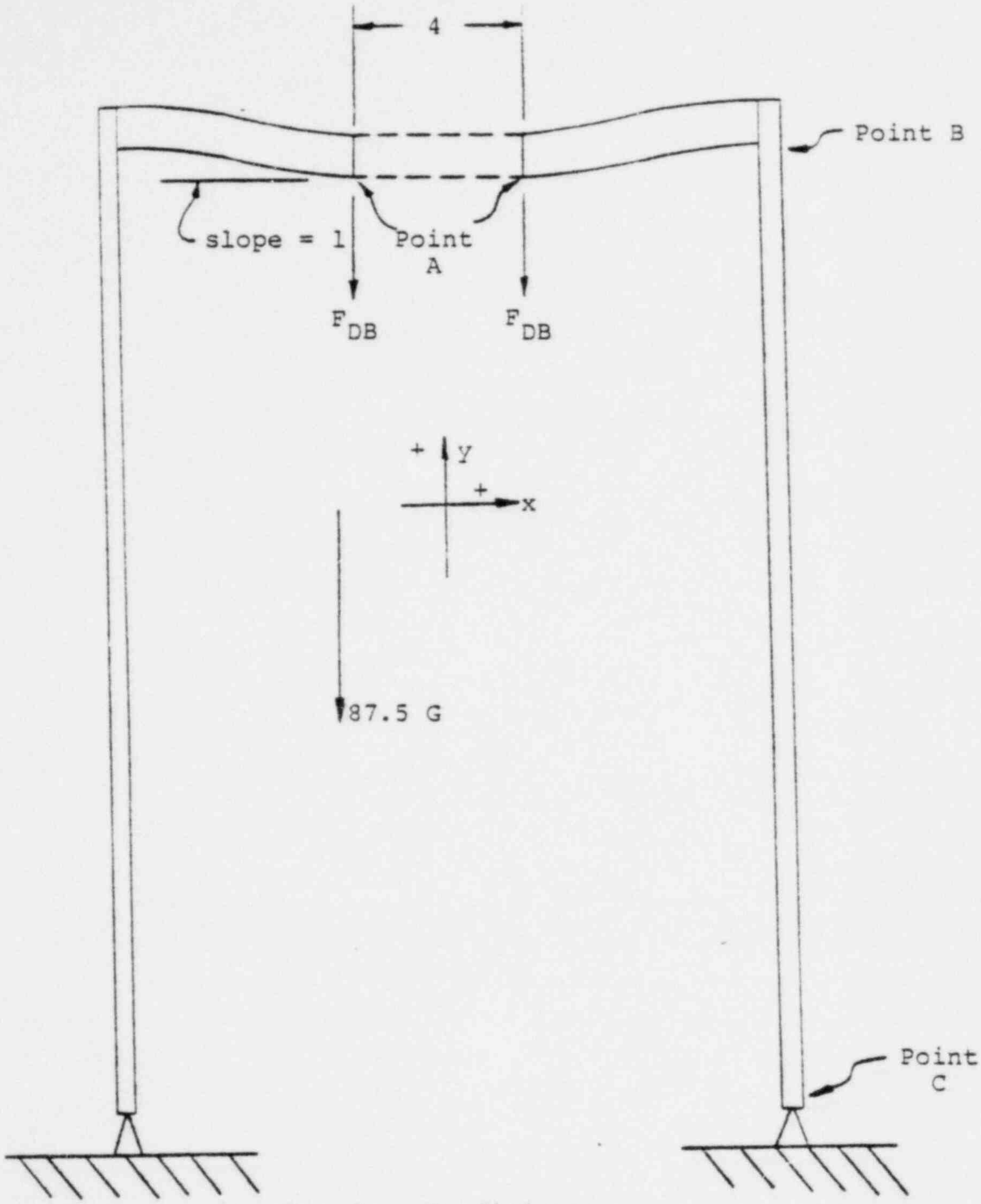

<u>Boundary Conditions</u>

At Pt. A Displacement x = 0
Slope = 0

At Pt. C Displacement y = Displacement x = 0
Moment = 0

FIGURE 2.4 MODEL OF FUEL CAN FOR TOP END FALL ORIENTATION

The MONSA program was first run for the static condition, i.e., the effect of the 1,000 pounds normal draw bolt load on the can. The results are summarized in Table 2.4. Under an impact condition, the inertial load of the anchor nut and bolt might either increase the load on the can or decrease it depending on the relative deformation between the can and the bolt. It is noted in Table 2.4 that for the 1,000 pound static condition the deformation of the can bottom at Point A is 0.00433. The MONSA computer program was then run to evaluate the effect of the inertia load of the can bottom and walls on the stresses in the can. As shown in Table 2.4, the can bottom at Point A would deflect 0.00607 inches if unsupported by the draw bolt. The total deformation then would be 0.01040 inches.

The deformation of the bolt under static and impact loads can be calculated by the relation:

$$e = \varepsilon L = \frac{\sigma}{E} = \frac{FL}{AE}$$

where

e = total deformation of bolt, inches

ε = unit strain

σ = stress in the bolt

E = Young's Modulus = $29(10^6)$ psi

L = length of the bolt = 49.75 inches

F = static force of 1,000 pounds or impact force at 87.5 G, pounds

A = area of the 1-1/4 OD x 1/4 wall bolt = 0.7854 square inches

g = impact force = 87.5 G .

TABLE 2.4 RESULTS OF ANALYSIS OF TOP END IMPACT ORIENTATION

	At Point A[a]			At Point B[a]		At Point C[a]	
	Stress, psi		Deflection relative to Point G, inches	Stress, psi		Stress, psi	
Load Condition	Inner Surface	Outer Surface		Inner Surface	Outer Surface	Inner Surface	Outer Surface
Static 1,000 lb	5,412	-5,492	-0.00433	-5,333	4,862	472	-943
Inertia of can bottom and can walls only, no restraint from bolt	3,624	-3,715	-0.00607	-6,299	5,317	3,608	-7,217
Total	8,036	-9,207	-0.01040	-11,632	10,179	4,080	-8,160

(a) Refer to Figure 2.4

For the static load condition, the bolt would be elongated 0.00218 inches. For the impact case, it was assumed that the effective force acting at the top of the bolt is equal to half the weight of the bolt plus the weight of the anchor nut. The weight of the bolt is 2.67 pounds per foot, and the weight of the 4-inch-diameter nut is 42.73 pounds per foot. Thus, the total effective force is:

$$F = (1/2)(2.67)(49.75)(87.5)/12$$

$$+ (42.73)(3.5)(87.5)/12 = 1575 \text{ pounds} \quad .$$

Therefore, the total compressive deformation is 0.00344 inches. The effect of the inertia loading on the bolt itself would be to relieve the tensile load on the bolt and place it in a compression. Its total deflection then is 0.00344 + 0.00218 = 0.00562 inches. Since the bolt would only deflect 0.00562 inches and the bottom, if unsupported, would deform 0.01040 inches, the bolt will provide a significant degree of restraint to deformation of the can. Thus, the greatest stress which the can will experience is probably 1/2 to 1/3 the maximum stress of 11,632 psi, shown in Table 2.4. The margin of safety, based on a 30,000 psi yield strength, will be greater than 1.5,

$$(MS = \frac{30,000}{11,632} - 1 = 1.58)$$

The can also acts as a column under compressive loading. By inspection, it is seen that the case for the bottom end impact is more severe than for the top end impact, since the impact force, 368 G, is greater and the cover is heavier than the can bottom. Thus, the column action of the can was not evaluated here.

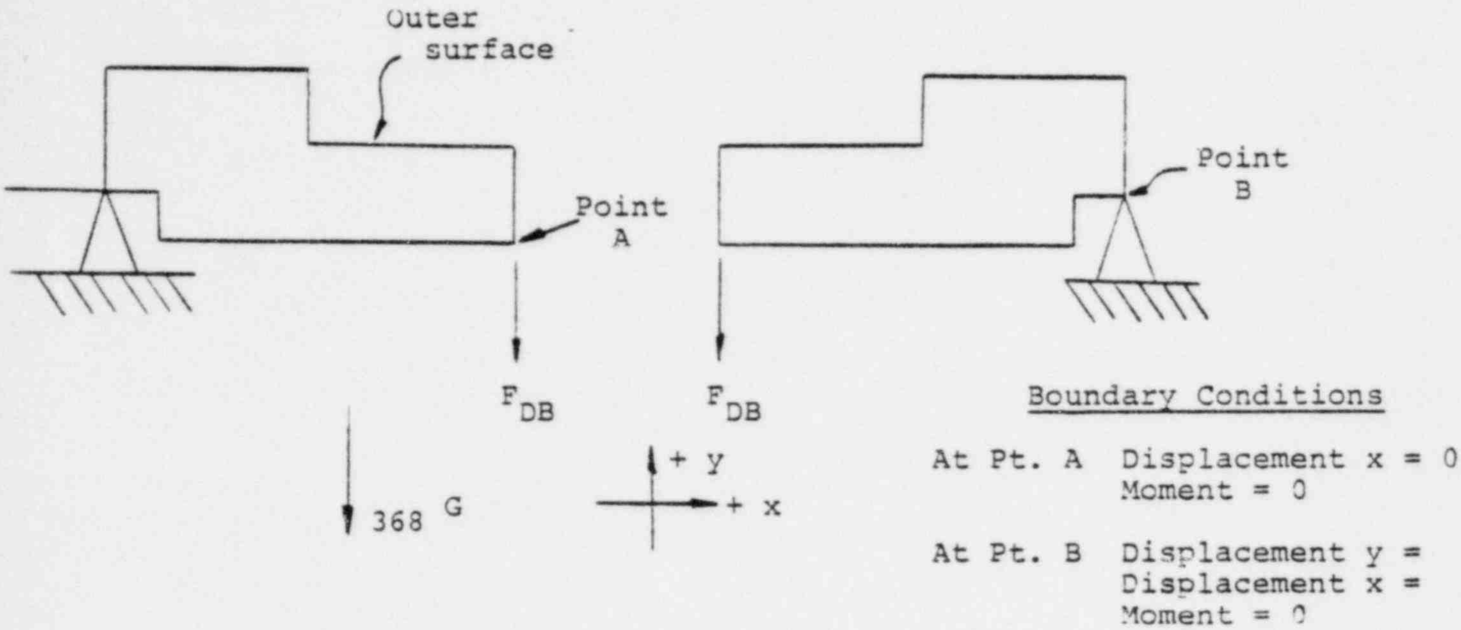

a) Cover

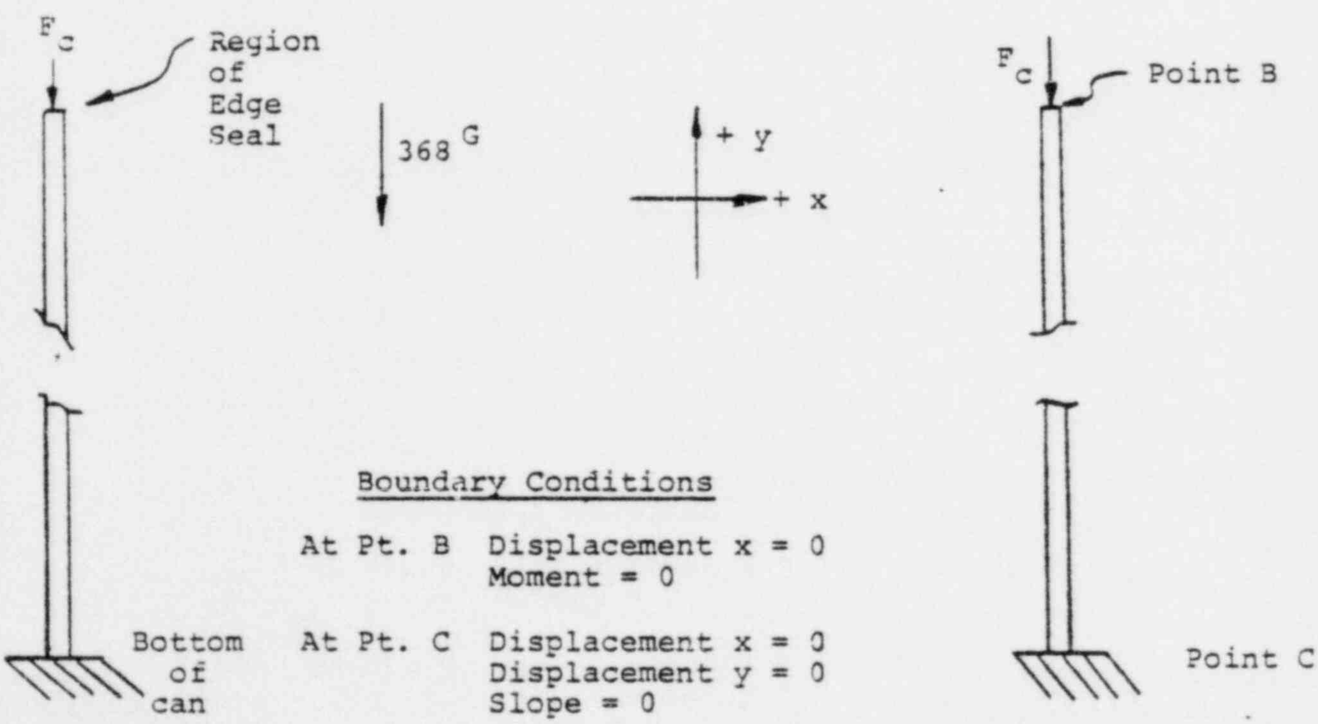

b) Shell

FIGURE 2.5 ANALYTICAL MODEL FOR BOTTOM END IMPACT ORIENTATION

Analyses of the effect of the added load from the can on the draw bolt was not considered necessary. The bolt closely fits through cover and thus misalignment during impact is prevented. Should the bolt experience any plastic deformation during the impact, it would not be detrimental to the seal. Any "shortening" of the bolt due to the impact would produce a greater tensile load in the bolt tending to keep the cover in place. Therefore, the above analyses have indicated that the integrity of the can and seal are maintained during a top end impact condition.

(b) Bottom End

In the event of an impact on the bottom end, the inertia force of the cover will tend to increase the pressure on the seal at the edge of the cover. However, the pressure on the seal under the head of the draw bolt could be lessened. The possibility of this occurring is evaluated below. The MONSA computer program was used to evaluate the model shown in Figure 2.5a for the static condition and for the inertia effect on the cover as if the draw bolt were not present. The maximum deflection of the cover, Point A in Figure 2.5a, relative to the outer seal, Point B, was calculated to be 0.00340 inch under the combined static and inertia load, Table 2.5. The MONSA program was then used to analyze the model of the can shell alone, shown in Figure 2.5b. The force F_c is 1,000 pounds for the static case and, for the impact case, F_c is the total inertia force of the cover acting on the top edge of the can. The cover weighs 65.67 pounds. Thus, for the 368 G inertia load, the force F_c is 24,170 pounds. The total deflection of the shell alone under the static load is 0.00042 inch. Under the inertia load of the cover and the shell, the deflection is 0.01507 inch (Point B to Point C in Figure 2.5b). Thus, the total deflection of the shell only is 0.01549 inch, and the total deflection of the cover, Point A, relative to the bottom of the can Point C, is 0.01889 inch.

TABLE 2.5 RESULTS OF ANALYSIS OF BOTTOM END IMPACT

	At Point A[a]			At Point B[a]			At Point C[a]	
	Stress, psi		Deflection relative to Point B inches	Stress, psi		Deflection relative to Point C, inches	Stress, psi	
Load Condition	Inner Surface	Outer Surface		Inner Surface	Outer Surface		Inner Surface	Outer Surface
Static load on cover only	-423	-1,689	-0.00044	145	36	--	--	--
Inertia load on cover only	1,391	-2,787	-0.00296	1,493	373	--	--	--
Total, static and inertia of cover on cover only	968	-4,476	-0.00340	1,638	409	--	--	--
Static load on shell only	--	--	--	-236	-236	-0.00042	-107	-364
Inertia load of shell and cover on shell only	--	--	--	-5,696	-5,696	-0.01507	-5,146	-17,293
Total, static and inertia of cover and shell on shell only	--	--	--	-5,932	-5,932	-0.01549	-5,253	-17,667

(a) Refer to Figure 2.5

It was shown above that the bolt is elongated 0.00218 inch under the static 1,000 pound load. It was also shown that the bolt will compress axially 0.00344 inch under a 87.5 G load. Thus, under a 368 G load, the bolt will compress (368)(0.00344)/ 87.5 or 0.01466 inch. Thus, the total deflection which the bolt will experience is 0.00218 + 0.01446 = 0.01664 inch. Since this is less than the deflection of the cover, the bolt does not contribute any load to the cover under the impact condition. These calculations indicate that the compression on the seal under the bolt head will be relieved 0.00225 inch. However, the seal is initially compressed about 0.030 inch so that this amount of relief under impact represents only about 7.5 percent of the initial amount. Stated another way, the O-ring is still compressed over 90 percent of its initial amount which is considered sufficient to maintain the seal.

The maximum stress in the can, Table 2.5, is 17,667 psi. The margin of safety is:

$$MS = \frac{30,000}{17,667} - 1 = 0.70 \quad .$$

The can also acts as a column under a compressive load equal to the inertia weight of the cover and can shell. It was assumed that the total inertia load experienced by the can as a column is equivalent to the cover weight and half of the inertia "weight" of the shell. From above, the inertia weight of the cover is 24,170 pounds. The static weight of the shell is 63.27 pounds. Thus, total inertia load on the can shell as a column is:

$$P = 24,170 + (1/2)(368)(63.27) = 35,810 \text{ pounds} \quad .$$

The critical buckling load for a column rigidly fixed at one end is:

$$P_{crit} = \pi^2 EI/4L^2 \quad ,$$

where

E = Young's Modulus = $29(10^6)$ psi

I = Moment of inertia = $\pi d^3 t/8$

d = Mean diameter = 14.91 inches

t = Thickness = 0.09 inches

L = Length = 51.75 inches .

Then

$$P_{crit} = 3.13(10^6) \text{ pounds} \quad .$$

Thus, the can will not buckle.

As above, any deformation or shortening of the draw bolt due to the impact incident would not be detrimental to the integrity of the seal. Therefore, it was not considered necessary to evaluate the impact effect on the bolt.

(c) Side Drop

The safety analysis report for the BMI-1 shipping cask indicated that the impact force on the cask in the region of contact between the cask and the unyielding surface may be as great as 400 G. The impact force on the basket and contents of the cask may be only 200 G or less, due to attenuation by the lead filled cask wall and the interface between the cask cavity and the basket. The degree of attenuation is difficult to predict, however, and thus, for purposes of analysis, the impact force on the basket was conservatively assumed to be the same as that calculated for the exterior of the cask, 400 G.

For the side impact orientation, the side of the can and the cover are supported by the full length of the cask cavity. Thus, the critical regions which must be considered include the stress and deflection in several regions of the draw bolt and the integrity of the seal under loads and moments transmitted by the bolt. A general schematic model of the can is shown in Figure 2.6. As shown, the bolt is rigidly supported at the bottom by the anchor nut, and at the top by the close fitting hole in the cover. It also nominally has a center support, the spacer can bottom, except that the spacer can has a 0.031 inch radial clearance and thus, the center of the bolt could deflect about 0.036 inch (the spacer can guide clearance plus the bolt clearance) before any degree of support could be expected.

Consider the model in Figure 2.7. The bolt is represented as a beam under a tensile load, restrained at the ends from bending and with a center support available after 0.036 inch of deflection. In the actual situation, the "center" support is about 1.38 inches from the midlength of the bolt. For purposes of analysis, it was considered sufficiently accurate to assume that deflections at the center and 1.38 inches from the center were essentially the same. Then from Roark[10], Table VI, Case 18, the deflection at the center is:

$$y = \frac{wl^2}{8p}\left[\frac{4U(1 - \cosh U/2)}{\sinh U/2} + U^2\right] .$$

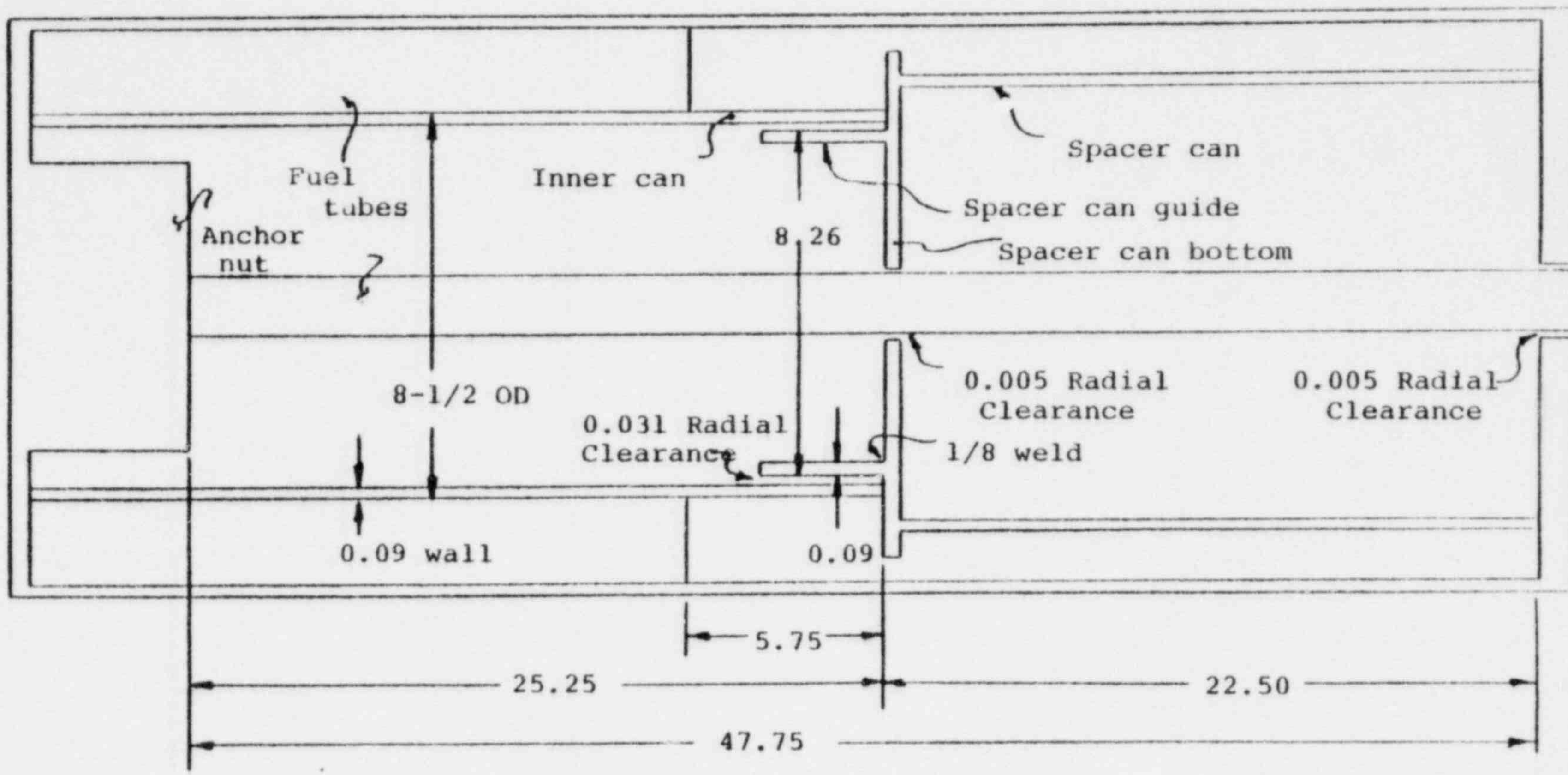

FIGURE 2.6. SCHEMATIC OF FUEL CAN FOR SIDE IMPACT ORIENTATION

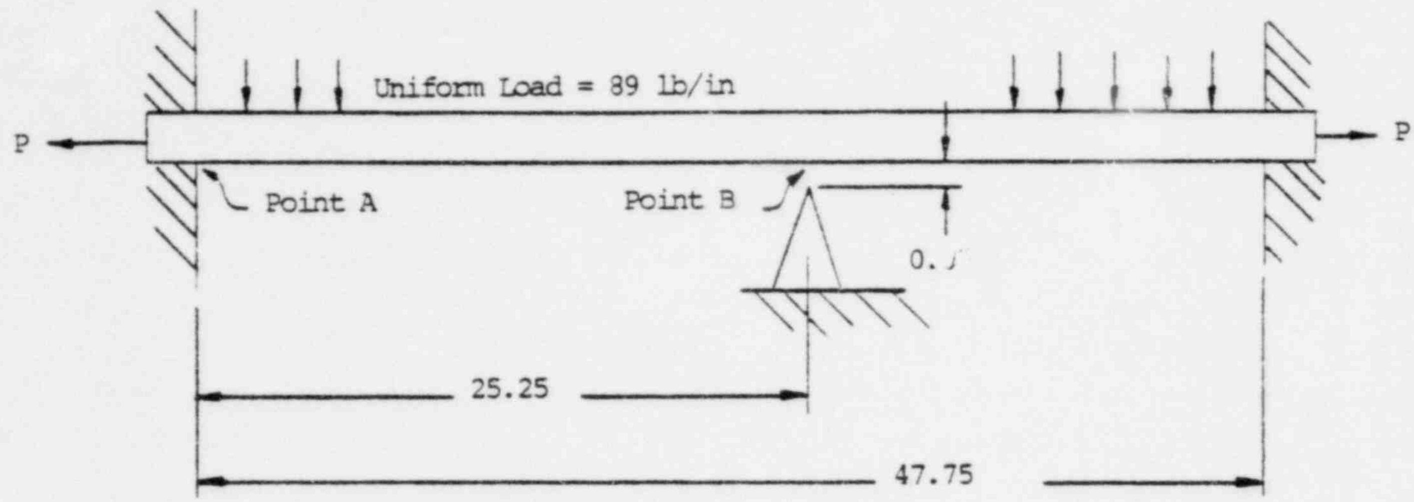

FIGURE 2.7. MODEL OF DRAW BOLT FOR SIDE IMPACT ORIENTATION

where

w = uniform load

$j = \sqrt{\frac{EI}{P}}$

E = Elastic modulus = $29(10^6)$ psi

I = Area moment of inertia = $\pi(D_o^4 - D_i^4)/64$

D_o = OD of draw bolt = 1.25 inches

D_i = ID of draw bolt = 0.75 inch

P = Tensile load = 1,000 pounds

$U = L/j$

L = Length of the bolt = 47.75 inches .

This equation was solved for w for the case where y = 0.036. At this deflection, w = 8.19 pounds per inch. However, the bolt weighs 2.67 pounds per foot and therefore, under a 400 G impact force, the distributed load would be 89.0 pounds per inch. Since this is more than the 8.19 pounds per inch distributed load required to deflect the center of the bolt 0.036 inch, the bolt will receive support from the spacer can bottom under the 400 G impact. The maximum moment in the bolt occurs at the end and is expressed as:

$$M = wj^2 \left[(U/2)/\tanh U/2 - 1 \right] .$$

With a distributed load of 8.19 pounds per inch, the moment is 1,538 inch pounds.

After the bolt receives support from the spacer can bottom, it then, for practical purposes, will respond as before, a beam with fixed ends and under a tension load. This is not truly the case since the "center" support is not truly at the midspan but 1.38 inches away. However, it is felt that negligible error will be introduced by this assumption. The calculation is as above then, except that the uniform load and the beam length are changed. The uniform distributed load for this case is the difference between the total impact load under the 400 G force, 89.0 pounds per inch, and the distributed load of 8.19 pounds per inch required to bring the draw bolt into contact with the spacer can bottom. Thus, w = 89.0-8.19 = 80.81 pounds per inch. The length of the beam is the distance from the spacer can bottom to the bottom of the can, Point A in Figure 2.7. Thus, L = 25.25 inches. Then, M = 4,278 in pounds. The total moment at the end of the draw bolt is the sum of this moment and the moment produced at the instant of contact of the draw bolt with the spacer can bottom. Thus, M_{ToT} = 1,538 + 4,278 = 5,816 in pounds. The fiber stress is:

$$\sigma = M_{tot}C/I$$

where

C = maximum fiber distance from neutral axis of the 1-1/4 inch bolt in end of draw bolt (at thread root) = 0.5335 inches

I = moment of inertia of 1-1/4 inch bolt at tread root =

$\pi C^4/4$.

Then the fiber stress is

$$\sigma_{fm} = 48{,}770 \text{ psi} \quad .$$

The fiber stress developed by the 1,000 pound tensile load in the bolt is:

$$\sigma_{ft} = P/A$$

where

P = 1,000 pounds

A = area of the 1-1/4 inch bolt at the thread root = 0.8942 square inch .

Then

$$\sigma_{ft} = 1,120 \text{ psi} \quad .$$

The total fiber stress is:

$$\sigma_f = 48,770 + 1,120 = 49,890 \text{ psi} \quad .$$

The shear stress is:

$$\sigma_{sh} = \frac{F_{sh}}{A} \quad .$$

The shear force, F_{sh}, was taken as half the impact force or

$$F_{sh} = wL/2 = (89.0)(25.25)/2 = 1,125 \text{ pounds} \quad .$$

The shear area, A, at the thread root, is 0.8942 square inch.

The shear stress is:

$$\sigma_{sh} = 1,125/0.8942 = 1,260 \text{ psi} \quad .$$

The combined stress is:

$$\sigma_{comb} = \sqrt{\sigma_f^2 + \sigma_{sh}^2} = 48,790 \text{ psi} \quad .$$

The threaded section of the bolt is made of A 325 steel which has a yield strength of 92,000 psi. The margin of safety is:

$$MS = \frac{F_y}{\sigma_{comb}} - 1 = \frac{92,000}{48,790} - 1 = 0.89 \quad .$$

At the center of the span, the bending moment is:

$$M = wj^2\left(1 - \frac{U/2}{\sinh U/2}\right)$$

where the terms are defined as above. At the instant of contact of the draw bolt with the spacer can bottom, the moment at the center of the 47.75 inch long span is 758 inch
loading beyond this point, the support at the center causes the location of the maximum moment to shift toward the center of the two short spans. The maximum load experienced by the short spans is the total inertia load. Thus, w = 89.0 pounds per inch and L = 25.25 inches. Then:

$$M = 2,350 \text{ inch/pounds} \quad .$$

The stress is:

$$\sigma_f = Mc/I \quad ,$$

where

M = 2,350 inch/pounds

c = Maximum fiber distance = 1.25/2 = 0.625 inches

I = Moment of inertia = $\pi(D_o{}^4 - D_i{}^4)/64$

D_o = 1.25 inches

D_i = 0.75 inch .

Then

$$\sigma_f = 12,260 \text{ psi} \quad .$$

The body of the bolt is made of C-1018 cold rolled carbon steel which has a yield strength of 60,000 psi. The margin of safety is:

$$MS = \frac{60,000}{12,260} - 1 = 3.89 \quad .$$

The above analyses assume that the center support, i.e., the spacer can bottom will not move radially more than about 0.036 inch. The spacer can is supported by the guide tube which fits into the inner can. The inner can is rigidly held by the nest of fuel tubes except for the endmost 5.75 inches into which the spacer can guide fits. This 5.75 inch extension, therefore, acts as a cantilever beam in supporting the spacer can bottom. Consider the model of Figure 2.8. The fiber stress in the inner can is:

$$\sigma = \frac{MC}{I} = \frac{FLc}{I} \quad ,$$

where

F = Inertia force of bolt and spacer can
L = Length of inner can extension = 5.75 inches
c = Maximum fiber distance = 4.25 inches
I = Moment of inertia = $\pi d^3 t/8$
d = Mean diameter = 8.41 inches
t = Thickness = 0.09 inch .

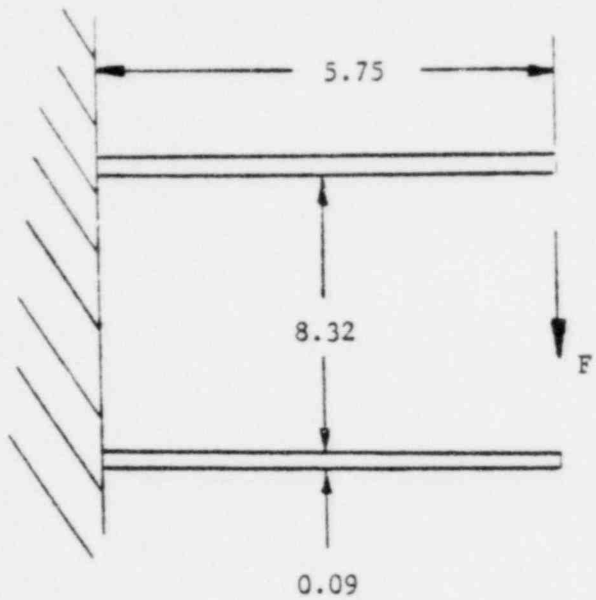

FIGURE 2.8 MODEL OF INNER CAN

The force was taken as half the inertia weight of the bolt and 3/4 the inertia weight of the spacer can. The spacer can has a static weight of about 35 pounds. Then the inertia force is:

$$F = (89.0)(47.75)/2 + (400)(35)(3/4) = 12{,}620 \text{ pounds.}$$

Then

$$\sigma_f = 14{,}680 \text{ psi} \quad .$$

The shear stress is

$$\sigma_{sh} = F/A = 12{,}620/(\pi dt) = 5{,}300 \text{ psi.}$$

The combined stress is

$$\sigma_{comb} = \sqrt{\sigma_f^{\,2} + \sigma_{sh}^{\,2}} = 15{,}600 \text{ psi} \quad .$$

The margin of safety for the inner can which is made of Type 304 stainless steel is

$$MS = \frac{F_y}{\sigma_{comb}} - 1 = \frac{30{,}000}{15{,}600} - 1 = 0.92 \quad .$$

The total deflection is:

$$y = FL^3/3EI = 0.0013 \text{ inch} \quad .$$

Thus, the spacer can will move 0.0013 inch more than the 0.036 inch assumed above. This difference is only 3.6 percent and thus will not significantly change the results presented above.

The integrity of the weld between the spacer can guide and the spacer can bottom must also be evaluated. The stress is:

$$\sigma_{sh} = F/A = 12{,}620/(0.707\pi dt) \quad ,$$

where

d = mean weld diameter ≅ 7.90 inches

t = weld thickness = 0.12 inch .

Then

$$\sigma_{sh} = 5{,}990 \text{ psi} \quad .$$

The margin of safety is

$$MS = \frac{F_{sh}}{\sigma_{sh}} - 1 = \frac{15{,}000}{5{,}990} - 1 = 1.50 \quad .$$

In the side fall incident, the bending moment present in the bolt at the cover will tend to "lift" one edge of the seal. The close fit of the bolt in the cover negates any possibility of "lifting" of the seal under the bolt head. However, the tendency for lifting of the seal at the edge of the cover must be evaluated. Consider the model in Figure 2.9. The moment, M, tends to lift the seal at Point B while the moment of the draw bolt tensile force, P, about Point A tends to maintain the seal at Point B. The moment, M, is assumed to be the same as the moment in the draw bolt at the anchor nut. (It actually will be slightly less since the unsupported span of the top part of the bolt is 2.75 inches shorter than the bottom part.) Then, M = 5,816 in pounds. The restoring moment is:

$$M_R = Pd/2 = (1{,}000)(15/2) = 7{,}500 \text{ inches/pounds} \quad .$$

This is about 30 percent greater than the moment tending to open the seal. Thus, the tendency for lifting is sufficiently restrained to maintain the seal.

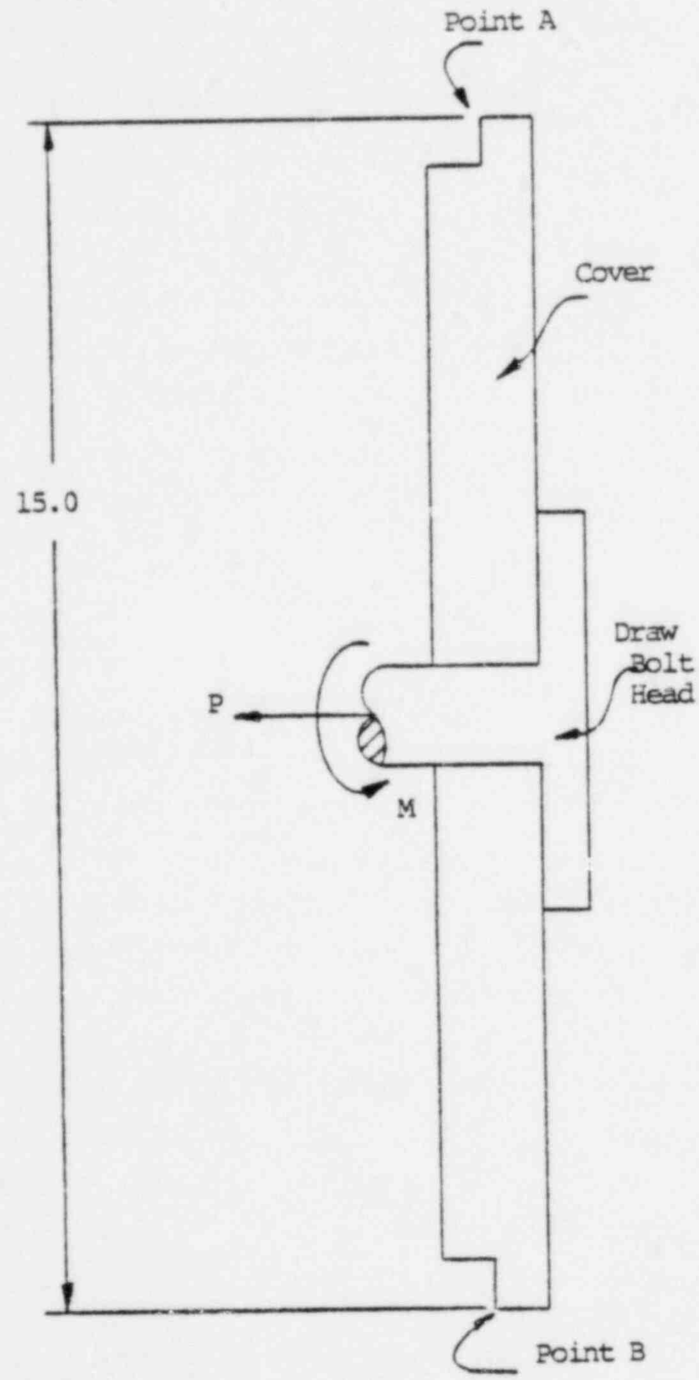

FIGURE 2.9. MODEL OF FUEL CAN COVER FOR SIDE IMPACT ORIENTATION

The conclusion of the above analysis is that the integrity of the fuel can and seal is maintained in the event of a side fall impact orientation.

(d) Corner Drop

The fuel can fits in the cask cavity with only nominal clearance. Thus, for the corner drop orientation, the can is supported both on the side and an end. Since the impact loads for the corner drop orientation are less severe (153 G) than for the impact loads for the bottom end drop or side drop configurations, the analyses for the bottom corner drop configuration need not be evaluated. For the case of a top corner impact orientation, the 153 G impact force is greater than that experienced by the cask for the top end drop configuration, 87.5 G. However, the aspect ratio of the cask (L/d) is relatively large; thus, the top edge drop orientation is very close to the vertical orientation of the end fall condition. The response of the fuel can to a top corner impact orientation can then be evaluated by taking the conservative approach and assume it strikes on the top end with the 153 G impact force. This is conservative since for the end impact orientation, no support is considered by the side walls of the cask cavity.

The response of the fuel can is proportional to the impact load. Since for the assumed case here the impact force is 153 G, the stresses and deflections experienced by the fuel can would be 153/87.5 = 1.75 times greater than for the case of the top end drop orientation. By inspection, it is seen that the stresses are well below the yield stress and thus, the can integrity is maintained. Similarly, by inspection it is seen that the seals will not be loosened for the top corner impact orientation and thus seal integrity is maintained.

2.10.2.2 Description of Welds on Fuel Element Tubes

The fuel elements are located in individual tube positioners for transport. These tubes are located in an annular region between the outer shell of the fuel can and an inner shell. Both the inner and outer shells are welded to the bottom plate of the fuel can with full circumferential welds, Drawing 1020, Rev. B. The tubes are held in place by the manner in which they fit in the annulus so that contact with adjacent tubes and the inner or outer shell of the fuel can prevents any relative motion between the tubes. The tubes in the annulus are attached to the bottom plate by one 0.090 inch wide x 0.50 inch long welds as shown in Figure 2.10. At the top of the tubes, each tube is welded to the adjacent tubes which touch it and to the inner or outer shell, Figure 2.10. Since each tube in the inner row of tubes contacts four other tubes and the inner shell, it has five welds, ~0.180 inch wide x 0.38 inch long around its top edge. Each tube in the outer row, touches two tubes in the inner row and the outer shell and thus, is welded at three locations, Figure 2.10.

2.10.2.3 O-Ring Material

All applicable drawings and operation procedures have been revised to reflect the use of only silicone rubber (silastic) seal materials.

2.10.2.4 Thread Sealant

There are no plugs on the fuel can which form part of the sealing system.

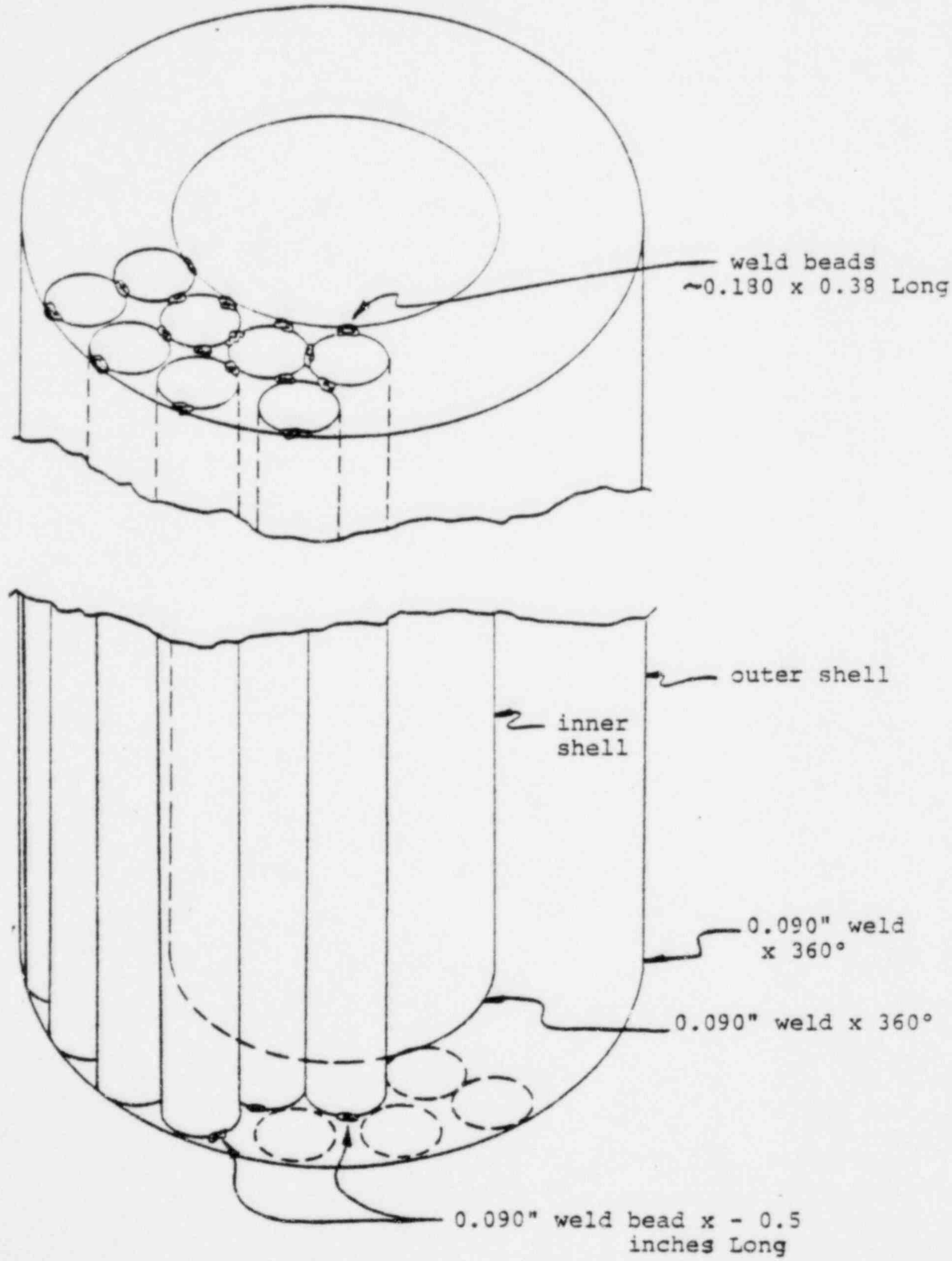

FIGURE 2.10 LOCATION OF FUEL TUBES IN FUEL SHIPPING CANNISTER.

2.10.3 Pulstar Fuel Pin Canister

Twenty-one irradiated fuel pins (ref. Westinghouse Canada, Ltd., Drawing 818C199) are loaded in a stainless steel tube. Twelve such canisters are loaded in a modified BMI-1 basket for shipment to the Idaho Chemical Processing Plant and subsequent storage in a pool. The loaded canisters are to be shipped in water. Each group of 21 pins weighs approximately 38 pounds.

The material selected for the canisters is 3 inches square, .120 inch wall, Type 304 stainless steel tubing. The design of the canister is shown on BCL Drawing Number 00-001-375. The base and cap plates are 3/16 inch, 304 S.S. plate as is the hoist fitting.

The canisters are analyzed for a 5 g handling load. Since they are transported in the BMI-1 basket, other transportation loads are analyzed as basket loads. The canisters are shipped dry and are sealed with Swagelock® fittings, Type SS-1610-C. The total weight of each canister and fuel is calculated to be 50.4 pounds. The total load in the basket is approximately 604.8 pounds.

2.10.3.1 Hoist Fitting

The load factor = 5.0 g

The maximum shear-out load on a canister hoist fitting = (50.4)(5.0) = 252 pounds.

Allowable shear stress (annealed value) = 20,000 psi.

Shear-Out of the Hoist Fitting.

$$\text{Shear area} = (2)(.95)(.125) = .238 \text{ inch}^2$$

$$fs = \frac{252}{.238} = 1,059 \text{ psi}$$

$$MS = \frac{20,000}{1,059} - 1 = 17.89 \quad .$$

2.10.3.2 Shear Load on Base Plate Weld

The base plate is welded to the 3 inch square tubing for a total of 12 inches of weld. Based on the annealed value for 304 SS, the allowable shear stress = 20,000 psi.

Width of weld = .06 inch minimum

The shear area = $(12)(.06)(\sqrt{2}) = 1.02 \text{ inches}^2$

Assume total weight acting on base = 50.4 pounds

Shear stress = $\frac{P}{A} = \frac{(50.4)(5)}{(1.02)} = 247$ psi

$MS = \frac{20,000}{247} - 1$ = very high .

2.10.3.3 Pressure Check of Stress and Deflection

Square Tubes x $\frac{1}{M}$ 3 inches x 3 inches x .12 inch 304 S.S.

Internal Pressure = 37 psig[11]

Test pressure = 120 x 37 = 44.4 psig .

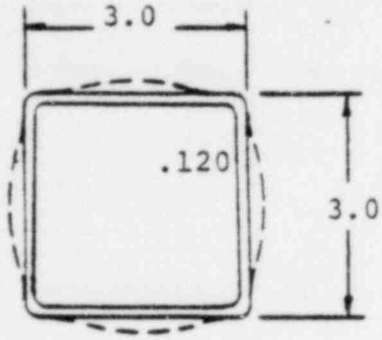

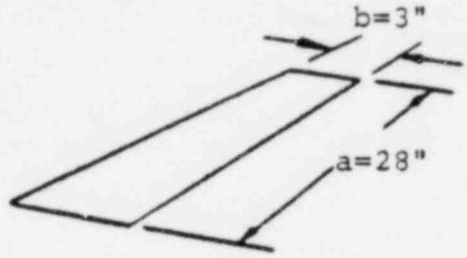

Assume all edges fixed--uniform load 44.4 psig:

$$\frac{a}{b} = \infty$$

$$\therefore \beta = .5 \text{ (Reference 12)}$$

$$\alpha \quad .0284 \quad .$$

The maximum stress occurs at the center of the long edges:

$$S_{max} = \beta\frac{wb^2}{t^2} = (.5)\ \frac{44.4(3^2)}{(.120^2)}$$

$$= 13875 \text{ psi} < 30{,}000 \text{ psi 304 SS yld.}$$

(annealed value)

$$y = \alpha\frac{wb^4}{Et^3} = (.0284)\ \frac{44.4(3^4)}{(28 \times 10^6)(.120^3)} = .00203 \text{ inch} \quad .$$

= .00203 inch each side of canister

2y = .00406 inch--well within space available of 0.31 inch .

Equivalent pressure load due to side drop imposed by fuel pins.

$w = 37.8$ pounds x 5 g's = 189 pounds .

Area of pin impact--assume 2.5 x 26 inches .

$A = 2.5 \times 26 = 65$ inches^2

$P = \frac{189}{65} = 2.91$ psi .

The wall deflection due to the pin load is negligible.

The total side presusre load = 44.4 + 2.9 = 47.3 psi.

$\therefore S_{max} = 13875 \frac{(47.3)}{(44.4)} = 14781$ psi, one side only

$y_{max} = .00196 \frac{(47.3)}{(44.4)} = .0021$ inch, one side only

$2y = .0042$ inch .

Internal pressure on end of tube:

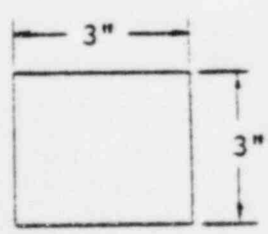

p = 44.4 psig

$\frac{a}{b} = 1$, $\beta = 0.3078$, $\alpha = 0.138$

$$Sb = \beta\frac{wb^2}{t^2} = (0.3078)\frac{(44.4)(3^2)}{(.1855)^2}$$

$$= 3{,}499 \text{ psi}$$

$$\text{Max } y = \alpha\frac{wb^4}{Et^3} = (0.138)\ \frac{(44.4)(3^4)}{(29 \times 10^6)(.1875)^3}$$

$$= .0026$$

Bottom load due to weight of 21 fuel pins:

$$w = (37.8)(5.0 \text{ gs}) = 189 \text{ pounds}$$

$$\text{Area} = 2.75 \times 2.75 = 7.5625^2$$

Equivalent pressure load $p = \frac{189}{7.5625} = 25$ psi

$$S_b = (3{,}499)\ (\frac{25}{44.4}) = 1{,}970 \text{ psi}$$

$$\text{Total } S_b = 3{,}499 + 1{,}970 = 5{,}469 \text{ psi}$$

$$\text{Max } y = .0026\ \frac{(25)}{(44.4)} = .0015 \text{ inch}$$

$$\text{Total } y = .0026 + .0015 = .0041 \text{ inch in center}$$

2.10.4 EPRI Crack Arrest Capsules

The six fission monitors consist of 0.25 inch OD x 0.38 inch long stainless steel tubes containing either 12 mg of U^{238} (3 monitors) or 20 mg of Np^{237} (3 monitors). Each tube is sealed and fits into a steel dosimeter block which is sealed by welding. Because of the way in which the fissile material is encapsulated, release into the cask cavity or to the environment is extremely remote. Moreover the quantities are much less than the maximum release permitted by the proposed regulations(13). The amount of U^{238} present is $1.2(10^{-8})$ curies and the amount of Np^{237} present is $4.2(10^{-5})$ ci. The maximum which can be released according to the proposed regulations is unlimited for U^{238} and 0.005 Ci for Np^{237}.

2.11 Baskets

2.11.1 Copper Basket for Fermi Fuel Elements

The BMI-1 cask was approved in July, 1964, and given AEC License SNM807 for use in transporting to a reprocessing site 24 spent BRR fuel elements per trip. Information regarding this structural analysis is recorded in Docket Number 70-813 at the AEC.

For the shipment of the Fermi fuel only a different fuel element basket and basket support are required. Drawing Number K5928-5-1 0049 Rev. 5/12/66, describes this modification. The entire assembly inside the cask including the fuel element, basket, and copper shield, has a calculated weight of 1,109 pounds. This assembly is supported by 12, 1/4 inch x 1-1/2 inch x 1-1/2 inch brass angles that extend the entire length of the cask cavity. The yield strength of the architectural bronze used in the angles is

20,000 psi. The cross sectional area of the 12 angles is 8.4 inches^2. Since all the side thrust is taken by the cask wall, only the compressive load must be supported by the angles. Thus, the normal stress on the supporting angles is 132 psi. If the loaded cask were to be subjected to some accident condition which would cause the angles to yield, the force on the fuel subassembly would be decreased and the unit displaced toward the point of contact. Axial motion of the unit in the cask should cause no damage to the fuel subassembly. All radial forces would be adequately restricted by the six, 0.75 inch x 2 inch x 36 inch copper ribs which are part of the copper shielding casting. Each rib would have an area of 27 inches^2 and a yield strength of 10,000 psi. Applying the entire weight of 1,109 pounds to one rib, the normal stress would be 41 psi. From the above description of the modifications inside the cask, it is obvious that the fuel subassembly is well protected within the cask.

2.11.2 BMI-1 Basket Modified for MTR Fuel

The only modifications made for shipment of the fuel from Texas A&M were to the fuel basket. Therefore, the cask itself meets all the structural requirements as shown in current license, SMN7 for the shipment of MTR type fuels. The analyses presented in this section show compliance of the modified basket with the regulations of 10CFR-Part 71. The applicable sections from those regulations affecting licensability of the modified basket are as follows:

Section 71.31(c) General Standards, Lifting Device
Section 71.36(a) Standards for Hypothetical Accident Conditions.

The details of the modified basket for the shipment of fuel from Texas A&M University to the University of Virginia are shown in BMI Drawing Number 00-000-236, Rev. A. The material used in the basket is Type 304 stainless steel. The mechanical properties used in the analysis are presented in Table 2.6.

TABLE 2.6 PROPERTIES OF TYPE 304 STAINLESS STEEL

Property	Design Stress, psi
Tensile yield stress	30,000
Tensile ultimate stress	75,000
Compressive yield stress	35,000
Shear yield stress	20,000
Shear ultimate stress	40,000
Bearing yield stress	50,000

The calculated weight of the modified basket is 269 pounds. Each fuel element weighs approximately 9.25 pounds.

2.11.2.1 Lifting Devices

The regulations state that the lifting devices should be able to support three times the weight of the loaded basket. This weight is calculated as 3(380 pounds) = 1,140 pounds. Assuming a 45 degree angle for the lifting cables, the force in each cable is:

$$T = \frac{W}{2(.707)} = \frac{1,140}{2(.707)} = 806 \text{ pounds} \quad .$$

The bending stress at the root of the handle can be calculated as:

$$S_b = Mc/I \quad ,$$

where

M = bending moment = (6.75)(.707)(W) inch/pounds
C = distance from neutral surface = .339 inch
I = moment of inertia of area = .7037 inch^4

$$S_b = \frac{(6.75)(.707)(806)(.339)}{.0737} = 17,700 \text{ psi} \quad .$$

The tensile stress can be calculated as:

$$S_t = \frac{P}{A} = \frac{(806)(.707)}{.625 \text{ inch}^2} = 912 \text{ psi} \quad .$$

The combined stress is therefore:

$$S_{max} = S_b + S_t = 18,600 \text{ psi} \quad .$$

The margin of safety is:

$$MS = \frac{30,000}{18,600} -1 = 0.61 \quad .$$

2.11.2.2 Free Drop

AEC Regulation 10CFR - Part 71, stipulates that the cask must withstand a fall of 30 feet to a hard, unyielding surface. The impact forces resulting from such a fall are presented in Table 2.3.

(a) Top End

In the event of a fall on the top of the cask, the cask would experience a maximum impact force of 87.5 G. It was conservatively assumed that no attenuation to this shock force would occur in the cask and that the basket would, therefore, also experience a force of 87.5 G. In the inverted position, the inertia force of the modified basket would be resisted by the two lifting bars. It is assumed that both bars strike the top of the cavity simultaneously and half of the force is resisted by each bar. Thus, the impact force on one bar is:

$$F = gw = \frac{(87.5\ G)(269\ \text{pounds})}{2} = 11{,}770\ \text{pounds} \quad .$$

The critical buckling load for a column in compression is given by Roark[14] as:

$$P' = \frac{\pi^2 EI}{(0.7l)^2} \quad ,$$

where

P' = critical buckling load, pounds

E = modulus of elasticity, 28×10^6 psi

l = length of bar, 6.75 inches

I = moment of inertia about bending axis = .0737 inch^4 .

$$P' = \frac{\pi^2 (28 \times 10^6)(0.0737)}{[0.7(6.75)]^2} = 9.12(10^5)$$

Since the impact force is 11,770 pounds, by inspection the margin of safety for buckling is large.

The maximum compressive stress on the bar is:

$$S_c = \frac{11,770}{(.625)} = 18,830 \text{ psi} \quad .$$

The margin of safety for yielding in compression is:

$$MS = \frac{35,000}{18,830} - 1 = 0.86 \quad .$$

<u>(b) Bottom End</u>

In the event of a bottom impact, the cask would experience a maximum impact force of 368 G. The 15 inch diameter spacer can must resist the impact force of the rest of the basket and the fuel elements. The combined weight of these two components is 347 pounds. The force which must be resisted by the spacer can is:

$$F = (368)(347) = 128,000 \text{ pounds} \quad .$$

Assuming this force is evenly distributed around the top edge of the can, Roark[15] gives the formula for the critical buckling stress as:

$$S = \frac{1}{\sqrt{3}} \; \frac{}{\sqrt{1-v^2}} \, \frac{t}{r} \quad ,$$

where

E = elastic modulus = $28(10^6)$ psi
v = Poisson's ratio = 0.3
t = wall thickness = 0.12 inch
r = radius of can = 7.5 inches

$$S = \frac{1}{\sqrt{3}} \frac{(29 \times 10^6)}{\sqrt{1-(.3)^2}} \frac{(0.12)}{(7.5)} = 272,000 \text{ psi} \quad .$$

The stress in the can is:

$$S = \frac{128,000 \text{ pounds}}{\pi(15)(0.12)} = 22,600 \text{ psi} \quad .$$

By inspection, the margin of safety for buckling is large.

The margin of safety for yielding in compression is:

$$MS = \frac{35,000}{22,600} -1 = 0.55$$

The potential of the fuel elements for puncturing the 1/2 inch thick stainless steel plate can be evaluated by considering the shear stress produced during impact,

$$\text{Shear strength} = \frac{\text{load for rupture}}{\text{area of material sheared}} \quad .$$

For the case of a fuel rod lower end guide puncturing the 1/2 inch plate, the shear area would be:

$$A = (0.5)(\pi)(2.06) = 3.24 \text{ inches}^2 \quad .$$

The impact load for one fuel element is:

$$F = (368\ G)(9.25 \text{ pounds}) = 3,400 \text{ pounds} \quad .$$

$$\frac{F}{A} = \frac{3,400}{3.24} = 1,050 \text{ psi} \quad .$$

The ultimate shearing strength of stainless steel is 40,000 psi. By inspection, the margin of safety against rupture is large.

The 1/2 inch plate is attached to the spacer can by a continuous weld. The shear stress in this weld can be computed as:

$$S_s = \frac{?}{0.707\ hl} \quad ,$$

where

P = impact load from fuel elements = ngw
n = number of elements = 12
g = impact force = 368 G
w = element weight = ?.25 pounds
h = size of weld, 0.1? inch
l = length of weld = ·(15) .

$$S_s = \frac{(12)(368)(9.25)}{(0.707)(0.18)(15)(\pi)} = 6,820 \text{ psi} \quad .$$

Assuming the ultimate shear stress for the weld to be the same as virgin metal, the margin of safety for shearing the weld is:

$$MS = \frac{40,000}{6,820} - 1 = 4.9 \quad .$$

The ultimate load that the plate can support before collapse is given by Roark[16] as:

$$Wu = Sy(2.814)\pi t^2 \quad .$$

The plate is assumed to have fixed edges since it s welded all around to the spacer can 1-3/4 inches below the rigid bottom of the original basket. It has been shown that the yield strength for impact loading is approximately 11 percent higher than the static yield stress[9]. Therefore, the load that the plate can support is:

$$
\begin{aligned}
Wu &= (30{,}000)(1.11)(2.814)(\pi)(0.5)^2 \\
&= 73{,}500 \text{ pounds} \quad .
\end{aligned}
$$

Since the impact load from the fuel elements is (12)(368)(9.25) = 40,900 pounds, the margin of safety for failure is:

$$MS = \frac{73{,}500}{40{,}900} - 1 = 0.80 \quad .$$

Assuming that the plate does not yield, the maximum deflection is given by Roark[17] as:

$$y_{max} = \frac{3W(m^2 - 1)a^2}{16\pi E\, m^2\, t^3} \quad ,$$

where

W = load = 40,900 pounds

m = reciprical of Poisson's ratio (= 1/0.3)

a = radius of plate (= 7.5 inches)

t = plate thickness (= 1/2 inch)

E = elastic modulus = $28(10^6)$ psi .

$$y_{max} = \frac{3(40{,}900 \text{ pounds})(3.33^2 - 1)(7.5^2)}{16\pi(28 \times 10^6)(3.33^2)(0.5^3)}$$

$$= 0.0357 \text{ inch} \quad .$$

The maximum stress under this loading is:

$$S_{max} = \frac{3W}{4\pi t^2} = \frac{3(40,900)}{4\pi(0.25)} = 39,000 \text{ psi} \quad .$$

This occurs at the outer edge. It is seen that the stress calculated is approximately 17 percent above the yield stress of stainless steel under impact conditions. Therefore, the deflection as calculated above, using equations based on elastic theory, is not exact. However, since the stress calculated is only 17 percent grater than the yield stress, the degree of plastic yielding and thus deflection beyond 0.0351 inches will be small. If the plastic yielding is assumed to increase the deflection by as much as 50 percent, the total deflection of the center of the plate will be about 0.053 inch. It is estimated that the fuel elements can be displaced vertically, about 0.25 inch, without affecting the criticality.

Thus, the margin of safety is about

$$MS = \frac{0.250}{0.053} - 1 = 3.7 \quad .$$

2.11.3 BMI-1 Basket Modified for Pulstar Fuel

The only modifications made for shipment of the fuel from the State University of New York were to the fuel basket. Therefore, the cask itself meets all the structural requirements as shown in current licenses for the shipment of Pulstar type fuels. The analyses presented in this section show compliance of the modified basket with the regulations of 10CFR-Part 71. The applicable sections from those regulations affecting licensability of the modified basket are as follows:

Section 71.31(c)	General Standards, Lifting Device
Section 71.36(a)	Standards for Hypothetical Accident Conditions

The details of the modified basket for the shipment of fuel from the State University of New York to the Idaho Chemical Processing Plant are shown in BMI Drawing Number 00-001-376, Rev. A. The material used in the basket is Type 304 stainless steel. The mechanical properties used in the analysis are presented in Table 2.7.

TABLE 2.7 PROPERTIES OF TYPE 304 STAINLESS STEEL

Property	Design Stress, psi
Tensile yield stress	30,000
Tensile ultimate stress	75,000
Compressive yield stress	35,000
Shear yield stress	20,000
Shear ultimate stress	40,000
Bearing yield stress	50,000

The calculated weight of the modified basket is 345 pounds. Each fuel canister weighs approximately 50 pounds.

2.11.3.1 Lifting Devices

The regulations state that the lifting devices should be able to support three times the weight of the loaded basket. This weight is calculated as (3)(950 pounds) = 2,850 pounds. The force in each cable is 2,850/2 = 1,425 pounds. A spacer bar between the cables is required at this load level to prevent bending at the handles. The tensile stress in the handles is calculated as:

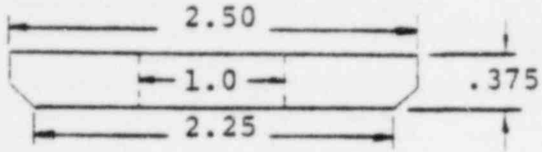

$$S_t = \frac{P}{A} = \frac{1,425}{.50} = 2,850 \text{ psi} \quad .$$

The margin of safety is:

$$MS = \frac{30,000}{2,850} - 1 = 9.52 \quad .$$

2.11.3.2 Free Drop

AEC Regulation 10CFR-Part 71 stipulates that the cask must withstand a fall of 30 feet to a hard, unyielding surface. The impact forces resulting from such a fall are presented in Table 2.3.

(a) Top End

In the event of a fall on the top of the cask, the cask would experience a maximum impact force of 87.5 G. It was conservatively assumed that no attenuation to this shock force would occur in the cask and that the basket would, therefore, also experience a force of 87.5 G. In the inverted position, the inertia force of the modified basket would be resisted by the two lifting bars. It is assumed that both bars strike the top of the cavity simultaneously and half of the force is resisted by each bar. Thus, the impact force on one bar is:

$$F = gw = \frac{(87.5 \text{ G})(345 \text{ pounds})}{2} = 15,094 \quad .$$

The critical buckling load for a column in compression is given by Roark[14] as:

$$P' = \frac{\pi^2 EI}{(0.7L)^2} \quad ,$$

where

P' = critical buckling load, pounds

E = modulus of elasticity, 28×10^6 psi

L = length of bar, 6.75 inches

I = moment of inertia about bending axis = .0737 inch^4 .

$$P' = \frac{\pi^2 (28 \times 10^6)(0.0737)}{[0.7(6.75)]^2} = 9.12(10^5)$$

Since the impact force is 15,094 pounds, by inspection the margin of safety for buckling is large.

The maximum compressive stress on the bar is:

$$S_c = \frac{15,094}{(.625)} = 24,150 \quad .$$

The margin of safety for yielding in compression is:

$$MS = \frac{35,000}{24,150} - 1 = 0.45 \quad .$$

(b) Bottom End

In the event of a bottom impact, the cask would experience a maximum impact force of 368 G. T e 15 inch diameter spacer can must resist the impact force of the rest of the basket and the fuel elements. The combined weight of these two components is 841 pounds. The force which must be resisted by the spacer can is:

$$F = (368)(950) = 349{,}600 \text{ pounds} \quad .$$

Assuming this force is evenly distributed around the top edge of the can, Roark[15] gives the formula for the critical buckling stress as:

$$S = \frac{1}{\sqrt{3}} \frac{E}{\sqrt{1-v^2}} \frac{t}{r} \quad ,$$

where

E = elastic modulus = $28(10^6)$ psi

v = Poisson's ratio = 0.3

t = wall thickness = 0.25 inch

r = radius of can = 7.5 inches

$$S = \frac{1}{\sqrt{3}} \frac{(28 \times 10^6)}{\sqrt{1-(.3)^2}} \frac{(0.25)}{(7.5)} = 566{,}490 \text{ psi} \quad .$$

The stress in the can is:

$$S = \frac{349{,}600}{\pi(15)(0.25)} = 29{,}675 \text{ psi} \quad .$$

By inspection, the margin of safety for buckling is large.

The margin of safety for yielding in compression is:

$$MS = \frac{35{,}000}{29{,}675} - 1 = 0.18 \quad .$$

The potential of the fuel canister for puncturing the 1/2 inch thick stainless steel plate can be evaluated by considering the shear stress produced during impact,

$$\text{Shear strength} = \frac{\text{load for puncture}}{\text{area of material sheared}} \quad .$$

For the case of a fuel canister puncturing the 1/2 inch plate, the shear area would be:

$$A = 2(3) + 2(.125)(0.5) = 3.125 \text{ inches}^2$$

The impact load for one fuel canister:

$$F = (368\ G)(50.4 \text{ pounds}) = 18{,}547 \text{ pounds}$$

$$\frac{F}{A} = \frac{18{,}547}{3.125} = 5{,}935 \text{ psi} \quad .$$

The resistance to shearing of stainless steel is 40,000 psi.[18] The margin of safety against puncture = $\frac{40{,}000}{5{,}935} - 1 = 5.74$.

The 1/2 inch plate is attached to the spacer can by a continuous weld both top and bottom. The shear stress in this weld can be computed as:

$$S_s = \frac{P}{0.707\ hl} \quad ,$$

where

P = impact load from fuel canisters = ngw

n = number of canisters = 12

g = impact force = 368 G

w = canister weight = 50 pounds

h = size of weld, 0.375 inch

l = length of weld = $\pi(15)$

$$S_s = \frac{(12)(368)(50.4)}{(0.707)(.375)(15)(\pi)} = 18{,}580$$

Assuming the ultimate shear stress for the weld to be the same as the parent metal, the margin of safety for shearing the weld is:

$$MS = \frac{40{,}000}{18{,}580} - 1 = 1.15$$

The support plate requires beam support for the bottom end drop accident. While the 1/2 inch plate can withstand the puncture load from the canister hoist fitting, the plate is not sufficiently thick to act as its own beam, nor is it practical from a weight or welding standpoint to increase the thickness. Therefore, three parallel, vertical webs have been welded to the bottom of the plate to stiffen it, and a vertical plate which acts as an intermediate support point for the beams and the plate has been welded to the inside of the cylinder. This plate provides a simple support only. The vertical plate and the cylinder walls are comparable to a standard 14 inch x 8 inch wide flange column with the same load capability.

The general arrangement is shown below.

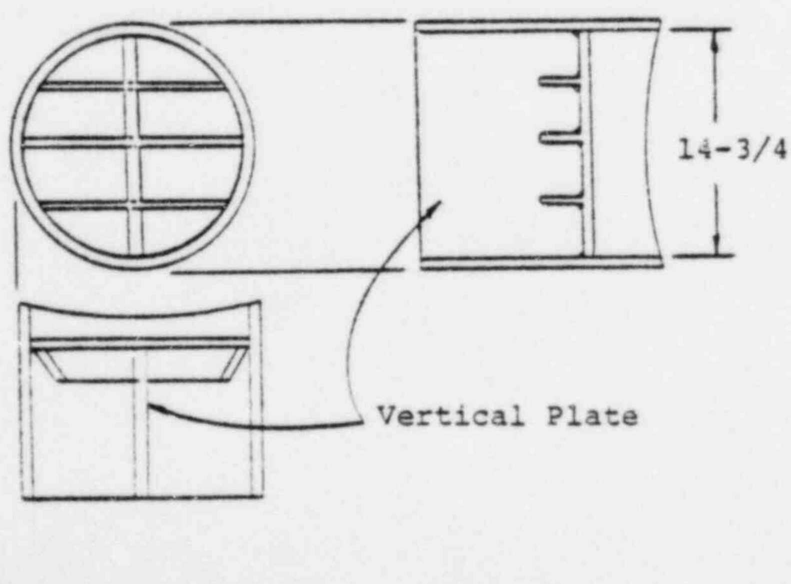

For ease of analysis, the plate will be assumed to be simply supported at the cylinder walls.

Four loading cases will be considered for the canisters. Case 1 will orient the canister base plates perpendicular to the direction of the three support beams. Case 2 will orient the canister base plates parallel to the beams as shown below. Cases 3 and 4 are discussed later.

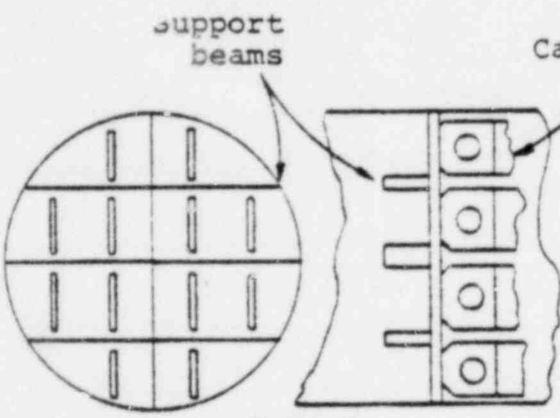

Case 1

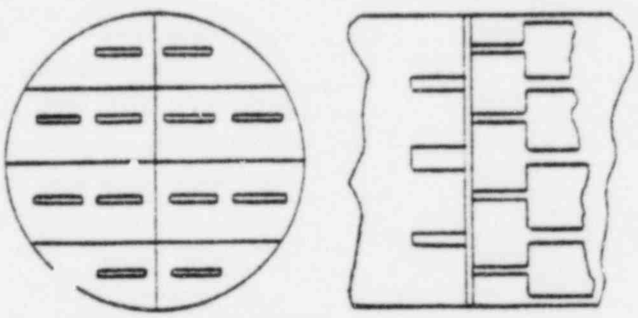

Case 2

Case 1 permits the consideration of the load as uniform on a continuous, multi span beam. This establishes a bending moment relationship for Case 2 as point loaded. A single vertical web, perpendicular to the three cross beams provides simple support to the plate upon which the canisters rest. The base plate is welded continuously, top and bottom, to the cylinder wall. The three support beams provide stiffness to the base plate enabling it to transmit half of the canister loads into the cylinder walls. The other half of the load is transmitted to the vertical web and thence into the cylinder walls and the cask bottom.

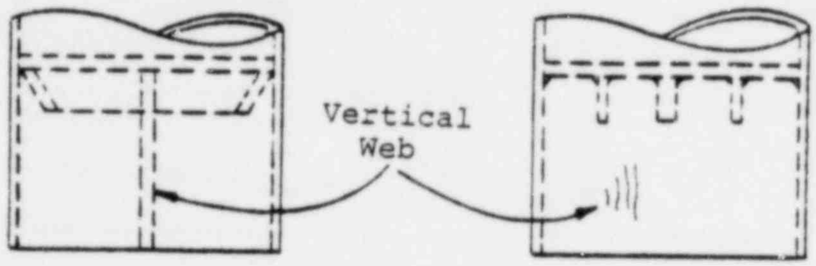

Assume the center portion of the plate carrying eight of the canisters to be a separate, simply supported, continuous beam with five supports as illustrated below. The load W1 represents the weight of the canister (50.4 pounds) times the g force (368).

(50.4)(368) = 18,550 pounds .

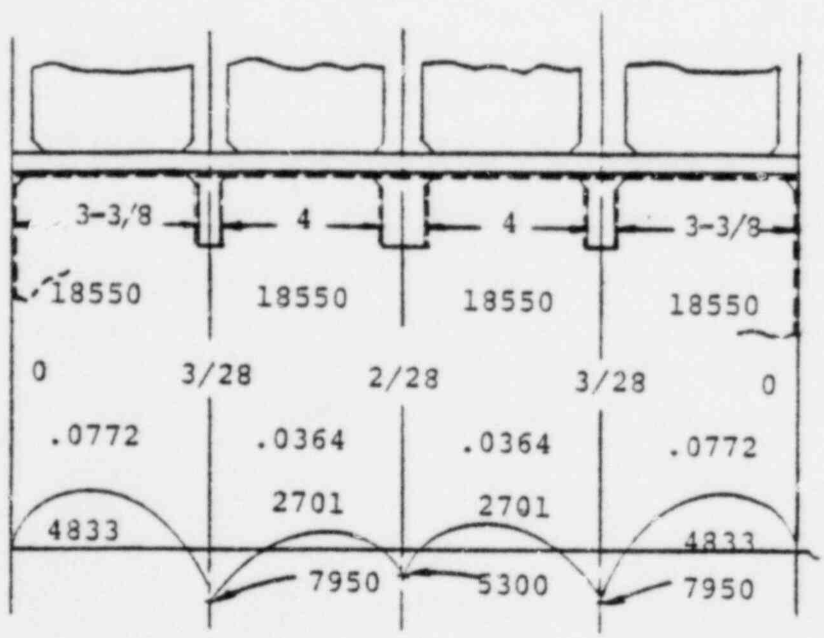

* 1/2 of load is carried by the center web shown in dotted outline.

Neglecting the support from the center web and the continuity of the plate at the sides, consider the bending stress in the plate as a beam. The maximum moment occurs at beams 1 and 3. The assumed width is 7.0 inches.

$$I = bh^3/12 = (7)(0.5)^3/12 = .073 \text{ inch}^4$$

$$fb = \frac{Mc}{I} = \frac{(7,950)(.25)}{.073} = 27,257 \text{ psi} < 75,000 \text{ psi ultimate} \quad .$$

The remaining half of the load is carried by the center web as a compression load. The web and the cylinder walls form an I section. This and other loads on the web will be summed up later.

Case 2 loads are based on the relationship of center span moments for uniformly loaded beams and point loaded beams. In this analysis, the center span moments are assumed to be three times the Case 1 moments.

On that basis, the maximum bending moment of 7,950 inches-pounds for Case 1 becomes, (1.5)(7,950) or 11,925 inches-pounds. The area moment of inertia is still .073 inch^4. The bending stress at the support is then:

$$(1.5)(27,257) = 40,885 \text{ psi} < 75,000 \text{ psi ultimate} \quad .$$

<u>Summation of Loads on Center, Vertical Web.</u> The center web, stabilized by the cylinder walls, carries one-half of the load from the eight canisters along the center web, and approximately 50 percent of the load from the remaining four canisters. The web and the walls form a wide flange column. The load is imparted to the web by the plate-beams and by direct bearing of the plate between the beams.

The shear at each of the supports is shown by:

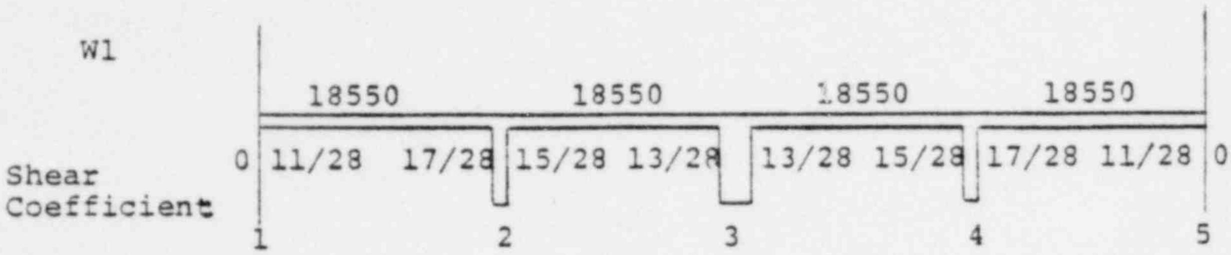

At 1, 5 $(\frac{11}{28})(18{,}500) =$ 7,287 pounds

At 2, 4 $(\frac{17}{28} + \frac{15}{28})(18{,}550) =$ 21,200 pounds

At 3, $(\frac{13}{28} + \frac{13}{28})(18{,}550) =$ <u>17,225</u> pounds

45,712 pounds x 2 = 91,424 pounds

The continuous beam shear loads from eight canisters is 91,424 pounds and an assumed 50 percent load from the remaining four is (.50)(4)(18,550) = 37,100 pounds for a total of 128,524 pounds. This load is assumed to be uniformly distributed on the top edge of the web. Neglecting the cylinder "flanges" the least radius of gyration ρ is found,

$$I = \frac{(14.75)(.5)^3}{12} = .1536 \text{ inch}^4$$

$$A = (14.75)(.5) = 7.375 \text{ inches}^2$$

$$\rho = \sqrt{\frac{.1536}{7.375}} = .1443 \text{ inch}$$

The allowable load is found from $P/A = C\pi^2E/(L/P)^2$

$$P = (7.375)(1.5)(\pi^2)(28 \times 10^6)/(13.25/.1443)^2$$

$$= 362,584 \text{ pounds}$$

∴ The web, stabilized by the cylinder will support the 128,524 pounds.

Case 3. The bending of the plate-beam combinations at 90 degrees to the foregoing analysis is presented next. The beams are more effective in this orientation. The center vertical web again reacts a large share of the canister loads as the center support for the beams.

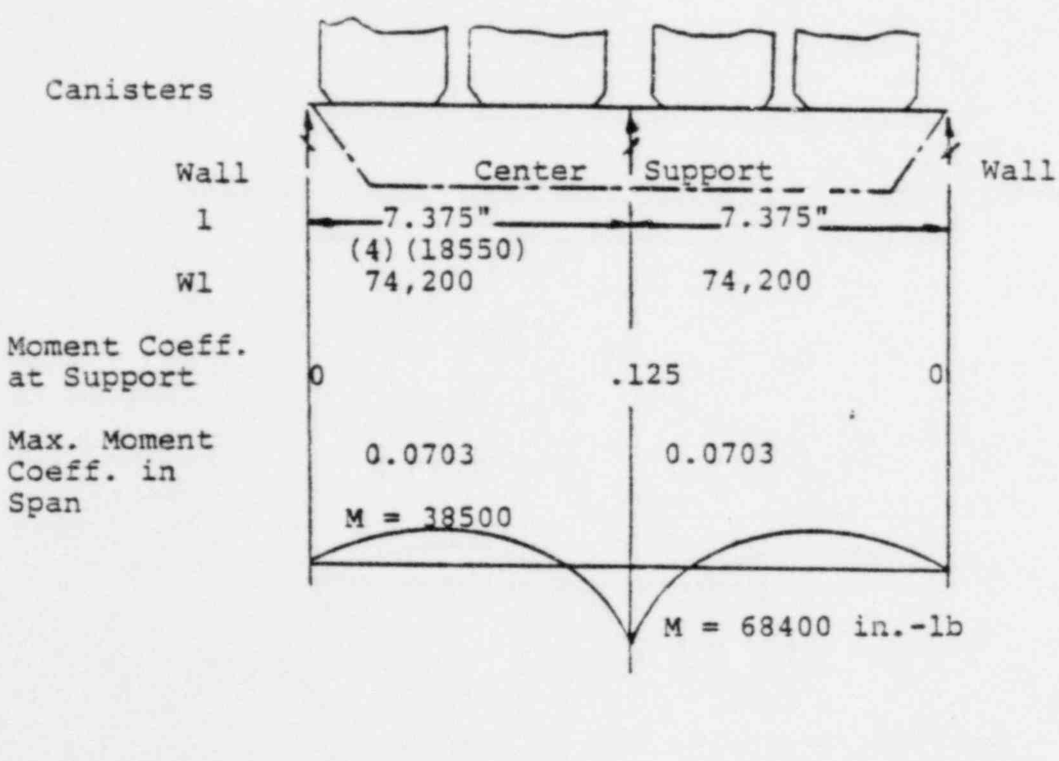

The beam plate area moment of inertia is based on the center 8 inch plate section, the center beam and one-half of each of the side beams.

This beam plate section carries eight of the twelve canisters. The other canisters are carried, two each, by a beam plate made up of the remaining half of the side beam, the cylinder wall and the section of the plate between the side beams and the cylinder wall.

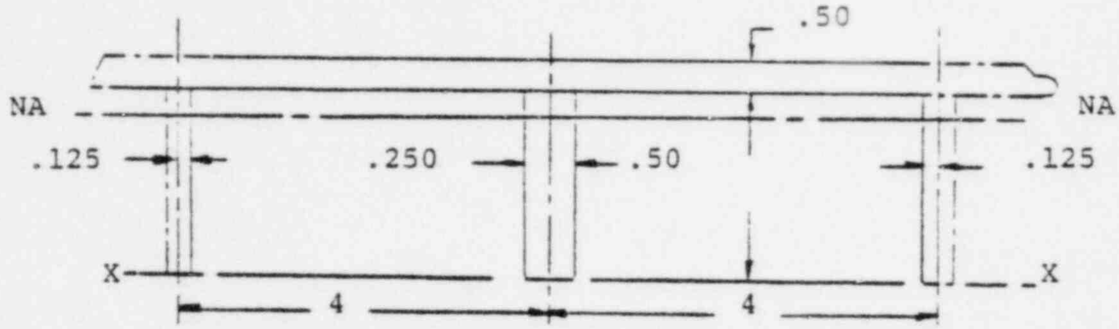

ITEM	A	Y	AY	AY^2	Io, $(bh^3/12)$
1 (8)(.5)	4.0	3.25	13.0	42.25	.0833
2 (.75)(3)	2.25	1.50	3.375	5.06	1.6875
	6.25		16.375	47.31	1.771

$$\overline{Y} = \frac{AY}{A} + 2.62 \text{ inches}$$

$$I_{NA} = Io + AY^2 - AY\,\overline{Y}$$

$$= 1.771 + 47.31 - (16.375)(2.62)$$

$$= 6.18 \text{ inches}^4$$

$$f_b = \frac{Mc}{I} = \frac{(68,400)(2.62)}{6.18} = 28,998 \text{ psi} < 75,000 \text{ psi}$$

$$M.S. = \frac{75,000}{29,000} - 1 = 1.58$$

The shear at the center support is (10/8)(W1) = 92,750 pounds. This is approximately the same value determined for Cases 1 and 2.

The side beam loads are illustrated as follows:

(The value of W is found by (50.4)(368) = 18,547)

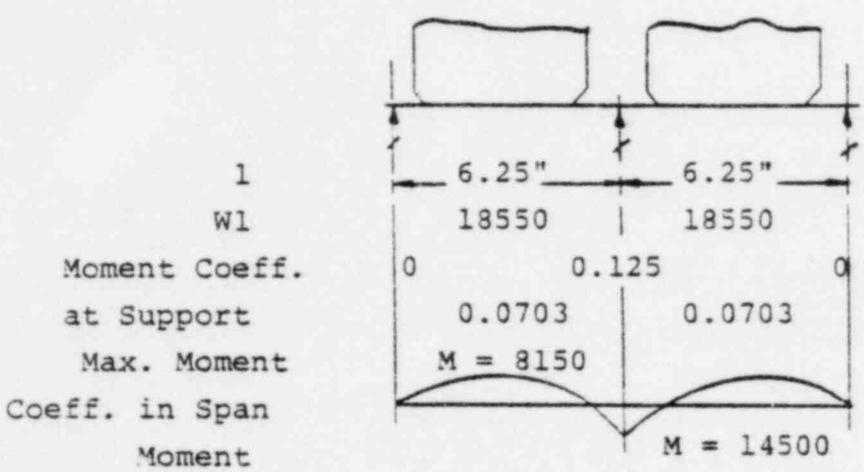

The area moment of inertia of the plate-beam is found below.

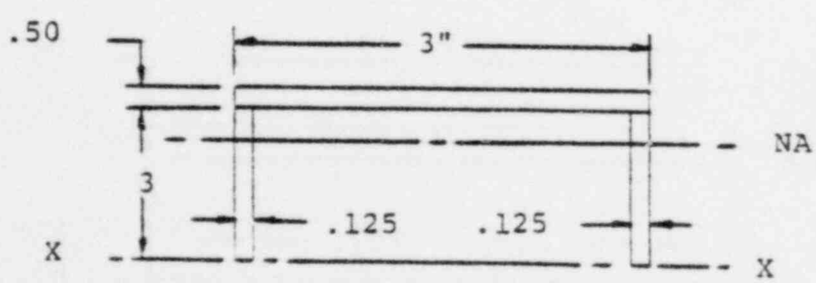

ITEM	A	Y	AY	AY^2	Io, $(bh^3/12)$
1 (3)(.5)	1.5	3.25	4.875	15.844	.031
2 (.25)(3)	.75	1.50	1.125	1.688	.562
	2.25		6.000	17.532	.593

$$\bar{Y} = \frac{AY}{A} = \frac{6.00}{2.25} = 2.67 \text{ inches}$$

$$I_{NA} = I_o + AY^2 - AY\,\bar{y}$$

$$= .593 + 17.532 - (6.0)(2.67)$$

$$= 2.105 \text{ inches}^4$$

$$f_b = \frac{Mc}{I} = \frac{(14,500)(2.67)}{2.105} = 18,390 \text{ psi} < 75,000 \text{ psi ultimate.}$$

Case 4. When the canisters are oriented 90 degrees to the foregoing, the plate alone is sufficient to bear the loads between the side wall and the side beam.

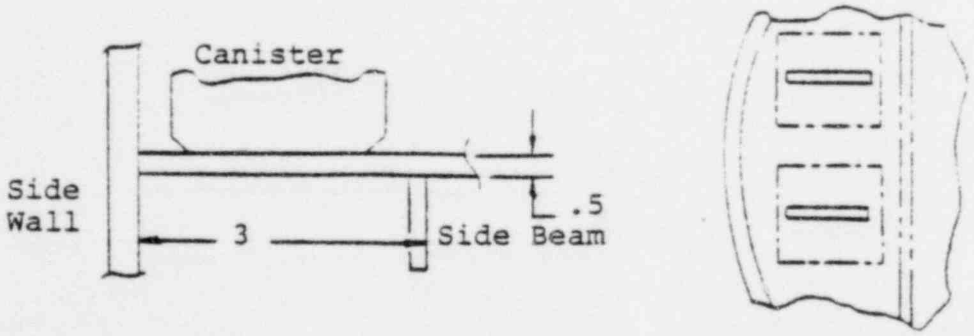

The area moment of inertia of the plate is found by:

$$I = \frac{bh^3}{12} = \frac{(3)(.5)^3}{12} = .031 \text{ inch}^4$$

W = 18,550 pounds (at 368 g's)

l = 30 inches .

Assuming a fixed end beam in this case, with a uniformly distributed load,

$$M = \frac{Wl^2}{12} \text{ where } Wl = W$$

$$= \frac{(18,550)(3)}{12} = 4,640 \text{ inches-pounds}$$

$$f_b = \frac{Mc}{I} = \frac{(4,640)(.25)}{.031} = 37,400 \text{ psi} < 75,000 \text{ psi ultimate}$$.

2.12 Appendix

2.12.1 References

(1) Metallic Materials and Elements for Aerospace Vehicle Structures, MIL-HDBK-5A, Change Notice 2, Sections 2.8 and 8.1, July 24, 1967.

(2) Wojtaszak, I. A., "Deformation of Thin Cylindrical Shells Subject to Internal Loading", Phil. Mag. 5.7, 18, (123), December, 1934, p 1099.

(3) Roark, R. J., Formulas for Stress and Strain, McGraw-Hill Book Co., 4th Ed., Equation 6, (1965), p 271.

(4) Nelms, H. A., "Structural Analysis of Shipping Casks, Vol 3, Effects of Jacket Physical Properties and Curvature on Puncture Resistance", Oak Ridge National Laboratory, ORNL-TM-1312, Vol 3, June, 1968.

(5) Lustman, B., and Kerze, F., The Metallurgy of Zirconium, p 626, McGraw-Hill Book Co., New York (1955).

(6) Tipton, C., Reactor Handbook, 2nd Ed., Vol I, Materials, p 727.

(7) Tipton, C., p 867.

(8) Roark, R. J., Equation 15, p 366.

(9) Brown, A. F. C., and Edmonds, R., "The Dynamic Yield Strength of Steel at an Intermediate Rate of Loading", Proceedings of the Institution of Mechanical Engineers, 159, 1948, p 11-23.

(10) Roark, R. J., Case 18, p 152.

(11) Private communication from Dr. Martin N. Haas, Associate Director, Nuclear Science and Technology Facility, State University of New York at Buffalo to Mr. R. Denney, Allied Chemical Company, 550 Second St., Idaho Falls, Idaho, 83401, File Ref. J-759.

(12) Roark, R. J., Case 41, p 227.

(13) Nuclear Regulatory Commission, Packaging of Radioactive Material for Transportation and Transportation of Radioactive Material Under Certain Conditions; Compatibility with IAEA Regulations, Proposed Rules 10CFR 71, August, 1979.

(14) Roark, R. J., Case 25, p 352.

(15) Roark, R. J., p 243.

(16) Roark, R. J., Case 6, p 217.

(17) Baumeister, T., Mark's Standard Handbook for Mechanical Engineers, 7th Ed., McGraw-Hill Book Co., New York, p 13-25 (1966).

2.12.2 Results of Cover Lifting Tests

Approved by: W. J. Madia

Battelle
Columbus Laboratories

Project Number 117-5865

Internal Distribution

W. J. Madia
T. R. Emswiler
D. E. Stellrecht
W. J. Gallagher
A. Parsons
D. E. Lozier

Date April 18, 1980

To R. J. Burian

From D. E. Lozier

Subject Testing of Lifting Handle on Cask BMI-1 Lid, February 27, 1980

The lid-lifting handle welded on the lid of cask BMI-1 was tested by attaching cask BCL-3, with its lid in place, to the BMI-1 lid with a chain. The assembly was then lifted off the floor and suspended for 3 minutes by a crane hooked to the BMI-1 lid-lifting handle. The certified weight of cask BCL-3 with lid is 2595 lb., placing a total weight on the lifting handle of >3695 lb. which is in excess of three times the weight of the 1100 lb. lid.

The weld was then checked by liquid dye penetrant in accordance with BCL QA Procedure HL-PP-60 with no defects detected.

DEL/cm

2.109

QUALITY ASSURANCE DOCUMENT

LIQUID PENETRANT INSPECTION
WORK COMPLETION RECORD

BATTELLE
Columbus Laboratories
505 King Avenue
Columbus, Ohio 43201

Prepared by

D. E. Lozier DEL

April 2, 1980
Date

APPROVED BY

[illegible] 4-2-80
Date

APPROVED BY

William [illegible] 4/4/80
Date

REV. A,
3-28-80

APPROVED BY

William [illegible] Gallacher 4-2-80
Date

APPROVED BY

D E Lozier 4/4/80
Date

2.110

LIQUID PENETRANT INSPECTION
WORK COMPLETION RECORD

1. Scope

This record documents the implementation and results of a liquid penetrant inspection.

2. Reference

2.1 BCL Hot Lab QA Manual (Sections HL-X-1 and HL-I-1).

2.2 HL-PP-60 Liquid Penetrant Inspection.

3. Work Completion Records

3.1 Work completion records shall be documented by the certified inspector performing the inspection and reviewed by a Q. A. respresentative.

3.2 Document the inspection on Record Form WC-60.

2.111

RECORD FORM WC-60
LIQUID PENETRANT INSPECTION

BMI-1 DES

1. Item inspected ____________

2. Inspection method (check method used).

   2.1 Visual Dye, i.e. spotcheck ✓

   2.2 Fluorescent Penetrant ____

	Initial	Date
3. Inspection performed as per HL-PP-60.	DES	2-27-80
4. Item approved as per acceptance criteria in HL-PP-60.	DES	2-27-80

5. Defects observed: None

6. Corrective action taken on defects:

   6.1 Reinspect after corrective action and document on another Record Form WC-60.

7. Inspection conducted by:
   ____________ Date 2-27-80

8. Reviewed by:
   ____________ Date 2-27-80

2.12.3 Description of MONSA Computer Program

MONSA (multilayer Orthotropic Nonsymmetric Shell Analysis) is a digital computer program written in FORTRAN IV. It is based on the multisegment numerical integration method for the analysis of boundary value problems.

MONSAS determines the displacements, forces, and stresses for a composite shell of revolution. A composite shell is defined as a shell composed of a number of distinct parts which may have the following shapes: cylindrical, spheroidal, ellipsoidal, paraboloidal, conical and toroidal. The shell wall may be composed of four different layers of orthotropic materials. The shell layers are specified by giving their location with respect to a reference surface.

Mechanical and temperature loadings can be applied to the shell. For nonsymmetric loadings, the user must determine the Fourier harmonics of the loadings and perform the appropriate number of shell calculations. Temperatures can vary along the shell meridian as well as through the thickness of the wall. The latter can be accomplished by specifying the temperature on the inner and outer surfaces and on three internal surfaces of the shell wall. A shell spinning about its longitudinal axis can be analyzed. A shell subjected to harmonically varying mechanical or temperature loadings can also be analyzed.

MONSAV will determine the natural frequencies and mode shapes of composite shells of revolution described above. The procedure is based on an iterative technique in which a trial frequency is picked and a determinant is calculated. The trial frequency becomes a natural frequency when the determinant vanishes.

Analysis of Shells of Revolution Subjected to Symmetrical and Nonsymmetrical Loads[1]

A. KALNINS

Assistant Professor
of Engineering and Applied Science,
Yale University,
New Haven, Conn.
Mem. ASME

The boundary-value problem of deformation of a rotationally symmetric shell is stated in terms of a new system of first-order ordinary differential equations which can be derived for any consistent linear bending theory of shells. The dependent variables contained in this system of equations are those quantities which appear in the natural boundary conditions on a rotationally symmetric edge of a shell of revolution. A numerical method of solution which combines the advantages of both the direct integration and the finite-difference approach is developed for the analysis of rotationally symmetric shells. This method eliminates the loss of accuracy encountered in the usual application of the direct integration approach to the analysis of shells. For the purpose of illustration, stresses and displacements of a pressurized torus are calculated and detailed numerical results are presented.

THE shell of revolution is an important structural element, and the literature devoted to its analysis is extensive. With regard to axisymmetric deformation, various methods have been employed to obtain solutions of the bending theory of shells of revolution by means of the H. Reissner-Meissner equations. For example, Naghdi and DeSilva [1][2] use asymptotic integration; Lohmann [2], Münz [3], Klingbeil [4], employ a direct numerical integration approach; Galletly, et al. [5] find the solution for an ellipsoidal shell of revolution by both the finite-difference and the Runge-Kutta method; and Penny [6], Radkowski, et al. [7], and Sepetoski, et al. [8] utilize the finite-difference technique. A number of additional references which deal with the solution of the H. Reissner-Meissner equations can be found in the papers cited.

For problems of bending in the absence of axial symmetry, a reduction of the governing equations of arbitrary shells of revolution to a system of four second-order differential equations involving four unknowns has been carried out by Budiansky and Radkowski [9]. A method for obtaining the solution of these equations is given in [9] which is an extension of that employed in [7] and [8]. Furthermore, treatments of nonsymmetric deformation of shells of revolution are found in papers by Goldberg and Bogdanoff [10], where a system of first-order differential equations for conical shells is derived, and by Steele [11] and Schile [12], where solutions of certain types are considered by means of asymptotic integration.

Among the papers which employ numerical analysis, two dif-

---

[1] National Science Foundation Grant No. 23922, Report No. 3, July, 1963.

[2] Numbers in brackets designate References at end of paper.

Presented at the Summer Conference of the Applied Mechanics Division, Boulder, Colo., June 9–11, 1964, of THE AMERICAN SOCIETY OF MECHANICAL ENGINEERS.

Discussion of this paper should be addressed to the Editorial Department, ASME, United Engineering Center, 345 East 47th Street, New York, N. Y. 10017, and will be accepted until October 10, 1964. Discussion received after the closing date will be returned. Manuscript received by ASME Applied Mechanics Division, July 31, 1963. Paper No. 64—APM-33.

Nomenclature

- ϕ, θ, ζ = coordinates of a point of shell
- s = distance measured from an arbitrary origin along meridian in positive direction of ϕ
- t_ϕ, t_θ, n = unit vectors tangent to coordinate curves (see Fig. 1)
- R_ϕ, R_θ = principal radii of curvature of middle surface
- r = distance of a point on middle surface from axis of symmetry
- E = Young's modulus
- ν = Poisson's ratio
- h = thickness of shell
- α = coefficient of thermal expansion
- $D = Eh^3/[12(1 - \nu^2)]$
- $K = Eh/(1 - \nu^2)$
- u_ϕ, u_θ, w = components of displacement of middle surface
- β_ϕ, β_θ = angle of rotation of normal
- p_ϕ, p_θ, p = components of mechanical surface loads
- m_ϕ, m_θ = components of moment of surface loads
- T, T_0, T_1 = temperature increment and temperature resultants
- $N_\phi, N_\theta, N_{\theta\phi}$ = membrane stress resultants
- $M_\phi, M_\theta, M_{\theta\phi}$ = moment resultants
- Q_ϕ, Q_θ = transverse-shear resultants
- N, Q = effective-shear resultants
- $J = 1/R_\phi + \sin\phi/r$
- $U = 1/R_\phi + \nu \sin\phi/r$
- $H = 1/R_\phi - \sin\phi/r$
- n = integer, designating nth Fourier component
- β = length factor
- $(\ )_{,x}$ = derivative with respect to any coordinate
- m = order of system of equations
- M = number of segments
- x = independent variable, either ϕ or s
- x_i = end point of segment
- $y(x)$ = $(m, 1)$ matrix, fundamental variables
- $A(x)$ = (m, m) matrix, coefficients of differential equations
- $B(x)$ = $(m, 1)$ matrix, nonhomogeneous coefficients
- $Y(x)$ = (m, m) matrix, homogeneous solutions
- $Z(x)$ = $(m, 1)$ matrix, nonhomogeneous solutions
- C = $(m, 1)$ matrix, arbitrary constants
- I = unit matrix

ferent methods of solution of the boundary-value problem of deformation of shells must be recognized; i.e., the direct integration [2–5] and the finite difference approach [5–9]. While the direct integration approach has certain important advantages, it also has a serious disadvantage; i.e., when the length of the shell is increased, a loss of accuracy invariably results. This phenomenon was clearly pointed out in [8]. The loss of accuracy does not result from accumulative errors in integration, but it is caused by the subtraction of almost equal numbers in the process of determination of the unknown boundary values. It follows that for every set of geometric and material parameters of the shell there is a critical length beyond which the solution loses all accuracy. The advantage of the finite-difference approach over direct integration is that it can avoid such a loss of accuracy. It is concluded from [8] that if the solution of the system of algebraic equations, which result from the finite-difference equations, is obtained by means of Gaussian elimination, then no loss of accuracy is experienced if the length of the shell is increased.

This paper is concerned with the general problem of deformation of thin, elastic shells of revolution, symmetrically or nonsymmetrically loaded, and with the development of a numerical method of its solution, which employs the direct integration technique, but eliminates the loss of accuracy owing to the length of the shell. The method developed here is applicable to any two-point boundary-value problem which is governed within an interval by a system of m first-order linear ordinary differential equations together with $m/2$ boundary conditions prescribed at each end of the interval. It is shown that the boundary-value problem of a rotationally symmetric shell can be stated in this form for any consistent linear bending theory of shells in terms of those quantities which appear in the natural boundary conditions on a rotationally symmetric edge.

The method of this paper offers definite advantages over the finite-difference approach. The main advantages are: (a) It can be applied conveniently to a large system of first-order differential equations, and (b) it permits an automatic selection of an optimum step size of integration at each step according to the desired accuracy of the solution. The first point means that the equations of the theory of shells of revolution, characterized in terms of first-order differential equations, can be integrated directly, and further reduction of the equations to a smaller number of unknowns is not necessary. The second point seems to be of great importance if a truly general method is desired which is expected to hold for arbitrary loads, shell configurations, thickness, and so on. With the finite-difference approach, a meaningful *a priori* estimate of the step size is often difficult, if not impossible, especially when rapid changes and discontinuities in the shell parameters are encountered. If a predictor-corrector direct integration approach is employed with the method of this paper, then the step size can be selected automatically at each step which ensures a prescribed accuracy of the solution and optimum efficiency in the calculation.

The method given in this paper can be divided into two parts: (a) Direct integration of $m + 1$ initial value problems over preselected segments of the total interval, and (b) the use of Gaussian elimination for the solution of the resulting system of matrix equations. The first part of this method is a generalization of that which is employed over the whole interval in [2–5]. Here, however, the initial value problems are defined over segments of the total interval, the lengths of which are within the range of the applicability of the direct integration approach. After the initial value problems are integrated over these segments, continuity conditions on all variables are written at the endpoints of the segments, and they constitute a simultaneous system of linear matrix equations. This system of matrix equations is then solved directly by means of Gaussian elimination. The result is that the direct integration method is employed and at the same time there is no loss of accuracy because the lengths of the segments are selected in such a way that the solutions of the initial value problems are kept sufficiently small. A convenient parameter is given from which the appropriate lengths of the segments can be estimated easily.

In the application of this method to the analysis of rotationally symmetric shells, the boundary-value problem is formulated in terms of first-order ordinary differential equations. For this purpose, starting with the equations of the linear classical bending theory of shells in which the thermal effects are included, first a system of equations is derived in the form of eight partial differential equations involving eight unknowns in such a manner that the system of equations contains no derivatives of the material parameters, thickness, or principal radii of curvature. The absence of the derivatives in the coefficients of the differential equations permits the calculation of the coefficients at a point without regard to the values of the shell parameters at preceding or following points. Then, assuming separability with respect to the independent variables, the desired system of eight first-order ordinary differential equations is obtained which together with the boundary conditions on two edges of the shell constitute a two-point boundary-value problem. The derived system of equations is applicable to rotationally symmetric shells with arbitrary meridional variations (including discontinuities) in Young's modulus, Poisson's ratio, radii of curvature, thickness, and coefficient of thermal expansion. While such a system of equations is derived in this paper only for one version of the classical theory of shells, it can be derived in the same way for all other consistent linear bending theories of shells, including those which account for the dynamic effects, transverse shear deformation, nonhomogeneity, and anisotropy.

Finally, with the use of the method and the equations given in this paper, stresses and displacements are calculated in a thin-walled torus subjected to internal pressure. The solution shows that the meridional membrane stress is almost identical to that predicted by membrane theory, but that the bending stresses even for a relatively thin torus may not be negligible.

Geometry and Basic Equations

The position of a point of a shell of revolution is given by the coordinates θ, ϕ, ζ measured along the triplet of unit vectors t_θ, t_ϕ, n, respectively, as shown in Fig. 1. The shape of the shell is determined by specifying the two principal radii of curvature R_ϕ, R_θ of the middle surface as functions of ϕ. Instead of R_θ, it is convenient to use the distance r from a point on the middle surface to the z-axis; from Fig. 1 it follows that

$$r = R_\theta \sin \phi \tag{1}$$

If the generating curve of the middle surface is given by $r = r(z)$, then

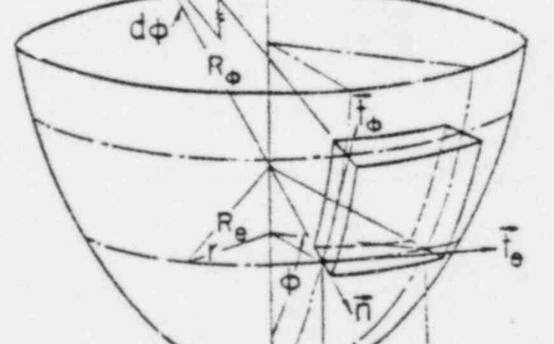

Fig. 1 Element of a shell of revolution

$$R_\phi = -\left[1+\left(\frac{dr}{dz}\right)^2\right]^{3/2} \Big/ \frac{d^2r}{dz^2}$$
$$R_\theta = r\left[1+\left(\frac{dr}{dz}\right)^2\right]^{1/2} \tag{2}$$

The following analysis requires frequent differentiation of r (or R_θ) with respect to ϕ, and it is convenient to express this derivative by the Codazzi relation

$$\frac{dr}{d\phi} = R_\phi \cos\phi \tag{3}$$

The displacement components of the middle surface of the shell and the rotations of the normal are defined by the expression of the displacement vector U of the form

$$\mathbf{U} = (u_\phi + \zeta\beta_\phi)\mathbf{t}_\phi + (u_\theta + \zeta\beta_\theta)\mathbf{t}_\theta + w\mathbf{n} \tag{4a}$$

The shell is subjected to the mechanical load vector $\mathbf{p}$, which is measured as force per unit area of the middle surface and written as

$$\mathbf{p} = p_\phi\mathbf{t}_\phi + p_\theta\mathbf{t}_\theta + p\mathbf{n} \tag{4b}$$

and the moment vector $\mathbf{m}$, which is measured as moment per unit area and given by

$$\mathbf{m} = -m_\theta\mathbf{t}_\phi + m_\phi\mathbf{t}_\theta \tag{4c}$$

With reference to Fig. 1, equations (4) serve the purpose for establishing the positive directions of the components of the displacement and mechanical load vectors.

The temperature distribution in the shell caused by some thermal loads is accounted for in the usual manner by means of the integrated temperature effect of the form

$$T_0(\phi, \theta) = \frac{1}{h}\int_{-\frac{h}{2}}^{\frac{h}{2}} T(\phi, \theta, \zeta)d\zeta \tag{5a}$$

$$T_1(\phi, \theta) = \frac{12}{h^2}\int_{-\frac{h}{2}}^{\frac{h}{2}} \zeta T(\phi, \theta, \zeta)d\zeta \tag{5b}$$

The derivation of a new set of equations carried out in the next section is based on a linear classical theory of shells given by Reissner [13]. When referred to arbitrary shells of revolution, the governing system of equations of [13] can be written in the following form. Equations of equilibrium:

$$N_{\theta,\theta} + \frac{r}{R_\phi}N_{\phi\theta,\phi} + 2\cos\phi\, N_{\theta\phi} + Q_\theta\sin\phi + rp_\theta = 0 \tag{6a}$$

$$N_{\theta\phi,\theta} + \frac{r}{R_\phi}N_{\phi,\phi} + (N_\phi - N_\theta)\cos\phi + \frac{r}{R_\phi}Q_\phi + rp_\phi = 0 \tag{6b}$$

$$Q_{\theta,\theta} + \frac{r}{R_\phi}Q_{\phi,\phi} + Q_\phi\cos\phi - N_\theta\sin\phi - \frac{r}{R_\phi}N_\phi + rp = 0 \tag{7}$$

$$M_{\theta,\theta} + \frac{r}{R_\phi}M_{\phi\theta,\phi} + 2\cos\phi\, M_{\theta\phi} - rQ_\theta + rm_\theta = 0 \tag{8a}$$

$$M_{\theta\phi,\theta} + \frac{r}{R_\phi}M_{\phi,\phi} + (M_\phi - M_\theta)\cos\phi - rQ_\phi + rm_\phi = 0 \tag{8b}$$

Stress-strain relations:

$$N_\theta = K(\epsilon_\theta + \nu\epsilon_\phi) - (1+\nu)\alpha KT_0 \tag{9a}$$

$$N_\phi = K(\epsilon_\phi + \gamma\epsilon_\theta) - (1+\nu)\alpha KT_0 \tag{9b}$$

$$N_{\theta\phi} = N_{\phi\theta} = (1-\nu)K\epsilon_{\theta\phi} \tag{9c}$$

$$M_\theta = D(\kappa_\theta + \nu\kappa_\phi) - (1+\nu)\alpha DT_1 \tag{10a}$$

$$M_\phi = D(\kappa_\phi + \nu\kappa_\theta) - (1+\nu)\alpha DT_1 \tag{10b}$$

$$M_{\theta\phi} = M_{\phi\theta} = (1-\nu)D\kappa_{\theta\phi} \tag{10c}$$

Strain-displacement relations:

$$\epsilon_\theta = \frac{1}{r}(u_{\theta,\theta} + u_\phi\cos\phi + w\sin\phi) \tag{11a}$$

$$\epsilon_\phi = \frac{1}{R_\phi}(u_{\phi,\phi} + w) \tag{11b}$$

$$2\epsilon_{\theta\phi} = \frac{1}{r}(u_{\phi,\theta} - u_\theta\cos\phi) + \frac{1}{R_\phi}u_{\theta,\phi} \tag{11c}$$

$$\kappa_\theta = \frac{1}{r}(\beta_{\theta,\theta} + \beta_\phi\cos\phi) \tag{12a}$$

$$\kappa_\phi = \frac{1}{R_\phi}\beta_{\phi,\phi} \tag{12b}$$

$$2\kappa_{\theta\phi} = \frac{1}{r}(\beta_{\phi,\theta} - \beta_\theta\cos\phi) + \frac{1}{R_\phi}\beta_{\theta,\phi} \tag{12c}$$

$$\beta_\theta = -\frac{1}{r}w_{,\theta} + \frac{\sin\phi}{r}u_\theta \tag{13a}$$

$$\beta_\phi = -\frac{1}{R_\phi}w_{,\phi} + \frac{1}{R_\phi}u_\phi \tag{13b}$$

The positive directions of the stress resultants in the foregoing equations are the same as the corresponding stresses on the edge of the shell. The definitions of the stress resultants are found in [13].

The order of the system of equations (6)–(13) is eight with respect to ϕ, and consequently it is possible to reduce (6)–(13) to eight first-order differential equations which involve eight unknowns. If the eight unknowns are those quantities which enter into the natural boundary conditions at the edge ϕ = const, then the boundary-value problem of a rotationally symmetric shell can be completely stated in terms of these unknowns. For this reason, the eight differential equations, derived in the following sections, and the eight unknowns are called the fundamental set of equations and the fundamental variables, respectively.

Derivation of Fundamental Set of Equations

According to the classical theory of shells, the quantities which appear in the natural boundary conditions on a rotationally symmetric edge of a shell of revolution include the effective shear resultants N and Q defined by

$$N = N_{\theta\phi} + \frac{\sin\phi}{r}M_{\theta\phi} \tag{14a}$$

$$Q = Q_\phi + \frac{1}{r}M_{\theta\phi,\theta} \tag{14b}$$

Thus, the fundamental variables, which are consistent with the theory of [13], are the four generalized displacements w, u_ϕ, u_θ, β_ϕ, and the four generalized forces Q, N_ϕ, N, and M_ϕ.

In the derivation of the fundamental equations, it is more convenient to employ the distance s, measured along the meridian of the shell, rather than the angular coordinate ϕ. However, after the equations are derived, the problem can again be easily formulated in terms of ϕ by means of the relation

$$\frac{1}{R_\phi}\frac{\partial}{\partial\phi} = \frac{\partial}{\partial s}$$

As a preliminary step, it is necessary to express N_θ, M_θ, $M_{\theta\phi}$ in terms of the fundamental variables. From (9a) it follows that

$$N_\theta = \nu N_\phi + K\frac{1-\nu^2}{r}(w\sin\phi + u_{\theta,\theta} + u_\phi\cos\phi) - \alpha K(1-\nu^2)T_2 \quad (15)$$

and from (10a) that

$$M_\theta = \nu M_\phi + D\frac{1-\nu^2}{r}\left(-\frac{1}{r}w_{,\theta\theta} + \frac{\sin\phi}{r}u_{\theta,\theta} + \beta_\phi\cos\phi\right) - \alpha D(1-\nu^2)T_1 \quad (16)$$

Elimination of $u_{\theta,s}$ and $w_{,\theta s}$ from equation (12c) leads to an expression for $M_{\theta\phi}$ in the form

$$M_{\theta\phi} = LD\frac{1-\nu}{2r}\left[2\beta_{\phi,\theta} + \frac{2\cos\phi}{r}w_{,\theta} + Hu_\theta\cos\phi - Ju_{\phi,\theta}\right] + \frac{LD}{K}\frac{\sin\phi}{r}N \quad (17)$$

where

$$L = \frac{1}{1 + \dfrac{\sin^2\phi}{r^2}\dfrac{D}{K}}$$

In the derivation of the four equations of the fundamental set which involve the derivatives of the stress resultants with respect to s, the use of (14) is essential. Elimination of Q_θ from (6a) and (8a) by means of (14a) leads to

$$N_{,s} = H\frac{\cos\phi}{r}M_{\theta\phi} - \frac{2\cos\phi}{r}N - \frac{1}{r}N_{\theta,\theta} - \frac{\sin\phi}{r^2}M_{\theta,\theta} - p_\theta - \frac{\sin\phi}{r}m_\theta \quad (18)$$

Similarly, elimination of Q_θ from (7) and (8a) gives

$$Q_{,s} = -\frac{2\cos\phi}{r^2}M_{\theta\phi,\theta} - \frac{\cos\phi}{r}Q + \frac{\sin\phi}{r}N_\theta + \frac{1}{R_\phi}N_\phi - \frac{1}{r^2}M_{\theta,\theta\theta} - p - \frac{1}{r}m_{\theta,\theta} \quad (19)$$

Solving (6b) from $N_{\phi,s}$ there results

$$N_{\phi,s} = -\frac{1}{r}N_{,\theta} + \frac{1}{r}JM_{\theta\phi,\theta} + \frac{\cos\phi}{r}(N_\theta - N_\phi) - \frac{1}{R_\phi}Q - p_\phi \quad (20)$$

and it follows from (8b) that

$$M_{\phi,s} = -\frac{2}{r}M_{\theta\phi,\theta} + \frac{\cos\phi}{r}(M_\theta - M_\phi) + Q - m_\phi \quad (21)$$

Wherever necessary, $N_{\theta\phi}$ and Q_ϕ were eliminated with the use of (14).

The fundamental set of equations consists of (18)–(21), where N_θ, M_θ, $M_{\theta\phi}$ can be replaced directly in terms of the fundamental variables by means of (15)–(17), and four additional equations involving the derivatives of w, u_ϕ, u_θ, β_ϕ with respect to s, which are obtained from (13b), (11c), (11b), (12b), respectively. Finally, the system of eight differential equations that governs the deformation of a shell of revolution can be expressed in terms of the eight fundamental variables and written as

$$w_{,s} = \frac{1}{R_\phi}u_\phi - \beta_\phi \quad (22a)$$

$$u_{\phi,s} = -Uw - \frac{\nu\cos\phi}{r}u_\phi - \frac{\nu}{r}u_{\theta,\theta} + \frac{1}{K}N_\phi + \alpha(1+\nu)T_2 \quad (22b)$$

$$u_{\theta,s} = -\frac{LD\sin 2\phi}{Kr^3}w_{,\theta} - \frac{1}{r}\left(1 - \frac{LDJ\sin\phi}{Kr}\right)u_{\phi,\theta} + \frac{\cos\phi}{r}\left(1 - \frac{LDH\sin\phi}{Kr}\right)u_\theta - \frac{2LD\sin\phi}{Kr^2}\beta_{\phi,\theta} + \frac{2}{(1-\nu)K}\left(1 - \frac{LD\sin^2\phi}{Kr^2}\right)N \quad (22c)$$

$$\beta_{\phi,s} = \frac{\nu}{r^2}w_{,\theta\theta} - \frac{\nu\sin\phi}{r^2}u_{\theta,\theta} - \frac{\nu\cos\phi}{r}\beta_\phi + \frac{1}{D}M_\phi + \alpha(1+\nu)T_1 \quad (22d)$$

$$\begin{aligned}Q_{,s} = {} & \frac{1-\nu}{r^4}\left[D(1+\nu)\frac{\partial^4}{\partial\theta^4} - 2LD\cos^2\phi\frac{\partial^2}{\partial\theta^2} + (1+\nu)Kr^2\sin^2\phi\right]w + (1-\nu)\frac{\cos\phi}{r^2}\left[\frac{1}{r}LDJ\frac{\partial^2}{\partial\theta^2} + (1+\nu)K\sin\phi\right]u_\phi \\ & - \frac{1-\nu}{r^2}\left[\frac{1}{r}LDH\cos^2\phi - (1+\nu)K\sin\phi + D(1+\nu)\frac{\sin\phi}{r^2}\frac{\partial^2}{\partial\theta^2}\right]u_{\theta,\theta} \\ & - D(1-\nu)\frac{\cos\phi}{r^3}(1+\nu+2L)\beta_{\phi,\theta\theta} + UN_\phi - \frac{\nu}{r^2}M_{\phi,\theta\theta} - \frac{LD\sin 2\phi}{Kr^3}N_{,\theta} - \frac{\cos\phi}{r}Q - p - \frac{1}{r}m_{\theta,\theta} \\ & - \alpha(1-\nu^2)\frac{1}{r}\left(K\sin\phi\, T_2 - \frac{1}{r}DT_{1,\theta\theta}\right)\end{aligned} \quad (22e)$$

$$\begin{aligned}N_{\phi,s} = {} & (1-\nu)\frac{\cos\phi}{r^2}\left[\frac{1}{r}LDJ\frac{\partial^2}{\partial\theta^2} + (1+\nu)K\sin\phi\right]w + \frac{1-\nu}{r^2}\left[(1+\nu)K\cos^2\phi - \tfrac{1}{2}LDJ^2\frac{\partial^2}{\partial\theta^2}\right]u_\phi \\ & + (1-\nu)\frac{\cos\phi}{r^2}[\tfrac{1}{2}LDJH + (1+\nu)K]u_{\theta,\theta} + JLD\frac{1-\nu}{r^2}\beta_{\phi,\theta\theta} \\ & - \frac{1}{R_\phi}Q - (1-\nu)\frac{\cos\phi}{r}N_\phi - \frac{1}{r}\left(1 - \frac{LDJ\sin\phi}{Kr}\right)N_{,\theta} - p_\phi - \alpha(1-\nu^2)K\frac{\cos\phi}{r}T_2\end{aligned} \quad (22f)$$

$$\begin{aligned}N_{,s} = {} & \frac{1-\nu}{r^2}\left[HLD\frac{\cos^2\phi}{r} - (1+\nu)K\sin\phi + (1+\nu)D\frac{\sin\phi}{r^2}\frac{\partial^2}{\partial\theta^2}\right]w_{,\theta} \\ & - (1-\nu)\frac{\cos\phi}{r^2}[\tfrac{1}{2}LDJH + (1+\nu)K]u_{\phi,\theta} \\ & + \frac{1-\nu}{r^2}\left[\tfrac{1}{2}LDH^2\cos^2\phi - (1+\nu)\left(K + \frac{D\sin^2\phi}{r^2}\right)\frac{\partial^2}{\partial\theta^2}\right]u_\theta \\ & - D(1-\nu)\frac{\cos\phi}{r^2}\left[(1+\nu)\frac{\sin\phi}{r} - LH\right]\beta_{\phi,\theta} - \frac{\nu}{r}N_{\phi,\theta}\end{aligned}$$

$$
-\frac{\cos\phi}{r}\left(2-\frac{LDH\sin\phi}{Kr}\right)N-\frac{\nu\sin\phi}{r^2}M_{\phi,\theta}-p_\theta-\frac{\sin\phi}{r}m_\theta
$$

$$
+\alpha(1-\nu^2)\frac{1}{r}\left(KT_{0,\theta}+D\frac{\sin\phi}{r}T_{1,\theta}\right) \quad (22g)
$$

$$
M_{\theta,s}=-(1-\nu)D\frac{\cos\phi}{r^4}(1+\nu+2L)w_{,\theta\theta}+LDJ\frac{1-\nu}{r^2}u_{\phi,\theta\theta}
$$

$$
+D(1-\nu)\frac{\cos\phi}{r^2}\left[(1+\nu)\frac{\sin\phi}{r}-HL\right]u_{\theta,\theta}
$$

$$
+D\frac{1-\nu}{r^2}\left[(1+\nu)\cos^2\phi-2L\frac{\partial^2}{\partial\theta^2}\right]\beta_\phi+Q-\frac{2LD\sin\phi}{Kr^3}N_{,\theta}
$$

$$
-(1-\nu)\frac{\cos\phi}{r}M_\phi-m_\phi-\alpha(1-\nu^2)D\frac{\cos\phi}{r}T_1 \quad (22h)
$$

Equations (22), (14), and (15) to (17) determine all unknown variables except Q_θ which can be found from (8a) and written in the form

$$
Q_\theta=\frac{1}{r}M_{\theta,\theta}+M_{\theta\phi,s}+\frac{2\cos\phi}{r}M_{\theta\phi}+m_\theta \quad (23)
$$

By calculating $M_{\theta\phi,s}$ from (17) and making use of (16), it is possible to express Q_θ directly in terms of the fundamental variables. This expression is lengthy and contains derivatives with respect to s of the shell parameters. Since Q_θ does not enter into any boundary conditions on the edge s = const, it is preferable to calculate Q_θ as the last unknown directly from (23). The derivative of $M_{\theta\phi}$ can be easily obtained by numerical differentiation.

The procedure for the derivation of an equivalent set of equations for other linear classical theories of isotropic shells is identical to that given before. For general anisotropic and/or nonhomogeneous shells of revolution with rotationally symmetric properties, the fundamental set of equations is derived in the same way as (22) except that (9) and (10) must be replaced by the appropriate stress-strain relations given, for example, by Ambartsumyan [14]. Otherwise, the derivation is straightforward. For the improved theory of shells, such as the one given by Naghdi [15], in which the effects of transverse-shear deformation are accounted for, the following ten fundamental variables are required: w, u_ϕ, u_θ, β_ϕ, β_θ, Q_ϕ, N_ϕ, $N_{\phi\theta}$, M_ϕ, $M_{\phi\theta}$. Since now Q_ϕ and Q_θ appear in (13), the elimination of Q_θ from (6a), (7), (8a), is done by means of (13a). The required equations for the derivatives of the generalized forces are obtained directly from the five equations of equilibrium (6), (7), (8). The remaining five equations are derived by following a procedure similar to that of the foregoing.

Fundamental Equations for Separable Solutions

For shells of revolution which consist of complete latitude circles, the surface loads are periodic with respect to θ with a period of 2π, and they can be assumed to be of the form

$$
\{p_\phi, p, m_\phi\}=\{p_{\phi n}, p_n, m_{\phi n}\}\begin{Bmatrix}\cos n\theta\\ \sin n\theta\end{Bmatrix} \quad (24a)
$$

$$
\{T_0, T_1\}=\{T_{0n}, T_{1n}\}\begin{Bmatrix}\cos n\theta\\ \sin n\theta\end{Bmatrix} \quad (24b)
$$

$$
\{p_\theta, m_\theta\}=\{p_{\theta n}, m_{\theta n}\}\begin{Bmatrix}\sin n\theta\\ \cos n\theta\end{Bmatrix} \quad (24c)
$$

where the variables with subscripts n depend only on s, and each integral value of n in (24) can be regarded as one Fourier component in a general Fourier series expansion of arbitrary periodic surface loads.

Separable solutions of (22), corresponding to the value of n in (24), are then obtained in the form

$$
\{w, u_\phi, \beta_\phi\}=\{w_n, u_{\phi n}, \beta_{\phi n}\}\begin{Bmatrix}\cos n\theta\\ \sin n\theta\end{Bmatrix} \quad (25a)
$$

$$
\{N_\phi, M_\phi, Q\}=\{N_{\phi n}, M_{\phi n}, Q_n\}\begin{Bmatrix}\cos n\theta\\ \sin n\theta\end{Bmatrix} \quad (25b)
$$

$$
\{u_\theta, N\}=\{u_{\theta n}, N_n\}\begin{Bmatrix}\sin n\theta\\ \cos n\theta\end{Bmatrix} \quad (25c)
$$

The s-dependent coefficients with subscripts n on the right-hand side of (25) are governed by a system of equations which is obtained from (22) and, after using the assumption that the shell is thin,[3] can be written as

$$
w_{n,s}=\frac{1}{R_\phi}u_{\phi n}-\beta_{\phi n} \quad (26a)
$$

$$
u_{\phi n,s}=-Uw_n-\frac{\nu\cos\phi}{r}u_{\phi n}\mp\frac{\nu n}{r}u_{\theta n}
$$

$$
+\frac{1}{K}N_{\phi n}+\alpha(1+\nu)T_{0n} \quad (26b)
$$

$$
u_{\theta n,s}=\pm\frac{D\sin 2\phi}{Kr^3}w_n\pm\frac{n}{r}u_{\phi n}+\frac{\cos\phi}{r}u_{\theta n}
$$

$$
\pm\frac{2Dn\sin\phi}{Kr^3}\beta_{\phi n}+\frac{2}{(1-\nu)K}N \quad (26c)
$$

$$
\beta_{\phi n,s}=-\frac{\nu n^2}{r^2}w_n\mp\frac{\nu n\sin\phi}{r^2}u_{\theta n}-\frac{\nu\cos\phi}{r}\beta_{\phi n}
$$

$$
+\frac{1}{D}M_{\phi n}+\alpha(1+\nu)T_{1n} \quad (26d)
$$

$$
Q_{n,s}=\frac{1-\nu}{r^4}[(1+\nu)n^4D
$$

$$
+2n^2D\cos^2\phi+(1+\nu)Kr^2\sin^2\phi]w_n
$$

$$
+(1-\nu)\frac{\cos\phi}{r^2}\left[(1+\nu)K\sin\phi-\frac{n^2}{r}DJ\right]u_{\phi n}
$$

$$
\pm\frac{(1-\nu)n}{r^2}\left[(1+\nu)D\frac{n^2}{r^2}\sin\phi+(1+\nu)K\sin\phi\right]u_{\theta n}
$$

$$
+n^2(1-\nu)(3+\nu)D\frac{\cos\phi}{r^3}\beta_{\phi n}-\frac{\cos\phi}{r}Q_n+UN_{\phi n}
$$

$$
\mp\frac{nD\sin 2\phi}{Kr^4}N_n+\frac{\nu n^2}{r^2}M_{\phi n}-p_n\mp\frac{n}{r}m_{\theta n}
$$

$$
-\alpha(1-\nu^2)\frac{1}{r}\left(K\sin\phi\,T_{0n}+D\frac{n^2}{r}T_{1n}\right) \quad (26e)
$$

$$
N_{\phi n,s}=(1-\nu)\frac{\cos\phi}{r^2}\left[(1+\nu)K\sin\phi-\frac{n^2}{r}JD\right]w_n
$$

$$
+\frac{1-\nu}{r^2}\left[(1+\nu)K\cos^2\phi+\frac{n^2}{2}DJ^2\right]u_{\phi n}
$$

$$
\pm\frac{(1-\nu^2)nK\cos\phi}{r^2}u_{\theta n}-\frac{n^2(1-\nu)}{r^2}DJ\beta_{\phi n}
$$

$$
-\frac{1}{R_\phi}Q_n-(1-\nu)\frac{\cos\phi}{r}N_{\phi n}\mp\frac{n}{r}N_n
$$

---

[3] In the derivation of the system of equations (6)–(13) the assumption is made that the shell is sufficiently thin, so that $1+h^2/12R^2\approx 1$, where R denotes the minimum principal radius of curvature. This same approximation is used to obtain the following equations from (22).

$$- p_{\phi n} - \alpha(1 - \nu^2)K \frac{\cos\phi}{r} T_{0n} \quad (26f)$$

$$N_{n,s} = \pm \frac{n(1-\nu)}{r^3}\left[(1+\nu)D\frac{n^2}{r^2}\sin\phi + (1+\nu)K\sin\phi\right]w_n$$

$$\pm \frac{(1-\nu^2)nK\cos\phi}{r^2}u_{\phi n} + \frac{n^2(1-\nu^2)K}{r^2}u_{\theta n}$$

$$\pm nD\frac{1-\nu}{r^3}\cos\phi\left[(1+\nu)\frac{\sin\phi}{r} - H\right]\beta_{\phi n}$$

$$\pm n\frac{\nu}{r}N_{\phi n} - \frac{2\cos\phi}{r}N_n$$

$$\pm \frac{\nu n\sin\phi}{r^2}M_{\phi n} - p_{\theta n} - \frac{\sin\phi}{r}m_{\theta n}$$

$$\mp \alpha(1-\nu^2)\frac{1}{r}\left(KT_{0n} + D\frac{\sin\phi}{r}T_{1n}\right) \quad (26g)$$

$$M_{\phi n,s} = n^2(1-\nu)(3+\nu)D\frac{\cos\phi}{r^3}w_n - n^2\frac{1-\nu}{r^3}JDu_{\phi n}$$

$$\pm nD\frac{1-\nu}{r^3}\cos\phi\left[(1+\nu)\frac{\sin\phi}{r} - H\right]u_{\theta n}$$

$$+ D\frac{1-\nu}{r^2}[(1+\nu)\cos^2\phi + 2n^2]\beta_{\phi n} + Q \mp \frac{2nD\sin\phi}{Kr^3}N_n$$

$$- (1-\nu)\frac{\cos\phi}{r}M_{\phi n} - m_{\phi n} - \alpha(1-\nu^2)D\frac{\cos\phi}{r}T_{1n} \quad (26h)$$

The double signs in (26) correspond to the top or bottom trigonometric function employed in (24) and (25).

The quantities which are not included in the fundamental variables can be expressed by means of separation of variables by

$$\{N_\theta, M_\theta, Q_\phi\} = \{N_{\theta n}, M_{\theta n}, Q_{\phi n}\}\begin{Bmatrix}\cos n\theta \\ \sin n\theta\end{Bmatrix} \quad (27a)$$

$$\{N_{\theta\phi}, M_{\theta\phi}, Q_\theta\} = \{N_{\theta\phi n}, M_{\theta\phi n}, Q_{\theta n}\}\begin{Bmatrix}\sin n\theta \\ \cos n\theta\end{Bmatrix} \quad (27b)$$

where the s-dependent coefficients with subscripts n must satisfy a set of equations obtained from equations (14)–(17) and (23) in the form

$$N_{\theta n} = \nu N_{\phi n} + (1-\nu^2)\frac{K}{r^2}(w_n\sin\phi + u_{\phi n}\cos\phi \pm nu_{\theta n})$$

$$- \alpha(1-\nu^2)KT_{0n} \quad (28a)$$

$$M_{\theta n} = \nu M_{\phi n} + (1-\nu^2)\frac{D}{r}\left(\frac{n^2}{r}w_n + \beta_{\phi n}\cos\phi\right.$$

$$\left.\pm n\frac{\sin\phi}{r}u_{\theta n}\right) - \alpha(1-\nu^2)DT_{1n} \quad (28b)$$

$$M_{\theta\phi n} = D\frac{1-\nu}{2r}\left(\mp\frac{2n\cos\phi}{r}w_n \pm nJu_{\phi n}\right.$$

$$\left.+ H\cos\phi\, u_{\theta n} \mp 2n\beta_{\phi n}\right) + \frac{D}{K}\frac{\sin\phi}{r}N_n \quad (28c)$$

$$Q_{\theta n} = \mp\frac{n}{r}M_{\theta n} + M_{\theta\phi n,s} + \frac{2\cos\phi}{r}M_{\theta\phi n} + m_{\theta n} \quad (28d)$$

$$N_{\theta\phi n} = N_n - \frac{\sin\phi}{r}M_{\theta\phi n} \quad (28e)$$

$$Q_{\phi n} = Q_n \mp \frac{n}{r}M_{\theta\phi n} \quad (28f)$$

The double signs again correspond to the top or bottom trigonometric function employed in (24), (25), and (27).

The remainder of this paper is concerned with the solution of the system of equations (26), subject to the boundary conditions on two edges s = const. It should be noted that after the expansion of the loads in Fourier series, the solution to (26) is obtained for each integral value of n separately, and then the solutions are superimposed to form a Fourier series expansion for the unknown variables.

Reduction to Initial Value Problems

This section is concerned with the reduction of a two-point boundary-value problem governed by

$$\frac{dy(x)}{dx} = A(x)y(x) + B(x) \quad (29a)$$

to a series of initial-value problems. In (29a), $y(x)$ is an $(m, 1)$ matrix which represents m unknown functions; x is the independent variable; $A(x)$ denotes the (m, m) coefficient matrix; and $B(x)$ is the $(m, 1)$ matrix of the nonhomogeneous terms. The elements of $A(x)$ and $B(x)$ are given piecewise continuous functions of x. The object is to determine $y(x)$ in the interval $a \leq x \leq b$ subject to m boundary conditions stated in terms of linear combinations of $y(a)$ and $y(b)$ in the form

$$F_a y(a) + F_b y(b) = G \quad (29b)$$

where F_a, F_b are (m, m) matrices and G is an $(m, 1)$ matrix, which are known from the statement of the boundary conditions of the problem. It should be clear that the governing system of equations (26) derived in the preceding section is stated in the form of (29a), and that the appropriate boundary conditions for a shell of revolution can be expressed in the form of (29b).

Let the complete solution of (29a) be written as

$$y(x) = Y(x)C + Z(x) \quad (30)$$

where the $(m, 1)$ matrix C represents m arbitrary constants, and $Y(x)$ is an (m, m) and $Z(x)$ an $(m, 1)$ matrix which are defined as the homogeneous and particular solutions of (29a) in the form

$$\frac{dY(x)}{dx} = A(x)Y(x) \quad (31a)$$

$$\frac{dZ(x)}{dx} = A(x)Z(x) + B(x) \quad (31b)$$

The initial conditions for determining $Y(x)$ and $Z(x)$ are

$$Y(a) = I \quad (32a)$$

$$Z(a) = 0 \quad (32b)$$

where I is the unit matrix.

Evaluation of (30) at $x = a$ leads at once, in view of (32a, b), to $C = y(a)$, and then (30) at $x = b$ can be written as

$$y(b) = Y(b)y(a) + Z(b) \quad (33)$$

Together with (29b), equation (33) constitutes a system of $2m$ linear algebraic equations from which the $2m$ unknowns, $y(a)$ and $y(b)$, are determined. Once $y(a)$ is known, the solution at any value of x is obtained from (30) provided that the values of $Y(x)$ and $Z(x)$ at that particular x are stored. This completes the reduction of a two-point boundary-value problem defined by (29) to $m + 1$ initial-value problems given by (31, 32).

As stated in the introduction, the solution for shells obtained by means of this procedure suffers a complete loss of accuracy at some critical length of the interval. The reason for this phenomenon can be seen clearly from (33). When the initial-value problems defined by (31, 32) are solved with the use of the equa-

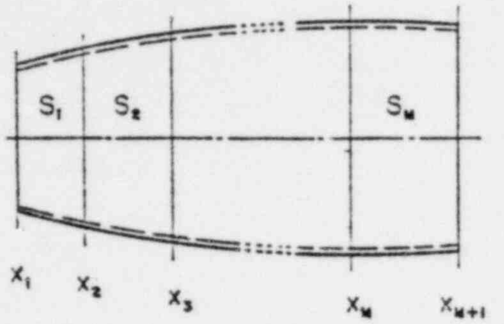

Fig. 2 Notation for division of total interval into segments

tions (26) for shells of revolution, it is observed that the elements of $Y(x)$ and $Z(x)$ increase in magnitude in such a way that if the length is increased by any factor n, then these solutions increase in magnitude approximately exponentially with n.

Consider, for example, the axisymmetric case when the deformation in the shell is caused by some prescribed edge conditions at $x = a$, say, by $M_\phi(a) = 1$ and $N_\phi(a) = Q(a) = 0$. It is reasonable to expect that the corresponding solutions at $x = b$ become smaller and smaller when the interval (a, b) is increased in length. The connection between $y(b)$ and $y(a)$ is given by the matrix equation (33) with the following magnitudes of the elements: $y(b)$-small, $Y(b)$-large, $y(a)$-unity. Clearly, the only way that the matrix product of (33) can give small values of $y(b)$ is that a number of significant digits of the large values of $Y(b)$ subtract out. When the length of the interval is increased, $Y(b)$ increase, while $y(b)$ decrease, and invariably all accuracy is lost at some critical length because all significant digits of $Y(b)$ in (33) are lost. This simple example serves as an illustration for the loss of accuracy encountered in the analysis of shells if the foregoing reduction technique is employed.

A convenient length factor, defined by

$$\beta = l[3(1 - \nu^2)]^{1/4}/(Rh)^{1/2} \tag{34}$$

where l is the length of the meridian of the shell and R is a minimum radius of curvature, can be used for an approximate estimate of the critical length of the shell. If the solutions $Y(x)$ and $Z(x)$ are obtained with a six-digit accuracy, then the foregoing procedure gives good results in the range $\beta \leq 3 - 5$.

However, the loss of accuracy of the solution can be avoided and shells of revolution with much larger values of β can be analyzed by means of the direct integration technique if the multisegment method given in the next section is employed.

Multisegment Method of Integration

Let the shell be divided into M-segments (denoted by S_i, where $i = 1, 2, \ldots, M$) of arbitrary length in each of which $\beta \leq 3$. Denote the coordinates of the ends of the segments by $x = x_i$, where the left-hand edge of the shell is at $x = x_1$ and the right-hand edge is at $x = x_{M+1}$, as shown in Fig. 2. In analogy to (30), the solution in the total interval $x_1 \leq x \leq x_{M+1}$ now can be written as

$$y(x) = Y_i(x)y(x_i) + Z_i(x) \tag{35}$$

where $Y_i(x)$ and $Z_i(x)$ denote the matrices corresponding to $Y(x)$ and $Z(x)$ in each segment $S_i(x_i \leq x \leq x_{i+1})$ and are given by

$$\frac{dY_i(x)}{dx} = A(x)Y_i(x) \tag{36a}$$

$$Y_i(x_i) = I \tag{36b}$$

$$\frac{dZ_i(x)}{dx} = A(x)Z_i(x) + B(x) \tag{36c}$$

$$Z_i(x_i) = 0 \tag{36d}$$

Requiring continuity of all elements of $y(x)$ at the points x_i, $i = 2, 3, \ldots, M + 1$, the following M-matrix equations are obtained from (35):

$$y(x_{i+1}) = Y_i(x_{i+1})y(x_i) + Z_i(x_{i+1}) \tag{37}$$

where $i = 1, 2, \ldots, M$. Equations (37) involve $M + 1$ unknown $(m, 1)$ matrices: $y(x_i)$, $i = 1, 2, \ldots, M + 1$. However, if the quantities prescribed at the edges of the shell are the fundamental variables, then the total number of unknowns is reduced by m, because $m/2$ elements of $y(x_1)$ and $m/2$ elements of $y(x_{M+1})$ are known. The same is true if the boundary conditions are stated in terms of linear combinations of the fundamental variables in the form of (29b). In this case, $y(x_1)$ and $y(x_{M+1})$ should be premultiplied by nonsingular (m, m) transformation matrices F_1 and F_{M+1}, respectively, so that the elements of the products contain the quantities prescribed at each edge. After eliminating $y(x_1)$ and $y(x_{M+1})$ from (37) by means of these products, it is concluded that (37) will retain its form if, after integration and before substitution into (37), $Y_1(x_2)$ is postmultiplied by F_1^{-1}, while $Y_M(x_{M+1})$ and $Z_M(x_{M+1})$ are premultiplied by F_{M+1}. In the following, it will be regarded that this transformation is carried out and that $y(x_1)$ and $y(x_{M+1})$ contain among their elements those quantities which are prescribed at $x = x_1$ and $x = x_{M+1}$, respectively.

Thus for all boundary conditions in the form of (29b), the system of M matrix equations (37) involves exactly M times m unknowns, and formally it can be solved by any method which is applicable to a large number of equations. However, the success of the procedure given in this paper lies in the application of Gaussian elimination directly on the matrix equations (37).

First a rearrangement of elements is performed. Since those $m/2$ elements of $y(x_1)$ and $y(x_{M+1})$ which are known through the boundary conditions can be any $m/2$ of the m-elements, it is necessary to rearrange the rows of $y(x_1)$ and $y(x_{M+1})$ so that the known elements are separated from the unknown elements. It is assumed here that the first $m/2$ elements of $y(x_1)$, denoted by $y_1(x_1)$, are known and that the last $m/2$ elements, denoted by $y_2(x_1)$, are unknown. On the other hand, $y_1(x_{M+1})$ are the unknown and $y_2(x_{M+1})$ are the known elements of $y(x_{M+1})$. Since the order of the variables in the column matrix $y(x)$ is arbitrary, it should be emphasized that this separation of elements does not involve any restriction on the boundary conditions, and that any natural boundary condition in the form of (29b) can be prescribed at each edge. The separation is achieved by a simple rearrangement of the columns of $Y_1(x_2)$ and the rows of $Y_M(x_{M+1})$ and $Z_M(x_{M+1})$ after integrating the initial-value problems defined by (36) to the ends of the segments S_1 and S_M and multiplying by F_1^{-1} and F_{M+1} as stated in the foregoing.

Once it is established which parts of $y(x_1)$ and $y(x_{M+1})$ are known, the continuity conditions (37) are rewritten as a partitioned matrix product of the form

$$\begin{bmatrix} y_1(x_{i+1}) \\ \hline y_2(x_{i+1}) \end{bmatrix} = \left[\begin{array}{c|c} Y_i^{11}(x_{i+1}) & Y_i^{12}(x_{i+1}) \\ \hline Y_i^{21}(x_{i+1}) & Y_i^{22}(x_{i+1}) \end{array}\right] \begin{bmatrix} y_1(x_i) \\ \hline y_2(x_i) \end{bmatrix} + \begin{bmatrix} Z_i^{1}(x_{i+1}) \\ \hline Z_i^{2}(x_{i+1}) \end{bmatrix} \tag{38}$$

so that each of the equations (37) turns into a pair of equations, given by

$$\begin{aligned} Y_i^{11}(x_{i+1})y_1(x_i) + Y_i^{12}(x_{i+1})y_2(x_i) - y_1(x_{i+1}) &= -Z_i^{1}(x_{i+1}) \\ Y_i^{21}(x_{i+1})y_1(x_i) + Y_i^{22}(x_{i+1})y_2(x_i) - y_2(x_{i+1}) &= -Z_i^{2}(x_{i+1}) \end{aligned} \tag{39}$$

The result is a simultaneous system of $2M$ linear matrix equations, in which the known coefficients $Y_i^{jk}(x_{i+1})$ and $Z_i^{j}(x_{i+1})$ are $(m/2, m/2)$ and $(m/2, 1)$ matrices, respectively, and the unknowns $y_j(x_i)$ are $(m/2, 1)$ matrices. Since $y_1(x_1)$ and $y_2(x_{M+1})$ are known, there are exactly $2M$ unknowns: $y_1(x_i)$, with $i = 2, 3, \ldots, M + 1$, and $y_2(x_i)$, with $i = 1, 2, \ldots, M$.

By means of Gaussian elimination, the system of equations (39) is first brought to the form

$$\left[\begin{array}{cccc:cc} E_1 & -I & 0 & 0 & 0 & 0 \\ 0 & C_1 & -I & 0 & 0 & 0 \\ 0 & 0 & E_2 & \cdot -I & 0 & 0 \\ 0 & 0 & 0 & C_2 & -I & 0 \\ \hdashline 0 & 0 & 0 & 0 & E_M & -I \\ 0 & 0 & 0 & 0 & 0 & C_M \end{array}\right] \left[\begin{array}{c} y_2(x_1) \\ y_1(x_2) \\ y_2(x_2) \\ y_1(x_M) \\ \hdashline y_2(x_M) \\ y_1(x_{M+1}) \end{array}\right] = \left[\begin{array}{c} A_1 \\ B_1 \\ A_2 \\ B_2 \\ \hdashline A_M \\ B_M \end{array}\right] \quad (40)$$

where the dots indicate the triangularized equations (39) with $i = 3, 4, \ldots, M - 1$. The $(m/2, m/2)$ matrices E_1, C_1 are defined by

$$E_1 = Y_1^2 \quad (41a)$$

$$C_1 = Y_1^4 E_1^{-1} \quad (41b)$$

and for $i = 2, 3, \ldots, M$

$$E_i = Y_i^3 + Y_i^1 C_{i-1}^{-1} \quad (41c)$$

$$C_i = (Y_i^4 + Y_i^3 C_{i-1}^{-1}) E_i^{-1} \quad (41d)$$

The $(m/2, 1)$ matrices A_i, B_i are given by

$$A_1 = -Z_1^1 - Y_1^1 y_1(x_1) \quad (42a)$$

$$B_1 = -Z_1^2 - Y_1^3 y_1(x_1) - Y_1^4 E_1^{-1} A_1 \quad (42b)$$

and for $i = 2, 3, \ldots, M - 1$

$$A_i = -Z_i^1 - Y_i^1 C_{i-1}^{-1} B_{i-1} \quad (42c)$$

$$B_i = -Z_i^2 - Y_i^3 C_{i-1}^{-1} B_{i-1} - (Y_i^4 + Y_i^3 C_{i-1}^{-1}) E_i^{-1} A_i \quad (42d)$$

Finally, for the Mth segment

$$A_M = -Z_M^1 - Y_M^1 C_{M-1}^{-1} B_{M-1} \quad (42e)$$

$$B_M = y_2(x_{M+1}) - Z_M^2 - Y_M^3 C_{M-1}^{-1} B_{M-1} - (Y_M^4 + Y_M^3 C_{M-1}^{-1}) E_M^{-1} A_M \quad (42f)$$

For brevity, in place of $Y_i^j(x_{i+1})$ and $Z_i^j(x_{i+1})$, the symbols Y_i^j and Z_i^j have been used.

By means of (41) and (42), the unknowns of (39) are obtained by

$$y_1(x_{M+1}) = C_M^{-1} B_M \quad (43a)$$

$$y_2(x_M) = E_M^{-1}[y_1(x_{M+1}) + A_M] \quad (43b)$$

and for $i = 1, 2, \ldots, M - 1$

$$y_1(x_{M-i+1}) = C_{M-i}^{-1}[y_2(x_{M-i+1}) + B_{M-i}] \quad (43c)$$

$$y_2(x_{M-i}) = E_{M-i}^{-1}[y_1(x_{M-i+1}) + A_{M-i}] \quad (43d)$$

It should be noted that (41)–(43) must be evaluated in succession, because each equation involves the result obtained by the preceding equation.

Once all the unknowns $y(x_i)$ are found, the fundamental variables are determined from (35) at any value of x at which the solutions $Y_i(x)$ and $Z_i(x)$ are stored during the integration of the initial-value problems of (36). The integration of (36) can be accomplished by means of any of the standard direct integration methods.

On the basis of the system of equations (26) given in an earlier section and the method of solution developed in the last two sections, the author has prepared a computer program[4] which has been applied to many shell configurations having large values of β and successfully tested against known results. One example of a pressurized torus with $\beta = 57$ is presented in the next section.

The program admits arbitrary meridional variations, including discontinuities, in all shell parameters. It also admits ring loads in the form of prescribed values of N_ϕ, M_ϕ, N, or Q at any value of ϕ on the shell. Such loads introduce discontinuities in the solution for the corresponding stress resultants, and they can be represented at every x_i by an $(m, 1)$ discontinuity matrix which is simply added to the matrix $Z_i(x_{i+1})$ on the right-hand side of (37). This feature is of great value if shell joints are considered. Any discontinuity, either in geometry or in loads, is easily handled by requiring that the end point of a segment coincides with the location of the discontinuity. Since integration is restarted at the beginning of each segment, the precise effect of the discontinuity is obtained. The program outputs all fundamental variables at a number of desired points within each segment, and it also computes the values of $y(x_i)$ twice; once from (43) and then from (35). If a certain number of significant figures of these values match, then the continuity conditions are known to be satisfied to the same number of figures. In this way, a convenient error estimate of the solution is obtained for every case.

Example: Pressurized Torus

In this section the stresses and displacements are determined in a complete torus subjected to a constant internal pressure. It is well known that the solution of this problem, when obtained by means of the linear membrane theory of shells, has a discontinuity in the displacement field. It has been shown by Jordan [16] and by Sanders and Liepins [17] that a satisfactory solution with regard to the displacement field for a sufficiently thin shell can be obtained if the nonlinear membrane theory of shells is employed. Subsequently, Reissner [18] established bounds on certain parameters which show when the nonlinear membrane and when the linear bending theory is applicable. It seems worthwhile to give here the solution for a pressurized torus as predicted by the linear bending theory.

The geometry of the torus is shown in Fig. 3. With regard to the quantities employed in equations (26), the two necessary parameters for a torus are given as

$$R_\phi = b \quad (44a)$$

$$r = a + b \sin \phi \quad (44b)$$

Because of symmetry with respect to the plane XX, Fig. 3, the

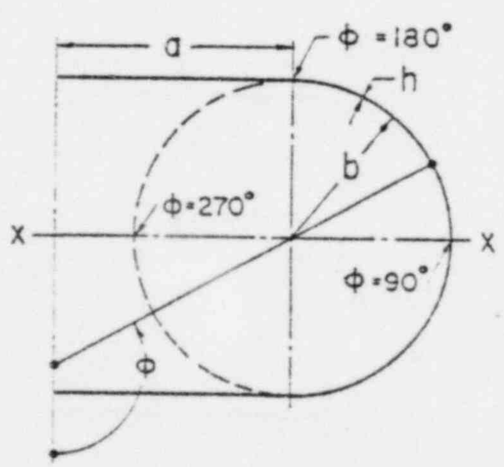

Fig. 3 Geometry of torus considered in example

[4] The program was written and all calculations were carried out by the author on the IBM 709 computer at the Yale Computer Center. The direct integration of (36) is performed by means of the Adams predictor-corrector method, which selects an optimum step size at every step according to a prescribed accuracy.

Table 1 Stresses and displacements of a pressurized torus; $pb/Eh = 0.002$, $a/b = 1.5$, $\nu = 0.3$

h/b / ϕ	$\sigma_{\phi m}/E \times 10^3$	$(\sigma_{\phi b}/E) \times 10^4$			$(w/b) \times 10^3$		
	0.005	0.05	0.02	0.005	0.05	0.02	0.005
90	1.601	−0.063	−0.031	−0.016	1.249	1.284	1.298
108	1.613	−0.188	−0.093	−0.019	1.261	1.315	1.328
126	1.650	−0.886	−0.123	−0.030	1.359	1.393	1.427
144	1.720	−1.915	−0.908	−0.020	1.786	1.597	1.625
162	1.832	−0.895	−1.378	−0.910	2.820	2.580	2.159
171	1.906	1.002	0.168	−0.605	3.467	3.493	3.297
180	1.990	3.089	2.277	1.482	3.994	4.334	4.815
184.5	2.042	3.890	3.035	1.968	4.150	4.576	5.243
189	2.104	4.270	3.119	1.520	4.208	4.637	5.151
193.5	2.175	4.178	2.580	0.530	4.156	4.509	4.693
198	2.254	3.610	1.589	−0.274	3.998	4.221	4.162
216	2.642	−0.587	−0.957	−0.079	2.652	2.527	2.481
234	3.168	−1.245	−0.291	−0.066	1.273	1.269	1.269
252	3.730	−0.717	−0.344	−0.077	0.416	0.417	0.414
270	3.997	−0.824	−0.331	−0.081	0.103	0.101	0.100

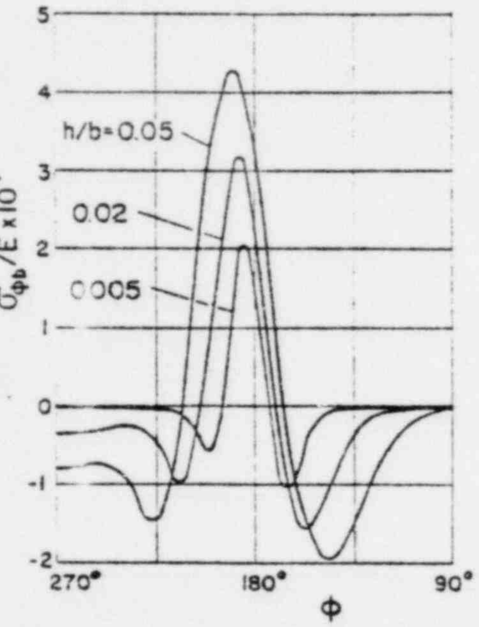

Fig. 4 Meridional bending stress $\sigma_{\phi b}$ at outer fiber versus meridional coordinate ϕ

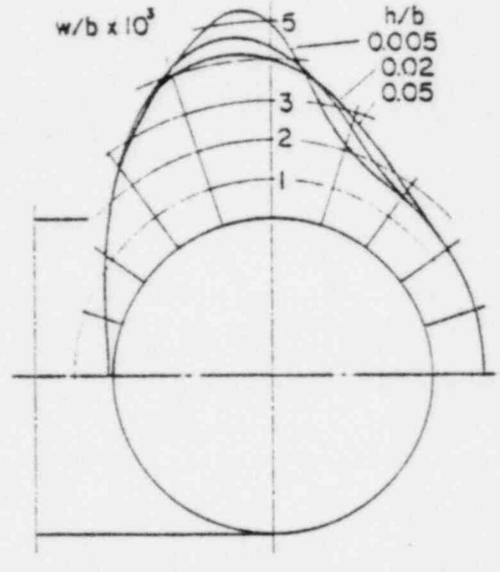

Fig. 5 Normal displacement w versus ϕ showing deformed section

integration of the initial-value problems is carried out from $\phi = 90°$ to $\phi = 270°$, and the boundary conditions at these endpoints are $u_\phi = \beta_\phi = Q = 0$. For the purpose of comparison with the results of [16] and [17], the load parameter is chosen as $pb/Eh = 0.002$ and $a/b = 1.5$.

The numerical values of the normal displacement, meridional membrane stress $\sigma_{\phi m} = N_\phi/h$, and meridional bending stress $\sigma_{\phi b} = 6M_\phi/h^2$ at $\zeta = h/2$ for a pressurized torus are shown in Table 1 and in Figs. 4 and 5. These results were taken from the output of the computer program prepared for an arbitrary shell of revolution after prescribing the geometric parameters as given by (44). The meridional membrane stress distribution agrees very well with that obtained in [17] by means of the membrane theory of shells and it shows only a small variation with h/b. The deformed shapes of the cross section of the torus shown in Fig. 5 for three values of h/b are in qualitative agreement with those given in [16] and [17], but their quantitative agreement cannot be expected because the values of h/b used in this example are outside the range where the bending effects are negligible. This is confirmed by the examination of the bending stresses shown in Fig. 4. The maximum value of $\sigma_{\phi b}$ occurs at $\phi = 189°$ for $h/b = 0.05$ and at $\phi = 184.5°$ for $h/b = 0.005$, which are also the points of maximum normal displacement and curvature as seen in Fig. 5. The comparison of the membrane and the maximum bending stress at various values of h/b is shown in Table 2.

Table 2 Maximum meridional bending stress and meridional membrane stress at $\phi = \phi_0$

h/b	0.05	0.02	0.005
ϕ_0	189°	189°	184.5°
$(\sigma_{\phi m}/E) \times 10^3$	2.053	2.082	2.042
$(\sigma_{\phi b}/E) \times 10^3$	0.427	0.312	0.197
$100\ (\sigma_{\phi b}/\sigma_{\phi m})$	20.8	15.0	9.6

It is of significance to note that even for the thickness ratio $h/b = 0.005$, which for many applications would be regarded as small, the maximum bending stress is about 10 percent of the membrane stress at the same point. Such effects of bending in a torus were previously noted by Clark [19], and they are also in agreement with the statement made by Goldenveizer [20] that when the middle surface touches a closed-plane curve, which in a torus corresponds to $\phi = 180°$, then in the vicinity of this curve bending stresses should be expected and the membrane theory is not applicable.

The boundary layer shown in Fig. 4 is also in agreement with the conclusions reached in [18] to the effect that when μ and ρ given by

$$\mu = [12(1 - \nu^2)]^{1/2}(b/a)(b/h)$$

$$\rho = 12(1 - \nu^2)(p/E)(b/h)^3$$

are large compared to unity, then a boundary layer in the neighborhood of $\phi = 180°$ should be anticipated. For the present example, μ ranges from 44 to 440 and p from 9 to 874. However, since p is the only load parameter of the problem, the solutions shown in Figs. 4 and 5 are proportional to p, and the boundary layer remains unaffected if p alone is varied. Of course, for very large values of p the deformation of the torus may exceed the limits of a linear theory which according to [18] restrict p to the range $p \ll \mu^{1/2}$.

Acknowledgments

This research has been supported by the National Science Foundation Grant #23922. Many ideas leading to this paper originated from the consulting work performed by the author for the United Technology Center, Sunnyvale, California. The author wishes to thank the staff of the Applied Mechanics Department of UTC for many illuminating discussions concerning this subject.

References

1 P. M. Naghdi and C. N. DeSilva, "Deformation of Elastic Ellipsoidal Shells of Revolution," *Proceedings of the Second U. S. National Congress of Applied Mechanics*, 1954, pp. 333–343.

2 W. Lohmann, "Beitrag zur Integration der Reissner-Meissnerschen Schalengleichung für Behälter unter konstantem Innerdruck," *Ingenieur-Archiv*, vol. 6, 1935, pp. 338–346.

3 H. Münz, "Ein Integrationsverfahren für die Berechnung der Biegespannungen achsensymmetrischer Schalen unter achsensymmetrischer Belastung," *Ingenieur-Archiv*, vol. 19, 1951, pp. 103–117, 255–270.

4 E. Klingbeil, "Zur Theorie der Rotationsschalen vom Standpunkt numerischer Rechnungen," *Ingenieur-Archiv*, vol. 27, 1959, pp. 242–249.

5 G. D. Galletly, W. T. Kyner, and C. E. Moller, "Numerical Methods and the Bending of Ellipsoidal Shells," *Journal of the Society of Industrial and Applied Mathematics*, vol. 9, 1961, pp. 489–513.

6 R. K. Penny, "Symmetric Bending of the General Shell of Revolution by Finite Difference Method," *Journal of Mechanical Engineering Science*, vol. 3, 1961, pp. 369–377

7 P. P. Radkowski, R. M. Davis, and M. R. Bolduc, "Numerical Analysis of Equations of Thin Shells of Revolution," *American Rocket Society Journal*, vol. 32, 1962, pp. 36–41.

8 W. K. Sepetoski, C. E. Pearson, I. W. Dingwell, and A. W. Adkins, "A Digital Computer Program for the General Axially Symmetric Thin-Shell Problem," Journal of Applied Mechanics, vol. 29, Trans. ASME, vol. 84, Series E, 1962, pp. 655–661.

9 B. Budiansky and P. P. Radkowski, "Numerical Analysis of Unsymmetrical Bending of Shells of Revolution," *AIAA Journal*, vol. 1, 1963, pp. 1833–1842.

10 J. E. Goldberg and J. L. Bogdanoff, "Static and Dynamic Analysis of Nonuniform Conical Shells under Symmetrical and Unsymmetrical Conditions," *Proceedings of the Sixth Symposium on Ballistic Missile and Aerospace Technology*, Academic Press, New York, N. Y., vol. 1, 1961, pp. 219–238.

11 C. R. Steele, "Shells of Revolution With Edge Loads of Rapid Circumferential Variation," Journal of Applied Mechanics, vol. 29, Trans. ASME, vol. 84, Series E, 1962, pp. 701–707.

12 R. D. Schile, "Asymptotic Solution of Nonshallow Shells of Revolution Subjected to Nonsymmetric Loads," *Journal of the Aerospace Sciences*, vol. 29, 1962, pp. 1375–1379.

13 E. Reissner, "A New Derivation of the Equations for the Deformation of Elastic Shells," *American Journal of Mathematics*, vol. 63, 1941, pp. 177–184.

14 S. A. Ambartsumyan, "Theory of Anisotropic Shells" (in Russian), *Gosudarstvennoye Izdatel'stvo Fiziko-Matematicheskoi Literatury*, Moscow, USSR, 1961, p. 91.

15 P. M. Naghdi, "On the Theory of Thin Elastic Shells," *Quarterly of Applied Mathematics*, vol. 14, 1957, pp. 369–380.

16 P. F. Jordan, "Stresses and Deformations of the Thin-Walled Pressurized Torus," *Journal of the Aerospace Sciences*, vol. 29, 1962, pp. 213–225.

17 J. L. Sanders, Jr., and A. Liepins, "Toroidal Membrane Under Internal Pressure," *AIAA Journal*, vol. 1, 1963, pp. 2105–2110.

18 E. Reissner, "On Stresses and Deformations in Toroidal Shells of Circular Cross Section Which Are Acted Upon by Uniform Normal Pressure," *Quarterly of Applied Mathematics*, vol. 21, 1963, pp. 177–187.

19 R. A. Clark, "On the Theory of Thin Elastic Toroidal Shells," *Journal of Mathematics and Physics*, vol. 29, 1950, pp. 146–178.

20 A. L. Goldenveizer, *Theory of Elastic Thin Shells*, Pergamon Press, New York, N. Y., 1961, p. 480.

3. THERMAL EVALUATION

3.1 Discussion

3.1.1 Summary of Results

For normal operation with 1.5 kw decay heat with a 130 F ambient temperature, the cask inner liner temperature will be about 227 F. During the hypothetical fire accident, the inner liner temperature will be about 560 F.

The Fermi fuel subassembly will be shipped in the BMI-1 shipping cask, which has been provided with a special basket. During shipment, the cask cavity is filled with water. The void spaces between the fuel rods in the subassembly are filled with a settled bed of copper shot in water. The cask is to be shipped by truck so that under normal conditions the maximum fuel and water temperature is about 230 F.

3.1.2 Maximum and Minimum Decay Heat

(a) BRR/MTR Fuel

The total fission product decay heat is calculated from the data in ORNL-2127[(1)]. Following the analysis in Reference (1), the Number U-235 atoms in a BRR fuel element is:

$$N = \frac{3.2 \times 10^{10} P}{\sigma\phi}$$

where

P = irradiation power (watts)

σ = fission cross section used in Tables = 580 barns

ϕ = thermal neutron flux.

(1) References to Section 3. found in Section 3.6.1.

The maximum U-235 burn-up in a BRR element is 17.5 percent For a fuel loading of 162 g U-235, with a capture to fission ratio of 1.18, the fission product production is 24.1 g. For an irradiation time of 313 days, the irradiation power is P = 24.1 MwD/313 D = 7.7×10^4 watts per element (assuming 1 g U-235 = 1 MwD). Thus, for $\phi = 10^{14}$ n/cm^2 sec:

$$N = \frac{(3.2 \times 10^{20})(7.7 \times 10^4)}{(580)(10^{14})} = 4.25 \times 10^{22} \text{ atoms U-235 per element.}$$

From the data in Reference (1), the total decay heat (beta plus gamma) for an irradiation time of 313 days and a cooling time of 90 days (with $\phi = 10^{14}$) is $q = 10^{-21}$ watts/atom U-235, or:

$$Q = (10^{-21})(4.25 \times 10^{22}) = 42.5 \text{ watts/element} \quad .$$

For 24 elements with the same irradiation history, the decay heat is 24 x 42.5 = 1.02 kw = 3,480 Btu/hr.

(b) Fermi Fuel

The heat transfer analysis is based on a total (beta plus gamma) decay heat of 1.5 kw in a maximum burnup subassembly. In such a subassembly, the fuel is irradiated at a power of 1.4 Mw for eight 28-day periods to a burnup of 1.6 percent. The reactor is shut down for 28 days between each 28-day irradiation period. The fuel is cooled 10 days before shipment. The axial power peaking factor is 1.23. The decay heat calculation is given in APDA Memo P-64-11[(2)].

IMAGE EVALUATION
TEST TARGET (MT-3)

6″

MICROCOPY RESOLUTION TEST CHART

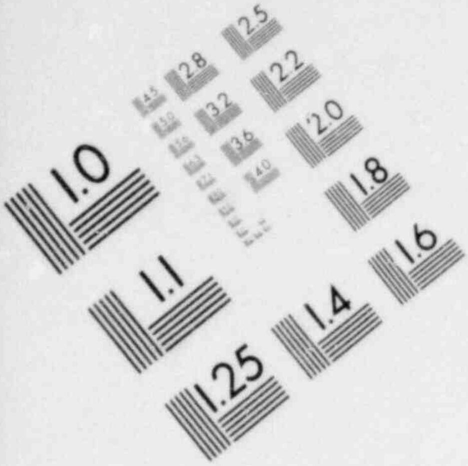

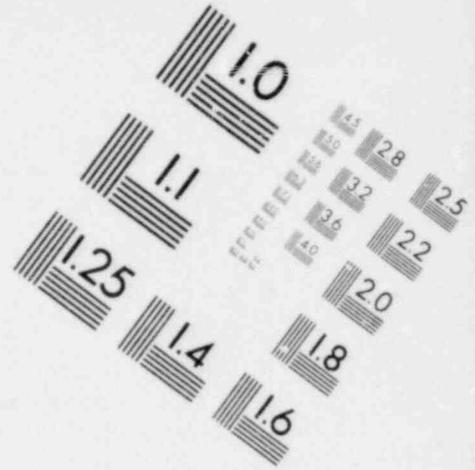

IMAGE EVALUATION
TEST TARGET (MT-3)

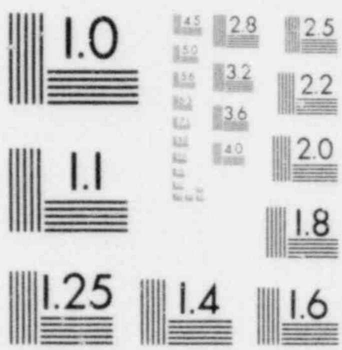

6″

MICROCOPY RESOLUTION TEST CHART

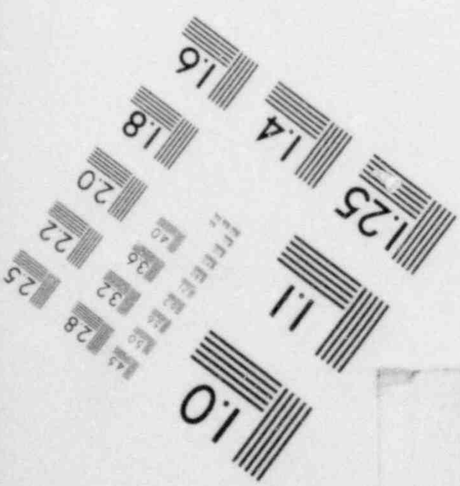

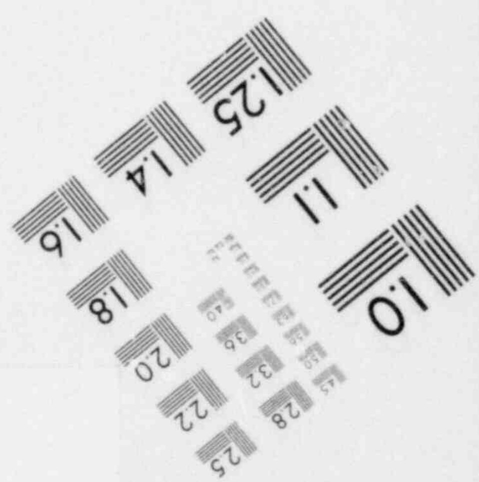

3.3 Documents: 11, 15,

(c) TRIGA Fuel

The fission product activity was estimated to be 250 curies per element in November, 1970 (based on radiation measurement made at that time). Assuming 2 MEV per event, the decay heat of the fuel is:

$$250 \text{ curies/element} \times 3.7 \times 10^{10} \text{ events/sec/curie} \times$$
$$2 \text{ MEV/event} \times 1.6 \times 10^{-13} \text{ watts/MEV/sec}$$
$$= 2.96 \text{ watts/element} \quad .$$

The total heat load for the cask is 112.5 watts. This is a very conservative estimate since the fuel has cooled $\sim$ 2 years and has a cooling factor greater than 3.0. The BMI-1 cask is licensed to handle up to 1.5 kw of decay heat. Thus, the thermal inventory for this shipment is well within the limits for the cask.

(d) PULSTAR Fuel

The average decay heat output per fuel pin at the time of shipment is 5.0 watts and the maximum heat output per pin is 7.0 watts. The heat source for the fully loaded cask will therefore be:

$$252 \frac{\text{pins}}{\text{cask}} \times 5.0 \text{ watts/pin} = 1{,}260 \text{ watts/cask} \quad .$$

Certificate of Compliance Number 5057 approves a heat load of 1.5 kw for the cask.

(e) EPRI Crack Arrest Capsules

The total decay heat generated by the capsule at discharge is 197 watts. The axial heat rate over the height of the capsule is (197)(12)/21.5 = 110 watts/ft. The cask is rated for contents whose decay heat is up to 1,500 watts. The cavity length is 54 inches. Thus, the axial heat rate permitted for the cask is (1,500)(12)/54 = [illegible] watts/ft. Thus, the decay heat is within permissible levels.

3.1.3 Solar Heat

From Reference (3), p 1,636, the solar heating is:

$$Q = 429T \left[\epsilon_H A_H \cos \theta_H + \epsilon_V A_V \cos \theta_V \right]$$

where

T = atmospheric transmittance = 0.6
ϵ = absorbtivity = 0.5
A = area of surface
H. = refers to horizontal surface or top of cask
V = refers to vertical surface or side of cask .

At noon during the summer solstice, at 40 degrees latitude:

$$\cos \theta_H = 0.96$$

$$\cos \theta_V = 0.284 \quad .$$

The outside of the cask is 33 inches in diameter and 72.375 inches in height. Thus:

$$A_H = \frac{\pi}{4} D^2 = 5.93 \text{ feet}^2$$

$$A_V = DH = 16.6 \text{ feet}^2 \text{ (protected area).}$$

The solar heat is:

$$Q = 429(0.6) \left[(0.5)(5.93)(0.96) + (0.5)(16.6)(0.284) \right]$$

$$= 732 + 607 = 1{,}339 \text{ Btu/hr.} = 0.392 \text{ kw}$$

3.2 Summary of Thermal Properties of Materials

The materials' thermophysical properties which were employed are shown in Table 3.1. Also, since it has been well demonstrated that the lead will contract away from the outer shell after casting (fabrication experience indicates a potential gap of 0.060-0.100 inch), the thermal model included a variable air gap (Node 118) which has an effective thermal conductivity that increases with temperature as shown in Figure 3.1.

3.3 Technical Specifications of Components

Relief Value - 75 psig

Pressure gauge - 30 in Hg vacuum to 100 psig pressure.

3.4 Thermal Evaluation for Normal Conditions of Transport

3.4.1 Thermal Model

The analysis for normal operation were performed assuming only radial heat flow from the contents through the cask walls to the environment.

Document: 4

TABLE 3.1 THERMOPHYSICAL PROPERTIES EMPLOYED FOR LEAD AND STEEL

Lead

Density = 705 pounds/feet^3
Melting Temperature = 621 F
Latent Heat = 10.5 Btu/pounds

Temperature, F	Thermal Conductivity, Btu/hr-ft-F	Specific Heat, Btu/lb	Emissivity
32	20.1	0.0303	1.0
212	19.6	0.0315	1.0
572	18.0	0.0338	1.0
621	8.8	0.0337	1.0
900	8.9	0.0326	1.0

Steel

Density = 488 pounds/feet^3
Latent Heat = 120 Btu/lb
Melting Temperature = 1,800 F

Temperature, F	Thermal Conductivity, Btu/hr-ft-F	Specific Heat, Btu/lb	Emissivity
32	8.0	0.11	0.8[a], 1.0[b]
212	9.4	0.11	0.8, 1.0
572	10.9	0.11	0.8, 1.0
932	12.4	0.11	0.8, 1.0
1,800	15.0	0.11	0.8, 1.0

(a) For steel surface exposed to flame, $\varepsilon = 0.8$.

(b) For steel surfaces viewing each other across internal air gaps, $\varepsilon = 1.0$.

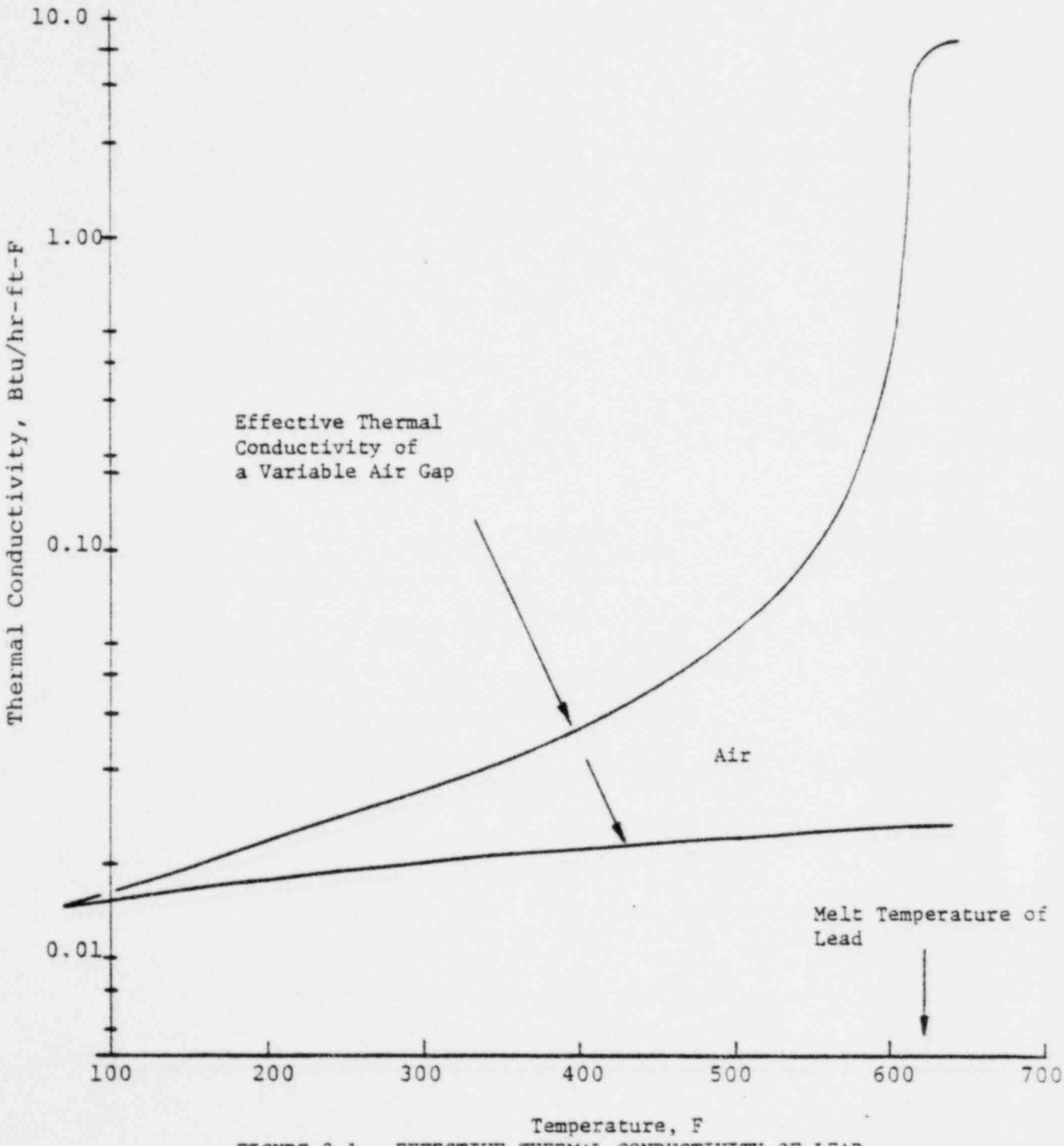

FIGURE 3.1. EFFECTIVE THERMAL CONDUCTIVITY OF LEAD TO-SHELL INTERFACE, GAP (NODE 118)

3.4.2 Maximum Temperature

3.4.2.1 BRR/MTR Fuel

(a) External Heat Transfer

During normal operation, heat is dissipated from the outside surface of the cask by radiation and natural convection in air. The heat transferred by radiation is:

$$Q_r = 0.173 \; \varepsilon A \left[\left(\frac{T_o}{100}\right)^4 - \left(\frac{T_a}{100}\right)^4 \right] ,$$

and the heat transferred by convection is:

$$Q_c = h_c A_c (T_0 - T_a) \quad ,$$

where

ε = surface emissivity = 0.5 for steel

T_o = cask surface temperature

T_a = ambient temperature = 100 F

$h_c = 0.19(T_o - T_a)^{1/3}$ (McAdams[4], p 173)

$A_r = A_c$ = heat transfer area .

Heat transfer from the outside corners and top of the cask is partly obstructed due to the air pockets built into the lead to provide for lead meltdown space in case of fire. The air pockets also insulate the cask from solar heating. Two estimates of the maximum heat load are made. In the first case, the full solar load and total cask surface area are considered.

In the second case, heat transfer from areas obstructed by air pockets is neglected, and only the solar load on the side is included. In the first case, the total heat load on the outside surface of the cask is Q = 3,480 + 1,339 = 4,819 Btu/hr; and, the heat-transfer area including the top and bottom is A = 52.1 + 11.36 = 63.96 ft^2. In the second case, the solar load is 540 Btu/hr for a total heat load of 4,020 Btu/hr; and the heat-transfer area, neglecting the top and corners, is A = 46.3 + 3.4 = 49.7 ft^2. In the first case, the heat flux is 75.4 Btu/hr ft^2, and in the second case is 80.9 Btu/hr ft^2. The second case is calculated below since it leads to conservative results (higher surface temperatures).

The total heat, removal capacity of the cask is: $Q=Q_r + Q_c$, or

$$Q = (0.173)(49.7) \left[\left(\frac{T_o}{100}\right)^4 - \left(\frac{560}{100}\right)^4 \right] + 0.19(49.7)(T_o - 560)^{4/3} .$$

For:

$$Q = 3,480 + 540 = 4,020 \text{ Btu/hr}, \quad 4,020 = 4.29 \left[\left(\frac{T_o}{100}\right)^4 - 981 \right]$$

$$+ 9.44(T_0 - 560)^{4/3} ,$$

and:

$$T_0 = 617 \text{ R} = 157 \text{ F}.$$

Thus, the maximum cask surface temperature will be 157 F, assuming there is no heat loss (or addition), through the top and corners of the cask. The surface temperature is below 180 F, which meets the AEC requirements.

(b) Heat Transfer in Cask Wall

The temperature drop across the lead in the wall of the cask is:

$$\Delta T = \frac{Q}{2\pi kL} \ln D_2/D_1 = 4.05 \text{ F},$$

where

$Q = 3,480$ Btu/hr
$k = 19$
$L = 5$ feet
$D_2 = 32$ inches
$D_1 = 16$ inches .

The total temperature drop across the inside (thickness = 0.25 inches) and outside (thickness = 0.5 inch) steel plates is $\Delta T = 0.7$ F.

As the lead solidifies in the manufacturing process, a small air gap is formed between the outside steel shell and the lead. The thickness of this gap is estimated to be 0.0817 inch. The heat transferred by conduction and radiation across the gap is:

$$Q = \frac{kA\Delta T}{t} + 0.173 \text{ FA } \frac{4T^3 \Delta T}{10^8}$$

where

$Q = 3,480$ Btu/hr
$A = 50.2 \text{ ft}^2$
$t = 0.0817$ inch

$$F = 0.231$$

$$T = 180\ F = 640\ R \quad .$$

The total temperature drop across the cask wall is ΔT = 23.8 F. It is expected that the lead will settle during transportation and close the air gap. Thus, the temperature drop across the wall of the cask should decrease in later shipments.

The total temperature drop across the cask wall is ΔT = 4.05 + 0.7 + 23.8 = 28.6 F. The temperature at the inside surface of the cask wall is T = 157 + 28.6 = 185.6 F.

(c) Internal Heat Transfer

During normal operation, the cavity of the cask is filled with water, and the fuel elements are cooled by natural circulation of the water. The water flows up through and around the fuel elements to the top of the cavity and then flows down through the space between the cask wall and the fuel elements. The heat absorbed by the water as it flows up through the elements is dissipated as the water flows down past the cooler cask wall.

The natural convection heat transfer can be calculated from the pertinent pressure drop and heat balance equations. These equations have been solved and placed in a form convenient for calculation in Reference 5. According to the analysis in Reference 5, the equations which must be solved for the maximum water temperature T(L) are:

$$T(L) = T_c = \frac{\gamma}{1-e^{-\alpha L}} \qquad (1)$$

$$\gamma = T(L) - T(o) = \frac{Q}{C\rho} \left(\frac{1}{AV} \right) \tag{2}$$

$$\alpha L - 2(F_A - 1) = \frac{384}{\rho g \beta} \left[(A_i D_i^{\,2})^{-1} + (A_o D_o^{\,2})^{-1} \right] \left(\frac{AV}{\gamma} \right) \tag{3}$$

$$\alpha L = \frac{P_H L}{C\rho} \left(\frac{h_o}{AV} \right) \tag{4}$$

$$h_o = 0.05 \left[\frac{\rho^2 k^2 g \beta c}{\mu} \right]^{\frac{1}{3}} \left(\frac{\gamma}{\alpha L} \right)^{\frac{1}{3}} \tag{5}$$

where

$T(L)$ = maximum water temperature (at top of cask)
$T(o)$ = water temperature at bottom of cask
T_c = cask cavity wall temperature
Q = decay heat
AV = flow velocity (ft^3/hr)
A_i = total element flow area (up-flow region)
D_i = equivalent diameter of element region
A_o = flow area of down-flow region
D_o = equivalent diameter of down-flow region
F_A = axial peaking factor
PH_L = heat-transfer area = area of cavity wall
g = gravitational constant

water properties:

c = specific heat
ρ = density
μ = viscosity
β = volume expansivity (F^{-1})
k = thermal conductivity .

The required numerical data are:

$T_{av} \sim 195$ F

$C = 1.0$ Btu/16 F

$\rho = 60.2$ pounds/ft^3

$\frac{384\mu}{\rho g \beta} = 0.28 \times 10^{-4}$

$\left[\frac{k^2 \rho^2 \alpha \beta C}{\mu}\right]^{\frac{1}{3}} = 487$

$F_A = 1.40$

$A_o = 68.5$ inches^2

$D_o = 2.76$ inches

$A_i = 88.7$ inches^2

$D_i = 0.477$ inches

$P_H = 48.7$ inches

$L = 52.5$ inches

$Q = 3{,}480$ Btu/hr

Using these numerical data, Equations (2), (3), (4), and (5) become:

$$\gamma = 57.8/AV \tag{2}$$

$$\alpha L = 0.8 + 0.03\ (AV/\gamma) \tag{3}$$

$$\alpha L = 0.295\ (h_o/AV) \tag{4}$$

$$h_o = 24.4\ (\gamma/\alpha L)^{\frac{1}{3}} \tag{5}$$

The solutions to these equations are $\gamma = 4.3$ F, $\alpha L = 0.896$, $AV = 13.5$ ft^3/hr, and $h_o = 41.2$ Btu/hr ft^2 F. From Equation (1), $T(L) - T_c = 7.3$ F.

From Section 3.4.2.1(b), the maximum inside cask wall temperature is $T_c = 185.6$ F. The maximum water temperature is $T(L) = 185.6 + 7.3 = 192.9$ F.

The design pressure of this cask is 100 psig so that the maximum permissible operating pressure is 50 psig. Thus, the maximum operating temperature (193 F) is well below the boiling point (298 F) at the maximum permissible operating pressure.

3.4.2.2 Fermi Fuel

Du... j normal conditions, the cask is water filled and the ambient temperature is 100 F. The decay heat load is 1.5 kw, and the solar load is 0.392 kw.

(a) External Heat Transfer

From Section 3.4.2.1(a), the surface temperature T_s of the cask is given by the equation:

$$Q = 4.29 \left[\left(\frac{T_s}{100}\right)^4 - \left(\frac{T_o}{100}\right)^4 \right] + 9.44 \; (T_s - T_o)^{\frac{4}{3}}$$

where

Q = 1.5 kw + 0.392 kw = 6,459 Btu/hr

T_o = ambient temperature = 100 F = 560 R

T_s = surface temperature

The solution to this equation is T_s = 643 R = 183 F. The surface temperature is slightly above 180 F, and access to the surface of the cask will be restricted when the ambient temperature is above 97 F.

(b) Temperature Drop in Cask Wall

A temperature drop of 29 F at 1.4 kw has been measured across the wall of the BMI-1 cask. At 1.5 kw, the temperature drop is:

$$\Delta T = \frac{1.5}{1.4} \times 29 = 31 \text{ F}$$

(c) Heat Transfer in Cavity

During normal conditions, heat is transferred from the surface of the basket to the cask wall by natural convection in water and by conduction through the six radial copper ribs extending from the basket to the wall. The heat transferred by natural convection from the basket to the water is:

$$Q = hA_b(T_b - T);$$

and the heat transferred from the water to the cask wall is:

$$Q = hA_w(T - T_w) \quad ,$$

where h = heat transfer coefficient = 100 Btu/hr ft^2 F,

(McAdams, Ref. 4, p. 175) .

A_b = basket area = 7.5 ft^2 .

A_w = wall area = 17.5 ft^2 .

T_b = basket temperature .

T_w = cask wall temperature .

T = water temperature .

From the equations above, the temperature drop $(T_b - T_w)$ is given by the relation:

$$Q = \frac{A_w A_b}{(A_w + A_b)} h \ (T_b - T_w) \quad .$$

If all the heat transferred by convection ($Q = 5,120$ Btu/hr) then $(T_b - T_w) = 9.8$ F. Heat transfer by conduction in the copper ribs will reduce this temperature drop a few degrees (see Section 3.5.4.2(b). From the above, the temperature of the outside surface of the copper basket is $T_b = 183 + 31 + 9.8 = 224$ F.

The temperature drop across the copper basket is:

$$\Delta T = \frac{Q}{2\pi kL} \ln \frac{D_2}{D_1} = 1.3 \text{ F}$$

where

$k = 200$ Btu/hr ft F

$Q = 5,120$ Btu/hr

$D_2 = 10.75$ inches

$D_1 \sim 4 \times 3.38/\pi = 4.3$ inches

$L = 34$ inches

Inside the cavity of the copper basket are contained successive layers of 0.125-inch-thick copper shot, and then the shot-filled fuel subassembly. Using the experimentally determined conductivity of wet copper shot bed $k = 6.1$ Btu/hr ft F, the temperature drop across the outer layer of copper shot is:

$$\Delta T = \frac{Qax}{kA}$$

$$= 5,120 \times 1.23 \frac{.125 \times 12}{6.1 \times 4 \times 3.38 \times 31} = 3.8 \text{ F}$$

where the axial peaking factor of 1.23 has been conservatively included in the total heat load. The temperature of the outside surface of the steel can is $T = 225 + 1.3 + 3.8 = 229$ F.

The temperature drop across the steel can, the inner layer of copper shot, and a dummy fuel subassembly was measured experimentally (Section 3.6.2). With a heat load of 0.350 kw in a 12-inch-long section of the dummy fuel subassembly, filled with shot and water, a temperature drop of 40 F was measured. Extrapolating this data to the actual subassembly which is 31 inches long with a decay heat of Q = 1.5 x 1.23 = 1.85 kw, taking into account the peaking factor, the temperature drop would be:

$$T = 40 \left(\frac{1.85}{.350}\right)\left(\frac{12}{31}\right) = 82 \text{ F} \quad .$$

It was observed experimentally (Section 3.6.2), however, that at the heat generation rate of the maximum burnup fuel subassembly the fuel pin temperature is uniform through the subassembly and comes to equilibrium at the saturation temperature corresponding to the ambient pressure. This condition was observed as long as the ends of the experimental assembly were covered with water. Under these circumstances, heat was apparently being removed from the subassembly primarily by evaporation and convection. When water was allowed to evaporate from the shot bed, a radial temperature distribution was observed which is typical of simple conduction heat transfer through the dry copper shot.

Based on the experimental evidence, heat transfer by means of evaporation-condensation and convection will cause the fuel element to come to an equilibrium saturation temperature corresponding to the pressure inside the cask with no loss of coolant. The equilibrium temperature in the fuel element would then be only a few degrees above the basket temperature of 229 F.

3.4.2.3 EPRI Crack Arrest Capsules

It was shown in the September 8, 1969 Addendum that for a 130 F ambient temperature and 1,500 watt thermal load, the outside wall temperature is about 190 F and the cask wall Δt is about 37 F. For a 100 F ambient with 1,500 watts decay heat the outside wall temperature would be 190-30 = 160 F. For the reduced heat load of 110 watts/ft, the outside wall temperature would be approximately (160-100)(110/333) + 100 = 120 F. The Δt through the cask wall would be (37)(110/333) = 12 F. Thus, the cavity wall temperature would be about 120 + 12 = 132 F. These temperatures are conservatively high since they assume no radial heat flow in the cask wall.

The temperature of the capsule is calculated assuming that all cooling take place by convection and radiation. The capsule will be transported without a canister. However, a wire mesh basket having a maximum wire size of 11 gage (0.125-inch) and minimum mesh size of 1.0 inches may be used to aid in handling the capsules. Thus, it is assumed that convection and radiation heat transfer will take place directly between the capsule wall and the cask inner cavity wall, Figure 3.2.

In order to facilitate the calculations, it is assumed that the cavity wall is a plane, as wide as the capsule (14 inches), as tall as the capsule (21.5 inches), and located approximately 4 inches away. From McAdams[6] the convection heat transfer correlation is given by:

$$Nu = \frac{C}{(L/x)^{1/9}} (Gr \cdot Pr)^n \quad .$$

where

$Nu = \frac{hx}{k}$

x = distance between planes = 1/3 ft

k = fluid thermal conductivity

L = height of planes = 1.79 ft

$Gr = a\, x^3\, \Delta t$

a = fluid property constants in Groshof Number

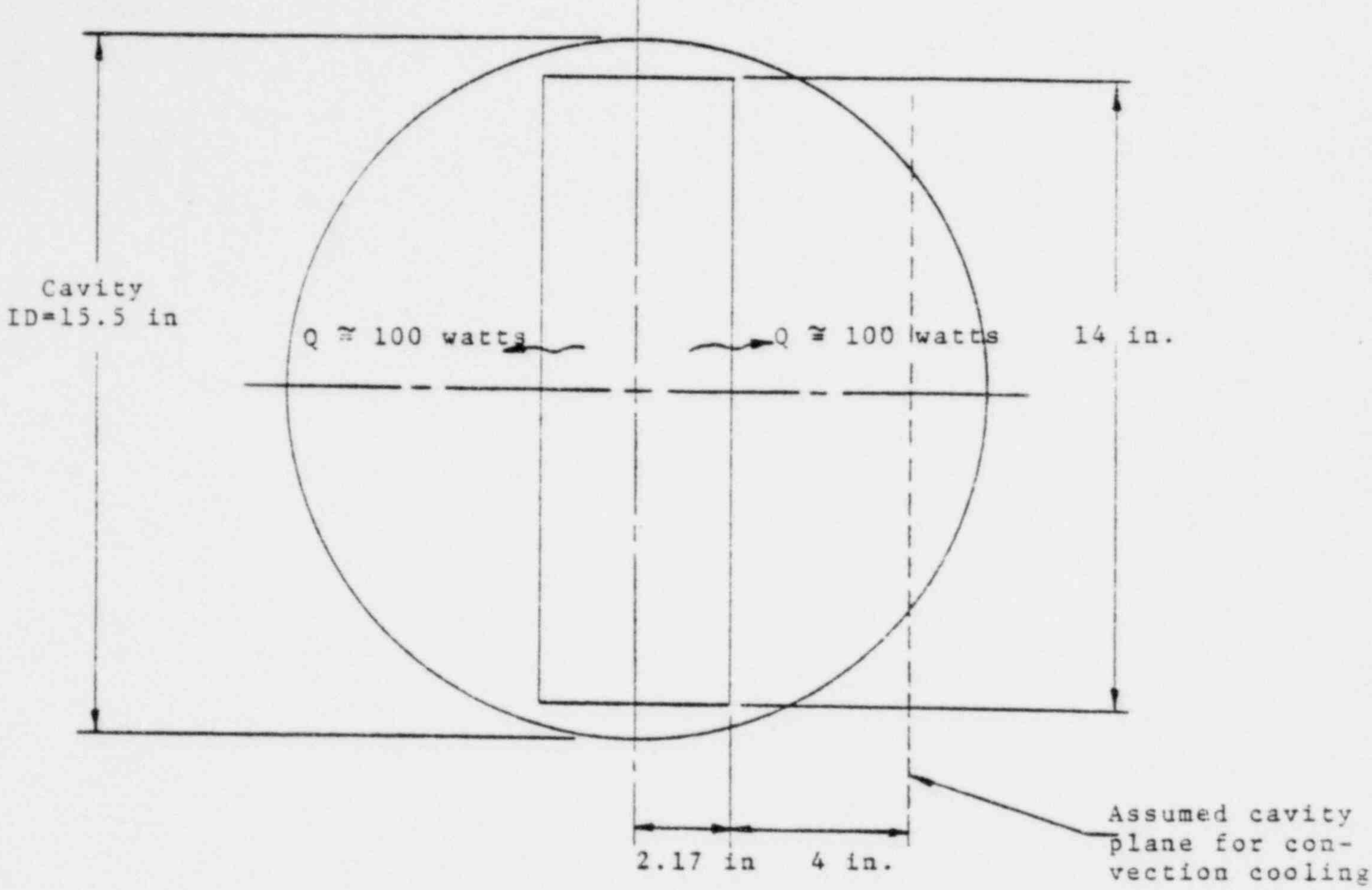

FIGURE 3.2. SKETCH OF MODEL FOR HEAT FLOW FROM EPRI CRACK ARREST CAPSULE TO CAVITY WALL

Pr = Prandl number which is function of fluid property.

For

$$Gr > 2(10^4);\ C = 0.071 \text{ and } n = 1/3 \quad .$$

Thus

$$h/k = 0.0589\ (aPr)^{1/3}\ \Delta t^{1/3}$$

Heat transfer by convection is expressed by:

$Q_{cv} = hA\Delta t$

A = area of plane surface = (14)(21.5)/144 = 2.09 ft^2

h = coefficient from above correlation .

Then

$Q_{cv} = 0.123\ k\ (aPr)^{1/3}\ \Delta t^{4/3}$

Heat transfer by radiation is expressed by:

$$Q_r = FeFa\sigma A(T_1^{\ 4} - T_2^{\ 4})$$

where Fe = emissivity factor

$$= \frac{1}{\frac{1}{E_1} + \frac{1}{E_2} - 1}$$

E_1 = emissivity of capsule = 0.2

E_2 = emissivity of cask wall = 0.5

$Fe = 0.167$

Fa = view factor = 1.0

$\sigma = 1.73\ (10^{-9})\ R^4$

$A = 2.09\ ft^2$

T_1 = capsule temperature, R

T_2 = cask cavity temperature, R

Thus

$$Q_r = 6.04\ (10^{-10})(T_1{}^4 - T_2{}^4)$$

It is assumed that the Δt is about 200 F and that the mean air temperature between the capsule and the cask wall is about 230 F. Then the air properties are:

$k = 0.0188$ Btu/hr ft F

$a = 4.78(10^5)/ft^3\ F$

$Pr = 0.68$

$T_1 = 460 + 132 + 200 = 792\ R$

$T_2 = 460 + 132 = 592\ R$

Substituting the values in the equations above results in the following:

$$Q_{cv} = 186\ \text{Btu/hr}$$

$$Q_r = 163\ \text{Btu/hr}$$

And the total heat flow is 349 Btu/hr = 102 watts. Thus, the capsule temperature for normal transportation is about 332 F.

3.4.3 Minimum Temperatures

From Section 3.4.2.1(c), the minimum water temperature is 192.9 - 4.3 = 188.6 F for an ambient temperature (T_a) of 100 F and a decay heat load (Q) of 3,480 Btu/hr. With no solar load, the water temperature is 180 F. For other values of T_a and Q, the water temperature (T) is approximately:

$$T = (180 - 100)\left(\frac{Q}{3,480}\right) + T_a \quad .$$

The water will freeze when T = 32 F, or $T_a = 32 - Q/43.5$. The water will not freeze at an ambient temperature of $T_a = -20$ F if the decay heat is greater than Q = 2,260 Btu/hr = 0.662 kw. When these conditions are satisfied, no antifreeze is needed in the water.

In later shipments it is expected that the temperature drop across the cask wall will decrease due to settling of the lead and closing of the air gap between the lead and outer steel shell. In this case, the water temperature may decrease from 180 F to about 160 F under normal conditions. Thus, in later shipments the decay heat will have to be over Q = 0.88 kw to prevent freezing at $T_a = -20$ F. Provisions will be made to cover the cask with a canvas blanket (which will decrease heat transfer from the outer surface) when ambient temperatures and cask internal temperatures indicate the possibility of freezing.

3.4.4 Maximum Internal Pressures

The design pressure of this cask is 100 psig so that the maximum permissible operating pressure is 50 psig. The maximum operating temperature (230 F) is 68 F below the boiling point (298 F) at the maximum permissible operating pressure.

3.5 Hypothetical Accident Thermal Evaluation

The thermal analysis presented in this section examines the thermal response, and associated effects, of the modified BMI-1 cask when subjected to the environmental fire condition outlined in Appendix B of 10-CFR-71. The fire is defined as a radiant thermal source having a temperature of 1,475 F lasting for 30 minutes. In addition, the "standard fire" is defined to have an effective source emissivity of 0.9, and the thermal absorptivity of the exposed cask surface is defined to be 0.8.

3.5.1 Thermal Model

The thermal transient analysis was carried out using the THT-D heat-transfer code (a generalized heat-transfer program available at Battelle). A cylindrical section, representative of the center region of the BMI-1 cask, was analyzed. Figure 3.3 illustrates the thermal model and THT-D node identification.

The primary modification to the BMI-1 cask, which is directed at fire survival, is the addition of a 1/8-inch-thick outer stainless steel shell (a thermal buffer shell) which encapsulates the existing 1/2-inch steel outer shell. The planned use of evenly spaced weld spots, 1/16-inch high, will assure an air gap between buffer shell and original outer shell. This air gap will impede the thermal pulse resulting from the hypothetical fire. A constant 0.060-inch air gap was employed in the transient calculations although it can be shown that a 1/8 - 3/16-inch air gap would exist due to differences in thermal expansions during the fire period.

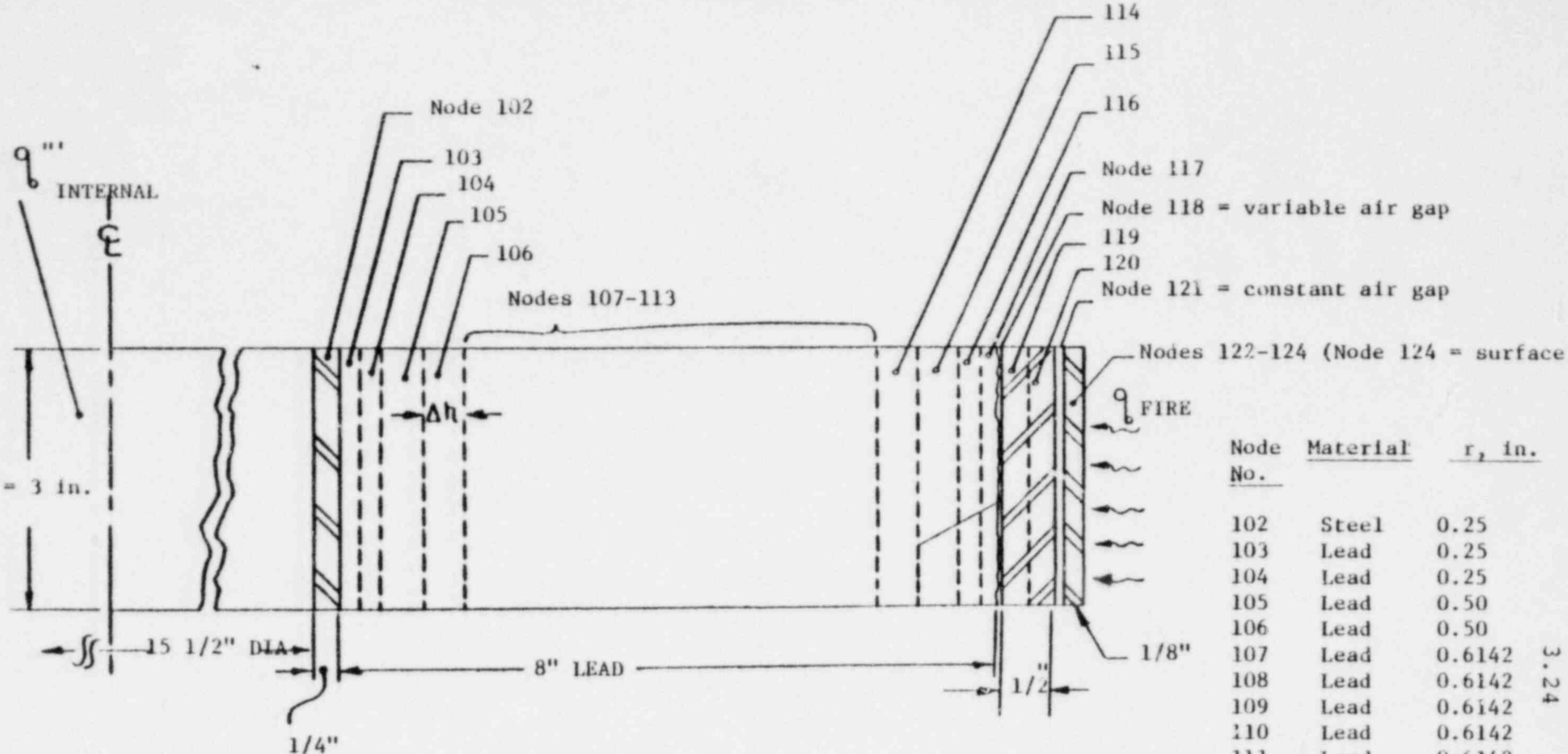

FIGURE 3.3. THERMAL MODEL EMPLOYED FOR BMI-1 FIRE THERMAL ANALYSIS

Node No.	Material	r, in.
102	Steel	0.25
103	Lead	0.25
104	Lead	0.25
105	Lead	0.50
106	Lead	0.50
107	Lead	0.6142
108	Lead	0.6142
109	Lead	0.6142
110	Lead	0.6142
111	Lead	0.6142
112	Lead	0.6142
113	Lead	0.6142
114	Lead	0.50
115	Lead	0.50
116	Lead	0.25
117	Lead	0.25
118	Air	0.010 (max.)
119	Steel	0.25
120	Steel	0.25
121	Air	0.0625
122	Steel	0.0625
123	Steel	0.0624
124	Steel	0.0001

3.5.2 Package Conditions and Environment

The starting temperatures (at start of the 30-minute fire) of the cask system, shown in Figure 3.4, were calculated for conditions corresponding to a 130 F day and a cask thermal load of 1.5 kw_t. The correlation of analytics with experimental data is shown in Figure 3.5, where the variation of cask outer surface temperature is shown as a function of thermal load and environmental temperature. The experimental point, measured for the BMI-1 cask without an outer shell, shows a measured outer shell temperature of 130 F on a 70 F day for a 1.4 kw_t thermal load. The calculated result is 133 F on a 70 F day. The external area change due to the addition of a 1/8-inch fire shell can be considered negligible. In addition, the experimental data for the 1.4 kw_t thermal load can be scaled to calculate an inner liner temperature of 227 F for the conditions of a 130 F day with a thermal load of 1.5 kw_t. Therefore, normal shipment with the contents contained in water will not result in any pressurization problems if the 1.5 kw_t heat load is not exceeded. The data contained in Figure 3.4 and 3.5 can be readily employed to assess other ambient and thermal load conditions.

For conservatism, the thermal capacitance of material(s) within the cask internal cavity was neglected, or an empty cavity was assumed for the thermal transient calculations.

The Fermi fuel subassembly will be shipped in the BMI-1 shipping cask, which has been provided with a special basket. During shipment, the cask cavity is filled with water. The void spaces between the fuel rods in the subassembly are filled with a settled bed of copper shot in water. The cask is to be shipped by truck so that under normal conditions the maximum fuel and water temperature is about 230 F.

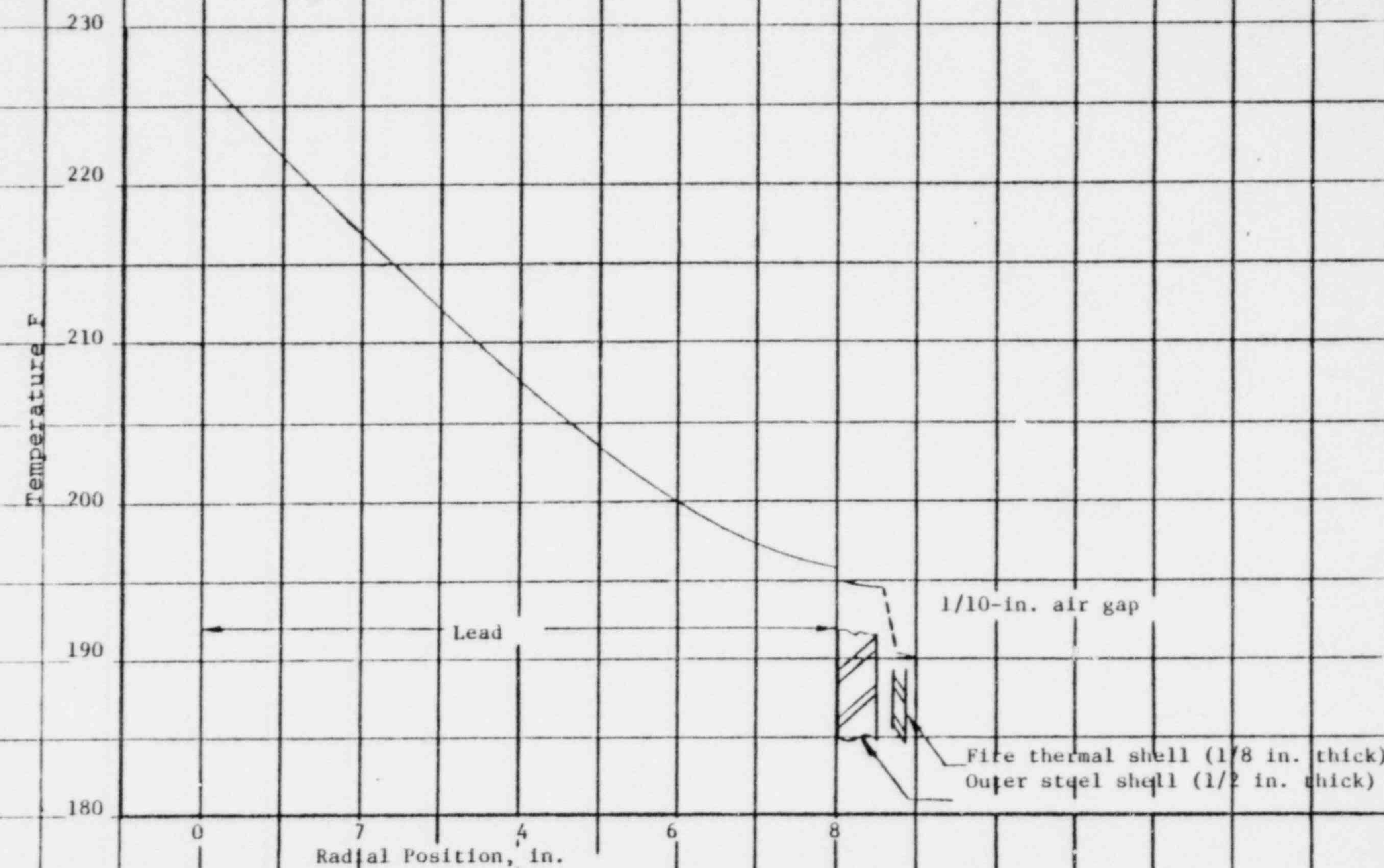

FIGURE 3.4. STARTING TEMPERATURES FOR BMI-1 FIRE ANALYSIS
(130 F DAY, 1.5-KW_T THERMAL LOAD)

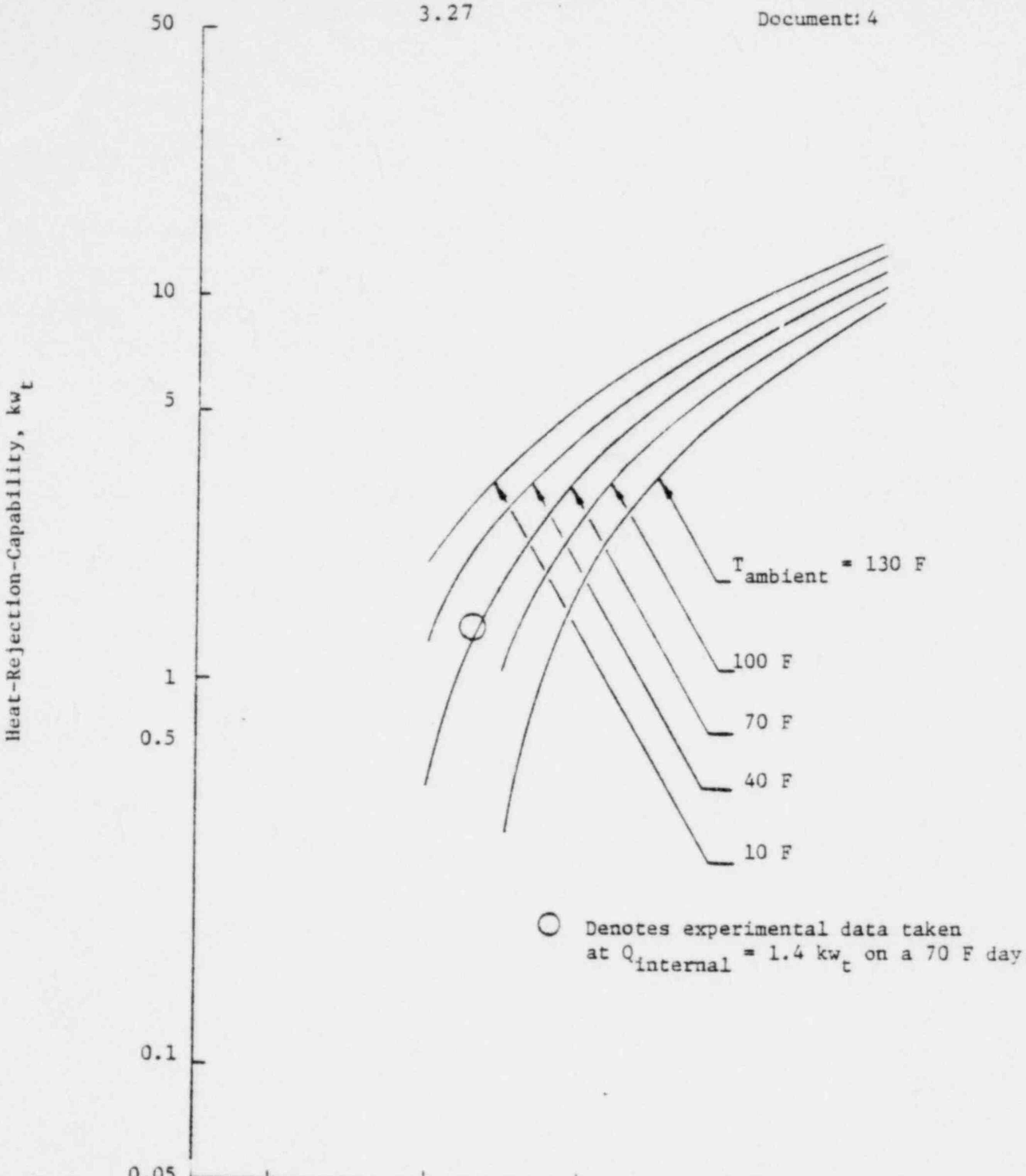

FIGURE 3.5. CALCULATED HEAT-REJECTION CAPABILITY VERSUS EXTERIOR WALL TEMPERATURE AND AMBIENT TEMPERATURE FOR BMI-1

3.5.3 Package Temperatures

The calculated thermal history of selective nodes (see Figure 3.3 for identification) is shown in Figure 3.6. The 1/8-inch outer shell, represented by Node 124 (a shell surface node), has little thermal capacitance and, therefore, responds very rapidly to the fire pulse. The outer shell, 1/2 inch thick, follows in succession, and since it also has only a nominal thermal capacitance, results in the closure of the internal air gap (Node 118). Commencement of lead melting is calculated to be at 16 minutes and the absorption of heat via latent heat capacity causes a reversal in the temperature response (see Figure 3.6) for a short time period. As the melt front travels inward, the outer shells then continue their temperature rise. The temperature reversal, and retardation, mentioned above are also the result of the thermal capacitance of the lead shield which has now become thermally coupled to the outer shell due to the lead-shrinkage gap (Node 118) being closed.

The "melt-front" boundary is shown in Figure 3.7, as a function of radial position and time.

3.5.4 Evaluation of Package Performance for the Hypothetical Accident Thermal Condition

3.5.4.1 Lead Melt

The cylindrical region of the BMI-1 cask was analyzed in detail to assess the potential for lead melting during a postulated hypothetical fire. The analysis assumed temperatures at commencement of fire corresponding to normal operation on a 130 F day with a 1.5 kw_t internal heat load.

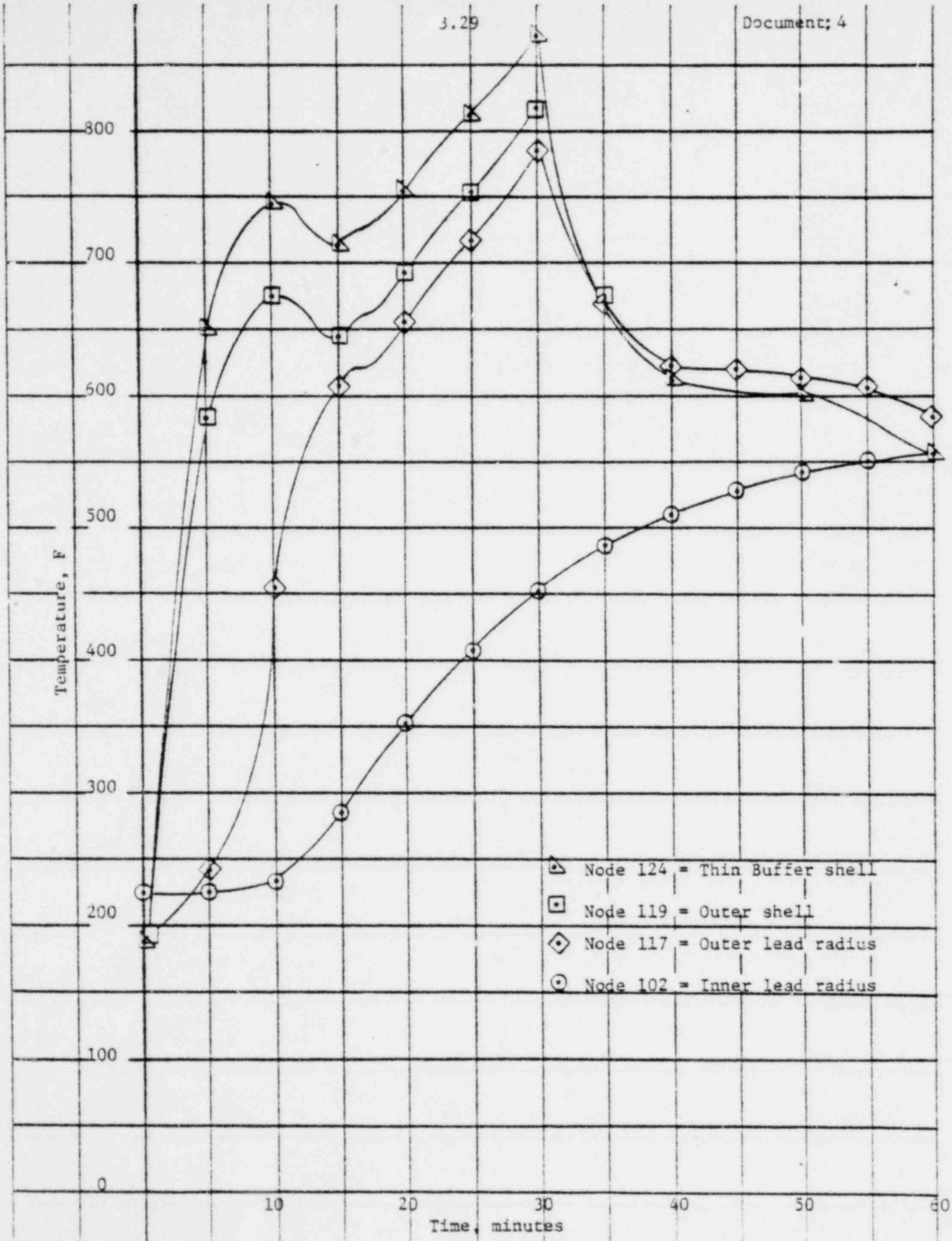

FIGURE 3.6. CALCULATED THERMAL HISTORY FOR THE MODIFIED BMI-1

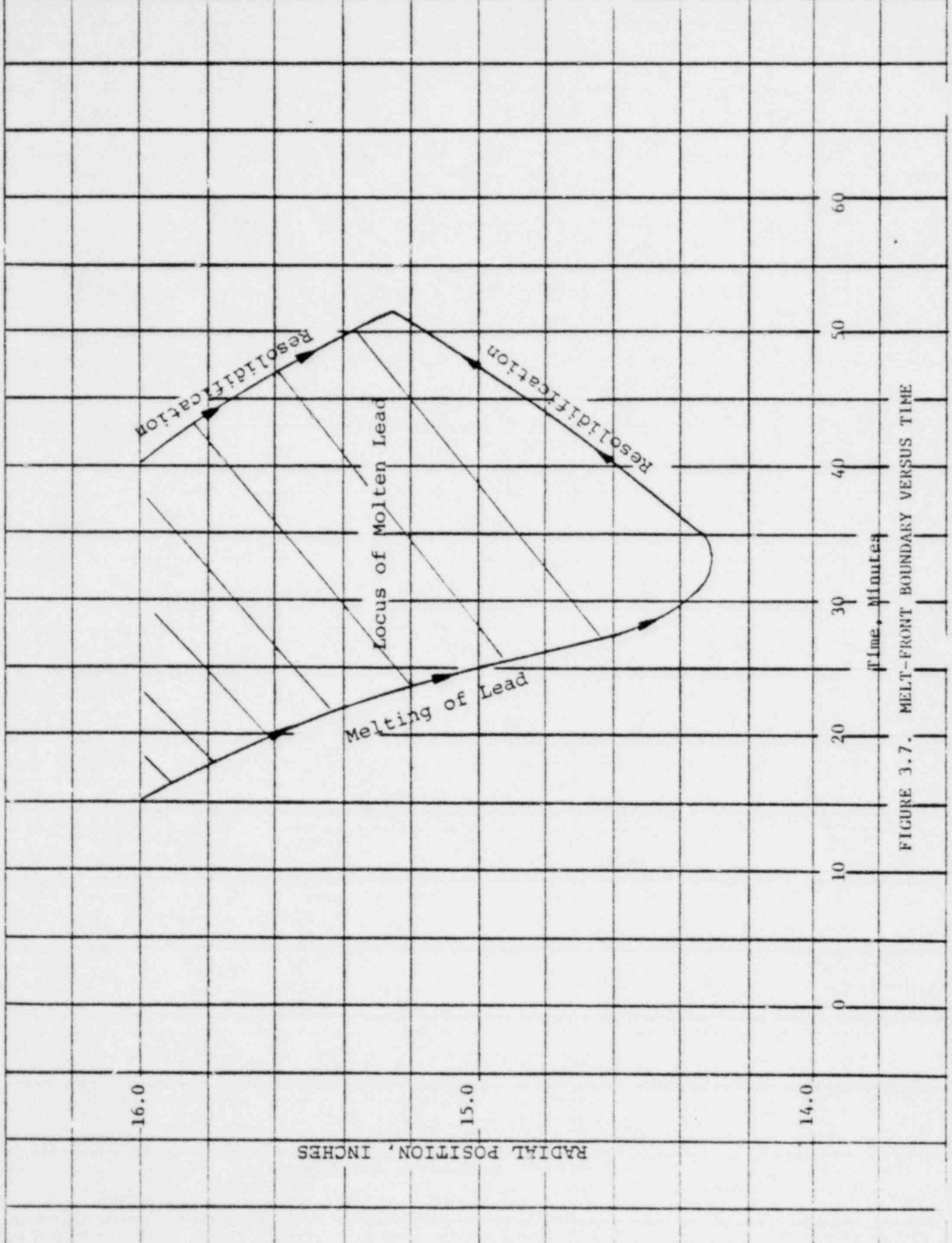

FIGURE 3.7. MELT-FRONT BOUNDARY VERSUS TIME

This analysis considers heat transfer through the cylindrical wall of the cask. This is the most severe thermal condition which could exist since the cover lid, corners, and bottom of the cask have sufficient thermal protection in the form of thick structural plates (i.e., 1-1/4-inch lid plate), skid I-beams, and corner lead-expansion voids. These structures provide a significant thermal capacitance and/or resistance.

The results of the thermal transient analysis indicate lead melt, within the outer regions of the lead shield.

The outer radius of the lead is 16.0 inches, and melting is calculated to proceed inward to a radial depth of 1.65 inches. Lead melting does not occur at the inner regions. Resolidification begins at about 33 minutes within the lead interior, followed by resolidification at the outer radius starting at 40 minutes. The results of these transient calculations indicate a maximum potential lead melt of 34 volume percent of the total lead if the cask is at the starting temperatures used in the calculation. Since expansion volume is provided for by shrinkage from the original casting, the expansion void needs only to accomodate the 3.8 percent increase in volume of the lead that melts. The built-in expansion void (752 inches^3) is more than sufficient to accommodate the excess volume of molten lead (574 inches^3), therefore, no pressure will be exerted on the wall of the cask. Also, no lead is lost. The adequacy of lead shielding after resolidification is discussed in the shielding section.

The lid, bottom, and corner volumes were not analyzed specifically since it is felt that the analysis presented above contains sufficient conservatism to permit extrapolation to those cask regions. For example, the lid cover is 1-1/8 inches thick and the corners at the loading end have 3/4-inch steel plates, respectively. The thermal capacitance of these plates, along with the internal air gaps (1/4 inch in the cover and expansion volumes in the corners) will very likely result in zero lead melt for those regions. The bottom of the cask also has corner-expansion volumes, and a 1-inch base plate. The base plate is furthermore thermal radiatively shielded by the I-beams employed in the skid. Previous calculations (i.e., NRBK-43) on similar cask systems have shown that the I-beam structure provides sufficient shielding from the fire to preclude, or minimize significantly, lead melting. Therefore, the bare cylindrical sides are the most susceptible to melting from a hypothetical fire, and were analyzed in detail. Based on the above analysis, the maximum canister flange temperature reached during/after a fire test is estimated to be less than 600 F.

3.5.4.2 Maximum Contents Temperature

(a) BRR/MTR Fuel, Loss of Coolant

The fuel element baskets in this cask contain two solid sheets of steel (neutron poison) which divide the baskets into quadrants containing three elements each. Since no heat is transferred between quadrants, the solid sheets have no effect on heat transfer. The three fuel elements in each quadrant are held in place by means of vertical steel strips on the corners of the elements. These strips partially obstruct radiation heat transfer, but have no effect on conduction or convection heat transfer.

Figure 3.8 is a sketch of one quadrant of the basket. Heat is transferred from Element 2 to Element 1 by radiation and conduction in air. Heat is transferred from Element 1 to the inner cask wall by radiation and convection. Analytically this is expressed as:

$$Q_{21} = 0.173\ F_{21}A_2 \left[\left(\frac{T_2}{100}\right)^4 - \left(\frac{T_1}{100}\right)^4 \right] + \frac{kA_2}{t} (T_2 - T_1) \quad (6)$$

$$Q_{1c} = 0.173\ F_{1c}A_1' \left[\left(\frac{T_1}{100}\right)^4 - \left(\frac{T_c}{100}\right)^4 \right] + h_c A_1\ (T_1 - T_c) \quad . \quad (7)$$

As discussed later, conduction in the aluminum elements smoothes out the axial temperature distribution so that the axial power peaking factor does not have to be included in Q_{21} or Q_{1c}. From Section 3.1.2(a), the total decay heat per element is 145 Btu/hr. Thus, Q_{21} = 145/2 = 72.5 Btu/hr and Q_{1c} = 145 x 3/2 = 218 Btu/hr. The heat transfer coefficient h_c is:

$$h_c = \frac{0.071}{\left(\frac{L}{t}\right)^{\frac{1}{9}}} \left[\frac{\rho^2 k^2 g \beta c}{\mu} \right]^{\frac{1}{3}} (T_1 - T_c)^{\frac{1}{3}} \quad . \quad \text{(McAdams[4] p 181)}$$

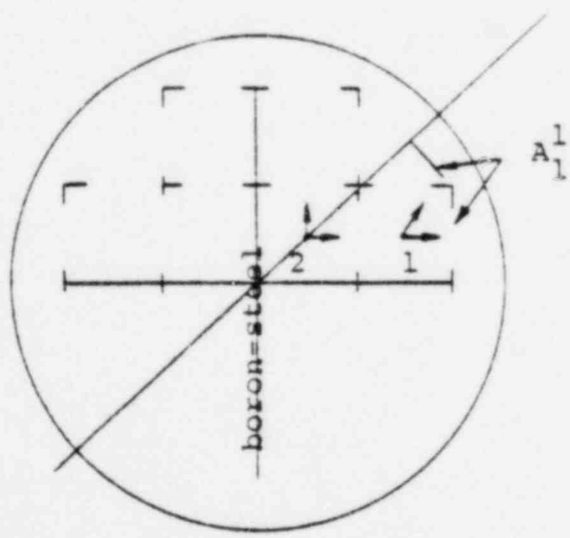

FIGURE 3.8. SKETCH OF FUEL BASKET

The numerical data needed to calculate h_c are:

$$T_{av} = 390 \text{ F}$$

$$L = 25 \text{ inches}$$

$$t = D_o/2 = 1.38 \text{ inches}$$

$$\left[\frac{\rho^2 k^2 g\beta c}{\mu}\right]^{\frac{1}{3}} = 1.25$$

and

$$h_c = 0.0643\ (T_1 - T_c)^{\frac{1}{3}} \quad .$$

Neglecting the effect of the corner strips, the radiation interchange factors F_{12} and F_{2c} are:

$$F_{21} = (2/\varepsilon_{Al} - 1)^{-1} = (2/0.15 - 1)^{-1} = 0.081$$

$$F_{1c} = (1/\varepsilon_{Al} + 1/\varepsilon_{Fe} - 1)^{-1} = (1/0.15 + 1/0.5 - 1)^{-1}$$

$$= 0.131 \quad .$$

For two steel surfaces, $F = 0.333$.

Now, consider the effect of the corner strips on radiation heat transfer. Assume that the surfaces A_1, A_2, and A_3 are parallel and that heat is transferred by radiation from A_1 to A_2 to A_3. Then:

$$Q_{12} = \sigma F_{12} A_1 (T_1^{\ 4} - T_2^{\ 4})$$

$$Q_{23} = \sigma\, F_{23} A_2 (T_2{}^4 - T_3{}^4)$$

and

$$\frac{Q_{12}}{\sigma F_{12} A_1} + \frac{Q_{23}}{\sigma F_{23} A_2} = T_1{}^4 - T_3{}^4 \quad .$$

Since $Q_{12} = Q_{23} = Q_{13}$ and $A_1 = A_2 = A_3$,

$$Q_{13} = \sigma \left[\frac{F_{12} F_{23}}{F_{12} + F_{23}} \right] A_1 (T_1{}^4 - T_3{}^4) \quad .$$

Thus, for the portion of the area between Elements 1 and 2 where the steel strips obstruct radiation heat transfer:

$$F_{21} = \frac{0.131 \times 0.131}{0.131 + 0.131} = 0.065$$

For the obstructed area between Element 2 and the cask wall:

$$F_{1c} = \frac{0.131 \times 0.333}{0.131 + 0.333} = 0.0935 \quad .$$

The steel corner strips obstruct one inch of the three inch element width. Averaging the radiation factors over the element width:

$$F_{21} = \frac{1(0.065) + 2(0.081)}{3} = 0.076 \quad ,$$

and

$$F_{1c} = \frac{1(0.0935) + 2(0.131)}{3} = 0.118 \quad .$$

The assembled numerical data needed to calculate T_2 and T_1 are:

$Q_{21} = 72.5$ Btu/hr $\qquad t = \frac{0.75}{12} = 0.0625$ ft

$Q_{1c} = 218$ Btu/hr $\qquad A_2 = 3 \times 25/144 = 0.52\ ft^2$

$F_{21} = 0.076$ $\qquad A_1 = 2A_2 = 1.04\ ft^2$

$F_{1c} = 0.118$ $\qquad A_1 = (1 + 1/\sqrt{2})\ A_2 = 0.89\ ft^2$

$T_c = 186\ F = 646\ R$ $\qquad k = 0.0239$ Btu/hr ft F .

$h_c = 0.0643(T_1 - T_c)^{\frac{1}{3}}$

Using these data, Equations (6) and (7) become:

$$72.5 = 0.00683 \left[\left(\frac{T_2}{100}\right)^4 - \left(\frac{T_1}{100}\right)^4 \right] + 0.199(T_2 - T_1) \qquad (6)$$

$$218 = 0.01815 \left[\left(\frac{T_1}{100}\right)^4 - 1{,}732 \right] + 0.067(T_1 - 646)^{4/3} \qquad (7)$$

The solutions to these equations are $T_1 = 461$ F and $T_2 = 615$ F. Thus, the maximum element temperature during loss of coolant is 615 F.

In the calculations above, the axial power peaking factor has been neglected since the aluminum in the fuel elements effectively evens out the axial temperature distribution. For a triangular power distribution with an axial peaking factor of 1.4, the fraction (1.4-1)/4 = 0.1 of the power is generated at a power greater than average. The temperature drop required to conduct this 10 per cent excess heat from the center to the end of the element is approximately:

$$\Delta T = \frac{0.10(\frac{Q}{2})L}{kA}$$

where

Q = 145 Btu/hr

L = 25/2 = 12.5 inches

k = 135(aluminum at 600 F)

A = 2.55 inches^2 .

$$\Delta T = \frac{(0.10)(72.5)(12.5)(12)}{(135)(2.55)} = 3.16 \text{ F} \quad .$$

Thus, the axial peaking factor increases the element temperature by 3.2 F.

It has also been assumed in the work above that the fuel elements are isothermal. The temperature drops across the elements themselves depend on the orientation of the fuel elements in the basket. In the worst case, the temperature drop would be about 15 F.

In conclusion, considering all the factors discussed above, the maximum fuel element temperature during loss-of-coolant will be T_2 = 615 + 3 + 15 = 633 F. This is a safe temperature for aluminum plate-type fuel elements.

Steam produced in the cask cavity during a fire is vented through a 1/16-inch-thick filter with a flow area of 20 inches^2. According to data obtained for pressure differentials (ΔP) up to about 20 psi, the flow capacities of these filters are W/A = 26.5 ΔP + 50 ft^3/min per ft^2 of filter area. Using this equation to extrapolate to ΔP = 75 psi, the flow capacity is W = 283 ft^3/min. (The pop-off value is set at ΔP = 75 psi.) At 89.7 psia, 283 pounds of water forms 1,382 feet^3 of steam. Thus, the cavity can be vented in t = 1,382/283 = 4.9 minutes. Ten minutes is considered a reasonable time to empty the cask. Thus, a 100 per cent safety factor in the design has been allowed, which is more than adequate to compensate for the possibility that the extrapolated filter-flow-capacity data is not accurate at ΔP = 75 psi.

(b) Fermi Fuel, Loss of Coolant

During the loss-of-coolant accident, the water drains from the cask and evaporates from the shot beds. The shot beds are held in place by a stainless steel can with porous steel end plates so that the shot will not drain out with the water. It is assumed during loss of coolant that the cask is exposed to 100 F ambient air and a solar heat load of 0.392 kw. From Section 3.4.2.2(a), the surface temperature of the cask is 183 F.

With water in the cask cavity, the temperature drop across the wall of the cask was 31 F. During loss of coolant, this temperature will be increased because the adjustable brass contact angles cover only 37 percent of the surface area of the inside wall of the cask. The temperature increase is less than:

$$T = \frac{Q}{2\pi kL} \ln \frac{D_2}{.37D_1} = 24 \text{ F} \quad ,$$

where

$$Q = 5,120 \text{ Btu/hr}$$

$$k = 19 \text{ Btu/hr ft F}$$

$$L \sim 3 \text{ ft}$$

$$D_2 = 32 \text{ inches}$$

$$D_1 = 16 \text{ inches}$$

The total temperature drop across the cask wall is less than $\Delta T = 31 + 24 = 55$ F.

The temperature drop across the six copper ribs and the copper basket is about 8 F. The temperature of the outside surface of the first layer of copper shot is thus T = 183 + 55 + 8 = 246 F.

Using the experimentally determined value for the conductivity of the dry cooper shot bed, k = 0.675 Btu/hr/ft/F, the temperature drop across the outer layer of cooper shot is:

$$\Delta T = \frac{Q\Delta x}{kA} = 5120 \times 1.23 \left(\frac{.125 \times 12}{0.675 \times 4 \times 3.38 \times 31}\right) = 28^{\circ}F,$$

where the maximum heating rate of Q = 5120 x 1.23 Btu/hr has been used in the calculation. The temperature of the surface of the steel can which contains the subassembly is thus T = 246 + 28 = 274°F. As discussed in an earlier section, the temperature drop across the steel can, the inner layer of copper shot, and a shot-filled dummy fuel subassembly was measured experimentally. In these experiments with a 12-in-long section of dummy subassembly, a temperature drop of 225°F was measured with a heat load of 0.648 kw. The temperature drop in a full size fuel subassembly would be

$$\Delta T = \left(\frac{1.5 \times 1.23}{0.648}\right) \left(\frac{12}{31}\right) 225 = 247^{\circ}F.$$

The maximum fuel subassembly temperature during loss of coolant is thus T = 274 + 247 = 521°F. This maximum temperature is well below the actual fuel operating temperature of 800°F in the Enrico Fermi Reactor.

(c) EPRI Crack Arrest Capsules

It was shown in the September 8, 1969 SAR Amendment, that for a full heat load of 1,500 watts, and starting into the hypothetical fire accident from condition for a 130 F ambient temperature, the maximum cask cavity wall temperature during the incident is about 560 F. Conservatively it is assumed that the Δt from the cask wall to the capsule is the same as for the steady state condition. Then the maximum capsule temperature during the hypothetical accident is 560 + (332 - 132) = 760 F. This is well below the melting temperatures for all the materials in the capsule. The maximum temperature of 760 F is a conservative value for the following reasons:

(1) The starting conditions are for an ambient temperature of 130 F. However, a 100 F ambient is allowed for determining starting conditions.

(2) The heat capacity of the capsule is neglected which will lower the maximum temperature in reality

(3) The Δt from the capsule to the cask cavity wall is assumed to be a constant over the temperature range. In reality, radiation heat transfer will become more dominant at the higher temperatures resulting in lower maximum capsule temperatures.

3.6 Appe dix

3.6.1 References

(1) J. O. Blomeke and M. F. Todd, "U-235 Fission Product Production as a Function of Flux, Irradiation Time, and Decay Time", ORNL-2127, Part I, Vol 2 (1957).

(2) Nims, J. B., "Generalized Subassembly Decay Heat Curves", APDA Memo P-64-11, January 14, 1964.

(3) L. S. Marks, "Marks' Handbook", McGraw-Hill, Inc. 5th Ed. (1951).

(4) W. H. McAdams, "Heat Transmission", McGraw-Hill, 3rd Ed. (1954).

(5) R. O. Wooton and H. M. Epstein, "Heat Transfer from a Parallel Rod Fuel Element in a Shipping Container", to be published, Battelle Memorial Institute (1963).

(6) McAdams, W. H. p 181, Eq7-9b.

3.6.2 Experimental Tests of Copper Shot

The shipment of an Enrico Fermi Core-A fuel subassembly with a decay heat output of 1.5 kw requires a heat transfer medium which remains in the cask under all conditions to prevent excessive fuel temperatures. Copper shot was considered to offer the most promise for this application.* To test this concept, experiments were performed with an actual Enrico Fermi Core-A fuel subassembly and a dummy subassembly fabricated using electrical resistance heaters to simulate fuel pins. The experiments were designed to investigate the thermal conductance of shot beds as applied to the Fermi fuel shipment. Details of these experiments and the results are discussed below.

3.6.2.1 Thermal Tests

A simulated fuel subassembly was constructed using actual cross-sectional dimensions including the proposed shipping basket. The unit had 12 inches of active length and thermal insulation was employed on the bottom to decrease the axial heat loss. The zirconium clad fuel pins were represented by stainless steel sheathed, magnesium oxide insulated, nichrome wire resistance heaters. These resistance heater pins had the same diameter (0.156-inch OD) as the Fermi fuel pins and were spaced on the same center to center distances as the Fermi fuel pins. The 18-ga. nichrome wire in the heater pins had a resistance of one ohm per foot and the radial heat transfer characteristics of the heater pin was calculated to be slightly less than that of Fermi fuel pins.

---

* This cooling concept is being patented by the Edward Lead Company, of Columbus, Ohio.

basket in the shipping cask. The heaters and both wrapper tubes were welded to a common bottom to make a liquid-tight unit. A drain tube covered by a porous stainless steel filter was welded to the bottom of the cavity.

To simulate the heat sink provided by the cask, an additional cylindrical can was welded to the common bottom plate. Inside this can was a copper cooling coil which was attached to a cold water line. Oil was used in this heat sink so that a higher range of temperatures could be used. The oil was continuously stirred by air bubbles to maintain as uniform heat sink temperatures as possible over the length of the apparatus.

The 144 heater wires were connected in series in four circuits which were connected in parallel to a controlled voltage power source. An attempt was made to regulate the heat input to approximate that of the center section of the Fermi fuel element. Precision meters monitored the circuits to maintain a constant heat input during the test periods.

Temperatures in this apparatus were measured in 13 locations with stainless-steel-sheathed, cromel-alumel thermocouples. The thermocouple sheath was 0.062-inch OD with the junction grounded to the sheath at the end. The thermocouples were positioned as shown on Drawing Number 0050D, and attached to a twelve-point recorder. A direct reading millivolt meter was used for the extra thermocouple. The thermocouples were placed so that Number 1 through Number 5 monitored center temperatures on two inch spacings from bottom to top, Number 3 being the center point. Thermocouples 6 through 10 were spaced at the 6-inch-height level (same as Number 3) progressing in 0.250-inch increments from center to outside. Thermocouples Numbers 11, 12 and 13 monitored the oil bath heat sink with Number 11 being at the 6-inch height.

One test was conducted with no shot or liquid in any of the apparatus to give an indication of temperatures under these conditions. The apparatus was then loaded with shot through openings in the spacer plate between the heater wires. The copper shot used in these tests were the same as that used in the flowability tests. The shot were thoroughly wetted before being added as a slurry into the water-filled apparatus. The shot readily displaced the water in the apparatus. As noted on Drawing Number 0050D, shot filled the space in the apparatus around the heater pins and between the wrapper tube and the basket tube. During the tests, most of the water was vaporized and passed readily through the porous shot bed. As the temperature approached 212 F, some water was forced ahead of the steam through the shot bed and appeared on the top of the apparatus. This movement of water and steam through the shot bed appeared to settle the bed slightly. Table Number 3.2 lists data from three of the tests.

During the testing, equilibrium conditions were reached about two hours after energizing the heaters. All the tests were run at least four hours and one test was continued for 51 hours. A slight improvement in the conductivity of the bed was noted in the 51 hour test as the test progressed. Figure Number 3.9 gives the time temperature relationships during a typical testing period. In Figure 3.9 time intervals are marked A through E to delineate significant periods during a typical test. The first 20 minutes, listed as "A", was required as a warm-up period with a full heat load. Section "B" marks the time during which evaporative and convective heat transfer took place. During this period, all the thermocouples in the shot bed registered the same temperature (approximately 212 F) and water vapor issued from the top of the apparatus. As the shot bed dried, Section "C", Number 3 thermocouple being in the center responded quite rapidly to an increase in temperature in that area. Other thermocouples quickly followed the rising temperature in the shot bed

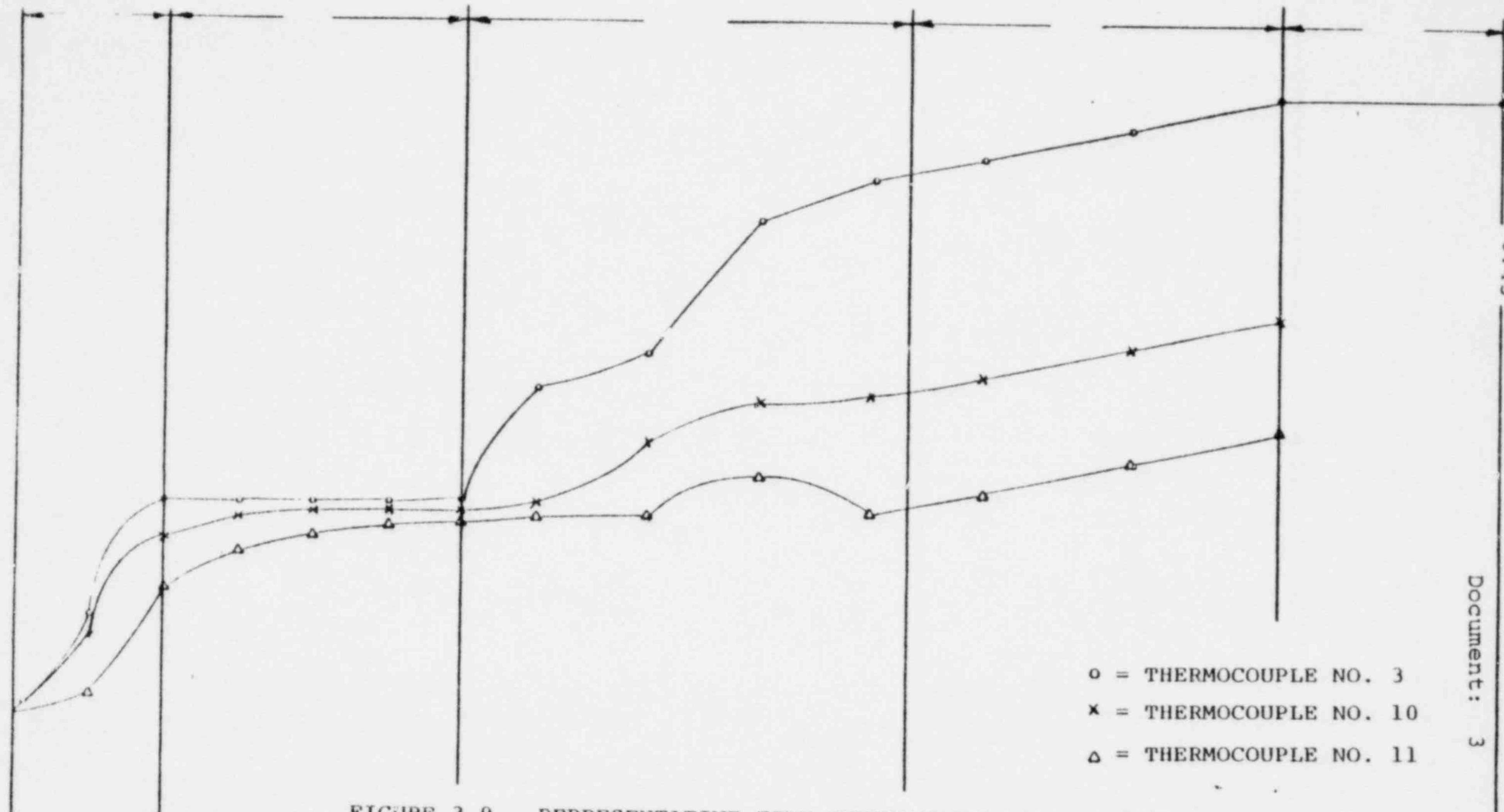

FIGURE 3.9. REPRESENTATIVE TIME-TEMPERATURE RELATIONSHIP IN SIMULATED FUEL SUBASSEMBLY WITH COPPER SHOT

TABLE 3.2 TEST DATA

Test Number	Thermocouple Numbers 1	2	3	4	5	6	7	8	9	10	11	12	13
	Temperatures in Degrees, F												
Test Number 1 Empty apparatus Heat input 491 watts	960	1133	1201	1201	1209	1172	1146	1065	783	373	165	156	
Test Number 2 Wet copper shot Heat input 350 watts	156	162	174	186	197	173	169	165	160	155	139	115	157
Test Number 3 Copper shot Heat input 648 watts	471	483	490	480	485	473	459	440	395	337	265	260	259

as it progressed from the center section of the apparatus. The heat transfer mode, during this time, was apparently changing from evaporative and convective to conductive via the residual copper shot bed. During the period represented by "C" some adjustments were made in the heat sink temperature by controlling the flow of water in the cooling coil. In periods "D" and "E", a constant ΔT is exhibited by the system indicating stabilized heat transfer conditions representative of complete loss of coolant. The rising temperatures in period "D" demonstrate the effect of raising the heat sink temperature.

Each test was made with a clean loading of shot, necessitating the removal of the shot between tests. During the tests with the copper shot, a crust of oxidized shot formed on the top and extended about 1/8 inch into the bed. Penetration of this crust permitted the remainder of the shot to be poured from the apparatus. From the experience with the test apparatus, it appears that very little difficulty would be encountered in removing the shot from a full size fuel element after a loss-of-coolant incident.

3.6.2.2 Calculation of Copper Shot Conductivity

The experimental heat transfer data were used to calculate the conductivity of the copper shot bed. Consider the dummy Fermi fuel subassembly to be a series of concentric cylinders in which the walls of the cylinders are composed of rows of fuel pins. The outer cylinder contains 44 pins, the next one 36 pins, the next 28, etc. The heat generated in a given cylinder is proportional to the number of fuel pins in it. The temperature drop across a given cylinder has contributions due to heat generated in interior cylinders and due to heat generated in the cylinder itself. (The calculated thermal conductance of the heater pins was very similar to that of an actual fuel pin.) Let R be the resistance to heat being conducted across a unit cell (fuel pin plus surrounding copper shot) of a cylinder. The resistance of a given cylinder is approximately inversely proportional to the number of cells in it. The resistance of the outer cell is approximately R/44; or in the general R/(8k-6) where k = 2, ..., 6 is the cylinder index number.

Proceeding in this manner, it can be shown that the temperature drop across the $k^{\underline{th}}$ cylinder is:

$$T_{k-1} - T_k = QR \left(\frac{2k^2 + 1}{4k - 3}\right) \quad ,$$

where

Q = decay heat per fuel rod (Btu/hr)
R = resistance of unit cell (F hr/Btu)
$k = 2, \ldots, 6: \quad (2, \ldots, 6) \quad .$

The total temperature drop is:

$$T_o - T_6 = QR \sum_1^6 \left(\frac{k^2 + 1}{4k - 3}\right) + 0.4\ QR = 23.58\ QR \quad .$$

The resistance of a unit cell of the Fermi element can be written approximately as:

$$R = \frac{\left(\frac{1.562}{k_1 L}\right)\left(\frac{2.42}{kL}\right)}{\left(\frac{1.562}{k_1 L}\right) + \left(\frac{2.42}{kL}\right)} + \left(\frac{0.21}{kL}\right) \quad ,$$

where

k_1 = fuel rod conductivity (Btu/hr ft F)

k = copper shot conductivity

L = fuel rod length (ft) .

This formulation of R assumes the unit cell is composed of three resistances, which are added as two parallel and one series resistance. For $k_1 = k$ the equation above should reduce to $R = 1/kL$; however, it reduces to $R = 1.16/kL$. Thus, the resistance is 16 per cent too large (for $k_1 = k$, at least); and the temperature drop is overestimated.

The conductivity of the shot bed can now be calculated from the experimental data using the above equations. The temperature drop across the fuel element and the layer of copper shot is:

$$\Delta T = 23.58\left(\frac{Q}{144}\right)R + \frac{Q\Delta x}{kA} \quad ,$$

where

Q = total heat load

Δx = thickness of shot layer

k = conductivity of shot

k_1 = rod conductivity = 8 Btu/hr ft F .

For the wet shot bed the experimental data gives:

$Q = 0.350$ kw, $L = 12$ inches, and $\Delta T = 35$ F (using readings from thermocouples Number 3 and Number 11). Substituting in the equation above,

$$35 = \frac{90}{0.19k + 2.42} + \frac{58.5}{k} \quad ;$$

and k = 6.1 Btu/hr ft F for the wet-shot bed.

For the dry copper shot bed, the experimental data gave $Q = 0.648$ kw, $L = 12$ inches, and $\Delta T = 225$ F. Substituting in the equation above:

$$225 = \frac{166}{0.19k + 2.42} + \frac{108}{k} \quad ;$$

and k = 0.675 Btu hr ft F.

4. CONTAINMENT

4.1 Containment Boundry

4.1.1 Containment Vessel

For certain uses as defined in Reference 1, (Section 4.4.1) the cask cavity liner provides the containment. For other uses, also defined in Reference 1, an inner containment vessel (canister) is also used to provide containment. These are described in Section 1, including the drawings in the Appendix to Section 1.

4.1.2 Containment Penetration

Penetrations to the cask cavity include the vent/pressure relief line at the top and a drain at the bottom. The specified relief pressure is 75 psig. The drain line is leak tight.

The special containment canisters used within the cask cavity do not have any penetrations.

4.1.3 Seals and Welds

Seals on both the cask cavity and inner canisters are elastometric as discussed in Section 1. All welds are full penetration welds.

4.1.4 Closure

The closure of the cask cavity is accomplished by twelve 1 inch x 8 studs with two lock nuts per stud. The initial tightening torque on the nuts is 50 feet/pounds. The closure of the canister is accomplished by ten 3/8 x 16 inch bolts. The initial tightening torque on the bolts is 60 inch/pounds.

4.2 Normal Conditions of Transport

The performance of the cask and inner canister during normal conditions of transport are presented in the applicable subsections of Section 2 and 3.

4.3 Hypothetical Accident Conditions

The performance of the cask and inner canister during the hypothetical accident conditions are presented in the applicable subsections of Sections 2 and 3.

4.4 APPENDIX

4.4.1 References

U.S. Nuclear Regulatory Commission Certificate of Compliance for Radioactive Materials Package Number 5957, Rev. 4, June 15, 1978.

5. SHIELDING ANALYSIS

5.1 Discussion and Results

5.1.1 Applicable Regulatory Criteria

Packages such as the modified BMI-1 cask which are transported in a vehicle assigned for the sole use of the consignor, and unloaded by the consignee from the transport vehicle in which they are originally loaded have radiation dose-rate limits [§173.393(j) of 49 CFR] under normal conditions of:

(1) 1,000 millirem per hour at 3 feet from the external surface of the package (closed transport vehicle only)

(2) 200 millirem per hour at any point on the external surface of the car or vehicle (closed transport vehicle only)

(3) 10 millirem per hour at 6 feet from the external surface of the car or vehicle and

(4) 2 millirem per hour in any normally occupied position in the car or vehicle (except in the case of private motor carriers).

Packages such as the modified BMI-1 cask which are transported by a commercial carrier have radiation dose-rate limits [§173.393(i) of 49 CFR] under normal conditions of:

(1) 200 mr/hr at any point on the external surface of the package and

(2) The transport index does not exceed 10 (i.e., 10 mr/hr at 3 feet from the surface of the package).

In addition to the above radiation limits for normal shipping conditions, the package must meet the shielding requirement for hypothetical accident conditions which is listed in §71.36(a)(1) of 10-CFR-71 as:

"The reduction of shielding would not be sufficient to increase the external dose rate to more than 1,000 milliroentgens per hour or equivalent at 3 feet from the external surface of the package."

5.1.2 Design Features

Lead shielding is provided in the BMI-1 cask to limit the surface dose to less than 200 mr/hr and the dose at 3 feet from the surface of the cask to less than 10 mr/hr. As required by the regulations, the dose will be measured before shipment to verify that these limits are not exceeded. The shielding for the sides of the cask is provided by 8 inches of lead and 0.875 inch of steel, where 0.25 inch of steel is in the inside cylinder and 0.025 inch of steel is in the outside cylinder and fire shield. The bottom is shielded by 7.75 inches of lead and 1.875 inches steel, where 0.75 inch of steel is in the inside plate and 1.125 inches is in the outside plate. The top is also shielded by 7.75 inches of lead and 1.875 inches of steel, where 0.75 inch of steel is in the inside plate and 1.125 inches is in the outside plate and fire shield.

5.2 Source Specification

5.2.1 Description of Radiation Sources

Types and quantities of radioactive materials analyzed for shipment in the modified BMI-1 cask fall within the transport groups and corresponding curie limits indicated in Tables 5.2 and 5.3. These analyses were carried out to determine the maximum quantity of radioactive materials in each transport group which, when transported in the BMI-1 container, result in compliance with the regulatory dose-rate limits.

5.2.2 Source Radiation Type and Intensity

Table 5.4 lists the radiation characteristics of the radionuclides which control the curie limit of each of the transport groups listed in Tables 5.2 and 5.3.

5.3 Model Specification

5.3.1 Source Geometry

All radiation sources were assumed to be right-circular cylinders 15.5 in. in diameter by 54 in. high with an average density equivalent to that of aluminum* (i.e., 2.7 g/cm^3).

5.3.2 Description of Shield

Figure 5.1 illustrates the shield configurations utilized in the dose-rate calculations for the modified BMI-1 cask under normal and hypothetical accident conditions. For purposes of analysis, the shield was assumed to consist of an annular lead cylinder 8.50** in. thick with end plates of 8.75-in. thickness.

---

* This material was used for purposes of simulating the average packing density of approximately 150 lb/ft^3 (2.4 g/cm^3) which is based on past shipping experience with the NECO-3 cask.

** For photon energies above 1.5 Mev and below 4 Mev, the 1-in. steel thickness is equivalent to about 0.75 in. of lead.

TABLE 5.1. SUMMARY OF MAXIMUM DOSE RATES
(mR/hr)

	Package Surface			3 Feet from Surface of Package		
	Side	Top	Bottom	Side	Top	Bottom
Normal Conditions						
Gamma					10	
Neutron						
Total						
Hypothetical Accident Conditions						
Gamma					<1000	
Neutron						
Total						
10 CFR Part 71 Limit	--	--	--	1000	1000	1000

TABLE 5.2 RADIONUCLIDES AND ASSOCIATED CURIE LIMITS PLANNED FOR TRANSPORT IN MODIFIED BMI-1 CASK (SOLE USE OF VEHICLE)

Transport Group*	Quantity (in curies)
I.	1,000
II.	8,120
General mixed fission products . . .	Unlimited**
III.	4,960
IV.	11,070
V.	8,120
VI and VII	800,000

* As defined in §173.390 of 49 CFT and Appendix C of 10-CFR-71.

** Limit will be imposed by dose-rate limits specified in §173.393(j) of 49 CFR.

TABLE 5.3 RADIONUCLIDES AND ASSOCIATED CURIE LIMITS PLANNED FOR TRANSPORT IN MODIFIED BMI-1 CASK (SHIPMENTS BY COMMERCIAL CARRIER)

Transport Group*	Quantity (in curies)
I.	1,000
II.	2,520
General mixed fission products . . .	Unlimited**
III.	1,540
IV.	3,440
V.	2,520
VI and VII	800,000

* As defined in §173.390 of 49 CFR and Appendix C of 10-CFR-71.

** Limit will be imposed by dose-rate limits specified in §173.393(i) of 49 CFR.

TABLE 5.4 RADIATION CHARACTERISTICS OF LIMITING RADIONUCLIDES

Transport Group	Limiting Radionuclide*	Radiation Type	Radiation Energy and Intensity	Limiting Radiation
I	Ac-228	β^-, γ	β 2.18 (10%), 1.85 (9.6%), 1.7 (6.7%), 1.11 (53%), 0.64 (7.6%), 0.45 (13%) γ 1.64, 1.59, 1.095, 1.035, 0.965, 0.907, 0.458, 0.410, 0.336, 0.232, 0.184, 0.174, 0.1275, 0.113, 0.0978, 0.0781, 0.0568	1.64 and 1.59 Mev γ
II	Kr-87	β^-, γ	β 3.8 (70%), 3.3 (5%), 1.3 (25%) γ 2.57 (25%), 0.85 (10%), 0.403 (50%)	2.57 γ's
III	Co-56	β^+, γ	β 1.5 (18%) γ 3.47 (1%), 3.25 (12%), 2.99 (1%), 2.6 (16%), 2.02 (11%), 1.75 (18%), 1.36 (5%), 1.24 (71%), 1.03 (16%), 0.845 (100%), 0.51 (36%)	3.47 - 1.36 Mev γ's
IV	Cl-38	β^-, γ	β 4.81 (53%), 2.77 (16%), 1.11 (31%) γ 2.15 (50%), 1.6 (40%)	2.15, 1.6 γ's
V	Kr-87**	β^-, γ	β 3.8 (70%), 3.3 (5%), 1.3 (25%) γ 2.57 (25%), 0.85 (10%), 0.403 (50%)	2.57 Mev γ's
VI and VII	Kr-85	β^-, γ	β 0.672 (100%) γ 0.517 (0.7%)	0.672 β's

* Radionuclide which results in the highest external dose rate for a given curie level.

** Uncompressed.

Document: 4

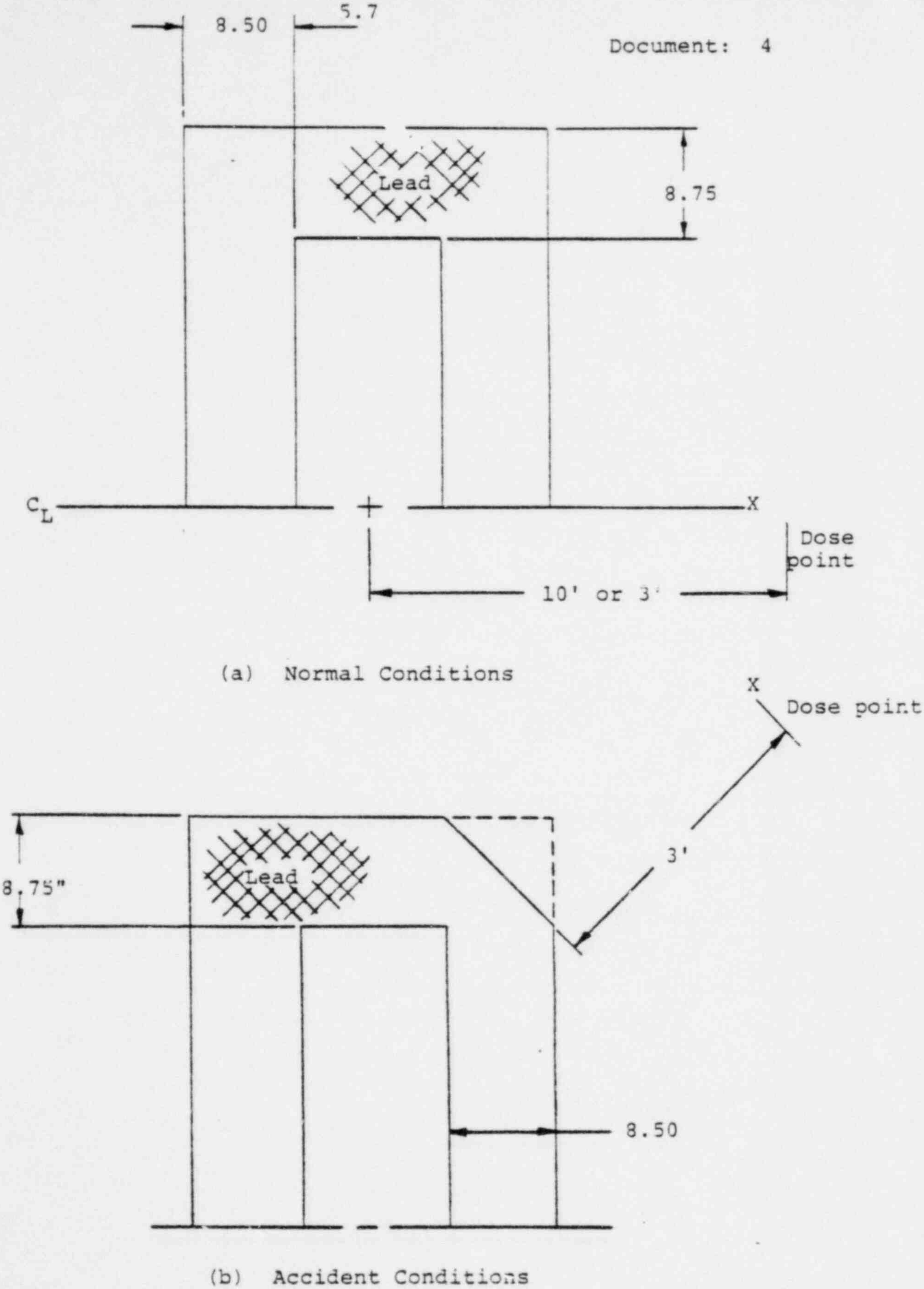

FIGURE 5.1 SHIELD CONFIGURATIONS UTILIZED IN THE DOSE RATE CALCULATIONS FOR THE MODIFIED BMI-1 CASK

5.4 Shielding Evaluation

5.4.1 Dose Rate Under Normal Conditions

5.4.1.1 General Contents

Point kernel integration techniques were utilized to calculate the gamma dose rates at 6 ft (the 10 mr/hr value at this distance is the most stringent of the aforementioned limits for sole use of vehicle transport) from the transport vehicle and 3 ft from the cask (the 10 mr/hr value at this distance is the most stringent of the aforementioned limits for shipment by commercial carrier) for various quantities of radionuclides. The basic equation employed was:

$$D_\gamma = \frac{K(E)B(E,\mu t)\ S_\gamma\ e^{\mu(E)t}}{4\pi r^2}$$

where:

D_γ = gamma dose rate at distance r from source, mrem/hr

$K(E)$ = flux-to-dose conversion factor as a function of photon energy, $\frac{\text{mrem/hr}}{\text{photon/cm}^2\text{-sec}}$

$B(E),\mu t)$ = dose buildup factor as a function of photon energy relaxation length in the shield

S_γ = source strength of photons with energy E, photons/cm^3-sec

$\mu(E)$ = linear attenuation coefficient for photons of energy E, cm^{-1}

t = shield thickness, cm

r = source-to-dose point separation distance, cm.

Parameters used in the above equation for the shield and source materials are listed in Table 5.5. The curie limits for each of the transport groups listed in Tables 5.2 and 5.3 were obtained by varying the source quantity and calculating the dose rate at 6 ft from the vehicle and at 3 ft from the cask until a maximum dose rate of 10 mr/hr was reached. Exceptions to this procedure were made for Transport Group I as well as for VI and VII in which cases curie limits of 1000 Ci and 800,000 Ci, respectively, were considered sufficiently high although the corresponding dose rates at the aforementioned distance were well below the allowable limit.

TABLE 5.5 LINEAR ATTENUATION COEFFICIENT OF THE SOURCE AND SHIELD MATERIALS

Group	Energy, Mev	μ_{source}, cm^{-1}	μ_{Pb}, cm^{-1}
1	4.0	0.071	0.474
2	3.0	0.081	0.476
3	2.0	0.099	0.500
4	1.55	0.110	0.585
5	1.0	0.140	0.729

Actually, the curie limit for Transport Groups VI and VII was established by the restrictions on internal heat load. That is, 800,000 Ci of Kr-85 corresponds to about 1500 watts of decay heat which is consistent with the value utilized for heat-transfer analyses (see thermal analysis section).

In the case where the shipper wishes to ship a mixture of radionuclides classified under various transport groups, the following conditional equation may be used to determine the shipping limits:

$$\sum_{K=1}^{7} \frac{Ci_K}{Limit_K} \leq 1 \quad ,$$

where:

Ci_K = number of curies in Transport Group K to be shipped

$Limit_K$ = curie limit (maximum shipment) for the $K^{\underline{th}}$ transport group

K = an index number assigned to each transport group (i.e., K=1 implies Transport Group I, etc.).

It should be noted that the curie limits referenced above are the "large-quantity" limits listed in Tables 5.2 and 5.3. These limits are based on a safety-related shielding analysis and, in several cases, involve inert gases* which will not be shipped); nevertheless, these limits will be maintained though overly restricted in the case of nongaseous elements.

5.4.1.2 Specific Contents

(A) Co-60

Gamma dose rates at the cask surface and a position 3 feet from the surface in the axial midplane were estimated to be 356 and 35.6 mrem/hour, respectively, for a 40,000-curie Co-60 source. These estimates were based on an assumed point isotropic source with no self-absorption. If the copper basket is placed around the Co-60 source, these dose rates are decreased to 12.2 and 1.22 mrem/hour, respectively.

* See Table 5.4 - Transport Groups II, V, VI, and VII.

(B) Fermi Fuel

The shielding of the BMI-1 cask has been increased by placing a 3.0-inch-thick cylinder of copper around the Fermi fuel subassembly. The gamma dose was calculated using the Perkins and King[1] data to obtain the radiation sources and Rockwell[2] data for the flux equations and cross-section data. The calculated doses without the 3-inch-thick copper shield were 1190 mr/hr at the surface and 47.7 mr/hr at three meters. The copper shield reduced these doses to 89 mr/hr and 3.6 mr/hr, respectively. Additional shielding is not needed at the ends of the subassembly because of the smaller angle subtended by the Fermi subassembly compared to the BRR fuel load.

(C) TRIGA Fuel

The stainless steel elements were measured at 1.6 R/hr at 10 ft in air in the summer of 1970, after approximately 6 months' cooling time. Assuming the Way-Wigner relation for fission product decay to be valid for this case indicates a cooling factor of 3.4, or that the current (December, 1971) activity of the SS elements is about 0.47 R/hr at 10 ft. The Al-clad elements have been measured at 0.30 R/hr at 10 ft in air (5-day cooling period). Using 0.5 R/hr as the maximum activity for one element at 10 ft, 38 elements in air would be 19.0 R/hr at 10 ft. (This assumes no self-attenuation). The BMI-1 cask has 8 in. of Pb shielding which is more than five 10th-value thicknesses. (The tenth value thickness of 1.5 MEV gamma is 1.5 in.). The 38 fuel assemblies surrounded by 8 in. of lead would have an activity of $\sim$0.2 mr/hr at 10 feet or $\sim$0.6 mr/hr at 3 ft. These values are well within the regulations.

(1) References to Section 5 are found in Section 5.5.1.

(D) Pulstar Fuel

In practice the shielding of the BMI-1 cask has been found to be conservatively designed for the types of applications for which it has been employed. The Pulstar fuel provides a less severe shielding requirement than that of previous shipments. Section 6.3 covers the shipment of 24 Battelle Research Reactor fuel elements at a loading of 200 grams ^{235}U per element. The integral burnup of the fuel shipped for this case was

$$\frac{200 \text{ gram}}{\text{element}} \times 0.45 \text{ atom percent burnup} \times \frac{1 \text{ gram fissioned}}{1.18 \text{ gram burnup}} \times$$

$$\frac{1 \text{ MWD}}{1 \text{ gram fissioned}} \times 24 \frac{\text{elements}}{\text{cask}} = 1830 \frac{\text{MWD}}{\text{cask}} \quad ,$$

whereas, for the Pulstar fuel the integral burnup at 10,000 MWD/MTU[3] is

$$\frac{10^4 \text{ MWD}}{10^6 \text{ g}} \times \frac{503.2 \text{ gU}}{\text{pin}} \times 252 \frac{\text{pins}}{\text{cask}} = 1270 \frac{\text{MWD}}{\text{cask}} \quad .$$

(E) EPRI Crack Arrest Capsules

The activity of the capsules was determined with the computer code ORIGEN using the material quantities given in Table 1.2 and the irradiation parameters given in Table 5.6.

The results indicated that shortly after discharge (~30 to 60 min), the activity is about 5200 Ci due entirely to isotopes in Transport Group IV. Since the present license for the BMI-1 cask permits up to 11,000 Ci of activity of materials in Transport Group IV the activity is within permissible levels.

TABLE 5.6. IRRADIATION PARAMETERS FOR EPRI CRACK ARREST CAPSULES

Target Fluence (E>1.0 Mev)	1 (10^{19}) n/cm^2
Fast Flux (E>1.0 Mev)	2.2 (10^{12}) n/cm^2-sec
Thermal Flux	1.8 (10^{12}) n/cm^2-sec
Fission in Fission Monitors	
U^{238}	1.2 (10^{14}) f/dosimeter
Np^{237}	1.5 (10^{15}) f/dosimeter

5.4.2. Dose Rate Under Accident Conditions

Accident conditions which can significantly alter the dose rate external to the cask are (a) the fire condition, (b) the 30-ft corner drop, and (c) the side drop in which case gross displacement of the lead occurs. Each of these cases is discussed in the following paragraphs.

5.4.2.1 Standard Fire

Since the amount of lead which could escape from the cask due to a fire is less than (i.e., 3 to 4 percent* of the melt or 574 in.^{3} would melt) the amount displaced in the 30-ft corner drop, the resulting dose rate at 3 ft from the surface of the cask would be below 1 R/hr.

* Due to expansion of the lead upon melting.

A drop in the lead level of 3 inches at the corner of the cask, will not increase the gamma dose above tolerable levels. Consider only the 2.18 Mev gamma dose from Pr-144 (which accounts for 70 percent of the dose) where $\mu_{Pb} = 0.493$ cm and $\mu_{Fe} = 0.307\ cm^{-1}$. For the most weakly shielded ray, the lead thickness is 3.25 in. and the steel thickness is 2.25 in. Compared to the side of the cask, this is 4.75 in. less lead and 1.5 in. more steel. The increase in dose along the most weakly shielded ray is proportional to

$$e^{4.75 \times 2.54 \times 0.493}\ e^{-1.5 \times 2.54 \times 0.307} = e^{4.78} = 119.$$

The increase in dose also depends on the angle subtended at one meter by the weakly shielded region. The ratio of the angles subtended by the weakly shielded region to the total source is about 1:7. Under normal conditions, the maximum dose one meter from the side of the cask is 13 mr/hr. Considering only the reduction in shielding, the dose at the upper corner after a fire would be less than 119 x 13 = 1.55 r/hr. When the angles subtended by the radiation sources are considered, the dose will be less than 1 r/hr at one meter after a fire.

5.4.2.2 Corner Drop

As shown in the section on structural integrity analysis, the maximum deformation of the lead shield at the corner resulting from the 30-ft drop onto an unyielding surface is 5.63 in. which results in a residual lead thickness of 4.53 in. at the point closest to the source region. This deformation results in a maximum dose rate of less than 1 R/hr at 3 ft from the surface of the cask for the curie levels listed in Tables 5.2 and 5.3. The analysis was conducted by numerically integrating* the previously defined point kernel over the source volume while incorporating the effects of the irregular shield geometry.

5.4.2.3 Side Drop

The maximum impact load on the side of the cask will cause 1.44 inches deformation of the lead. Since this is less than the 1.65 inches lead melted during the fire accident, which was previously demonstrated to be safe, the dose rate 3 feet from the surface after impact will be less than 1.0 rem/hour.

5.5 Appendix

5.5.1 References

(1) Perkins, J. F., and King, R. W., Nuclear Science and Engineering, Vol. 3, p 725, 1953.

(2) Rockwell, T., "Reactor Shielding Design Manual", TID-7004, 1956.

(3) Private communication from Dr. Martin N. Haas, Associate Director, Nuclear Science and Technology Facility, State University of New York at Buffalo to Dr. C. E. Williams, Manager, Idaho Operations Office, U.S. ERDA, 550 Second Street, Idaho Falls, Idaho 83401.

---

* By utilizing a simple three-dimensional code under development at Battelle.

6. CRITICALITY EVALUATION

6.1 Discussion and Results

6.1.1 Applicable Regulatory Criteria

Regulatory criteria pertaining to criticality which are applicable to Fissile Class I and II shipments are delineated in §71.37, §71.38, and §71.39 of 10-CFR-Part 71. These sections are summarized as follows:

§71.37 Evaluation of an array of packages of fissile material

(a) An array of packages shall be evaluated by subjecting a sample package to the conditions specified in 71.38, 71.39, or 71.40.

(b) In determining whether the standards of the Class I, II, and III sections are met, it will be assumed that, consistent with the condition of the package:

  (1) The fissile material is in the most reactive credible configuration.

  (2) Water moderation occurs to the most reactive extent.

§71.38 Specific standards for a Fissile Class I package.

A Fissile Class I package shall be so designed and constructed and its contents so limited that:

(a) Any number of such undamaged packages would be subcritical in any arrangement, and with optimum interspersed hydrogenous moderation unless there is a greater amount of interspersed moderation in the packaging, in which case that greater amount may be considered; and

(b) Two-hundred-fifty such packages would be subcritical in any arrangement, if each package were subjected to the hypothetical accident conditions.

§71.39 Specific standards for Fissile Class II package.

(a) For a Fissile Class II package; designed, constructed, loaded, and number limited so that:

(1) Five times the number of undamaged packages would be subcritical in any arrangement with close water reflection.

(2) Two times the number of packages damaged by the Appendix "B" tests would be subcritical in any arrangement with close water reflection and optimum interspersed moderation, or built-in moderation if it is greater.

(b) The number of radiation units to be fifty divided by the allowable number of packages, rounded up to next higher tenth.

6.1.2 Determination of Allowable Number of Packages

6.1.2.1 Fissile Class I

For Fissile Class I shipments a 1000 x 1000 x 1000 array was analyzed.

6.1.2.2 Fissile Class II

The number of allowable packages that can be shipped under Fissile Class II was calculated from the equation:

$$\frac{50}{N} = I_t \quad ,$$

where N is the allowable number of packages and I_t is the transport index or minimum number of radiation units. For the case of sole use of vehicle shipments, §173.396(f) of 49 CFR states that for nuclear criticality control purposes, the transport index must not exceed 10. Thus, using this transport index, the number of casks that could be shipped was calculated from the above equation and found to be 5.

On the basis of the allowable number of packages determined above, §71.39 of 10-CFR-Part 71 specifies that 5N or 25 packages remain subcritical under normal conditions and that 2N or 10 packages remain subcritical under accident conditions.

The container is shown to undergo little dimensional change in the accident conditions; thus, shipment of 25 packages will be the most reactive case.

6.1.3 Contents Evaluated

The following contents are evaluated for shipment in the BMI-1 cask

- General contents
- BRR Fuel Elements
- MTR Fuel Elements
- Fermi Fuel Elements
- TRIGA Fuel Elements
- PULSTAR Fuel Elements.

6.2 Criticality Evaluation for General Contents

6.2.1 Package Fuel Loading

A criticality evaluation was made of the modified BMI-1 cask using the KENO[1] computer code. The analysis was made for mutually exclusive shipments of U-235 or Pu-239. Two separate criticality analyses were performed for shipment with and without an inner container. In addition, a check calculation was made for the case of a critical solution of $U(30.45)O_2F_2$ in spherical geometry to verify the accuracy of the Hansen and Roach[2] cross sections used in the aforementioned analysis.

6.2.2 Shipment Without Inner Container

6.2.2.1 Calculational Model

The configurational model of the modified BMI-1 cask used for the criticality analysis is shown in Figure 6.1. The fissile material is assumed to contain the concentration of water required to make the material most reactive (i.e., optimum H/X atomic ratio) and is located in a spherical volume at the geometric center of the container. The remainder of the inner cavity of the container is assumed to be void.*

The criticality calculations (to determine X_{eff}) for Fissile Class II shipments were performed on a 3 x 3 x 3** array

---

* This represents the most reactive condition.

** For simplicity of the calculational model, 27 casks were used in lieu of 25.

---

(1) References for Section 6. are found in Section 6.8.1.

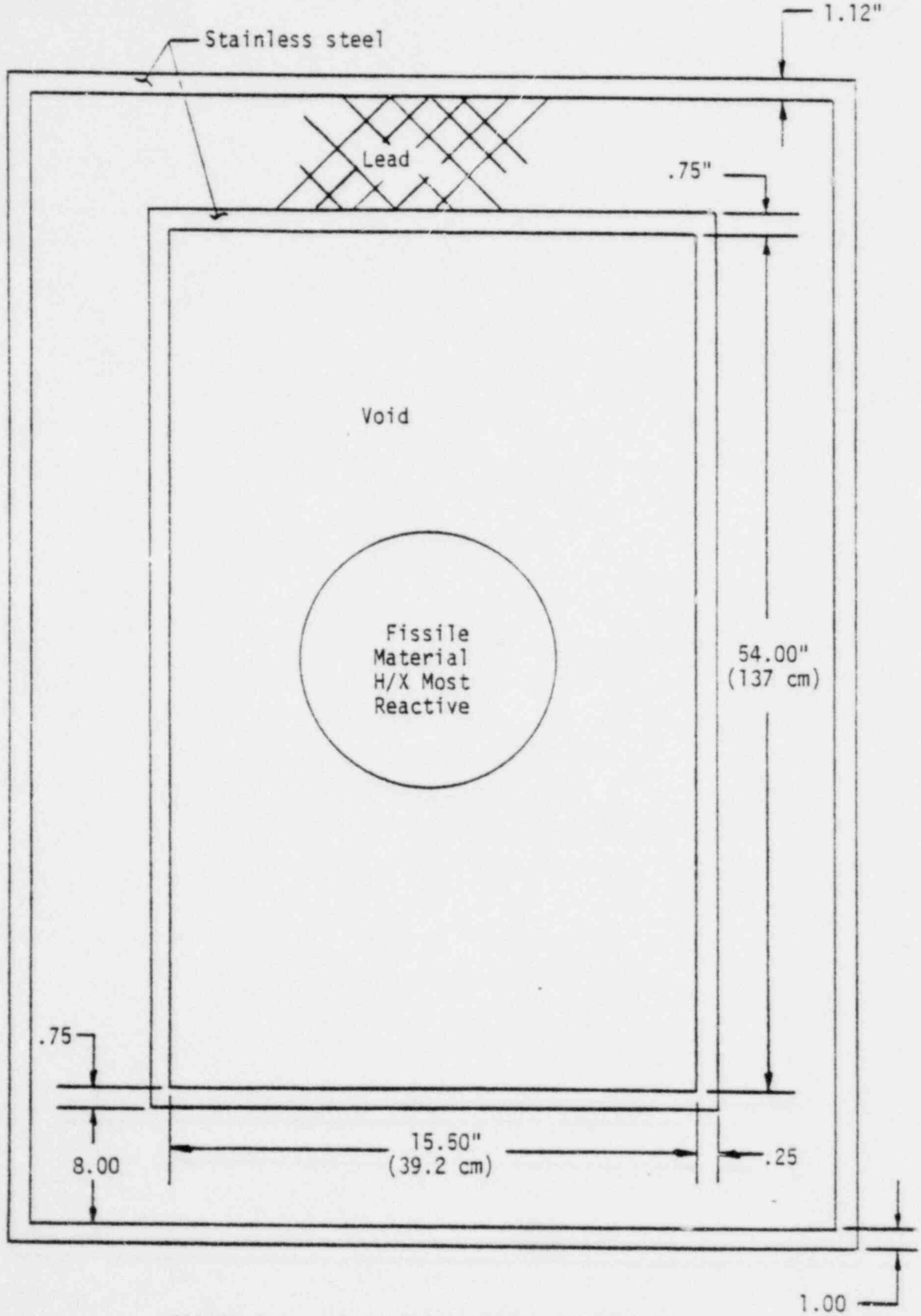

FIGURE 6.1. CALCULATION MODEL UTILIZED IN CRITICALITY EVALUATION

of BMI-1 casks. The array (shown in Figure 6.2) has a cubic lattice with a pitch of 33.0 inches, and the array is completely surrounded by a 10-inch water reflector.

The criticality calculations for Fissile Class I shipments were performed on a 1,000 x 1,000 x 1,000 array of BMI-1 casks. This array was assumed to be infinite for calculational purposes.

6.2.2.2 Results

The results of the KENO calculations for shipment without an inner container are given in Table 6.1. These results show that an infinite array (i.e., 1 billion units) of BMI-1 casks, each of which contains 500 g of U-235 or 280 g of Pu-239, remains subcritical. Since Pu-239 is more reactive on a mass basis than U-233, 280 g of U-233 in an infinite array would also be subcritical.

The difference in K_{eff} for 27 (i.e., 3 x 3 x 3 array) and 1 billion (i.e., 1,000 x 1,000 x 1,000) casks each containing 500 g of U-235 was found to be only 0.01. Thus, the lattice type was found to be unimportant in the case of the foregoing calculations.

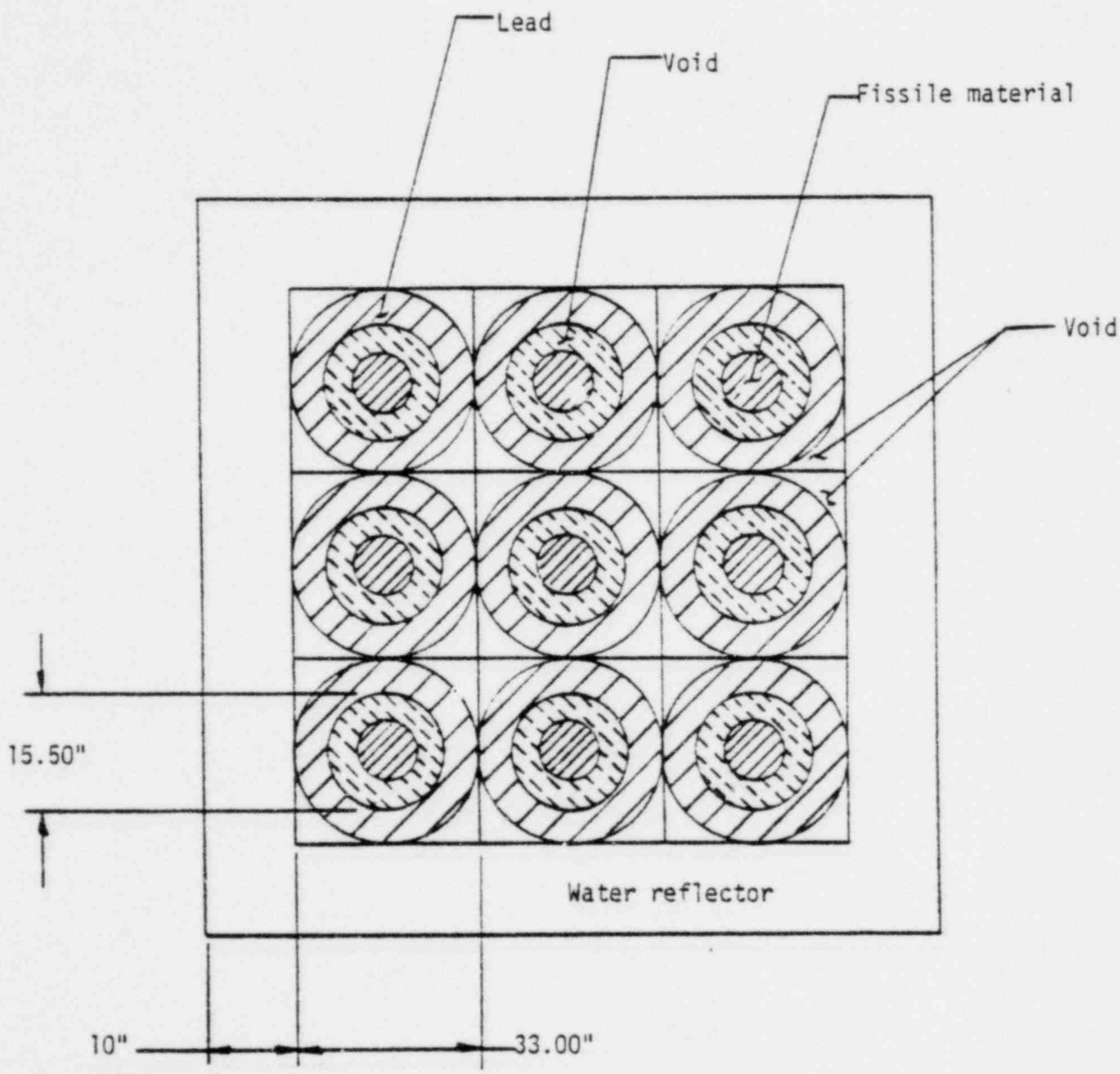

FIGURE 6.2. CROSS SECTION OF 3x3x3 ARRAY OF CASKS

TABLE 6.1. RESULTS OF THE KENO CODE CALCULATIONS OF K_{EFF} FOR SHIPMENT WITHOUT AN INNER CONTAINER

Run No.	Description	Fissile Material	Mass Fissile Material (grams)	H/X[a] Atomic Ratio	Calculated K_{eff}
1	Critical sphere test case[b]	U-235	991	573	1.01 ± 0.01
2	3 x 3 x 3 array - H_2O reflected (cubic lattice)	U-235	500	500	0.93 ± 0.02
3	1,000 x 1,000 x 1,000 array (cubic lattice)	U-235	500	500	0.94 ± 0.025
4	1,000 x 1,000 x 1,000 array (cubic lattice)	Pu-239	280	800	0.93 ± 0.02

(a) Reference 3, pages 12, 14, and 35.

(b) Reference 3, page 12.

In the case where the shipper wishes to ship a mixture of the fissile isotopes considered here, the following conditional equation may be used to determine the mass limit for shipment:

$$\sum_{k=1}^{3} \frac{M_K}{Limit_K} \leq 1 \quad , \tag{1}$$

where:

M_K = mass (grams) of $K^{\underline{th}}$ fissile isotope to be shipped

$Limit_K$ = mass limit (grams) (maximum shipment) for the $K^{\underline{th}}$ fissile isotope

K = an index number assigned to each fissile isotope (i.e., K=1 for U^{235}; K=2 for Pu^{239}; and K=3 for U^{233}).

6.2.3. Shipment with Inner Container

6.2.3.1 Calculational Model

The configurational model of the modified BMI-1 cask used for the criticality analysis is shown in Figure 6.3. The fissile material is assumed to contain an H/X ratio not greater than 20 and is located in a spherical volume at the geometric center of the container. The remainder of the inner cavity of the container is assumed to be void.

The criticality calculations for Fissile Class I shipments were performed on a 1,000 x 1,000 x 1,000 array of BMI-1 casks. This array was assumed to be infinite for calculational purposes.

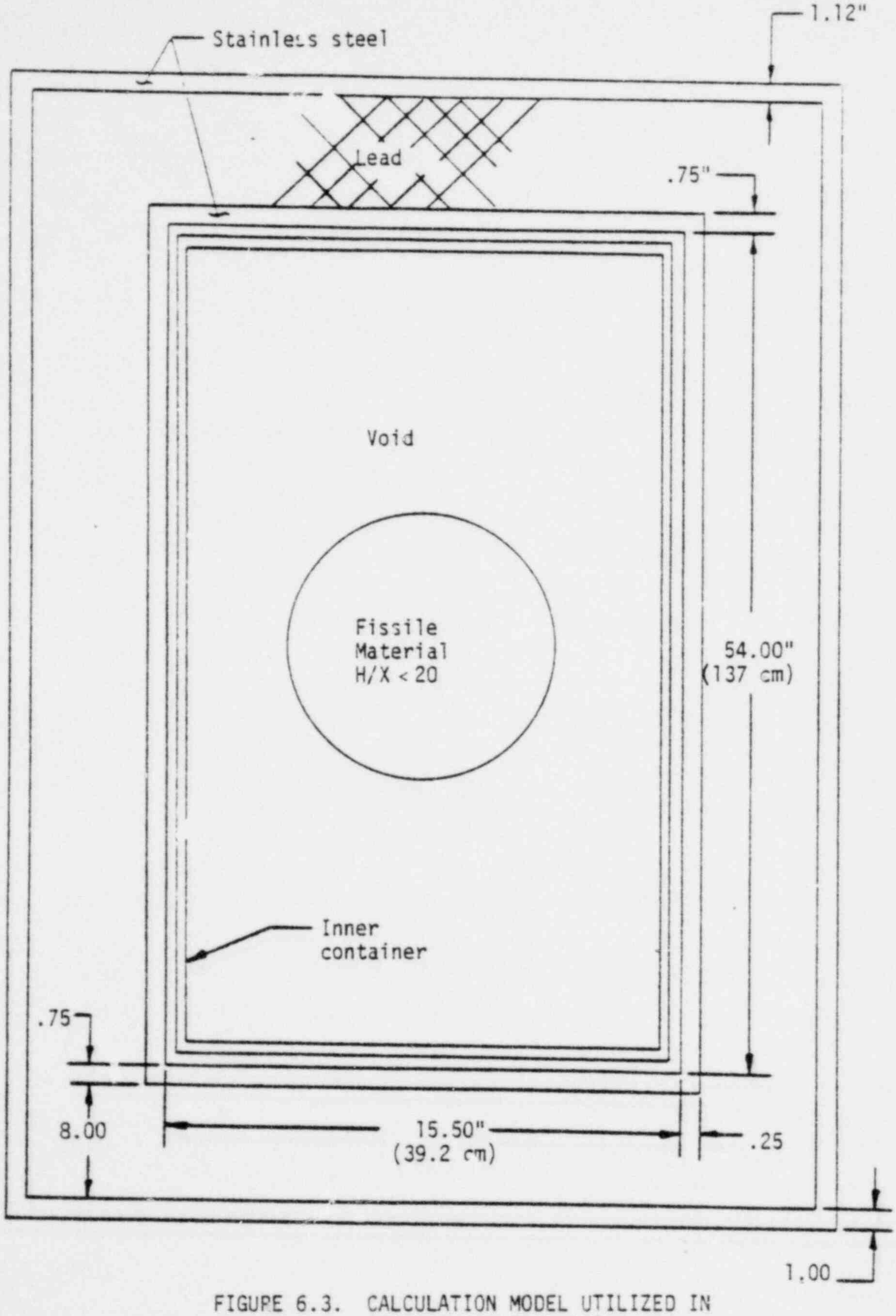

FIGURE 6.3. CALCULATION MODEL UTILIZED IN CRITICALITY EVALUATION

6.2.3.2 Results

The results of the KENO calculations are given in Table 6.2. These results show that an infinite array (i.e., 1 billion units) of BMI-1 casks, using an inner container each of which contains 1,000 grams U-235 or 600 grams Pu-239, remains subcritical. Since Pu-239 is more reactive on a mass basis than U-233, 600 grams of U-233 in an infinite array would also be subcritical.

Since the lattice extent was found to be unimportant for the arrays of casks without inner containers, it is obvious that a 3 x 3 x 3 cubic array of casks (Fissile Class II) with inner containers and with 1,000 grams U-235 or 600 grams Pu-239 would also be subcritical.

In this case where the shipper wishes to ship a mixture of the fissile isotopes considered here, Equation (1) may be used to determine the mass limit for shipment.

TABLE 6.2. RESULTS OF KENO CODE CALCULATIONS OF K_{EFF}
FOR SHIPMENT WITH AN INNER CONTAINER

Run No.	Description	Fissile Material	Mass Fissile Material (grams)	H/X Atomic Ratio	K_{eff}
1	1,000 x 1,000 x 1,000 array (cubic lattice)	U-235	1,000		0.83 ± 0.02
2	1,000 x 1,000 x 1,000 array (cubic lattice)	Pu-239	600	20	0.81 ± 0.02

6.3 Criticality Evaluation for BRR Fuel Elements

6.3.1 Package Fuel Loading

The modified BMI-1 shipping cask is a cylindrical, double-walled stainless-steel vessel, in which the space between the inner and outer shells is occupied by lead shielding. Fuel assemblies are positioned within the central cavity by two identical stainless-steel clad boral plates acting as center dividers as shown in Drawing 0004, Rev. B.

For this analysis, BRR fuel elements with 200 g of U-235 were considered. Each is 3.16 x 3.00 x 23.25 in., fueled length. A description of a standard fuel assembly for Battelle's Research Reactor is given in Figure 6.4. Each fuel assembly is a heterogeneous mixture of Al, H_2O, U-235, and U-238. The composition of a BRR fuel element is given in Table 6.3.

TABLE 6.3. COMPOSITION OF BRR'S FUEL ASSEMBLY

Material	Weight, gm	Atoms or Molecules per cc (Volume Homogenized)
H_2O	2725	2.5253×10^{22}
Al	2780	1.7188×10^{22}
U-235	200	1.41×10^{22}
U-238	15	1.05×10^{19}

A cross section of BMI-1 shipping cask's fuel basket is shown graphically in Figure 6.5 and in detail in Drawing 0004. This is the fuel basket used to ship the fuel element assemblies. The dimensions of each of the 12 cavities are 3.34 x 3.34 in. The fuel assemblies are shipped into these cavities.

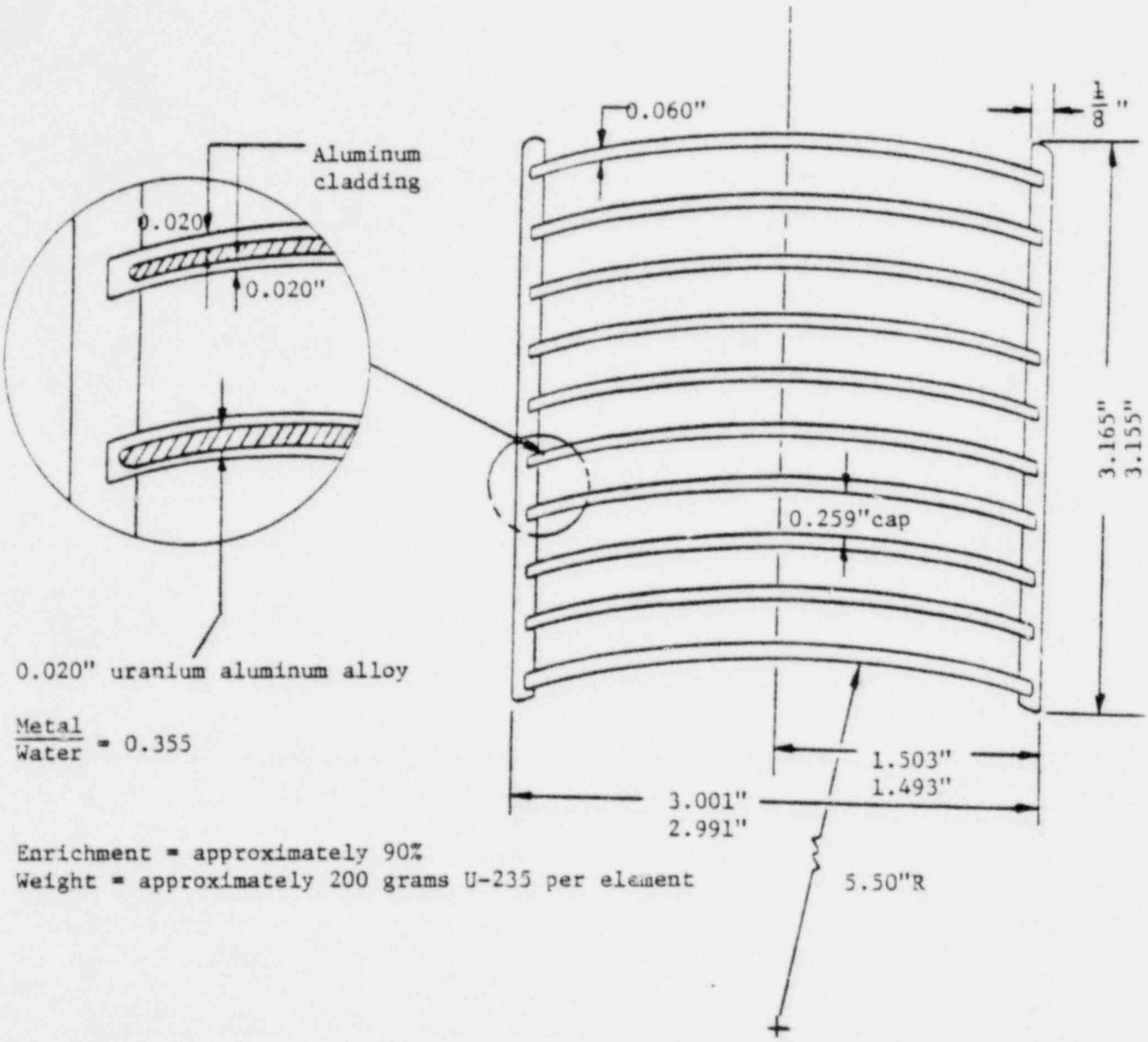

FIGURE 6.4. STANDARD FUEL ASSEMBLY FOR BATTELLE RESEARCH REACTOR

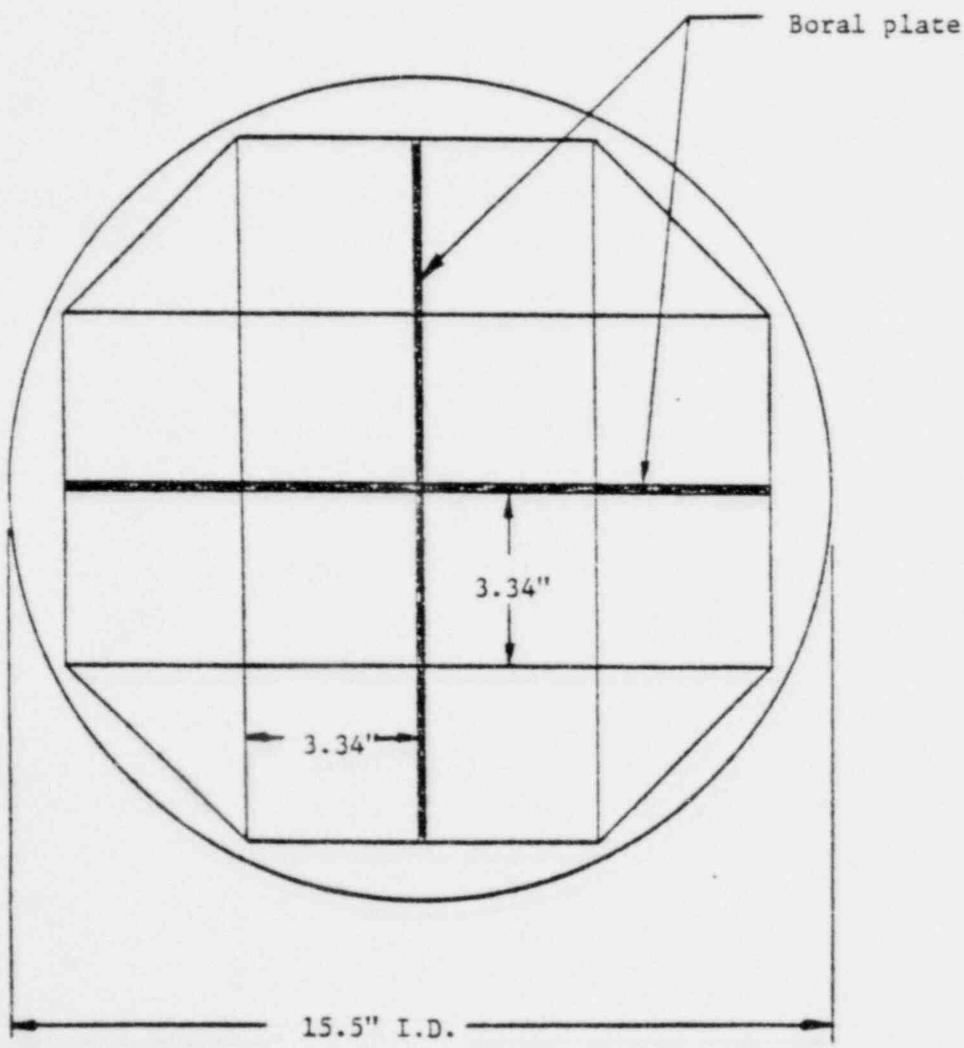

FIGURE 6.5. TOP VIEW OF SHIPPING CASK FUEL BASKET

6.3.2 Calculational Model

The fuel assembly was volume-homogenized for calculational purposes. Since the thermal flux is depressed in the fuel and peaks in the water of the cell, this is a conservative approximation, i.e., one that would tend to give relatively greater importance to the fuel and overpredict the value of K_{eff}.
The effect is known to be small.

In order to properly account for transverse leakage effects, Fe-Pb-Fe end plugs for the BMI-1 cask were incorporated into the two cask systems as shown in Figure 6.6.

A void region was also defined between the casks in order to increase the effect of neutron interaction between casks (see Figure 6.7 for details). The remainder of the two cask systems was immersed in a water reflector.

A 16-group set of cross sections was used. This modified Hansen-Roach set has been shown[4] to predict, accurately, values of K_{eff} when used in conjunction with the KENO program for systems such as the one described here.

6.3.3. Package Regional Densities

Table 6.4 gives the number densities for a basket cavity with a fuel assembly in it (volume fraction of fuel cell, 0.85, volume fraction of water, not in the cell, 0.15).

TABLE 6.4 NUMBER OF ATOMS PER CC IN THE HOMOGENIZED FUEL BASKET

Element	N x 10^{24}
H	0.052981
O	0.0264905
Al	0.0146098
U-235	0.0001199
U-238	0.0000089

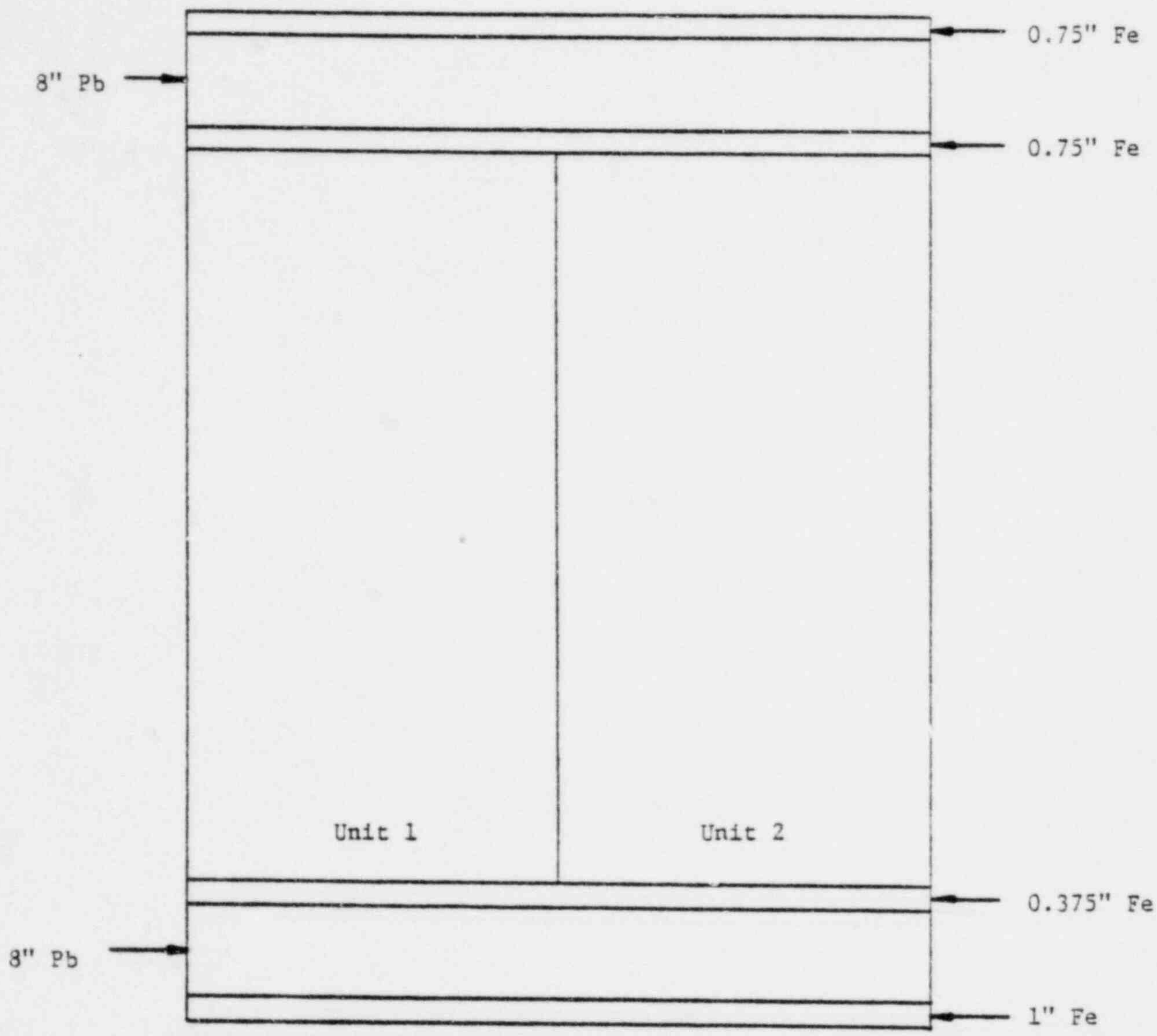

FIGURE 6.6. AXIAL REPRESENTATION OF THE SYSTEM
(SYSTEM IMMERSED IN WATER)

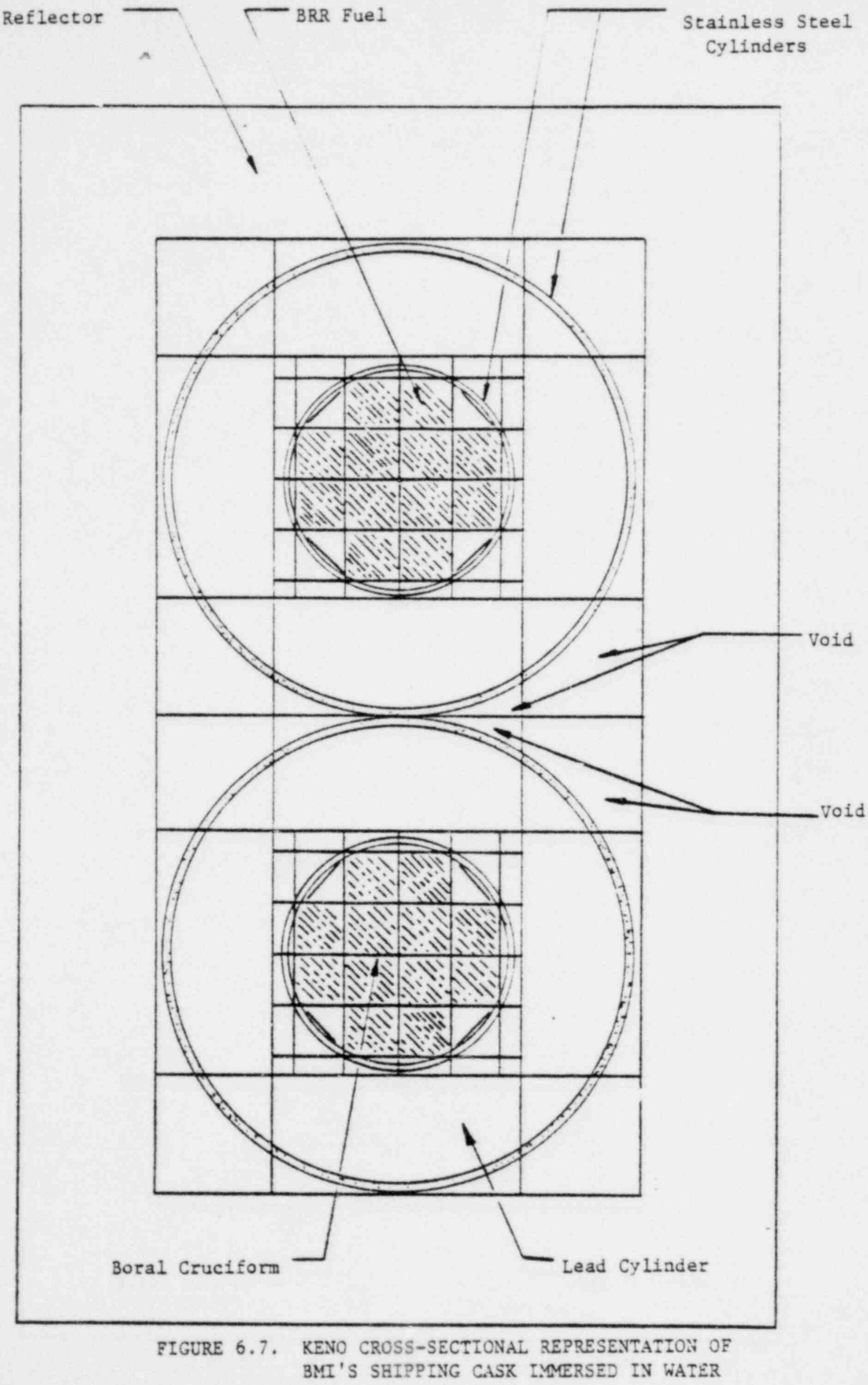

FIGURE 6.7. KENO CROSS-SECTIONAL REPRESENTATION OF BMI'S SHIPPING CASK IMMERSED IN WATER

When considering the cruciform boral plates a simple volume homogenization is not adequate since it does not account for self-shielding effects, and thus would tend to over-estimate the boron absorption.

The total reaction rate in the homogeneous mixture of absorber (boral plates) and diluent (Al-cladding and SS), $V_T\Sigma\phi$, can be related to the reaction rate of each of the components by:

$$V_T\overline{\Sigma}\ \overline{\phi} = V_a\overline{\Sigma}_a\overline{\phi}_a + V_d\overline{\Sigma}_d\overline{\phi}_d \tag{2}$$

where V_a, V_d, V_T, refer to the volumes of the absorber, the diluent, and the total, respectively. Equation (2) can be interpreted as a defining equation for proper homogenization, with the average flux defined by:

$$V_T\overline{\phi} = V_a\overline{\phi}_a + V_d\overline{\phi}_d \quad . \tag{3}$$

Using Equations (2) and (3), the properly homogenized number densities, N, are then found to be:

$$N \ \text{(absorber)} = \frac{V_a^f\ N^o\ \text{(absorber)}}{V_a^f + V_d^f\ \dfrac{\phi_s}{\phi_a}} \quad , \tag{4}$$

and

$$N \ \text{(diluent)} = \frac{V_d^f\ N^o\ \text{(diluent)}}{V_a^f\ \dfrac{\overline{\phi}_a}{\phi_s} + V_d^f} \quad . \tag{5}$$

where f indicates volume fractions and N^{o} are the true number densities of absorber and diluent materials. A ratio of the surface ($\bar{\Phi}_d = \bar{\Phi}_s$) to average flux in the absorber $\bar{\Phi}_s/\bar{\Phi}_a$ is equivalent to volume-homogenized number densities. The effect of using Equations (4) and (5) is to decrease the simple volume weighted number density of the absorber and to increase that of the cladding, as expected.

The boral plate, 62 mils thick, is composed of a o.103 cm thick B_4C-Al plate containing 35wt/o B_4C in the B_4C-Al mixture (65 w/o Al, 27.4 w/o B, 7.6 wt/o C), and clad with aluminum. There are also two outer SS plates, each 31 mils thick. The volume fractions of diluent Al, diluent SS, and absorber B_4C-Al mixture are, 17.3 percent, 50 percent, and 32.7 percent, respectively.

It has been shown[5] that conventional calculations of the absorption cross-section of boral do not consider channeling of neutrons due to B_4C lumping. Experimentally, it has been verified[6] that B_4C lumping in the boral plates reduces the thermal neutron absorption cross-section about 20 to 30 percent. This implies that the number density (above) of B should be reduced by that factor for computation of the absorption cross sections. It can be shown that:

$$\frac{\Phi_s}{\bar{\Phi}_a} = \frac{2(2 - \beta)}{\beta} \Sigma_a \frac{V}{S} \quad ,$$

where β is the capture fraction, and V and S refer to the volume and surface of the absorber. For a slab,

$$\frac{\Phi_s}{\bar{\Phi}_a} = \frac{(2 - \beta)}{\beta} \Sigma_a \ell \quad .$$

For heavy absorbers, $\beta \doteq 1$, we have

$$\frac{\phi_s}{\phi_a} = \Sigma_a \ell \quad .$$

Where Σ_a is the absorption cross section of B_4C-Al mixture and ℓ is the thickness of the plate. $\Sigma_a \doteq 17.664\ cm^{-1}$, $\ell = 0.103$ cm, therefore,

$$\frac{\phi_s}{\phi_a} = 1.82 \quad .$$

The properly homogenized number densities are then,

$$N_d\ (Al) = \frac{(0.173)\ (0.0602)\ x\ 10^{24}}{\frac{(0.327)}{(1.82)} + (0.173 + 0.5)} = 0.0122\ x\ 10^{24} \quad ,$$

$$N_a\ (Al) = \frac{(0.327)\ (0.0392)\ x\ 0.7\ x\ 10^{24}}{(0.327 + (0.673)\ (1.82)} = 0.00578\ x\ 10^{24} \quad ,$$

6.3.4 Results

The k_{eff} for two BMI-1 shipping casks loaded with 24 BRR fuel elements (200 g of U-235 per element), having the inner cavity filled with water, a void between the casks where they are in contact, and the cask systems surrounded by a water reflector was calculated to be:

$$k_{eff} = 0.934$$

with a standard deviation of $\pm$ 0.0099.

6.4 Criticality Evaluation for MTR Fuel Elements

The MTR fuel assemblies to be shipped comply in type and form to 5(b) (1) (i) of the present BMI-1 container license. The modified basket maintains the identical geometry for the active fuel portion of the MTR assemblies as the licensed package containing 24 assemblies. The criticality analysis for shipment of 24 assemblies is detailed in Section 6.3. The present shipment represents the same geometry as analyzed in Amendment 5 except the length of the active fuel is reduced from 48 inches to 24 inches. This is a less critical lc ıg and geometry than analyzed in Section 6.3 Thus, the shipment of 12 MTR assemblies in the modified basket will remain subcritical in the most reactive credible configuration.

6.5 Criticality Evaluation for Fermi Fuel Elements

The Fermi fuel subassembly contains 18.616 kg of uranium, including 4.771 kg of uranium-235. The subassembly as shipped is 2.6 inches square and 31 inches long. The H to U235 atomic ratio for the Fermi element is about 10. According to the Nuclear Safety Guide,[7] Figure 3 pp 15, safe infinite cylinder diameter is about 4.7 inches. With copper shot displacing water, the critical mass would be larger. Thus, under normal conditions, there is no criticality problem.

The melting points of all the materials in the fuel element are above 2000 F (U-10 w/o Mo fuel alloy with zirconium cladding). Since it is not expected that this temperature would be encountered during shipment, the fuel element configuration will be maintained, and there is no danger of meltdown.

6.6 Criticality Evaluation for TRIGA Fuel Elements

6.6.1 Package Fuel Loading

Irradiated Triga Type III fuel assemblies containing not more than 40 grams U-235 per assembly prior to irradiation. Uranium may be enriched to a maximum 20 w/o in the U-235 isotope. Active fuel length shall be 15 inches for stainless steel clad assemblies and 14 inches for aluminum clad assemblies.

38 fuel assemblies as contained in product containers specified in 5(a)(4) (iv).

6.6.2 Results

Experiments have shown that in an optimally moderated array, critcality is achieved with 60 TRIGA fuel elements. Information on these experiments is contained in "Torrey Pines TRIGA MARK III Reactor Startup and Post Critical Tests", GAMD-7445. Only 38 elements will be shipped in the BMI-1 cask and the geometry for shipment is highly nonideal. Structural analysis shows the basket maintains its integrity during the accident sequence. Thus the shipment of 38 elements will remain subcritical under both the normal and accident conditions for transport.

6.6.3 Criticality Measurements

Following are the results of the loading-to-critical experiment in the University of Arizona TRIGA. The aluminum-clad fuel is the fuel which we anticipate shipping to the University of Utah at Salt Lake City, Utah. The measured value of k for the 38-element loading in the most reactive configuration is seen to be 0.83; however, by curve fitting as shown in Figure 6.8 the best value would be a k of 0.80.

TABLE 6.5. MEASURED RESULTS DURING LOADING TO CRITICAL IN TRIGA AT THE UNIVERSITY OF ARIZONA

Fuel Elements	CPM	$\frac{1}{M} = 1 - k$
0	188	1
6	188	1
16	317	0.76
25	495	0.38
33	678	0.28
38	1135	0.17
42	1543	0.12
46	2111	0.09
50	3722	0.05
58	Critical	0

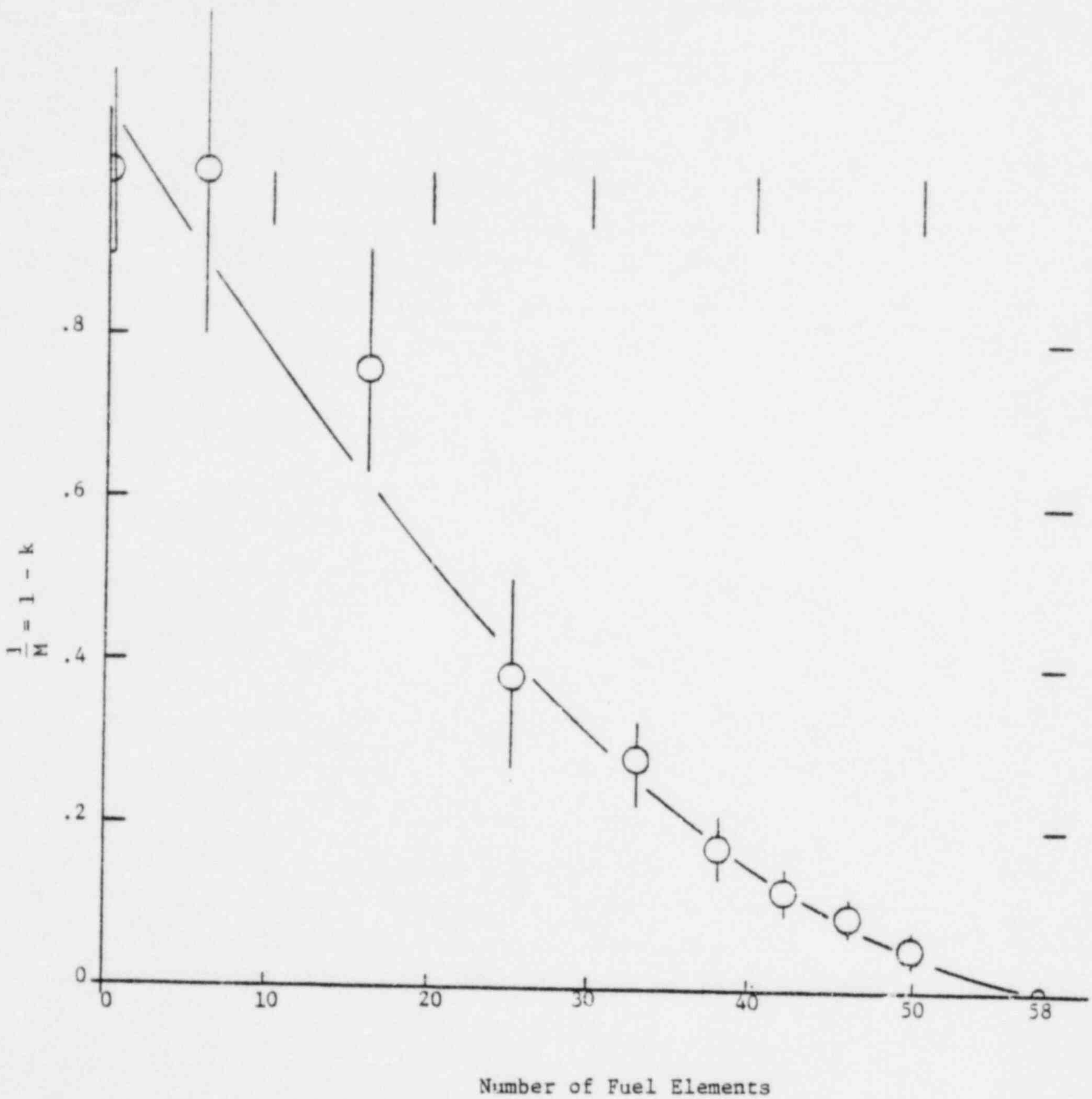

FIGURE 6.8. LOADING TO CRITICAL RESULTS IN TRIGA USING ALUMINUM-CLAD FUEL ELEMENTS.

6.7 Criticality Evaluation for PULSTAR Fuel Elements

6.7.1 Package Fuel Loading

The BMI-1 shipping cask is a cylindrical, double-walled stainless steel vessel, in which the space between the inner and outer shells is occupied by lead shielding. Fuel assemblies are positioned within the central cavity by a stainless steel fuel basket (containing 12 fuel assemblies) and are supported by a circular stainless steel plate welded to a stainless steel cylinder which occupies the bottom part of the central cavity of the cask. A permanent neutron poison is provided by stainless-steel clad boral plates which serve as center dividers of the basket.

The spent fuel to be shipped is of the Pulstar type with 6 percent enriched UO_2 encased in Zircaloy-2 cladding. Each fuel pin is 26-1/8 inches long with an OD of 0.474 inch. Each fuel pin contains an average of 572.80 grams of UO_2, 505.2 grams of U, and 30.28 grams of U-235. The fuel pellets are 24 inches long. The cladding is 0.020 inch thick and Zircaloy caps are welded at the ends of the fuel pin. These fuel pins are to be loaded into stainless steel canisters (see Figure 6.9), 21 per canister. The canisters are to be loaded into the BMI-1 shipping cask, 12 per cask. A cross-section of the fuel basket is shown in Figure 6.5. The 12 canisters fit into the 3.34-inch-square spaces provided for by the basket. The basket spacers are made of 1/10-inch stainless steel except the central ones (both vertical and horizontal). These are 1/8-inch stainless steel clad boral plates.

Figure 6.10 shows the overall geometry of the loading in the vertical plane. This geometry fits snugly into the central cavity of the cask. This cavity is 15-1/2 inches in diameter by

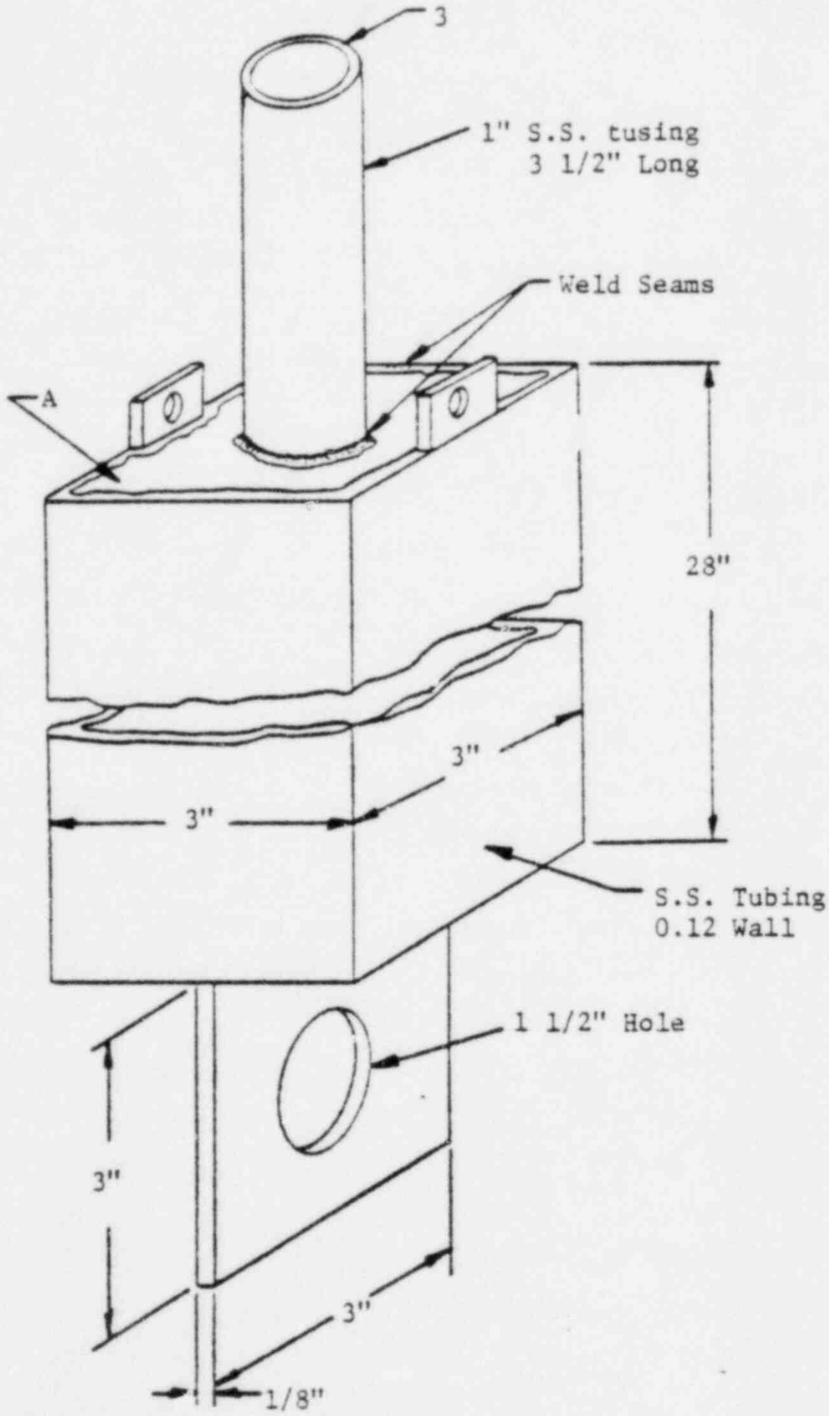

NOTE A: Top and Bottom Lid are 3/16" S.S.

NOTE B: Canister will be sealed with 1" S.S. Swagelock Cap

FIGURE 6.9. FUEL STORAGE CANISTER

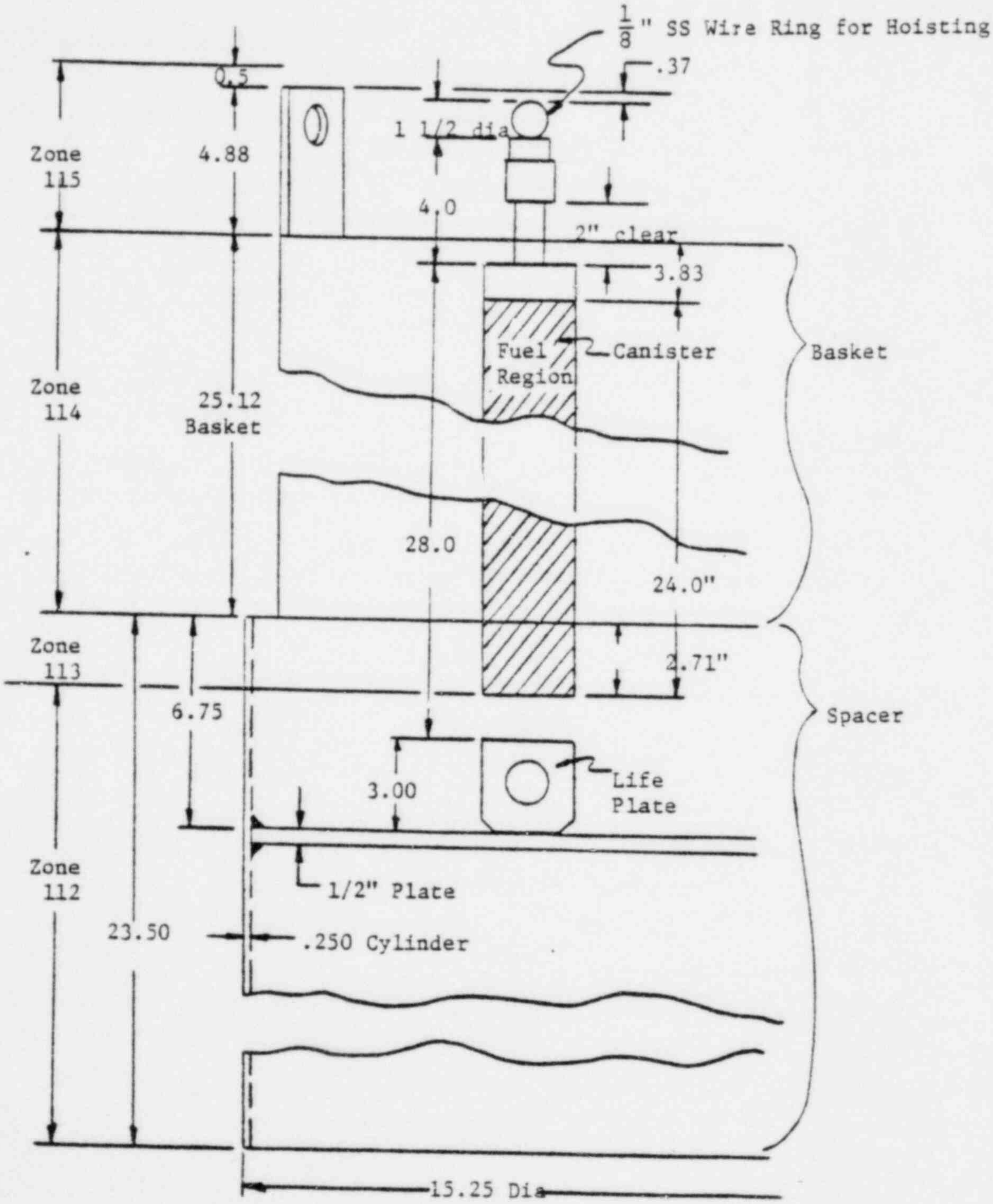

FIGURE 6.10 FUEL LOADING ARRANGEMENT

54 inches long. The cask has an inner stainless steel cylindrical shell which is 1/4-inch thick, an outer stainless steel cylindrical shell which is 5/8-inch thick, and 8 inches of lead between these shells on the sides. The stainless steel shell below the cavity is 3/4-inch thick, the cask bottom is 1-1/8 inch thick, and there is 7-3/4 inches of lead below the cask cavity. The removable plug at the top of the cask has 3/4-inch stainless steel at the bottom, 7-3/4 inches of lead, 1-1/8 inches of stainless steel at the top, and 1/4-inch stainless steel cylindrical sides.

6.7.2 Normal Conditions

The shipment of fuel is to be made dry. The total mass of U-235 in the 12 canisters, each containing 21 pins, is then 7.631 kg. The minimum critical mass of 92.5 percent enriched uranium, full reflected, is 22.8 kg[7]. Thus even for two dry packages in contact and reflected on all sides by water, $k_{eff} < 1$.

6.7.3 Accident Conditions

6.7.3.1 Calculational Model

Under accident conditions for Fissile Class III materials, one shipment of packages is to remain subcritical with optimum hydrogenous moderation and close reflection by water.

In this case the first task is to find what loading of the fuel storage canister is most reactive when the canister is flooded with water. As a guide in this determination it is noted here that based upon initial cold, clean conditions the minimum number of fuel assemblies required for criticality is slightly in excess of 16 for light water moderation[8]. Each fuel assembly consisted of 25 fuel pins with a nominal pitch from pin to pin of 0.606 inch. Furthermore[8], as indicated by the decreasing curvature of the plot of inverse count rate vs number of fuel assemblies the Pulstar design results in an undermoderated core for the 6 percent enrichment. For this loading there are 25 pins in a square with sides of length approximately 6 x 0.606 or 3.636 inches. Thus there is about 0.53 square inches per pin. At this same areal density a fuel loading canister which is square and of length 2.76 inches on the inside will hold $(2.76)^2/0.53 = 14.38$ pins. Since this loading is undermoderated, maximum reactivity for the accident condition should occur at a loading of less than 14 pins/can.

To determine the pin/canister loading at which maximum reactivity occurs, a number of computer calculations were made in which this loading was varied. All of the calculations were done using the 23 group neutron structure available with the AMPX-1 modular code system(9). This consists of the 80 GAM-II groups combined with a 30 group THERMOS structure below 1.86 ev. For each of 4 pins per canister loadings the value of K_∞ was found in the following way. First a NITAWL(9) calculation was made for a unit fuel cell configuration. NITAWL corrects for resonance self-shielding in the U-238 of the fuel pin using the Nordheim Integral Treatment and "cell-averages" the resonance cross sections. Then an XSDRNPM(9) calculation was done. This is a one-dimensional transport calculation of k_∞. XSDRN also spacially weighs the cross sections of the unit fuel cell, i.e., it generates cross sections consistent with mocking up a cellular configuration as a homogenized region. The spatial "disadvantage factors" are taken into account in the weighing. These cross sections can then be used as input to a KENO calculation to find k_{eff} of a finite system.

The results of these code calculations are shown in Figure 6.11. A loading of 12 pins per canister was selected as being the most reactive. The spacially weighed cross sections

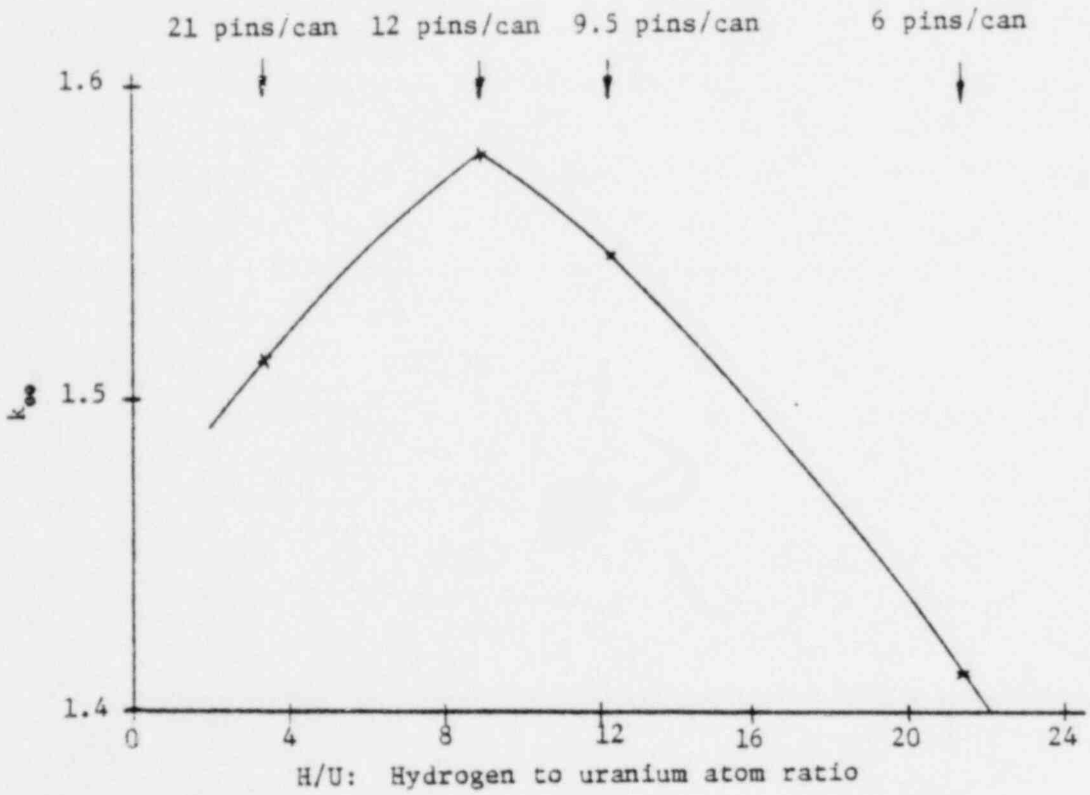

FIGURE 6.11 k_∞ VERSUS FUEL PIN LOADING

found in this run are the ones used to represent the fuel region in a KENO[10] run which was done to find the value of k_{eff} for the hypothetical accident condition.

The KENO calculation was done using the generalized geometry package (GEOM), which allows any system that can be described by a collection of planes and/or quadratic surfaces arbitrarily oriented and intersecting in arbitrary fashion. Figure 6.12 shows a horizontal cross sectional representation of the loaded BMI shipping cask flooded with water and immersed in water. In the vertical direction the geometry was divided into six zones. These zones, in order from bottom to top correspond to the following six regions: bottom of 6-inch reflector to bottom of cask, bottom of cask to bottom of fuel, bottom of fuel to bottom of basket, bottom of basket to top of basket top of basket to top of cask, and top of cask to top of 6-inch water reflector. The third zone from the bottom was further divided into four blocks (quadrants) for ease of representation and the fourth zone from the bottom was divided into eight blocks. The modeling of the geometry was made conservative in that in zone 112 the canister material was replaced with water, in zone 114 the fuel region was extended to 3.83 inches upward to the top of the basket, and in zone 115 the canister material was again replaced with water.

6.7.3.2 Package Regional Densities

The KENO calculation requires as input the number densities of five mixtures. These are the homogenized fuel, the stainless steel, the boral poison plates, the lead shield, and the water moderator and reflector. The fuel loading is that of 12 pins per canister with a volume of $(2.76)^2 \times 24$ in.^{3} or

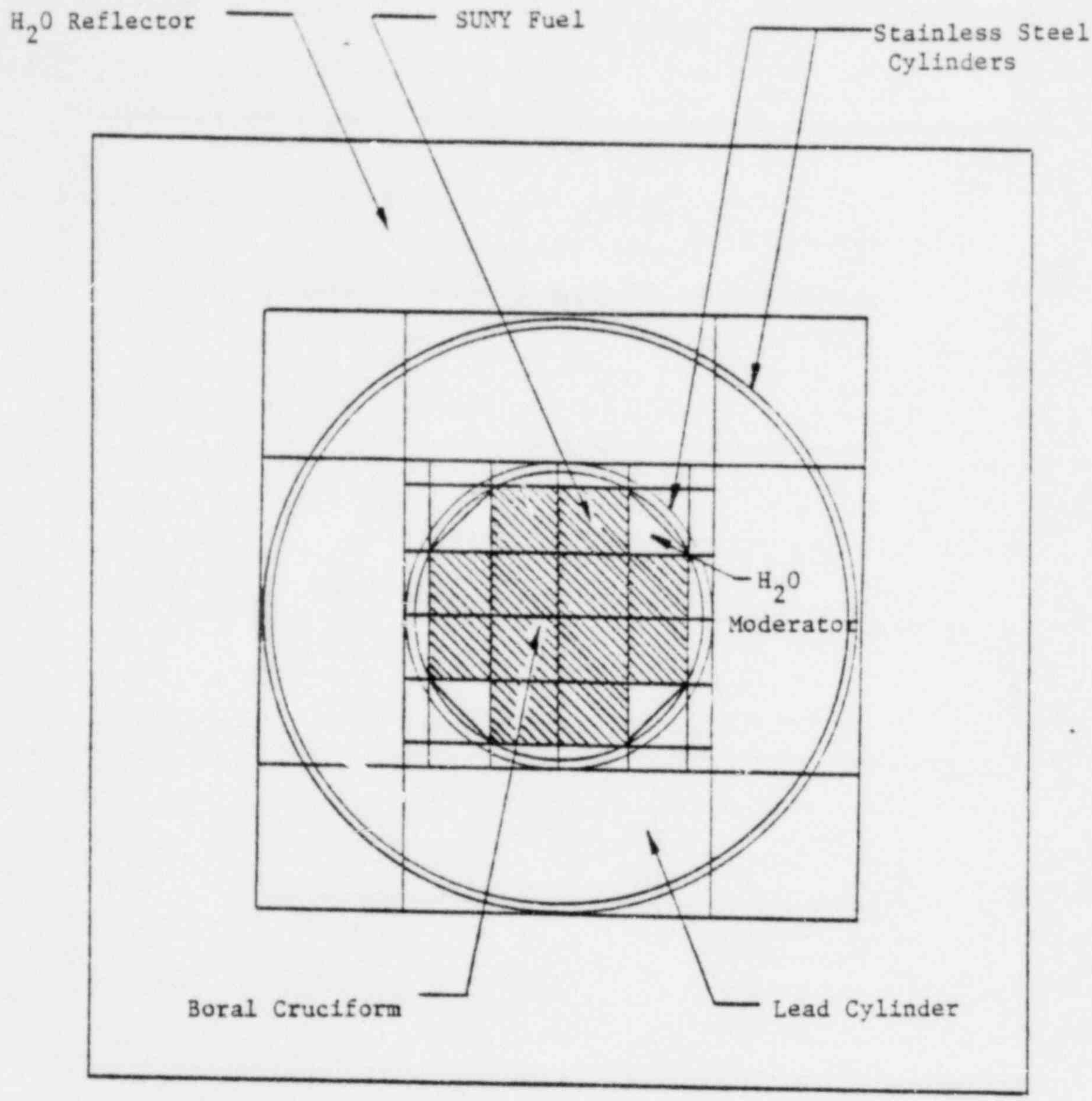

FIGURE 6.12 KENO CROSS-SECTIONAL REPRESENTATION OF BMI'S SHIPPING CASK IMMERSED IN WATER

2995.92 cc. The 12 pins occupy a volume of 832.80 cc and water occupies the remaining 2103.12 cc. The 20 mil zircalloy cladding occupies a volume of 134.63 cc. The homogenized number densities for this configuration are given in Table 6.6.

TABLE 6.6. NUMBER OF ATOMS PER CC IN THE HOMOGENIZED FUEL REGION

Element	$N \times 10^{24}$
U-238	0.0048140
U-235	0.0003109
H	0.0482800
O	0.0342200
Zr	0.0019110

The stainless steel is a mixture of 19 percent chromium, 10 percent nickel, and 71 percent iron with a density of 7.904 grams/cc. The resultant number densities are given in Table 6.7.

TABLE 6.7. NUMBER OF ATOMS PER CC IN STAINLESS STEEL

Element	$N \times 10^{24}$
Cr	0.017400
Ni	0.008114
Fc	0.060520

When considering the poison boral plates, a simple volume homogenization is inadequate since this does not account for self-shielding effects and thus would tend to over-estimate the neutron absorption of the boron. Experimentally it has been shown[5] that B_4C lumping in the boral plates reduces the thermal neutron absorption cross section by 20 to 30 percent. Thus the number density of boron should be reduced by this factor for the computation of absorption. In order to be conservative, only 1/2 the calculated boron number density was used in the KENO computation. The plate was made up of a B_4C-Al core with a thickness of 0.04 inch, a density of 2.64 g/cc, and containing 35 wt percent B_4C and 65 wt percent aluminum. On each side of the core were an aluminum cladding with density $\rho = 2.71$ and thickness 0.011 inch and a stainless steel cladding of thickness 0.031 inch. The number densities are given in Table 6.8.

TABLE 6.8. NUMBER OF ATOMS PER CC IN BORAL POISON PLATE

Element	$N \times 10^{24}$
B	0.00648
C	0.00324
Al	0.02311
Cr	0.00870
Ni	0.00405
Fe	0.03026

The number density in the lead with a density of 11.005 g/cc is 0.03199×10^{24} atoms/cc. Water with a density of 1.0 contains 0.066863×10^{24} atoms/cc of hydrogen and 0.033432×10^{24} atoms/cc of oxygen.

6.7.3.3 Results

The computed value of k_{eff} is

$$k_{eff} = 0.843 \pm 0.010 \quad .$$

Table 6.9 gives a summary of criticality results.

TABLE 6.9. FISSILE CLASS III (I, II, III)

NORMAL CONDITIONS	Fissile Class I	II	III
Number of undamaged packages calculated to be subcritical (Fissile Class I, must be infinite; Fissile Class II, must be at least 25; Fissile Class III, must be at least identical shipment).			2
Optimum interspersed hydrogenous moderation; yes, required for Fissile Class I.			No
Closely reflected by water; yes, required for Fissile Class II and III.			Yes
Package size, cu cm			1.04×10^7

ACCIDENT CONDITIONS	I	II	III
Number of damaged packages calculated to be subcritical (Fissile Class I must be at least 250; Fissile Class II must be at least 10).			1
Optimum interspersed hydrogenous moderation, full water reflection			Yes
Package size, cu cm			1.04×10^7
Fissile Class II, minimum transport index (must not exceed 10).			

6.8 APPENDIX

Document: 3, 5, 9, 15

6.8.1 References

(1) Whitesides, G. E., "Adjoint Biasing in Monte Carlo Criticality Calculations", Trans. Am. Nucl. Socl., 11, 159 (1968).

(2) Bell, G. E., et al, "Los Alamos Group-Averaged Cross Sections", LAMS-2941 (September, 1963).

(3) TID 7028

(4) Whitesides, G. E., Private Communication.

(5) Burrus, W. R., "How Channeling Between Chunks Raises Neutron Transmission Through Boral", Nucleonics, 16, 91-94 (January, 1958).

(6) BMI - Internal Memo from R. O. Wooton to E. C. Lusk (April 9, 1964).

(7) Nuclear Safety Guide, TID-7016, Rev. 1, Goodyear Atomic Corporation (1961).

(8) Private communication from Martin N. Haas, Associate Director, Nuclear Science and Technology Facility, State University of New York at Buffalo to Dr. Richard Denning, Battelle Memorial Institute, Columbus, Ohio 43201 (March 15, 1977).

(9) RSIC Computer Code Collection, ORNL-TM-3076, AMPX-1, Oak Ridge National Laboratory, Oak Ridge, Tennessee 37830.

(10) Petrie, L. M., and Cross, N. F., "KENO IV, An Improved Monte Carlo Criticality Program", ORNL-4938, Oak Ridge National Laboratory, Oak Ridge, Tennessee 37830.

7. OPERATING PROCEDURES

7.1 Procedures for Loading The Package

The procedures outlined in this section are applicable for handling the BMI-1 Cask during loading of the package at Battelle-Columbus Hot Laboratory at West Jefferson, Ohio. It should be used by other facilities as a guide in their operational planning.

7.1.1 Preuse Test and Examination

7.1.1.1 Preuse Test

The Preuse Tests shall be performed immediately before or during loading for each use. At each use the canister (if applicable) and cask shall be individually subjected to a 50 psig minimum pressure test after they have been loaded and the lid secured in place.

The purpose of the pressure leak test is to establish that the seal of the canister and cask has been accomplished and meets the sealing requirements. The maximum permissible leak rate permitted for the BMI-1 cask is 9.24×10^{-3} atm-cc/sec. According to ANSI Standard N-14.5, the required sensitivity of a leak test to detect this degree of leak is 4.62×10^{-3} atm-cc/sec. The Soap Bubble Leak Test Procedure described below has a sensitivity of 1×10^{-3} atm-cc/sec and, therefore, meets the requirements.

Procedure, Soap Bubble Leak Test

(1) Load and close containment canister or cask according to the loading procedure.

(2) Attach a pressurized air or inert gas line to the pressure port as applicable. Use Teflon

tape or other compatible sealant material on threads.

(3) Slowly pressurize to 50^{+1}_{-0} psig.

(4) With a "soap bubble" detection liquid (i.e., SNOOP), flood the seal region and pressure port attachment.

(5) Observe for a minimum of (2) minutes reapplying solution as required to maintain heavy liquid film layer.

(6) At the completion of a successful test, depressurize slowly and remove solution by convenient method.

(7) Remove pressurization line and insert plug in pressure port according to the loading procedure. Close pressure port valve if applicable.

(8) The acceptance criteria is that there shall be no evidence of bubble formation indicative of a leak. Failure to meet this criteria constitutes failure of the test and requires that the cognizant supervisory personnel be notified and corrective action be initiated.

7.1.1.2 Preuse Visual Examination

Prior to each use the following visual examinations shall be performed.

(1) Cask Body. The cask shall be examined for any obvious deformities or flaws especially in weld area which would impair the safety of the cask. The lid bolt holes shall be examined to assure that they are clean and free of any foreign material and that the threads are not damaged. The bolts shall be examined for damage and

replaced if needed. The drain valve shall be inspected to assure that it operates freely. The threads and gaskets on the drain housing and drain housing cover plate shall be examined to assure that the cover fits properly on the housing. The O-ring seat on the cask body and cover shall be inspected to assure that they are free of any scratches which would impair their sealing ability. The lid O-ring shall be inspected for cuts, deformities or other irregularities. The safety plugs shall be inspected for any flaws. The upper pressure relief valve and pressure gage shall be inspected for flaws and proper operation before each cask use and the gage calibrated on an annual schedule.

(2) Skid. The skid shall be examined to assure that it is not twisted, bent, or otherwise damaged such that it would impair the safety of the package. If the skid is not attached to the cask, the bolt holes in the skid shall be inspected to assure that they are free of foreign material and that the threads are not damaged; and the bolts shall be examined to assure that they are not damaged.

(3) Canisters and Baskets. The canisters and baskets shall be inspected for any deformed areas. Any O-ring and seal surfaces shall be examined for scratches or other irregularities which would impair the sealing ability. The bails or lifting eyes shall be inspected to assure that they are not frayed or otherwise damaged and that their attachments to the units are secure. Pressure ports and plugs shall be inspected for any damage

or deformed threads which would affect the sealing ability. Welds shall be inspected for cracks and flaws.

7.1.2 Preloading Operations

Prior to each use the following shall be verified as being in compliance with USNRC Certificate of Compliance Permit Number USA/5957/B()F:

(1) Permit is current and applicable.

(2) Shipper is registered as a user under Section 71.12(b) of 10 CFR Part 71.

(3) Assure contents will qualify as to material type, form, and maximum quantity. This shall include meeting the limits for decay heat, fissile quantities and external radiation limits.

(4) Determine the requirement for an internal containment canister or basket.

(5) The maximum gross weight of the cavity contents shall not exceed 1800 pounds.

(6) Verify that the consignee is properly licensed to receive the material and that its license is current.

7.1.3 Loading the Cask

Conduct the loading procedures as stated below after the preloading operations have been completed. Notify the cognizant supervisor if any damage or deficiency is noted and perform corrective action as directed.

Procedure

(1) Carefully lift the cask, by using the lifting yoke or by lifting beneath the skid with a forklift truck. Move to wash area if required, otherwise to preparation and loading area.

(2) Wash the cask and place it on blotting paper, if required.

(3) Remove the cover from cask drain valve housing.

(4) Remove the plug from the drain, assuring the drain valve is closed before the plug is removed. (Pressure gauge should read zero.)

(5) If the cask was not opened upon last receipt, perform an internal pressure and liquid check using NS-PI-1.4 (Section 7.4.2) as a guide.

(6) Inspect the drain valve.

(7) Remove all cask lid bolts.

(8) Insert hooks into the cask lid lifting plate.

(9) Remove the cask lid with continuous monitoring by Health Physics.

(10) Perform the preuse inspection described in Section 7.1.1 and perform any required corrective maintenance.

(11) Pour liquid into cask cavity and collect from drain valve to insure clear drain line.

(12) Ensure that the cask O-ring is properly seated in the lid groove.

(13) Close the drain valve and insert drain plug if loading dry. Leave open if loading plan requires underwater loading.

(14) Check all dimensions of containers, cask, loading areas, crane travel, etc. to assure that all operations can be performed.

(15) Move the cask to the loading area.

(16) Perform a preuse inspection of the containment canister or basket (if one is used) according to the procedures described in Section 7.1.1.2 and perform any required corrective maintenance.

(17) Load the canister or basket with the radioactive material.

(18) Place the lid on the canister or basket and bolt in place. Torque the canister bolts to 60 ± 10 inch-pounds.

(19) Perform the canister-cask pressure leak test according to the procedures described in Section 7.1.1.1. Decontaminate the canister if applicable.

(20) Lift the canister or basket using a suitable method and insert it into the cask cavity. Do Not Drop.

(21) Place the lid on the cask and secure with at least two lid bolts.

(22) Remove the cask from the loading area, monitor the cask to assure that radiation limits for shipment outlined in Section 7.1.4.1 will not be exceeded, and then move to a designated area.

22a. Check the coolant (if liquid shipment) for activity after the cask has stood for at least 4 hours (activity shall not exceed that specified for 10 CFR 71.35A3 or DOE Manual Chapter 0529).

22b. Drain 5 percent of the water from the cask to provide expansion space for the water due to changes in ambient temperatures. Close and plug drain and flush valves. When needed, use a compatible antifreeze mixture to prevent damage to any components of the package due to freezing.

(23) Insert the remaining cover bolts and tighten in alternating sequence to 50 foot-pounds.

(24) Perform a preliminary smear survey and decontamination, if required, to meet the facility handling requirements.

(25) Perform a preuse pressure leak check on the cask lid seal, pressure system, and drain valve according to procedures described in Section 7.1.1.1.

(26) Install the plugs in all valve outlets using Teflon tape or suitable material on threads.

(27) Install all cover plates after inspection to assure the areas are contamination free prior to covering.

(28) Remove the lid-lifting hooks from the lid and attach cover plates to the four lifting eyes.

(29) Transfer the cask to the skid.

(30) Bolt the cask onto the skid and secure the cask to the skid with turnbuckle anchors.

(31) Assure the cask temperature requirements as follows.

(1) Temperatures on any accessible surface may not exceed those specified in 10 CFR 49 Section 173.393e2. (In the shade, assuming still air at ambient temperatures.)

(a) 122 F nonsole-use vehicle..

(b) 180 F sole-use vehicle.

(2) For liquid shipments, insert thermocouple into well in the lid and follow the cask temperature until it comes to equilibrium.

The equilibrium coolant temperature may not exceed 270 F minus the difference between 100 F and actual ambient temperature.

7.1.4 Final Preparation for Shipment of Package

7.1.4.1 Radiation Surveys

The following procedures shall be followed to assure compliance with the applicable Federal Regulations and BCL requirements for commercial motor freight shipments.

(1) Perform and record a complete radiation survey of the cask and support equipment. The shipping limits are as follows:

- (a) Dose rate may not exceed 200 mRem/hr at cask surface or personnel barrier and is not to exceed a transport index of 10 per package and 50 total for all packages for nonexclusive use of vehicle and any other open transport vehicle.
- (b) Dose rate on cask may not exceed 10 mRem/hr at 3 feet from the cask surface, as per the Certificate of Compliance, and 200 mRem/hr on the external surfaces of the vehicle (exclusive use, closed transport vehicle only.)
- (c) Dose rate may not exceed 10 mRem/hr at 6 feet from the vertical planes projected from the outer edges of the vehicle (open or closed vehicle).

(d) If the dose rates exceed these levels, notify the cognizant engineer, and await his instructions for corrective action before proceeding.

7.1.4.2 Smear Survey

Procedures

(1) Decontaminate the cask until removable contamination on all accessible surfaces is <2200 dpm/100 cm^2 $\beta\gamma$ and <220 dpm/cm^2 α. These limits may be exceeded if the conditions and limits specified under 49 CFR 173.397 are met.

(2) Document the smear survey on Form HPS-S1-73 (Section 7.4.3).

7.1.4.3 Security Seal

Procedure

(1) Attach a seal to the cask lid, drain line cover, and upper pressure port cover, which is not readily breakable and which, while intact, will be evidence that the package has not been illicitly opened.

(2) Record the seal number on Form HPT-1-76 (Section 7.4.4) for the consignee's verification upon receipt.

7.1.4.4 Label and Markings

Procedure

(1) Attach two address labels identifying both consignor and consignee and their addresses.

Additional identification may be added as applicable.

(2) Fill out and attach two radioactive material hazards labels or "Empty" labels as applicable.

(3) Verify that all container identification information is attached as required by the regulations.

7.1.4.5 Packing List

Procedure

(1) Attach a packing list to the cask container at a minimum, the completed Form HPT-1-76 (Section 7.4.4) and Operating Manual NS-COM-1.[1] (Unless previously supplied to receiver.) Additional information which may assist the motor carrier and consignee may also be included.

7.1.4.6 Shipping Documents

Procedure

(1) Prepare and obtain required signatures on a Bill of Lading (Commercial or Government) in accord with applicable regulations.

(2) Complete Form HPT-1-76 (Section 7.4.4) for attachment in packing list and for internal and external distribution.

7.1.5 Quality Assurance

(1) To assure that all critical functions are performed, the shipper for all shipments originating outside BCL shall complete the applicable

(1) References for Section 7. are found in Section 7.4.1.

Work Completion Check Sheet in Section 7.4.5, or provide similar documentation.

(2) For shipments originating within BCL, the Quality Assurance Documents of NS-PI-1[2] shall apply.

7.1.6 Package Transport

(1) Transfer the cask to the trailer.
(2) Secure the cask on the trailer using four chains and binder sets, attach each set to the four tiedown eyes provided at the top of the cask, and rigidly secure to the trailer. The chain shall be at least the equivalent to Columbus-McKinnan 5/16" G-70 with a working load of 4700 pounds and an ultimate load of 18,800 pounds. The binders shall have an equivalent rating. The supporting yoke shall be secured to the trailer bed with chains and binders of the same rating.
(3) Apply Radioactive placards to all four sides of the trailer if applicable.
(4) Obtain approval of the driver and cognizant facility supervisor that the load and trailer are properly secured, marked, and sealed.
(5) Seal the trailer doors and record if applicable.
(6) Review any Emergency Instructions with the driver and be sure they are clearly understood by him.
(7) Ensure that all trailer lights and brakes are operating properly, and that tires are in satisfactory condition.
(8) Transmit all applicable documents to the driver. These should include but not be limited to copies of:

(a) Bill of Lading

(b) Radioactive Shipment/Receipt Form, HPT-1-76 (Section 7.4.4)

(c) Emergency Instructions.

(9) Release shipment to vehicle driver.

7.1.7 Postshipment Requirements

The following actions shall be taken after the vehicle leaves the facility.

(1) Notify the consignee of the shipment, ETA, and any special instructions by mail, telephone, or telegraph as applicable.

(2) Distribute documents internally as applicable.

(a) For shipments of accountable material the consignee's and consignor's Materials Accountability Section shall be notified no later than the day of the shipment.

(3) Maintain contact with the consignee to verify safe arrival of the shipment.

7.2 Procedures for Unloading the Package

7.2.1 Receipt of Package

(1) Move the transport vehicle to the unloading ar a. Secure the trailer prior to removing the tractor (if applicable).

(2) Survey and smear the tractor compartment and semi-trailer bed and remove any barriers.

2.1 Limits are per Sections 7.1.4.1 and 7.1.4.2.

2.2 If radiation and smear limits are exceeded, perform a major survey and decontamination.

(3) Perform radiation and smear surveys on external surfaces of the cask and support equipment. Record the results.

3.1 Limits are per Sections 7.1.4.1 and 7.1.4.2.

(4) Notify the Facility Supervisor of the survey results, seal and damage inspections, and obtain his authorization and instructions to unload the cask from the trailer and move it to a designated area.

(a) Check the seal identification and integrity. Compare the seal identification with that appearing on the shipper's documents. Notify a cognizant supervisor of any apparent security violation and await his instructions.

(b) Inspect the external cask components and support equipment for apparent damage or deficiencies and report these to a cognizant supervisor.

(5) Remove the cask from the carrier by using the yoke provided or suitable chain or cable.

(6) Survey and smear the trailer area where the cask was located.

6.1 Limits are per Sections 7.1.4.1 and 7.1.4.2.

6.1.1 The radiation dose rate on any accessible surface of an empty transport vehicle shall not exceed 0.5 mRem/hr at the time it is released for public use.

(7) Move the cask to a designated area.

(8) Clean road dirt from the cask if required.

(9) Loosen the tension on the tiedowns with the turnbuckles and detach the tiedowns from the cask.

(10) Unbolt the cask from the skid plate.

(11) Mark the orientation of the lid in relation to the cask body.

(12) Move the cask to the facility storage or unloading area.

(13) Tag the cask with identification of the contents and radiation survey data.

7.2.2 Unloading the Empty or Loaded Cask

The following unloading procedures shall be followed at the BCL Hot Laboratory and should be used as a guide for operational planning by other facilities.

Procedure

(1) Review unloading instructions and any special handling, safety, and security procedures.

(2) Check the cask for internal pressure by observing the pressure gage in the pressure control system box. Check for undocumented liquid using Procedure NS-PI-1.4 (Section 7.4.2) as a guideline. Some shipments are authorized to be shipped wet.

(3) Remove the lid bolts. Insert hooks into the lid-lifting plate.

(4) Lift the lid from the cask in an area properly controlled for radiation and contamination. Perform a radiological survey as required.

(5) Remove the containment canister or other internal containment devices from the cask cavity using suitable equipment.

5.1 If the canister is empty, perform radiological surveys on the canister and cask cavity and clean both as required in the designated cleaning area.

5.1.1 Return the canister to the cask cavity if applicable, replace the cask lid, secure the bolts, and proceed to Step 13.

5.2 If the canister contains radioactive material proceed to Step 6.

(6) Empty the canister and return it to the cask cavity (if applicable).

(7) Replace the cask lid and lid bolts.

(8) Remove the cask from the unloading area and take it to the cleaning area.

(9) Remove the lid bolts and lid.

(10) Remove the canister and clean it.

(11) Flush and clean the cask cavity with a minimum of 1 gallon of water remove the drain valve cover drain plug and open the drain.

(12) Drain all liquid from the cavity, close the drain, replace the drain plug and place the cover on the drain housing, replace the canister (if applicable), replace the cask lid, and secure the cover bolts.

(13) Decontaminate the cask exterior surface as required.

(14) Label the cask "Empty" and remove it to a storage area.

(15) If the cask contains an empty canister, this should be noted on a tag or label.

7.3 Preparation of an Empty Package for Transport

The procedures for shipment of the empty BMI-1 cask are the same as the applicable procedures prescribed for loading the package, Section 7.1.

7.4 Appendix

7.4.1 References

(1) Operating Manual for BCL Radioactive Materials Package No. BMI-1, NS-COM-1, Revision 0, Battelle's Columbus Laboratories, November 5, 1979.

(2) Procedures for the Use of BCL Radioactive Materials Shipping Packages - Casks and Canister, Battelle Columbus Laboratories, NS-PI-1, Revision 0, April 17, 1979.

7.4.2 Pressure Check Procedures NS-PI-1.4

(1) Cask Internal Pressure and Liquid Check

1.1 To ensure that no cask is opened in a pressurized condition, or contains undocumented liquids, a pressure check shall be made prior to release for shipment, and after the cask has been moved to the cask unloading area following its receipt. The following procedure shall be implemented upon receipt of a cask.

(2) General Considerations

2.1 Connect the manifold (Figure 7.1) to the cask cavity drain valve.

2.2 In the event that liquid enters the manifold and passes through the filter, the in-line filter element shall be replaced after the pressure check.

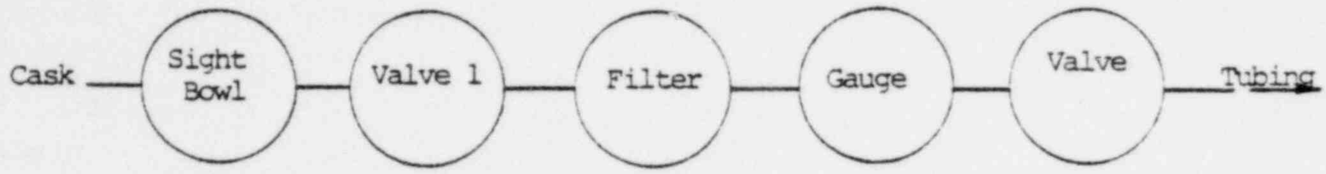

Pressure and Liquid Check Manifold

FIGURE 7.1

2.2.1 This is done to assure the integrity of the manifold filter during pressure checks.

2.3 If any liquid is found in the cask cavity, it shall be collected and disposed of in a "hot" drain.

(3) Procedures

3.1 Remove the cask valve cap from the selected cavity relief or drain valve.

3.2 Ensure that all cask valves are closed.

3.3 Remove appropriate sealing plug from valve to which manifold will be attached.

3.4 Assemble the following manifold device (See Figure 7.1).

3.4.1 1/4 in. pipe nipple - 4 in. length minimum - to be attached to the cask.

3.4.2 Absolute in-line filter.

3.4.3 Pressure gage - 0-50 psig minimum - gage must be approved for pneumatic and hydraulic use.

3.4.4 1/4 in. globe type valve; two required.

3.4.5 Sufficient heavy wall Tygon tubing, or equivalent, to reach from the cask to a contamination controlled area.

3.4.6 Sight bowl, type ERNST E-57-0, or equivalent.

3.4.7 Sufficient pipe fillings as necessary to complete assembly of manifold.

3.5 With the cask valve and manifold valves closed, attach the manifold to the cask valve.

3.6 Slowly open the cask valve.

3.7 Observe the sight bowl for the presence of liquid. Proceed to 3.8 if no liquid is observed.

3.7.1 If liquid is present, slowly open Valve 1 and read pressure in cask cavity.

3.7.2 If no pressure is present, proceed to 3.7.3.

3.7.2.1 When pressure and/or liquid is present, place the exit end of the exhaust tubing into the airborne contamination control area.

3.7.2.2 Slowly open Valve 2 and collect the liquid while bleeding off the pressure.

3.7.2.3 Continue the liquid collection and pressure bleeding under constant observation until all liquid is drained from the cask and the manifold gage reads zero.

3.7.2.4 Dispose of collected liquid in a "hot" drain.

3.7.2.5 Proceed to 3.9.

3.7.3 Perform Steps 3.7.2.1 through 3.7.2.4 deleting the portion pertaining to pressure bleed off.

3.8 Slowly open Valve 1 and read internal cask pressure on the pressure gauge. If no internal pressure exists, proceed to 3.9.

3.8.1 If the cask is in a pressurized condition, perform Steps 3.7.2.1 through 3.7.2.3 deleting the portion pertaining to liquid collection.

3.9 Close the cask valve.

3.10 Close the manifold valves.

3.11 Remove the manifold from the cask.

3.12 Replace the cask valve plug.

3.13 Package and store the manifold assembly as internally contaminated equipment.

(4) Documentation

4.1 Record and document cavity pressure and above operations on the following form.

Internal Pressure Check Traveler

Procedure Number NS-PI________, Rev.________.

Cask Identification Number________.

	Initial	Date
1. Cask pressure gage present and registering 0 psig or manifold assembled as required	______	____
1.1 Manifold attached to cask drain line	______	____
2. Cask drain valve opened to pressure gage	______	____
3. Record gage reading:		
3.1 Gage at __________psig	______	____
4. Pressurized cask: (if applicable)		
4.1 Pressure slowly released from cask	______	____
4.2 Record gage reading:		
4.2.1 Gage at _________psig	______	____
5. Cask valve closed	______	____
5.1 Manifold removed from cask	______	____

Comments:____

____

____

____

Work Completed by:__________________________ Date__________
Operator

Reviewed by:______________________________ Date__________
Operations Supervisor

Work Completed by:__________________________ Date__________
Operator

Reviewed by:______________________________ Date__________
Operations Supervisor

7.4.3 Form HP-S1-73

7.22

BATTELLE-COLUMBUS LABORATORIES

HEALTH PHYSICS SERVICES

SMEAR SURVEY REPORT

Building ________________ Date ______________ Area ______________________________

Surveyor ________________ Nature of Suspected Activity ___________________________

Counted with ☐ Solid State Alpha-1 ☐ Scintillation Detector ☐ Gas Proportional Detector

Give exact location either by writing, attached floor plan, or sketch on back of this form.

Results of Survey

Efficiency of Detector: α_____ βγ_____ Counted by________________________

Background of Detector: α_____ βγ_____ Date______________________________

Action Limits: α_____cpm, βγ_____cpm Action Limits: α_____dpm, βγ_____dpm

Location	Alpha				Beta Gamma			
	Ctg. Time	c/m Gross	c/m Net	d/m/ 100 cm^2	Ctg. Time	c/m Gross	c/m Net	d/m/ 100 c[illegible]

7.4.4 Form HPT-1-76

7.24

(Form HPT 1-76 Rev. 1)

RADIOACTIVE SHIPMENT AND RECEIPT RECORD

File No. ______

Battelle
Columbus Laboratories
505 King Avenue
Columbus, Ohio 43201

TO: ______

ATTN: ______

FROM: ______

Date Shipped ☐
Date Received ☐ ______

Shippers No. ______
Purchase No. ______

Collect ☐ Cost $ ______
Prepaid ☐ ______

Carrier ______

Special Handling ______

TELEPHONE NUMBERS

BCL Shipper ______
BCL 24 Hr. ______
Consignee ______

Item No.	Material Description	Unshielded-hr/hr Contact	Unshielded-hr/hr 1-Meter	Curies	Container-mr/hr Contact	Container-mr/hr 1-Meter

CONTAINER EXAMINED:
No evidence of deterioration or damage ______
signature

RETURN CONTAINER TO:
(Freight Address Only)
______

CONTAINER DESCRIPTION

Serial No. ______
Permit No. ______
Weight, Gr. ______
Volume ______
LSA ☐ A ☐ B ☐ B/F ☐
Steel ☐ Lead ☐ Wood ☐
Other: ______ ☐

MATERIAL CATAGORY

Empty ☐
Low Specific Activity (LSA) ☐
Limited Quantities ☐
Type A Quantities ☐
*Type B Quantities ☐
*Fissile Quantities ☐
*Fissile and Large Quan. ☐

PHYSICAL FORM

Normal ☐ Special ☐
Solid ☐ Liquid ☐ Gas ☐
Encap. Source ☐
Empty—Residual Contam. ☐

CHEMICAL FORM ______

TRANSPORT GRP

I ☐ II ☐ III ☐
IV ☐ V ☐ VI ☐
VII ☐ Spec. Form ☐

TYPE RADIATION

Alpha ☐ Beta ☐
Gamma ☐ Neut. ☐

FISSILE CLASS

NONE ☐
Fissile Exempt ☐
Fissile I ☐
Fissile II ☐
Fissile III ☐
Special Controls ______

HM SHIPPING NAME

Radioactive Material,
1 N.O.S. ☐
2 LSA, N.O.S. ☐
3 Limited Quantity, N.O.S. ☐
4 Special Form, N.O.S. ☐
5 Fissile, N.O.S. ☐
6 ______ ☐

LABELS REQUIRED

LSA—Radioactive ☐
White I ☐
Yellow II ☐
Yellow III ☐
Empty ☐
None Required ☐
Other ______ ☐

ACCOUNTABILITY/SECURITY CONTROL

Classified ☐ Unclassified ☐ Approval Received ☐ Verified ☐
Recipients License No. ______ Exp. Date ______ On File ☐
Consignee Notified ______ Method ______ ______
Date Initial

By Product ☐ DOE ☐ IRR ☐
SNM ☐ NRC ☐ UNIRR ☐
Source ☐

741 Tran. No. ______
BCL Lot No. ______
BCL Code No. ______

Isotope						
Percent Iso.						
Weight						

HAZARD CLASS

Radioactive Material ☐
Other ______ ☐

PLACARDS

Radioactive—(4) ☐
None Required ☐

HP SURVEY

Carrier-mr/hr		
Cab	Sides/Rear	
Contact	Contact	6 FT

PACKAGE/CARRIER EXTERNAL CONTAMINATION

$\beta\gamma$ ______ dpm/100 cm^2
α ______ dpm/100 cm$_2$
Surveyer ______

CONTAINER INSPECTION

Pressure Checked ☐
Shipping Pressure ______ psig ☐
"O" Ring Inspected/Approved ☐
Valves Closed/Plugged/Sealed ☐
Lid Torqued ______ ft.-lbs. ☐
Labels/Pack. List/Address Applied ☐
Coolant: Type ______ Quan. ______ ☐
Support Equipment Present ☐

Transport Index No. ______
(mr/hr at 3 feet)
Seal Nos. ______

CARRIER INSPECTION

Tiedowns Secure ☐
Survey Complete ☐
Enclosure Secured ☐
Placards (4) ☐
Routing Plan ☐
Emergency Inst. ☐
Bill of Lading Comp. ☐
Fissile III Warning ☐

***10CFR71 REQUIREMENTS**
(For Fissile/>Type A Quan.)

Meets 71.53 (Pre.Det.) ☐
Meets 71 Sub C (Pkg. Std.) ☐
Moderator/Neutron Absorb. OK ☐
Internal Pressure OK ☐
Coolant Contamination OK ☐
Irr Decay History OK ☐
QA Document Completed ☐

Remarks ______

This is to certify that the above named articles are properly classified, described, packaged, marked and labeled, and are in proper condition for transportation according to othe applicable regulations of the Department of Transportation. Signature ______

Distribution

Originator ☐ Recipient ☐
Packing List ☐ Health Phy ☐
Accountability ☐ Other ☐
W. J. Security ☐ ______

Remarks ______

BCL Authorization

Signature ______

Title ______

REV. A. 3-28-80

7.4.5 Work Completion Check Sheet

Work Completion Check Sheet - Cask BMI-1
(Shippers Other Than BCL)

Date____________________

Facility____________________

Operator(s)____________________

Shipper____________________

Material Composition____________

Material Identification__________

Est. Decay Heat____________ Watts

1. UNLOADING CASK FROM TRANSPORTER	Initial	Date
1.1 Radiation survey of cask ________ mr/hr β-γ	______	____
1.2 Smear survey of cask ________ DPM α-β-γ	______	____
1.3 Cask removed from transporter	______	____
1.4 Radiation survey of transporter under cask, ________ mr/hr β-γ	______	____
1.5 Smear survey of transporter under cask, ________ DPM α-β-γ	______	____
1.6 Copy of all documents to transportation coordinator	______	____
1.7 Cask seals checked and recorded	______	____
1.8 Cask inspected for damage and so recorded	______	____
1.9 Cask tagged to identify contents	______	____

	Initial	Date
2. PREUSE EXAMINATION AND PROCEDURES		
2.1 External components visual inspection and approval	______	____
2.2 Preloading operations performed	______	____
3. CASK LOADING		
3.1 All cover bolts removed	______	____
3.2 Cask moved to loading area	______	____
3.3 Cask cover removed	______	____
3.4 Canister (if used) loaded	______	____
3.5 Canister cover bolts torqued to 60 $\pm$ 10 inch-pounds	______	____
3.6 Pressure leak test performed and canister seal satisfactory	______	____
3.7 Canister loaded in cask cavity	______	____
3.8 Cover placed on cask and secured with	______	____
bolts torqued to 50 foot-pounds	______	____
3.9 Pressure leak test performed on cask cover seal and drain valve	______	____
4. CASK UNLOADING		
4.1 Internal cask cavity pressure checked	______	____
4.2 All cover bolts removed	______	____
4.3 Cask moved to unloading area	______	____
4.4 Cask cover removed	______	____
4.5 Canister removed from cask	______	____

		Initial	Date
4.6	Canister unloaded, if applicable, and returned to cask cavity	_______	_____
4.7	Cask cover replaced	_______	_____
4.8	Cask removed from unloading area	_______	_____
4.9	Cask cavity and canister cleaned	_______	_____
4.10	Canister returned to cask cavity and cover bolted in place	_______	_____
4.11	Cask decontaminated externally	_______	_____
4.12	Cask transferred to storage area	_______	_____

5. PREPARATION FOR SHIPMENT

5.1	Radiation survey completed	_______	_____
5.2	Cask decontaminated to acceptable level of removable contamination	_______	_____
5.3	Form HPS-SI-73 (Appendix E) completed	_______	_____
5.4	Radioactive Shipment Form (Appendix D) completed	_______	_____
5.5	Cask properly sealed, labeled, marked, and identified	_______	_____
5.6	Cask properly secured on transporter	_______	_____
5.7	Transporter vehicle inspected and sealed	_______	_____
5.8	Driver instructed and given proper papers	_______	_____

8. ACCEPTANCE TESTS AND MAINTENANCE PROGRAM

8.1 Acceptance Tests

The BMI-1 Shipping Cask has been in use in its present configuration since 1970. Tests of the package, therefore, properly are part of the maintenance program discussed in the next section.

8.2 Maintenance Program

8.2.1 References

RDT-E12-7T - Inspection and Preventive Maintenance of Radioactive Shipping Containers
10 CFR71 Appendix E - Quality Assurance
RDT-F8-11 - Fuel Shipping Container Tiedown for Truck Transport
AECM - 0529 - Safety Standards for the Packaging of Fissile and Other Radioactive Materials
ANSI - N 14.5 - Leakage Tests on Packages for Shipment of Radioactive Materials

8.2.2 Inspections

8.2.2.1 Types

The following types of inspections shall be performed and documented:

Periodic - Annual; Biennial
Preusage
Postaccident.

8.2.2.2 Frequency

(a) Periodic inspections shall be performed before initial use of the packaging and annually thereafter except during periods of prolonged storage. Items specified for biennial inspection may be included in the annual inspection on alternate years. No packaging shall be used which has not been inspected in the immediately preceding year for the items of Section 8.3.3.1 and the preceding 2 years for the items of Section 8.3.3.2.

(b) Preusage inspections shall be performed immediately prior to each offsite shipment of the packaging.

(c) Postaccident inspections shall be performed prior to use of the packaging after it has been subjected to unusual stress conditions including fire, moving transportation accident, nuclear incident, free drop, internal or external explosion, pressurization above maximum design specification, exposure to materials corrosive to structural components, or freezing of liquid contents.

8.2.2.3 Inspecting Personnel

(a) Inspections shall be performed by personnel representing Quality Assurance organizations that are qualified in accordance with 10 CFR 71 Appendix E.

(b) Postaccident inspections shall be directed by a person in charge, designated by the responsible performing organization on the basis of engineering competence, and familiarity with the Safety Analysis Report for the packaging (container) in question.

8.2.2.4 Records

(a) A corrosion-resistant metal tag indicating expiration date of most recent periodic inspection shall be firmly and securely affixed in a conspicuous location on the body of the packaging. A similar metal tag shall be affixed to any optional use components such as inserts. Where permanent attachment of a metal tag would damage the component, other durable methods of marking the expiration date, compatible with the materials and service environment, shall be used.

(b) A record of each periodic inspection, including a description of defects and corrective actions which were taken, shall be prepared by the person in charge, and shall indicate his organizational title or responsibility. This record of inspection shall be placed in the Quality Assurance record file required in accordance with AECM 0529.

(c) A detailed description of all tests and inspections performed and the results thereof shall be prepared by the engineer responsible for performing a postaccident inspection. This record shall be placed in the Quality Assurance record file for the packaging. If the results of this inspection indicate the original design specifications are no longer applicable, then revisions of outstanding drawings, reports, specifications, licenses, and certificates of compliance reflecting the change shall be obtained.

(d) Handling and shipping procedures of the user of packaging shall contain appropriate instructions for preusage inspections and tests ensuring compliance with design and permit requirements. Record copies of these inspections shall be retained for at least 2 years after the shipment.

8.2.3 Periodic Inspections

8.2.3.1 Annual

An annual inspection together with the biennial inspection shall verify that the packaging continues to meet design specifications. Items for annual inspection shall include, but are not limited to the following:

(a) Surfaces. Surfaces shall be free of corrosion, gouges, cracks, or other deformations as determined by visual inspection. Painted surfaces shall be free of cracks, chips, or blisters.

(b) Sealing Surfaces. These surfaces shall be inspected for pits, scratches, burrs, corrosion and other imperfections.

(c) Sliding Surfaces. Surfaces which move relative to one another shall be inspected for excessive wear or roughness not within design tolerances.

(d) Welds. Welds shall be determined to be sound by visual inspection.

(e) Closure Devices. Bolts and nuts shall conform to original design specifications and shall not be bent or otherwise deformed. Threads shall be uniform and free of burrs. Provision for installing seal wires shall be present. Latches shall work smoothly and engage properly.

(f) Alignment Devices. Guide pins, lugs, etc., shall not be deformed and shall operate as intended. Match marks shall be clearly visible.

(g) Lifting Lugs, Eyes, and Trunnion. Visual inspection shall indicate no misalignment, wear, or other deformation which would significantly affect strength. Engagement guides and retainers shall be sound and operable as intended. Bearing surfaces shall be smooth to prevent binding.

(h) Valves, Lines, and Connections. Valves shall be freely operable by hand pressure. Lines shall be determined to be free of restrictions. Threaded connections shall be free of deformation or damage. "Quick-disconnect" type fittings shall operate freely. Plugs or caps shall be provided for all line ends except those downstream of pressure relief devices.

(i) Filters. Filters shall be replaced or inspected and tested to verify performance in accordance with design specifications.

(j) Reuseable Gaskets. These gaskets shall have no visible evidence of deterioration or damage. They shall be retained in position on one of the sealing surfaces in a manner which will not affect the seal. One-time-use gaskets are not inspected on periodic inspections.

(k) Tiedown. The tiedown shall comply with RDT F 8-11.

(l) Leaktightness. A test shall be performed to demonstrate leaktightness at least of the degree corresponding to the basis for the certificate of compliance, and in accordance with procedures in ANSI N 14.5.

8.2.3.2 Biennial

Items to be inspected include the following:

(a) Welds. Welds which are subject to stress and which must be sound for safe operation or for compliance with regulations shall be inspected by dye penetrant, radiographic, or ultrasonic methods.

(b) Pressure Relief Valves and Instruments. Pressure relief valves and instruments such as pressure gages and thermocouples shall be bench-tested and calibrated as necessary to verify performance in accordance with specifications.

8.2.4 Preusage Inspections

Inspections shall be performed before each shipment of a loaded package or contaminated empty packaging to establish compliance with applicable regulations and standards. Items to be inspected include, but are not limited to, the following:

8.2.4.1 General Condition

Visual inspection shall be made for deformation of structural members, missing components, and other possible deficiencies. Any necessary maintenance shall be performed. Requirements may differ for loaded packages and empty packaging.

8.2.4.2 Closure

Reusable gaskets shall be inspected visually and determined to be sound before closure is made. Gaskets which are permanently deformed by normal use shall be replaced at each use. Rupture disks shall be visually inspected and determined to be free of imperfections, damage, or corrosion. All valves shall be closed, bolts and nuts shall be determined to be tightened within design torque specifications, and wire seals shall be installed.

After a loaded or internally contaminated package is closed, it shall be determined to be sealed by a leakage test of the sensitivity specified in ANSI N 14.5 to be used before each shipment, or by an alternative procedure approved by the USNRC or DOE Contracting Office having jurisdiction of the packaging if a leakage test of such sensitivity is impractical with the package loaded for shipment. When a potential leakage point is submerged in liquid on the upstream side and clearly visible on the downstream side, a hydrostatic test at 15 psig or more is acceptable, with any observed drops or seepage being cause for rejection. If a hydrostatic test is used with loss of pressure as a measure of leakage, account shall be taken of possible gas in the containment vessel, solubility of gas, temperature change, liquid compressibility, and stretch of the vessel.

8.2.4.3 Radiation and Contamination

Radiation and surface contamination surveys shall be performed on the loaded package. The results of these surveys shall fall within applicable BCL limits.

8.2.4.4 Tiedown

The tiedown shall comply with design specifications and RDT F 8-11.

8.2.5 Postaccident Inspections

8.2.5.1 Purpose

Performance of postaccident inspection shall verify that the package complies with original design or permit specifications. Where characteristics have changed, but remain within permitted variances, these changes shall be noted in the Quality Assurance file.

8.2.5.2 Items of Inspection

Items of inspection shall include, but are not limited to the following:

(a) Dimensional Stability. Measurements shall be taken to verify that all dimensions which affect performance are within specified tolerances. Particular attention shall be paid to flatness, straightness, or uniformity tolerances affecting fit between parts.

(b) Welds. Welds whose function is simple closure or joining shall be determined to be sound by visual inspection. Welds required to sustain stress shall be determined to be sound by nondestructive examination such as radiographic examination, liquid penetrant and/or ultrasonic means.

(c) Package Shielding. Where the nature of an accident is such that internal shielding material may have melted, deformed, or cracked, the shielding characteristics of the package shall be reevaluated. This shall be accomplished by enclosing a gamma source of known high energy level in the package cavity. Radiation measurements shall be taken on the surface of the package and shielding effectiveness shall be calculated. The effectiveness thus calculated shall not deviate significantly from that which would be expected from the original shielding design. Where neutron shielding is required, a similar test shall be performed using a neutron source.

(d) Heat Transmission. The heat transmission characteristics of the package shall be reevaluated by enclosing a heat source of design value in the package cavity and, after equilibrium with ambient conditions is achieved, measuring surface and internal temperature of the package. These transmission characteristics shall agree with the requirements of the certificate of compliance.

8.2.6 Preventive Maintenance

8.2.6.1 Definition

Preventive maintenance shall consist of repair, replacement, and adjustment during periods of usage or storage to ensure specified functioning and to avoid deterioration.

8.2.6.2 Frequency

Preventive maintenance shall be performed as follows:

(a) At the time of periodic inspection and at the time of inspection before each shipment, as considered necessary by the person in charge, to correct deficiencies which might lead to failure or damage.

(b) Before any period of protracted storage, to provide necessary protection against corrosion or other avoidable deterioration.

8.2.6.3 Records

All maintenance repairs will be recorded and documented per BCL Quality Assurance procedures.

8.2.6.4 Items

Preventive maintenance is intended to be performed before failure or inoperability occurs. Such work shall include, but not be limited to, the following:

(a) Parts Replacement. Damaged, missing, deteriorated, or badly worn parts such as nuts, bolts, filters, gaskets, valves, cables, pressure relief devices and rupture disks shall be repaired or replaced. Such rework shall meet design specifications.

(b) Decontamination. Prior to shipment, the external surfaces of packages shall be decontaminated to levels within the limits specified by applicable regulations. Prior to storage, the external surfaces of packages shall be decontaminated to levels permitted in the specific storage area. The interior of packages shall be decontaminated as required to maintain consistency with the levels of contamination of items to be shipped therein. Decontamination shall remove contaminants. Application of paint, plastic film, or similar surface coatings to cover or shield contamination is not permitted.

8.2.7 Documentation

All Inspections and Preventive Maintenance Activities shall be recorded and documented on the applicable BCL-QA documents.